The Natural Ventilation Augmented Cooling (NVAC) Greenhouse: Design Development, Analysis of Greenhouse Climate, and Plant Response

By

Lucas McCartney

A thesis submitted to McGill University

in partial fulfillment of the requirements of the degree of Doctor of Philosophy

August, 2017

Department of Bioresource Engineering

21111 Lakeshore Road, Sainte-Anne-de-Bellevue, Quebec H9X 3V9 McGill University,

Montreal, Canada

Acknowledgements

First and foremost, I would like to thank my parents, Cathy Shannon and Kurt McCartney, who have provided me with continuous support during my doctorate. Without my family's cherished influence on my life and heartfelt support, including my sibling Chloe and grandparents, none of this would have been possible.

I would like to express my sincere gratitude to my supervisor Dr. Mark G. Lefsrud for the continuous support of my Ph.D. work and related research, and for his patience and motivation to pursue the project. I thank Dr. Lefsrud for pushing me to strive for higher and better, and for giving me the opportunity to join scientific groups and committees, travel to international conferences to present our work, and lecture courses. I am grateful for all I have learned from these experiences.

Thank you Dr. Valérie Orsat, my co-supervisor and Chair of the Department of Bioresource Engineering, for guidance through my graduate (and undergraduate) studies, and for providing me with support and perspective on many important topics of my dissertation.

I am particularly thankful to Werda Saeed for her continuous support throughout the years of my doctorate, especially in the last months when the days were long with redaction of my dissertation. Thank you for being there during every part of it and for proof-reading my thesis.

Thank you to Simon and Sandra Cannon, owners of the greenhouse operation in Trents, Barbados. Without your kindness, support and trust in allowing me work in your greenhouses, this project would not have been possible.

I am also thankful for the support from Dr. Danielle J. Donnelly who provided me with valuable knowledge and guidance in terms of plant science throughout my entire doctorate program. I would like to acknowledge the technical and engineering support provided by Mr. Yvan Gariepy who offered a solution to nearly every problem that I presented to him. Thank you to Dr. Robert Williams who proof-read my earlier work and provided much needed horticultural and chemistry guidance. I would like to acknowledge support from Dr. Ian Strachan and Mrs. Kelly Nugent, Department of Natural Resources Sciences, for their kind assistance with sonic anemometry. Finally, thank you to Mr. Michael Bleho, Mr. Guy Rimmer and Mr. Ian Ritchie for providing the facilities to test the prototypes.

Thank you to Mrs. Susan Mahon and the staff of the Bellairs Research Institute in Holetown, Barbados, for support during time in and away from Barbados. A particular thank you to Mrs. Krista Houser and Mrs. Kim McGrath, and the McGill Office of Sustainability (MOOS) for support of the Bellairs Research Institute Greenhouse Project.

This work has also benefited from the help and support provided by many friends and colleagues both at and outside of McGill University. A thank you to James Cumberbatch, Ryan Knight, Dillon Fields, Zainab Iqbal, Emmet Austin, Carmen Raffa, Dominic Silk, Brittany Curry-Sharples, Rachael Warner, Jessica Xavier and Rhys Burnell who assisted me in Barbados with the construction and testing of many NVAC greenhouses. Thank you to Bo-Sen Wu, Lara Hendry, Mahnaz Mansoori and all other colleagues and friends from the Biomass Lab for helping me with different aspects of the project.

Contributions of Authors

In accordance with the McGill Guidelines for a Manuscript Based Thesis, the contributions made by the candidate and the co-authors to the completion of this work are described here.

Chapter 3 was coauthored by the candidate and Mark G. Lefsrud. In Chapter 3, the candidate reviewed the literature and identified challenges during experiments conducted in the field, while building the test greenhouses. The candidate was responsible for compiling the information and writing the manuscript. The coauthor Mark G. Lefsrud served as the Ph.D. advisor and provided critical review of the manuscript. Chapter 4 was coauthored by the candidate and Mark G. Lefsrud. In Chapter 4, the candidate was responsible for the NVAC greenhouse design and construction, experimental design, sensor choice and calibration, data collection, interpretation of data, analysis, and writing of the manuscript. The coauthor Mark G. Lefsrud served as the Ph.D. advisor, was involved in greenhouse and experimental design and provided critical review of the manuscript. Chapter 4 is under review with the journal *HortTechnology*. Chapter 5 was coauthored by the candidate, Valérie Orsat and Mark G. Lefsrud. In Chapter 5, the candidate was responsible for the NVAC greenhouse design and construction, experimental design, sensor choice and calibration, data collection, interpretation of data, analysis, and writing of the manuscript. Valérie Orsat served as the Ph.D. co-advisor and provided critical review of the manuscript. The coauthor Mark G. Lefsrud served as the Ph.D. advisor and provided critical review of the manuscript. Chapter 5 is under review with the journal *Biosystems Engineering*. Chapter 6 was coauthored by the candidate and Mark G. Lefsrud. In Chapter 6, the candidate was responsible for experimental design, sensor choice and calibration, data collection, interpretation of data, analysis, and writing of the manuscript. The coauthor Mark G. Lefsrud served as the Ph.D. advisor and provided critical review of the manuscript. Chapters 7 and 8 were coauthored by the candidate and Mark G. Lefsrud. In Chapters 7 and 8, the candidate was responsible for measurement device choice and development of the apparatus, computing program choice, writing of program script, experimental design, data collection, interpretation of data, analysis, and writing of the manuscripts. The coauthor Mark G. Lefsrud served as the Ph.D. advisor and provided critical review of the manuscripts.

Journal Papers

1. McCartney, L., & Lefsrud, M.G. (2017). Field Trial of The Natural Ventilation Augmented Cooling (NVAC) Greenhouse. HortTechnology, (under revision).
2. McCartney, L., Orsat, V., & Lefsrud, M.G. (2017). An experimental study of the cooling performance and air movement in a Natural Ventilation Augmented Cooling (NVAC) greenhouse by means of direct measurement and tri-sonic anemometry. Biosystems Engineering, (under revision).
3. McCartney, L., & Lefsrud, M.G. (2017). Protected Agriculture in Extreme Environments: A Review of Controlled Environment Agriculture in Tropical, Arid, Polar and Urban Locations. Applied Engineering in Agriculture, (under revision).
4. McCartney, L., & Lefsrud, M.G. (2017). Photosynthesis, fluorescence and transpiration responses in bell pepper plants to high temperature and to the Natural Ventilation Augmented Cooling (NVAC) greenhouse design. HortTechnology, (to be submitted).
5. McCartney, L., & Lefsrud, M.G. (2017). Measurement of diurnal fruit growth patterns in tomato using machine vision. Machine Vision and Applications, (under revision).
6. McCartney, L., & Lefsrud, M.G. (2017). The study of diurnal growth patterns of tomato fruit under arid conditions and conditions of the natural ventilation augmented cooling (NVAC) greenhouse, HortTechnology, (to be submitted).

Abstract

Greenhouses create an optimal growing environment for crops through climate control and protection from harsh weather and pests. This research project assessed the current challenges that exist within the protected agriculture industry and developed a new greenhouse design accordingly. The work focused on a new method of greenhouse cooling, for use in warm climates. A strong emphasis was put on affordability, ease of access to technology, and water and energy efficiency. The result of this research is the Natural Ventilation Augmented Cooling (NVAC) greenhouse. The NVAC greenhouse is naturally ventilated and improved by augmenting the thermal buoyancy and wind effects with a strategically placed misting system. The greenhouse structure is comprised of tall sidewalls, oversized side vents, a roof vent and an additional inside roof. The misting system is located above the gutters of the greenhouse and sprays a mist of water horizontally between the top roof and the added inside roof. The added roof guides the cooled air to the plant space and prevents water droplets from reaching the crop foliage. Test units were built a) at the Macdonald Campus of McGill University in Ste-Anne-de-Bellevue, QC, Canada b) in Trents, Barbados and c) in the controlled environment of a research greenhouse at the Macdonald Campus of McGill University. In its final design under field conditions, the NVAC greenhouse provided temperatures 1.3 to 3.6 °C cooler than outside temperatures, while increasing relative humidity by 5.7 to 17.7%. This is in contrast to inside temperatures being warmer than outside conditions in most natural ventilation greenhouses. The temperature response was rapid, dropping by 3.3 °C within 120 s after activation of the system. Under field use, the NVAC greenhouse used 5.6% of the electricity required to run a pad and fan system in a comparable greenhouse. Under the low wind conditions of the controlled environment research greenhouse, the cooling performance of the NVAC greenhouse design varied from 1.9 to 12.6 °C while the relative humidity increased by 1.4 to 31.2%, depending on the ambient conditions. Accordingly, the NVAC greenhouse was able to reduce the vapor pressure deficit (VPD) by 0.3 to 4.9 kPa. It was shown that the NVAC greenhouse can provide air movement in the plant space of the greenhouse at velocities up to 0.40 $m \cdot s^{-1}$ without the use of fans. The conditions provided by the NVAC greenhouse offered an improved greenhouse climate in terms of plant growth and plant stress by means of cooling and an increase in relative humidity. In contrast to conditions of high temperature, the photosynthetic rate (P_n) in mature and fruiting bell pepper (*Capsicum annumm*, var. Bell Boy) was 28% higher under NVAC

system conditions. Plant fluorescence (F_v/F_m i.e. ratio of variable to maximum chlorophyll fluorescence), an indicator of plant stress, was not depressed and the transpiration rate of the plants was reduced, by an average of 31%, with the use of the NVAC greenhouse. By monitoring diurnal tomato fruit growth, it was found that the NVAC greenhouse moderated the plant water status and prevented fruit shrinkage. By means of the cooling and humidity control of the NVAC greenhouse, the diurnal fruit growth patterns were more uniform in comparison to hot, harsh conditions. Under low wind condition, the NVAC greenhouse is capable of providing an improved climate that is comparable to that provided by pad and fan and fogging systems, and offers advantages over these traditional systems such as prevention of foliage wetting. The NVAC misting system can be used either intermittently or continuously to lower greenhouse temperatures and alter relative humidity conditions year-round or to extend the growing season. Site-specific conditions such as wind gusts and natural variations in daily temperature and relative humidity must be considered as they play a large role in the performance of the NVAC greenhouse.

Résumé

Les serres créent un environnement de croissance optimal pour la culture végétale. Ce projet de recherche a identifié les défis actuels qui existent au sein de l'industrie de la culture en serre et a mis au point un nouveau type de serre. Cette serre fait l'objet d'une nouvelle méthode de refroidissement pour utilisation dans les climats chauds. Un accent a été mis sur la facilité d'accès à la technologie et à l'efficacité énergétique et de l'utilisation de l'eau. Le résultat est la serre à ventilation naturelle avec refroidissement augmenté (VNRA). La serre VNRA est naturellement ventilée et son environnement est amélioré en augmentant les effets du vent et de la flottabilité de l'air sur la masse d'air intérieure avec un système de brumisation à basse pression stratégiquement installé. La structure de la serre est composée de hautes parois latérales, d'ouvertures latérales surdimensionné, d'une ouverture de toit en longueur et d'un toit additionnel placé à l'intérieur. Le système de brumisation est situé au-dessus du niveau des gouttières de la serre et vaporise un brouillard d'eau dans une direction horizontale dans l'espace créé par le toit intérieur et le toit dominant extérieur. Le toit intérieur guide l'air refroidi vers l'espace principale de la serre et empêche les gouttelettes d'eau de la brumisation d'atteindre le feuillage. Des prototypes ont été construits 1) sur le Campus Macdonald de l'Université McGill à Ste-Anne-de-Bellevue, QC, Canada, 2) à Trents, à la Barbade et 3) dans l'environnement contrôlé de la serre de recherche sur le Campus Macdonald. Dans sa conception finale, sous conditions extérieures typiques, la serre VNRA a fourni de 1,3 à 3,6 °C de refroidissement lorsque comparée aux températures extérieures. L'humidité relative a été augmenté par 5,7 à 17,7 %. Les répercussions, en termes d'effet sur la température intérieure, ont été rapides, avec de 3,3 °C de refroidissement dans les 120 secondes suivants l'activation du système VNRA. Le system VNRA n'utilise pas plus de 5,6 % de l'électricité nécessaire pour la fonction d'un système de refroidissement 'pad and fan', dans une serre comparable. Sous des conditions de vents faibles dans un environnement contrôlé, la performance de refroidissement de la serre VNRA a varié de 1,9 à 12,6 ° C alors que l'humidité a augmenté de 1,4 à 31,2 % par rapport au conditions ambiantes sans refroidissement. La serre a également été en mesure de réduire le 'vapor pressure deficit' (VPD) de 0,3 à 4,9 kPa par rapport au conditions ambiantes sans refroidissement. Il a été démontré que la serre NVAC peut fournir un mouvement d'air dans la serre à des vitesses allant jusqu'à 0,40 $m \cdot s^{-1}$, sans l'utilisation de ventilateurs. La serre VNRA offre un climat amélioré en termes de stress apporté à la plante. Contrairement à l'état des plants

sous des conditions de haute température, sous les conditions de la serre VNRA, le taux de photosynthèse (P_n) de plants de poivron (*Capsicum annumm*, var. 'Bell Boy') était 28 % plus élevé, et la fluorescence de la feuille (F_v/F_m i.e. ratio de fluorescence chlorophyllienne) n'a pas été réduit. Le taux de transpiration des plants de poivrons a été réduit de 31%, mais n'a pas été complètement refoulé. Par la mesure des variations de croissance à court terme des fruits sur les plants de tomates, les effets apportés par la serre VNRA sur les fruits a été comparé aux conditions de hautes températures. Le system VNRA offre des avantages tel que la prévention du mouillement du feuillage. Le système VNRA peut être utilisé pour de courtes périodes ou en continu, au besoin, pour abaisser la température intérieure de la serre. Les conditions climatiques particulières du site où la serres VNRA se trouve, tels que les conditions de vent (présence de rafales de vent, par exemple) et les variations naturelles de température et d'humidité relative, doivent être considérées comme elles jouent un rôle important dans la performance de la serre.

Nomenclature and Abbreviations

ACMG	The Haughton Mars Project's Arthur Clarke Mars Greenhouse in the Canadian High Arctic
Af	tropical rainforest in the Köppen climate classification system
A_G	greenhouse floor area
Am	tropical monsoon in the Köppen climate classification system
As	tropical savannah in the Köppen climate classification system
ASABE	American Society of Agricultural and Biological Engineers
ASHRAE	American Society of Heating, Refrigerating and Air-Conditioning Engineers
A_V	ventilator opening area
Aw	tropical wet and dry in the Köppen climate classification system
BER	blossom end rot
BS	steppe or arid climate in the Köppen climate classification system
BW	desert arid climate in the Köppen climate classification system
CELSS	controlled ecological life support system
CING	Canadian Integrated Northern Greenhouse at McGill University
CPPS	closed plant production systems
e	ellipticity
E	actual vapor pressure
EAHES	earth-to-air heat exchanger systems
E_C	water vapor input by the evaporative cooling system
ECD	equivalent circular diameter
EF	icecap climate in the Köppen climate classification system
Eff.	efficiency
E_S	water vapor evaporating from the soil or hydroponic systems
Es	saturation vapor pressure at the dry-bulb temperature
ET	polar tundra climate in the Köppen climate classification system
E_T	water vapor input by plant transpiration
E_V	water vapor that enters or exits the greenhouse via ventilation

EVA	ethylene-vinyl acetate
E_w	saturation vapor pressure at the wet-bulb temperature
FIR	far-infrared radiation
F_o	minimum chlorophyll fluorescence
F_v/F_m	ratio of variable to maximum chlorophyll fluorescence
HIS	hue, saturation, intensity
HPS	high pressure sodium (lighting)
i_u	turbulence intensity of the air (note: unitless)
$i_{u\ avg}$	average turbulence intensity of the air (note: unitless)
LED	light emitting diode
LVDT	linear voltage displacement transducer
n	number of data points
NFT	nutrient film technique
NIR	near infrared radiation
NVAC	Natural Ventilation Augmented Cooling
o.d.	outer diameter
P	barometric pressure
PAR	photosynthetically active radiation
PFAL	plant factories with artificial lighting
P_n	photosynthetic rate
PSII	photosystem II
PVC	polyvinyl chloride
Q_G	heat transfer via convection and conduction
Q_L	latent heat transferred to water
Q_P	heat transfer to and from the plants and other greenhouse components
Q_R	solar radiation heat transfer
Q_S	heat transfer to and from the soil
Quonset	a building made of corrugated metal and having a semicircular cross section
Q_V	heat transfer via air exchange by ventilation
R	ratio between surface areas of the roof vent openings and side vent

	openings
R’	ratio of ventilator opening area to greenhouse floor area
RGB	red-green-blue
RH	relative humidity
RH_i	average inside relative humidity
RH_m	average relative humidity inside the greenhouse with the use of the NVAC misting system
RH_o	average outside relative humidity
rms	root mean square
RSI	Système international d'unités unit for the thermal resistance unit R-value
S_{VR}	surface area of the roof vent openings
S_{VS}	surface area of the side vent openings
T	temperature
T_{db}	dry-bulb temperature
T_i	average inside temperature
T_m	average temperature inside the greenhouse with the use of the NVAC misting system
T_o	average outside temperature
T^s_{air}	corrected temperature measurements obtained from the sonic anemometer
u	air velocity, can have subscripts x, y and z for axis direction
u_{avg}	average air velocity
u_{max}	maximum air velocity
u_{min}	minimum air velocity
V	volt
var.	variety
VNRA	ventilation naturelle avec refroidissement augmentée
VPD	vapor pressure deficit
VPD_c	vapor pressure deficit during cooling of the NVAC misting system
VPD_i	vapor pressure deficit without NVAC misting system
X	photosynthetically active radiation sensors
Z	elevation in meters (m) used for barometric pressure calculation

η	efficiency of a pad and fan evaporative cooling process
η_c	cooling efficiency of the NVAC greenhouse
η_c'	cooling efficiency of the NVAC greenhouse comparable to the methodologies used for pad and fan evaporative cooling systems
σ	variance of air velocity
ΔRH	difference in relative humidity
ΔT	difference in temperature
$\Delta_{i\text{-}o}$	difference between inside and outside conditions without NVAC misting
$\Delta_{m\text{-}o}$	difference between inside and outside conditions with NVAC misting
+	temperature and relative humidity sensors
$\otimes$	wet-bulb and dry-bulb aspirated air sensors
ϕ	angle of air velocity vector

Table of Contents

List of Tables

List of Figures

List of Equations

1. Chapter 1: Thesis Introduction

Chapter 1 provides the background information, brief descriptions of subject matters, and the rationale that has led to the development of this research. The hypothesis and the objectives of this research are stated below, while a description of the organization of this thesis can be found at the end of this chapter.

1.1 Background

Greenhouse crop production is a growing industry worldwide (Jensen & Malter, 1995). The global greenhouse vegetable cultivation area was estimated at 473 466 ha in 2016, a 14% increase from 2015 (Hickman, 2017). Some recent estimates suggest that greenhouse cultivation, of all crops combined, surpasses 5.4 million ha globally (Farrell et al., 2017). Most greenhouses are built in mild climate areas, and more than 90% of these are plastic film greenhouses (von Zabeltitz, 2011; Giacomelli, 2008). Greenhouse plant production has become widespread because protected agriculture, in its various forms, has become important for local populations around the world as a source of fresh food and income (von Zabeltitz & Baudoin, 2005). Greenhouses increase crop yield and quality, and therefore have the potential to address the growing concerns of food security due to climate change and urbanization (Lawrence et al., 2014; Despommier, 2011; Jensen & Malter 1995).

Various methods of ventilation, heating and cooling are used to control the climate found within a greenhouse. However, greenhouse cooling can be complex and far more difficult than heating. Unlike heating, for which the technology is well developed, greenhouse cooling frequently presents complex problems as it depends heavily on local environmental conditions, ease of operation and maintenance, and economic viability (Kumar et al., 2009; Sethi & Sharma, 2007). Current cooling technologies demand large investments and involve high-energy consumption (Kittas et al., 2005). Cooling is typically accomplished first by ventilation, either mechanically, via exhaust fans, or naturally via wind and thermal buoyancy (Teitel et al., 2004; Willits, 2003). Natural ventilation is the preferred greenhouse climate control system as it is simple and cheap. Therefore, the study of the greenhouse climate under natural ventilation has been the object of many studies (Teitel & Tanny, 1999; Boulard et al., 1996; Willits & Li, 2005; Kittas et al., 1997). In most cases however, the outcome is informative but not generally applicable (Bakker et al., 1995; Mutwiwa et al., 2007).

When ventilation alone is not sufficient to cool greenhouses, evaporative cooling is used. Evaporative cooling systems are used in many industries, and can be found in agricultural applications, primarily in poultry barns (Bottcher et al., 1991) and greenhouses (Sethi & Sharma, 2007; Fuchs et al., 2006; Giacomelli, 2003). The most widespread solutions for greenhouse cooling are pad and fan systems and high-pressure fog systems (Al-Ismaili & Jayasuriya, 2016; Jensen, 2001; Montero, 2006; Arbel et al., 2003). Both systems rely on evaporative cooling, which is considered the most effective cooling method for controlling the temperature and relative humidity inside a greenhouse (Kumar et al., 2009). Considerable research has been devoted to the experimental study of greenhouse environments under both pad and fan systems (Kittas et al., 2001; Kittas et al., 2003; López et al., 2010; López et al., 2010) and fog systems (Arbel et al., 1999; Arbel et al., 2003, Hayashi et al., 2007; Hayashi et al., 2005).

The Mediterranean coastal area is home to the largest concentrations of greenhouses in the world, with approximately 20% of the worldwide greenhouse area (Castilla & Hernández 2005; Franco et al., 2011), consisting for the most part of natural ventilation greenhouses (Baille, 2001). It is estimated that there are over 27 000 ha of greenhouse cultivation in the region of Almería, Spain alone (Molina-Aiz et al., 2011), which continues to expand with an average net growth rate of 500 $ha \cdot yr^{-1}$ (Sanjuan, 2007). In recent years, the Almería-type greenhouse has seen a massive expansion in use in other warm climate areas such as Mexico, Colombia, Morocco and China (Molina-Aiz et al., 2011). This established greenhouse industry, that once did not demand cooling strategies, is now seeking alternative cooling solutions. Previous trends for crop growth management in subtropical Mediterranean greenhouses were to adapt the plants to suboptimal environments, instead of adapting the greenhouse design and climate control measures for a maximum of plant yield, quality, and health (Montero, 2009; Castilla et al. 2008; Castilla, 2002). The advantage of applying cooling technologies to this greenhouse industry is the additional security and stability of the production (Castilla & Montero, 2008). Moreover, with rising market competition for high quality produce, greater yield demand, and higher temperatures occurring in the greenhouses, due to limited airflow from the growing use of improved insect netting (Castilla & Montero, 2008), growers are seeking new cooling solutions to improve greenhouse conditions (a first-hand account of this is presented in Appendix A). Financial constraints are limiting the widespread use of pad and fan systems and high-pressure fog systems with forced ventilation. Current advances in Mediterranean greenhouse technology have tended towards improving natural ventilation systems (Garcia et al., 2011) and incorporating new cooling techniques.

Furthermore, there is an emerging and expanding greenhouse industry in regions of the world relatively new to greenhouse technology. Due to food security concerns related to growing populations (Lawrence et al., 2014; von Zabeltitz, 2011), rapidly declining soil quality (Mendelsohn & Dinar, 1999; Battisti & Naylor, 2009), harsher climates (Lawrence et al., 2014; Stocking, 2003), and increasing awareness of declining freshwater availability (Al-Ismaili & Jayasuriya, 2016), greenhouses are a growing trend in regions of the Middle East (Farrell et al., 2017), Africa (Thipe et al., 2017), the Caribbean (Lawrence et al., 2014) and Southeast Asia (von Zabeltitz, 2011). These regions share an important characteristic: year-round or seasonal high temperatures that limit the use of natural ventilation greenhouses. Moreover, there are constraints impacting the use of typical greenhouse cooling strategies in these developing regions. These issues are largely rooted in the design of the structures being used which cause them to be outright ineffective in warm climates, fail prematurely or to be too costly to operate (Sachs, 2001; Lawrence et al., 2014; Lawrence et al., 2011). Although evaporative cooling solutions, such as pad and fan systems, are successful in certain regions of the world, the optimization of greenhouse ventilation and cooling with respect to local climatic and economic conditions remains a challenge for many other regions (von Elsner, 2000, Sethi & Sharma, 2007). The inaccessibility to technology, rising cost of energy and the unreliability of certain power grids renders cooling systems that rely on forced ventilation unfeasible for many growers by constraining profits (Sachs, 2001). In addition, water scarcity in many regions of the world limit the use of many greenhouse evaporative cooling techniques even if the systems are financially possible (Abdel-Ghany et al. 2012). According to the World Bank, research in greenhouse technologies should concentrate on the design and engineering of lowest-cost controlled environment agriculture systems to be ventilated, cooled or heated as much as possible by natural phenomena and alternative energy sources (Jensen & Malter, 1995).

In this research, a new evaporative cooling technique was developed to be used with naturally ventilated greenhouses. The design is called a Natural Ventilation Augmented Cooling (NVAC) greenhouse. The design of the greenhouse structure is based on well-known design parameters for natural ventilation in high temperature environments. The use of enlarged side and roof vents is essential to enhance natural airflow and profit from wind driven ventilation, whereas greater greenhouse heights are used to maximize greenhouse volume (von Zabeltitz, 2011; von Zabeltitz & Baudoin, 2003). To improve the natural ventilation process, the NVAC greenhouse makes use of an evaporative cooling misting system in a simple, energy efficient and water efficient way. The use of fog evaporative cooling in combination with natural ventilation is a well-established way to control greenhouse temperature and relative humidity (Hayashi & Kozai, 2005; Hayashi et al., 2007; Toida et al., 2006). However, the high operational and procurement costs of high-pressure fog systems can limit their use (Montero, 2006). The proliferation of diseases through wetting of the plant foliage is a possible drawback that limits the use of fog systems (Toida et al, 2006; Kittas et al., 2003). To counter high costs, the NVAC greenhouse makes use of a relatively low-pressure, low-cost and simple misting system. Moreover, the NVAC greenhouse design includes an added roof placed inside the greenhouse to capture unevaporated water droplets from the misting system, recover the water for further use, and guide the cooled air into the greenhouse space. This novel greenhouse design is the first of its kind in providing cooling and additional air movement at the plant level without the use of fans, by relying solely on the evaporative cooling process. The design is protected under three patents: Canadian patent CA 2838296, American patent US 20150173308 A1, and Australian patent 2013273819.

In this dissertation, we have demonstrated the performance and efficiency of the NVAC greenhouse design in terms of temperature, relative humidity, vapor pressure deficit (VPD), and air movement control, by means of a series of experimental methods. The design required development through build-iterations under field conditions to ensure adequate performance outside of the laboratory. With a functional design established, a test unit in a controlled environment space was used to demonstrate the ideal performance of the NVAC greenhouse in a variety of climates. This test unit served as a model to investigate the air movement capabilities of the NVAC greenhouse design, independent from external influences such as wind. Lastly, a series of non-invasive methodologies were established and used to measure the plant responses to the greenhouse climate provided by the NVAC greenhouse. It was demonstrated that the NVAC greenhouse provided an improved plant growing environment through greenhouse cooling and improved air movement. Throughout the study, we highlighted the importance of energy and water efficiency in greenhouse systems, and the need for sustainable and locally available greenhouse technologies. The NVAC greenhouse was designed to be affordable and locally available worldwide with energy and water efficiency in mind.

1.2 Statement of Research Objectives

All current greenhouse cooling methods increase production costs (Samaniaego-Cruz et al., 2002). There is therefore a need to develop efficient greenhouse cooling techniques, adapted to both existing and emerging protected agriculture markets. Preliminary tests indicated that the NVAC greenhouse design can provide cooling and air movement to the greenhouse crop. It is therefore of interest to evaluate the potential of the NVAC greenhouse design in providing an improved greenhouse environment in warm climates. It was hypothesized that different performances in terms of cooling and air movement will result from the use of the NVAC greenhouse design in varying climates. Moreover, the cooling that occurred using the NVAC greenhouse design would result in an increase in humidity in the greenhouse air. Through the measurement and analysis of the environmental parameters of the greenhouse, the driving forces of the NVAC system could be identified and explained. The plant response to the NVAC greenhouse design would be a valuable tool used to explain how the improved greenhouse climate could lead to better crop production. It was hypothesized that the NVAC greenhouse would provide an improved environment in terms of plant growth and quality of production.

The objectives of this research are therefore as follows:

- Objective 1:
  Design and build functional NVAC greenhouse test units in warm climates using affordable and locally available materials.
  - Through preliminary design tests, develop an NVAC greenhouse unit capable of being subjected to field tests.
  - Develop an effective misting system design to be used in the NVAC greenhouse.
  - Measure and analyze environmental parameters, consisting of air temperature, relative humidity, vapor pressure deficit (VPD) and solar radiation, inside and outside of the NVAC greenhouse test units.

- Determine if the NVAC greenhouse can provide significant air temperature, relative humidity, VPD and solar radiation differences under field conditions compared to that measured under usual natural ventilation conditions and outside conditions.
- Bring improvements to the NVAC greenhouse design based on the results from the analysis of the environmental parameters.

- Objective 2:
  Design and build an NVAC greenhouse test unit in a controlled research environment capable of reproducing a range of climatic conditions.
  - Measure and analyze environmental parameters (air temperature, relative humidity, VPD, solar radiation and air movement) inside and outside of the NVAC greenhouse test units.
  - Determine if the changes in greenhouse climate brought about by the NVAC system vary amongst different climates and how different climatic conditions affect the performance of the system.
  - Determine the performance of the NVAC greenhouse design, in terms of cooling potential and water usage.
  - Through removal of the wind effect, determine the uniformity of the conditions inside the greenhouse that are brought about by the NVAC system.
  - Through removal of the wind effect, describe the air movement inside the greenhouse that is brought about by the NVAC system.
- Objective 3:
  Determine the plant responses to the NVAC greenhouse design and if the NVAC greenhouse can provide an improved growing environment.
  - Use plant gas exchange and chlorophyll fluorescence to measure plant responses to the NVAC greenhouse design in comparison to stress conditions.
  - Develop an experimental design to measure plant transpiration under NVAC greenhouse conditions and under high temperature conditions.
  - Develop an experimental design to measure diurnal growth in plant fruit under NVAC greenhouse conditions and under high temperature conditions.

- Carry out a series of plant response experiments under NVAC greenhouse conditions and high temperature conditions and analyze the findings to determine if the NVAC greenhouse design can provide an improved growing environment.

- Objective 4:

  Evaluate the NVAC greenhouse design's applicability in the greenhouse industry.
  - Review the situation of protected agriculture in extreme climates including high temperature climates, with a focus on greenhouse technology.
  - Identify current issues in the protected agriculture industry, with a focus on greenhouse technology.
  - Present current solutions and future trends in the protected agriculture industry.

1.3 Choice of Methodology

The nature of this research project remained the development of the NVAC greenhouse design and the advancement in understanding of the driving forces behind its performance and its effect on plant growth and crop production. Given the novelty and uniqueness of the design, necessity to test crop response and the availability of the proposed physical test sites, including a controlled environment test site, simulation in the proposed research project was accomplished with physical models. Other techniques have been used to measure, improve and predict the internal greenhouse environment such as tracer gas techniques, experiments with measurements on physical model test units and simulation and modelling using computational fluid dynamics. Tracer gas techniques do not allow determination of real and specific air movement but may help characterize effective flow and leakage through openings of a greenhouse and air exchange (Boulard et al., 1997). The tracer gas technique therefore does not seem appropriate for use in this research project. Climate simulation and modelling by Kozai et al., 1980, Chalabi and Bailey, 1989, Fernandez and Bailey, 1993, Bot, 1983, De Jong, 1990, Fernandez and Bailey, 1992, Boulard and Draoui, 1995, Kittas et al., 1995 and Papadakis et al., 1996 were reviewed. As compared with physical experiments, computer simulation methods may be performed quicker in less expensive, more flexible and repeatable ways (Wang and Boulard, 2000). However, the complexity of greenhouse simulation and modelling is countered through simplification of the design of key greenhouse elements, and through emphasis on single specific elements of interest, such as vent size.

1.4 Organization of Thesis

This dissertation consists of eight chapters, the references and appendices. Chapter 1, the introduction, provides research background, rationale, the hypothesis and objectives. Chapter 2, the literature review, provides brief discussion on the subject matters involved in this research. Chapters 3 provides further insight into and detailed explanations relating to the commercial and research controlled environments industries. Chapters 4, 5, 6, 7 and 8 each present the research and experiments conducted to reach the stated objectives. Between Chapters 3, 4, 5, 6, 7 and 8, connecting texts provide the transition and rationale between each experiment. Chapter 9 provides a summary of each experiment, describes the significant contributions to knowledge that this research has brought, and presents suggested further studies on the research topic. The references and appendices follow. Appendix A provides an up-to-date (October 2017) description of the public and industry interest in the NVAC greenhouse. Appendix B and C provide a detailed account of functional NVAC greenhouses built by the candidate in Trents, and Holetown, Barbados. Appendix D provides the MATLAB scripts used to capture and process the images for Chapters 7 and 8. Appendix E and F provide license documentation for the use of copywritten images. International System of Units (SI) units are used throughout but imperial units were preferred for certain descriptions and measurements in which case SI units follow in parentheses.

2. Chapter 2: Literature Review

2.1 Energy and Water Vapor Balances of a Greenhouse

2.1.1 Energy Balance

The energy transfer into and out of a greenhouse impacts the internal environment and determines what systems, such as cooling or heating systems, are needed for environmental control. Energy balance models of varying complexity have been proposed to predict the performances of many greenhouse designs under a variety of conditions and for a range of crops (Bot, 1983; Critten & Bailey, 2002; Singh et al., 2006). A simplified equation can summarize the energy relations of a greenhouse in warm climates using the greenhouse air as the control volume, the greenhouse cladding, the ground, components within the greenhouse, and the vents as the control surfaces. Therefore, the energy transferred across these surfaces involves both sensible and latent heat exchanges (Boulard & Wang, 2000). The energy balance equation is therefore represented by the following equation (Sabeh, 2007):

$$Q_R + Q_G + Q_V + Q_S + Q_P + Q_L = 0 \qquad \text{Equation 1}$$

As illustrated in Figure 1, Q_R is the heat transfer by solar radiation. Q_G is the heat transfer across the cladding, and depends on the temperature difference between the outside and inside air to transfer energy both by conduction and convection. Q_V is the heat transfer by ventilation, which removes energy from the greenhouse. Q_S is the heat transfer between the ground and greenhouse air and depends on their temperature difference. Q_P is the heat transfer by the various greenhouse components, including structural components, irrigation systems, and evapotranspiration of plants, which transfer latent heat energy to the greenhouse air. Q_L is the latent heat transfer of sensible energy in the air to water from evaporative cooling systems, if cooling is used.

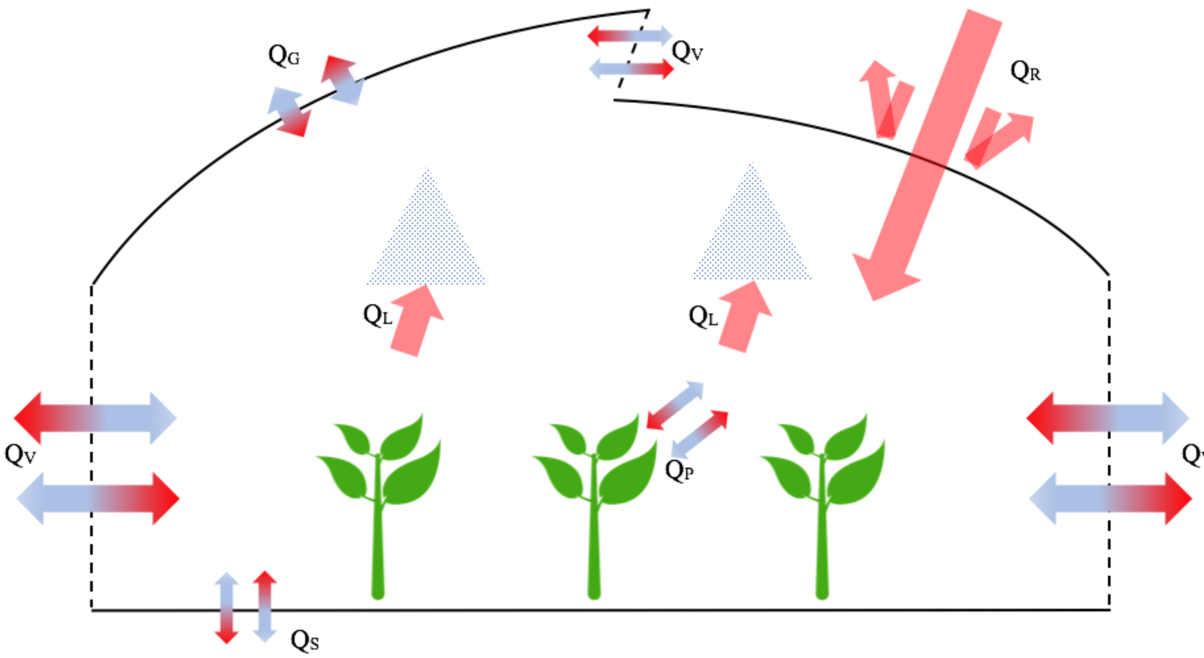

Figure 1. Heat transfer in a warm climate greenhouse. Q_R is solar radiation, Q_G is convection and conduction across the greenhouse cladding material, Q_V is the heat transfer via air exchange by ventilation, Q_S is the heat transfer to and from the soil, Q_P is the heat transfer to and from the plants and other greenhouse components such as irrigation systems, and Q_L is the latent heat transferred to water in evaporative cooling systems, in this case a fog or mist system.

2.1.2 Water Vapor Balance

The amount of water vapor in the greenhouse is determined by the transfer of water vapor into and out of the greenhouse. Using the greenhouse air as the control volume, the simplified control surfaces include the cladding, ground, plants, and vents. Therefore, water vapor transferred across these surfaces will comprise the water balance equation, which is represented in the following equation (Sabeh, 2007):

$$E_V + E_C + E_S + E_T = 0 \qquad \text{Equation 2}$$

As illustrated in Figure 2, E_V is the water vapor that enters or exits the greenhouse via ventilation, E_C is the water vapor input by the evaporative cooling systems, if cooling is used, E_S is the water vapor evaporating from the soil or hydroponic systems, and E_T is the water vapor input by plant transpiration.

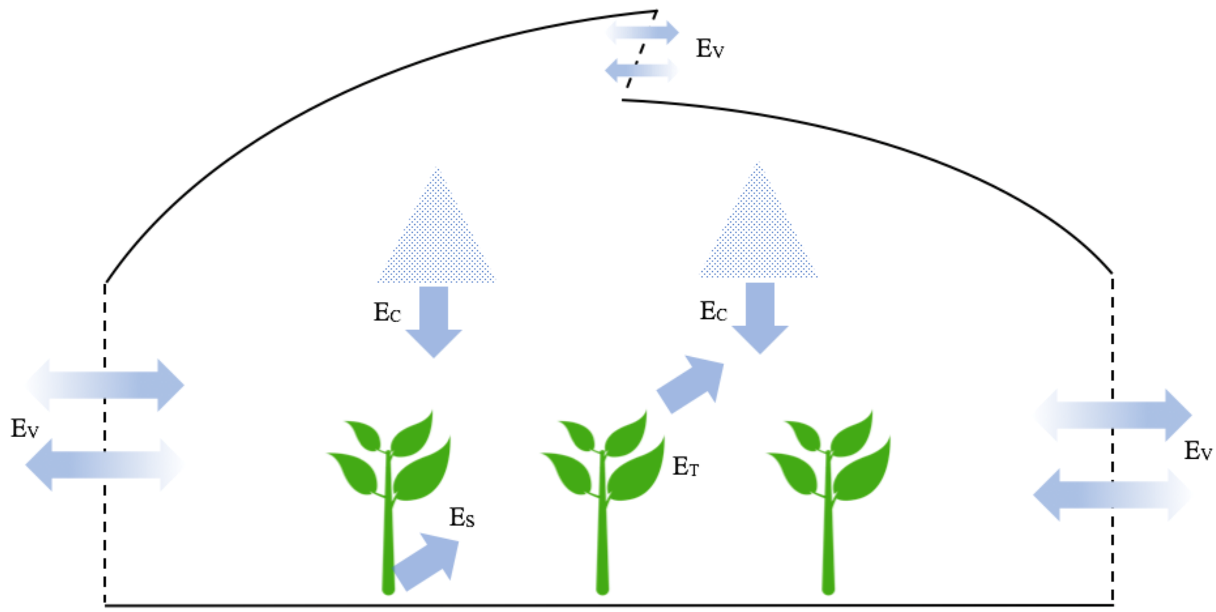

Figure 2. Water vapor transfer in a warm climate greenhouse. E_V is the water vapor lost or gained via air exchange by ventilation, E_C is the water vapor gained through evaporative cooling, in this case a fog or mist system, E_S is the water vapor gained from the irrigation or hydroponic system, and E_T is the water vapor gained via plant transpiration.

2.2 Greenhouse Cooling and Ventilation

The greenhouse ventilation process is the driving force for airflow, climate and crop transpiration heterogeneity in greenhouses (Bot, 1983; De Jong, 1990; Fernandez & Bailey, 1992; Boulard & Draoui, 1995; Boulard et al., 1996). Greenhouse cooling is required when the heat entering the greenhouse is greater than the heat transfer to the outside components. Ventilation is the first step taken to lower greenhouse temperatures. However, when ventilation is not sufficient or when temperatures lower than outside temperatures are required, evaporative cooling systems are used. These systems are based on the conversion of sensible heat into latent heat in mechanically supplied evaporated water (Arbel et al., 1999).

2.2.1 Natural Ventilation

Natural ventilation is widely used in greenhouses around the world. It requires little to no energy input and additional equipment, and is therefore the cheapest method of cooling a greenhouse (Willits & Li, 2005). The main driving forces of natural ventilation are caused by a combination of pressure differences induced by multiple effects (Boulard & Baille, 1995; Kittas et al., 1997; Baptista et al., 1999). The buoyancy effect (chimney effect) induces pressure differences between the side and the roof openings (Bruce, 1978; Bruce, 1982). The wind effect induces pressure differences around the greenhouse, mainly between the windward and the leeward parts of the greenhouse (Boulard et al., 1996; Kittas et al., 1997). The turbulent effect of the wind, seen across the greenhouse openings and into the plant space, affects the air movement of ventilation (Boulard et al., 1996). These effects generate a vertical ventilation flux due to the chimney effect and a horizontal ventilation flux due to the wind effects (Kittas et al., 1997).

In the absence of any of these influences, such as in low wind conditions, these fluxes may be altered, minimized or eliminated entirely. Winds stronger than 1.8 to 2.0 $m \cdot s^{-1}$ can dominate the ventilation process and under wind conditions, buoyancy can be neglected (Bot, 1983; Papadakis et al., 1996). Buoyancy driven ventilation is more important if the wind velocity is lower than 0.5 $m \cdot s^{-1}$. In the intermediate cases where wind velocity is between 0.5 and 2 $m \cdot s^{-1}$, the ventilation is driven mostly by the wind effect and some influence of the buoyancy is observed (Kacira et al., 2004). The necessity of installing insect netting in order to prevent proliferation of diseases and pests induces a pressure loss, thereby reducing the ventilation efficiency by up to 50% (Miguel et al., 1997; Kittas et al., 2002; Bailey et al., 2003).

Because natural ventilation depends on outside conditions, air exchange rates and direction, it can be unpredictable (Sabeh, 2007). Moreover, no cooling beyond that of ambient conditions is possible in solely natural ventilation designs (Giacomelli et al., 1985).

2.2.2 Shading

Greenhouse shading using screens or whitening is aimed at reducing the quantity and modifying the quality of radiation transmitted into a greenhouse, mainly focusing on the reduction of infrared radiation entry (Baille et al., 2001). For example, during summer months in the Spanish Mediterranean greenhouse region, growers whiten the roofs by whitewashing with calcium hydroxide, commonly called slaked lime, to reduce incident radiation and avoid excess heating and humidity of growing crops inside. At the end of the warm season, this slaked lime layer is removed to allow enough solar radiation inside for winter and spring crops (Campra et al., 2008). The removal process is sometimes viewed as a drawback of this system. The main drawback however is that the whitening agent is permanent throughout the day and is not selective with regards to the photosynthetic active radiation and near infrared radiation (Garcia et al., 2011).

Shading material comprised of aluminized high-density polyethylene strips woven with plastic threads is commonly used and effective at reducing greenhouse temperatures (Kittas et al., 1999). These systems can be permanent or mobile in the greenhouse, offering adaptive and changing levels of solar radiation (Garcia et al., 2011). However, when these systems are installed inside the greenhouse the most noticeable disadvantage observed is the obstruction of airflow (Lorenzo et al., 2005).

Some solutions include the development of plastic films with filtering properties (Verlodt & Verschaeren, 1997; Hemming et al., 2006) and the development of shading paints (von Elsner & Xie, 2003). Evaporative cooling coupled with active ventilation and shading can reduce greenhouse air temperature by up to 8°C, though some reports show cooling up to 12 °C is possible in hot arid regions (Kittas et al., 2003; Arbel et al., 1999; Al-Jamal, 1994; Landsberg et al., 1979). However, shading reduces the amount of photosynthetically active radiation (PAR) reaching the plants and can therefore only be used under high solar radiation conditions. Similar to natural ventilation, temperatures lower than outside conditions are not possible with the use of shading as a means of cooling.

2.2.3 Fan Systems

The effects of solar radiation on greenhouse air temperature are reduced by increasing the ventilation rate (Critten & Bailey, 2002). Systems comprised of exhaust fans and circulating fans can supply immediate air movement and high air exchange rates whenever needed. These systems are limited as they allow maintenance of the inside temperature to a level slightly higher than the outside temperature (Sethi & Sharma, 2007). Although financially viable in certain regions, the use of fans for greenhouse ventilation is not feasible in many areas as initial equipment costs and energy costs are too high (von Zabeltitz & Baudoin, 2005). This is true in regions such as the Caribbean, and many other developing island states. Increasing the ventilation rate has a diminishing return when it comes to lowering the greenhouse air temperature (Sabeh, 2007), and little advantage has been shown to using ventilation rates greater than 0.035 $m^3 \cdot m^{-2} \cdot s^{-1}$ (Critten & Bailey, 2002) and 0.05 $m^3 \cdot m^{-2} \cdot s^{-1}$ (Willits, 2003). Greenhouse ventilation must be limited in warmer regions such as arid and semi-arid climates, as they can be unfavourable by stressing the crop through increased transpiration (Kittas et al., 2003).

2.2.4 Evaporative Cooling Systems

Evaporative cooling is the most effective cooling method for controlling the temperature and humidity inside a greenhouse (Kumar et al., 2009). It is done by spraying water droplets in a naturally ventilated building, or by forcing ambient air through wet pads. The change from liquid to vapor requires energy, which is extracted from the greenhouse air, cooling it and increasing its humidity (Franco et al., 2010). This brings about a change from sensitive heat to latent heat which implies a drop in temperature and an increase in water content of the air (Sethi & Sharma, 2007; Franco et al., 2010). In thermodynamics, this is known as the adiabatic process, and the enthalpy of the system remains nearly constant (ASHRAE, 1985). Such a change in greenhouse conditions decreases the vapor pressure deficit (VPD) of the greenhouse air and moderates the crop transpiration (Katsoulas et al., 2001).

The efficiency of evaporative cooling systems is impacted by conditions of high ambient humidity (Franco et al., 2010). The relative humidity in greenhouses can vary considerably throughout the day and evaporative cooling systems can become effective during the midday period, when the ambient temperature is highest and relative humidity is lowest. A study by Dagtekin et al. (2009) on evaporative cooling systems in the Mediterranean region found that these systems are effective when the relative humidity drops below 50%.

2.2.4.1 Pad and Fan Systems

The pad and fan technique utilizes a fan system to draw air through a curtain of wetted pads, often made from corrugated cellulose. Pad materials can vary from cellulose to aspen fiber (ASABE, 2006), experimental date-fronds leaves (Al-Massoum, 1998) and PVC sponges (Liao & Chiu, 2002). It is the preferred cooling solution in many commercial and research greenhouses (Kittas et al., 2003). Installation, operation and maintenance are expensive and continuous operation and poor water quality cause progressive clogging of the pads, resulting in declining cooling performance (Arbel, 1999; von Zabeltitz, 2011). Furthermore, pad and fan systems require large amounts of water, which can be a rare commodity in some regions of the world, such as in arid climates and some tropical climates (von Zabeltitz, 2011). The inaccessibility to technology, rising cost of energy and the unreliability of certain power grids renders cooling systems that rely on forced ventilation unfeasible in many regions (Sachs, 2001).

2.2.4.1.i Pad and Fan System Performance

Under proper use, these systems can lower the greenhouse air temperature by 4 to 6 °C if used alone, and by 4 to 12 °C if used with shading (Koazai & Sase, 1976; Landsberg et al., 1979; Jain & Tiwari, 2002; Kittas et al., 2003; Sethi & Sharma, 2007). The main disadvantage of cooling pad systems is the creation of large temperature gradients inside the greenhouse, pads are placed on one side of the greenhouse and extracting fans are placed on the opposite side (López et al., 2010). Kittas et al. (2003) reported temperature gradients up to 8 °C when comparing the temperature at the cooling pads to the temperature at the fans.

2.2.4.1.ii Pad and Fan System Water Usage

The water consumption of cooling pads increases linearly with the ventilation rate (Sabeh et al., 2007). Al-Helal (2007) reported that the average consumption of cooling water varied from 0.65 to 1.08 $L \cdot h^{-1} \cdot m^{-2}$. Sabeh (2007) suggests consumption values range from 0.36 to 1.1 $L \cdot h^{-1} \cdot m^{-2}$ of greenhouse for 150 mm cellulose pads in semi-arid conditions. In conditions of extreme aridity, the values can range from 0.61 to 1.3 $L \cdot h^{-1} \cdot m^{-2}$ of greenhouse area for 100-mm corrugated cellulose pads (Al-Helal, 2007).

2.2.4.2 Mist and Fog Systems

Both high and low-pressure misting are used in greenhouses to maintain high humidity, prevent excessive water loss from leaf surfaces and cool the greenhouse air (Jackson & Darby, 2010). Fog systems require clean water, free of any soluble salts, to prevent clogging of the nozzles (Zhang & Shipp, 2002). Jensen and Malter (1995) stated that as misting becomes more cost competitive, it will become more frequent. To separate high pressure misting from low pressure misting systems, high pressure misting is often referred to as fogging systems.

2.2.4.2.i Mist Systems

Mist systems may be located at bench top level for direct water application to the plant, or it may be located overhead to provide increased humidity and some cooling throughout the greenhouse. As the droplets evaporate, air temperature is reduced. This solution is highly effective in hot and dry climates to humidify the greenhouse and provide cooling. However, this method alone, without consideration of structural design and local climate often involves excess humidity in stagnant air.

2.2.4.2.ii Fog Systems

Fog systems rely on a low volume, high pressure water line and provide tiny water droplets which can evaporate faster than the larger droplets from the mist. High quality and expensive water and filtration systems are important to reduce the problem of nozzles clogging, even more so than in traditional misting systems. Arbel et al. (1999) found that fog systems provided more uniform temperature and humidity conditions than a fan and pad system under similar environmental conditions.

Fog systems have been used in natural ventilation greenhouses (Hayashi & Kozai, 2005), but must be used intermittently to avoid wetting of the plants. A combination of forced ventilation and fog systems for greenhouse cooling can be used to provide more effective cooling, as presented by Arbel et al. (2003). As with pad and fan cooling systems, high pressure fog systems have up-front, operation and maintenance costs (Montero, 2006), and therefore are not financially accessible to all greenhouse growers.

2.2.4.2.iii Mist and Fog System Performance

Montero et al. (1994) used an air water fogging system to cool the greenhouse with shade screen of 45% perforations. It was reported that the maximum temperature reduction during sunny days was 5 °C. The cooling performance of a fog system by Arbel et al. (2003) based on a greenhouse in the arid climate of Israel varied from 8.5 to 12 °C.

2.2.4.2.iv Mist and Fog Systems Water Usage

The water in a mist systems is supplied at a relatively low pressure of 40 psi (280 kPa) at a flow rate of roughly 0.25 $L \cdot min^{-1}$. The nozzle spacing occupies approximately 3.3 m^2 of greenhouse area per nozzle. Timing of the misting periods, frequency, and duration must be controlled to prevent excessive wetting and subsequent over-watering of the crop below.

Fog systems operate at higher pressures than mist systems, ranging from 1015 psi to 2030 psi (7000 to 14 000 kPa) and with very low volume nozzles of roughly 4.5 $L \cdot h^{-1}$

(Giacomelli, 2003). Current greenhouse misting systems typically use high pressure (4000 to 7000 kPa) water lines with compressed air (Berlinger et al., 1999; Zhang & Shipp, 2002).

2.2.5 Other Cooling Systems

Roof evaporative cooling consists of sprinkling water onto a surface of the greenhouse roof so as to form a thin layer. The air temperature inside the greenhouse is reduced from the heat required to evaporate the thin layer of water. In a variety of experiments, greenhouse cooling using this system ranged from 3 to 6 °C (Giacomelli et al., 1985; Giacomelli & Roberts, 1989; Mannan & Cheema, 1981; Sutar & Tiwari, 1995).

Earth-to-air heat exchanger systems (EAHES) circulate greenhouse air through buried pipes (2 to 4 m below grade) for dissipation of heat to the underground soil. Experimental and model studies by Santamouris et al., (1995) and Ghosal et al. (2004) have tested the design and have suggested that it can lower greenhouse temperatures by 3 to 4 °C. However, literature shows limited studies exclusively related to exploring the cooling potential of EAHES for agricultural greenhouses (Sethi and Sharma, 2007).

The seawater greenhouse (Davies & Paton, 2005) successfully uses seawater in place of freshwater in a greenhouse providing both cooling and desalination. Cooling of over 10 °C was possible in the hot and arid climates in which the design is intended for. A 200-m by 50-m seawater greenhouse yielded 125 $m^3 \cdot d^{-1}$ of fresh water in its cooling and condensing processes. Some systems combine desiccation with evaporative cooling, but remain energy intensive. For example, Jain et al. (1994) compared systems that use liquid desiccants focusing on large-scale systems in hot and humid climates, such as greenhouses. These liquid desiccant air conditioners remove both moisture and latent heat from process air via a liquid desiccant material, such as lithium chloride (LiCl) (Dieckmann et al., 2008). Other salt solutions and triethylene glycol can also be used in these systems (Oberg & Goswami, 1998).

The Watergy greenhouse is a concept developed by Buchholz et al. (2006). It is a closed greenhouse with a passive cooling and dehumidification strategy, allowing for a reduction of water consumption by 75% and continuous plant production even during hot summer conditions in Southern Spain. The greenhouse temperature during daytime ranged from 20 to 35 °C. The innovative element in the Watergy design is a cooling tower in the center of the greenhouse. During the daytime, hot air rises from the vegetation area, through the roof area into the tower

(Buchholz et al., 2005). To increase the energy and water content of the rising air, it is further humidified in the roof area by sprinklers on an inner roof. Although this may resemble some of the concepts of the NVAC greenhouse design, some stark dissimilarities remain. First, the closed aspect of the Watergy system does not relate to the natural ventilation basis of the NVAC system. There is also the water tower, water condensation, heat exchange and energy storage aspects of the Watergy system that are not present in the NVAC greenhouse design.

Hemming et al. (2004) worked on a greenhouse design for the tropical lowlands of Indonesia. The design incorporated existing technologies to provide resistance against local wind loads using natural ventilation and insect netting for pests control. Polyethylene film of a thickness of 8 mil (~200 µm), with a lifetime of about 3 years in Indonesia was developed. The film contains an ultraviolet-blocking pigments and has highly light diffusing properties. Other film prototypes were developed that selectively reflect near infrared radiation (NIR) to reduce greenhouse temperatures.

2.3 Greenhouse Climate

2.3.1 Greenhouse Temperature

Air temperature is a major component of the greenhouse microclimate (Mutwiwa et al., 2008). Regardless of climate, greenhouse air temperatures are generally higher in the daytime and lower at nighttime. Variations in temperature are the result of complex and interactive heat and mass exchanges between the inside air and the several elements of the greenhouse. Some key elements include the structure and vegetation, and the outside boundaries such as outside air, weather conditions and solar radiation (Frausto & Pieters, 2004).

High temperatures can affect greenhouse crop growth during the warmest months of the year in regions with temperate, subtropical and semi-arid climates. In Mediterranean countries where vast amounts of produce are grown in greenhouses, high temperatures and VPDs over 35 °C and 3 kPa, respectively, are commonly observed in greenhouses during summer (Katsoulas et al., 2001). Not surprisingly, high greenhouse temperatures are also a problem in hot arid climates and tropical climates, sometimes year-round. In many regions of the Middle East and Northern Africa, the average summer daytime temperatures inside ventilated greenhouses can reach 46 °C without the use of evaporative cooling strategies, with the average outside temperature commonly over 38 °C (Al-Ismaili & Jayasuriya, 2016; Mattara et al., 2015; Al-Helal

& Alhamdan, 2009; Ali et al., 1990). In Al-Jamal (1994) the maximum temperature in an unvented greenhouse in south-east Jordan, was measured at 75 °C when the outside ambient temperature was about 37 °C. Tropical climates can have very distinct seasons, offering a variety of conditions ranging from mild to hot, and humid to very dry. Tropical rainforest (e.g. Innisfail, Australia or Singapore) and tropical monsoon (e.g. Miami, United States or Chittagong, Bangaldesh) climates offer yearround humid and rainy conditions, with very short to inexistent dry periods. Tropical wet and dry (or savanna) climate (e.g. Lagos, Nigeria or Barbados) can offer extended dry periods lasting months, with certain months of the year being more humid and rainy (Kottek et al., 2006). Inevitably, without ventilation or cooling systems, greenhouse temperatures in such climates exceed outside conditions. Some recommendations suggest that if the mean maximum outside temperature is greater than 27 °C, roof ventilation is necessary in a hot and humid climate. Evaporative cooling may be recommendable if conditions permit. If the mean maximum outside temperature is greater than 36 °C, evaporative cooling is necessary (von Zabeltitz, 2011).

Yield potential in many common vegetable crops reduces at temperatures above 26 °C, with fruit set being one of the first processes that is negatively influenced by daytime temperatures greater than 32 °C and nighttime temperatures greater than 26 °C, even with specialized cultivars (Heuvelink, 2008; Sato et al, 2006). Generally, plants grown under protected cultivation are particularly adapted to average temperatures ranging from 17 to 27 °C (von Zabeltitz, 2011). Optimal temperatures can therefore range between 22 and 28 °C in the daytime and 15 to 20 °C at night (Castilla & Hernandez 2007). The optimum temperatures for tomato cultivation, for instance, are between 25 and 30 °C during the photoperiod and 18 to 25 °C during the dark period (Husey, 1965; Camejo et al., 2005), although this can vary between cultivars. The mean absolute maximum temperature for most greenhouse crops should not be higher than 35 to 40 °C (Verlodt, 1999; von Zabeltitz, 2011).

2.3.2 Greenhouse Relative Humidity

A recommended greenhouse relative humidity range is between 40-70% (Wees, 2016), although this can vary greatly depending on the air temperature, type of crop and age of the crop. For instance, a relative humidity range of 70 to 90% can be considered safe for most vegetable and flower crops in warm climates (von Zabeltitz, 2011). Recommendations suggest that if outside daytime relative humidity is lower than 55 to 60% in warm climates, greenhouse relative humidity should be increased via evaporative cooling techniques (von Zabeltitz, 2011).

It is suggested that the most common purpose of humidity control in a greenhouse is to sustain a minimal rate of transpiration in the crops (Stanghellini, 1992), and avoid water stress (Grange & Hand, 1986). Several studies have demonstrated that increasing the relative humidity with fog or mist systems reduces transpiration rates and therefore reduces plant water stress (Katsoulas et al., 2001; Urban & Langelez, 2001). In arid climates, elevating humidity inside the greenhouse is crucial as it causes a reduction in crop evapotranspiration by 60 to 80% (Al-Ismaili & Jayasuriya, 2016), beyond reduced plant stress, translates to large water savings (Fernandez et al., 2003). However, the amount of water required for evaporative cooling in many greenhouse operations is much more than water needed for irrigation (Al-Ismaili & Jayasuriya, 2016; Al-Mulla, 2006), and a certain amount of management is required to optimize crop health and water use.

Conversely, extreme high humidity in greenhouses can have detrimental effects on crop health (Hand, 1988) and pest management (Shipp et al., 2003). Calcium disorders are present in almost every fruit and vegetable crop (Shear, 1975), such as tip-burn in lettuce and blossom end rot in tomato and pepper fruit, and high humidity can cause or aggravate a variety of these disorders (Hand, 1988). High relative humidity in greenhouse cultivation is tightly related to fungal disease incidence (Stanghellini, 1992), such as grey mold (*Botrytis cinerea*) and leaf mold (*Fulvia fulva*), in tomato, and downy mildew (*Bremia lactucae*) in lettuce (Hand, 1988). There may be occasions when high greenhouse humidity is desirable. For instance, in generating root pressure to avoid calcium deficiency in fruit or young leaves, when using pathogenic fungi to control insect pests, and in the propagation of plants from leafy cuttings or in tissue culture (Grange & Hand, 1986).

Both extreme high or low relative humidity levels have been found to impact the photosynthetic rate in plants (Hand, 1988). Both humidity extremes have shown detrimental effects in crop growth and yield (Hoffman, 1979; Swalls & O’Leary, 1975; Swalls & O’Leary, 1976).

2.3.3 Greenhouse Vapor Pressure Deficit

Vapor pressure deficit (VPD) is a valuable climate control measurement as it can be used to evaluate plant disease threat, condensation potential, and irrigation needs of a greenhouse crop through transpiration control (Prenger & Ling, 2001; Wollaeger & Runkle, 2015). VPD is the difference between the amount of moisture in the air and how much moisture the air can hold when it is saturated at a certain temperature. Once air becomes saturated, water will condense on all surfaces, including plant leaves. If a film of water forms on a plant leaf, it becomes far more susceptible to disease. As the VPD increases, the plant will draw more water from its roots. The effect of humidity is best given in terms of VPD between the plant leaf and greenhouse air (Zhang et al., 2015). For instance, Aphalo and Jarvis (1991) concluded that VPD is a more appropriate variable for describing stomatal responses to humidity than solely relative humidity.

VPD can impact plant growth in a variety of ways (Pettigrew et al., 1990), and the repercussions of VPD extremes are similar to that of relative humidity extremes. A VPD between 0.3 and 1 kPa is considered ideal for most greenhouse crops, and variation within this range has little effect on the crop (Hand, 1988). A VPD beyond 2 kPa has been reported to cause high transpiration rates and low water potential in leaves of well-watered rooted plants (El-Sharkawy et al., 1986). According to Rylski and Spigelman (1986) both high VPD (> 2 kPa) and low VPD (< 0.2 kPa) can lead to heat injury as leaf temperatures increase. A low VPD suppresses transpiration and significantly impacts the energy balance of the plant canopy. Without sufficient plant transpiration, under high temperatures, incoming solar radiation can rapidly increase leaf temperatures (Zolnier et al., 2000).

2.3.4 Greenhouse Air Movement

Proper air circulation improves temperature, relative humidity and carbon dioxide uniformity in the greenhouse. The ASHRAE Fundamentals Handbook (1985) states that greenhouse air velocities in the range of 0.5 to 0.7 $m \cdot s^{-1}$ are optimal (Kittas et al., 2003). In terms of plant productivity and quality, the velocity of the air movement in a greenhouse is suggested to not exceed 1 $m \cdot s^{-1}$ across the plants (ASHRAE, 1985).

In Mediterranean-style natural ventilation greenhouses, the air velocity typically observed in the plant space can vary from 0.1 to 0.5 $m \cdot s^{-1}$, which includes the wind effect (Molina-Aiz et al., 2003, Molina-Aiz et al., 2004, Jiménez-Hornero et al., 2005; Teitel et al., 2005). Airflow will vary depending on the greenhouse design, the weather and the season, and that in many regions, sufficient greenhouse airflow cannot be sustained by natural ventilation alone (Latimer, 2009). The type of crop and crop arrangement can influence airflow in the greenhouse (Sase et al., 1984).

In a multi-span greenhouse located in the Mediterranean region of Almería, Spain, average air velocities of 0.21 and 0.26 $m \cdot s^{-1}$ were reported inside the greenhouse, with and without crop, respectively (López et al., 2010). In the study by López et al. (2010), it was shown that the flow of air that passed through the evaporative pads underwent a sharp drop in velocity when it encountered the dry, warm air inside, contributing to the large temperature gradients found in pad and fan cooled greenhouses.

In a study by Fernandez and Bailey (1994), air velocity was measured inside an empty greenhouse with side vents (no cooling pads), with and without circulation fans, which showed that the fans provided significantly greater air velocities. The average air velocities inside the greenhouse without the use of circulation fans was 0.12 $m \cdot s^{-1}$, whereas with the use of fans was 0.64 $m \cdot s^{-1}$.

A Quonset style greenhouse with exhaust fans and an evaporative cooling pad systems was studied by Willits (2003). Two levels of ventilation rate were considered, 0.041 $m^3 \cdot m^{-2} \cdot s^{-1}$ versus 0.087 $m^3 \cdot m^{-2} \cdot s^{-1}$. Based on measurements, air velocities were 0.15 $m \cdot s^{-1}$ near the cover, 0.33 $m \cdot s^{-1}$ through the canopy and 0.26 $m \cdot s^{-1}$ over the floor for the lower ventilation rate. Those for the higher ventilation rate were 0.53 $m \cdot s^{-1}$ near the cover, 0.69 $m \cdot s^{-1}$ through the canopy and 0.43 $m \cdot s^{-1}$ near the floor.

2.4 Plant Responses to Greenhouse Climate

Transpiration rate and leaf temperature are the two most common parameters used to study plant responses to their greenhouse climate (Sabeh, 2007). Other plant responses that can be measured are leaf water potential, stomatal conductance, carbon dioxide (CO_2) exchange rate, fluorescence and diurnal fruit growth. This work focuses on transpiration rate, CO_2 exchange rate, fluorescence, and diurnal fruit growth.

2.4.1 Transpiration

The transpiration rate of a greenhouse crop can be impacted by air temperature, relative humidity, VPD and air velocity. Jolliet and Bailey (1992) have quantified climate effects on young and mature tomato plants. They found that for a mature crop, an increase in solar radiation of 1 $MJ \cdot m^{-2} \cdot day^{-1}$ resulted in an increase in transpiration of 0.14 $mm \cdot day^{-1}$ and an increase in VPD of 0.1 kPa (dehumidification of 4% relative humidity at 20 °C) increased transpiration by 0.24 $mm \cdot day^{-1}$. The effects were felt less on young tomato plants.

Studies have shown that the smallest internal resistance to transpiration occurs at 23 to 25 °C for several varieties of tomato plants, which may indicate the temperature range where the plants have optimum transpiration rates (Papadakis et al., 1994). Results presented by Montero et al. (2001) indicate that Geranium (*Pelargonium zonale*) did not show any significant reduction of canopy conductance and transpiration rate for VPD values from 1.4 to 3.4 kPa and ambient temperature up to 36 °C. However, this crop response was explained by considering that the crop had been grown from its early stages in a highly evaporative demanding environment. Other studies have shown no correlation between transpiration and air temperature (Jolliet and Bailey, 1992). It seems that temperature in combination with relative humidity, through VPD, contributes to changes in plant transpiration rates.

In fact, transpiration rate and air VPD follow a linear relation even under very high VPD conditions (> 2.5 kPa) (Lorenzo et al., 1993). It has been reported that high VPD conditions reduce fruit xylem influx and increase fruit transpiration, but hardly affected fruit phloem influx (Guichard et al., 2005). In this case, net fruit water accumulation and growth rate were reduced, and a xylem efflux even occurred during the warmest and driest hours of the day. Such results suggest that the transpiration rate can surpass the water uptake rate of the plant, and cause drastic changes in plant water relations, notably by affecting diurnal fruit growth rate. This involves the stem water potential dropping below the fruit water potential (Johnson et al., 1992).

Plant transpiration rates have been positively correlated with high greenhouse air velocity as air movement reduces stomatal resistance (Jolliet & Bailey, 1992). This is particularly true in arid climates (Kittas, 2003). Other studies, however, have demonstrated that high ventilation rates (0.13 $m^3 \cdot m^{-2} \cdot s^{-1}$) have little effect on transpiration (Willits, 2003).

Studies have shown a linear relationship between plant transpiration rate and solar radiation (Baille et al., 1994; Jolliet & Bailey, 1992). However, poor correlations have been reported when solar radiation is greater than 300 $W \cdot m^{-2}$, and transpiration has been shown to level off (Prenger et al., 2002). Johnson et al. (1992) showed that the stem water potential dropped below the fruit water potential only under higher solar radiation (> 400 $W \cdot m^{-2}$), compared to lower solar radiation (80 $W \cdot m^{-2}$).

2.4.2 Photosynthesis

Photosynthesis is known to be one of the most heat-sensitive processes and it can be completely inhibited under high temperatures before other symptoms of stress are detected (Berry & Bjôrkman, 1980). Reductions in photosynthetic rate can result from the inhibition of photosystem II (PSII) activity, which has been shown to be the most thermally fragile component of the electron transport chain (Quinn & Williams, 1985; Havaux et al., 1991).

In a study on tomato plants under varying VPD, the photosynthetic rate was 18% greater at a VPD of 0.5 kPa than at 1.0 kPa (Acock et al., 1976). In another study on tomato, the photosynthetic rate began to decline when air VPD exceeded a threshold value of 1 kPa (Romero-Aranda, 1995).

2.4.3 Chlorophyll Fluorescence

Three different occurrences can happen when light energy is absorbed by chlorophyll molecules in a plant: the energy can be used to drive photosynthesis (photochemistry), excess energy can be dissipated as heat or it can be reemitted as light-chlorophyll fluorescence. These three processes occur in competition, such that any increase in the efficiency of one will result in a decrease in the yield of the other two (Maxwell & Johnson, 2000). Hence, by measuring the yield of chlorophyll fluorescence, information about changes in the efficiency of photosynthesis and heat dissipation can be obtained.

Chlorophyll fluorescence has been successfully used as an early indicator of various types of plant stress (Mohammed et al., 1995; Andrews et al., 1995), including high temperature stress (Janssen et al., 1992). Although the total amount of chlorophyll fluorescence is very small (only 1 or 2% of total light absorbed) (Maxwell & Johnson, 2000), the measurement of fluorescence is a sensitive and reliable method for detection and quantification of temperature-induced changes in the photosynthetic apparatus (Krause & Weis, 1991). For instance, a strong increase in PS I fluorescence in the far-red region (720-740 nm) occurs when leaf tissue is cooled. These changes in emission spectra are quantified and can serve as a measurement scale.

The measurement of fluorescence relies on the measurement of isolated leaf areas. The full interpretation of the complex signals emanating from intact photosynthetic organisms, particularly from leaves of higher plants, is still problematic (Krause & Weis, 1991). Certain measured parameters are of empirical value only and therefore chlorophyll fluorescence is often combined with other plant stress indicators, such as photosynthetic rate measurement.

2.4.4 Diurnal Fruit Growth

Crops cultivated in greenhouses during warm summer conditions are negatively affected by stressful temperature and humidity conditions, which in turn influence yield and product quality (Katsoulas et al., 2009). High radiation and air temperature associated with elevated VPD cause serious problems for the production of fresh tomato fruits, as yield and quality are reduced (Guichard et al., 2001). In particular, problems of blossom end rot and cuticle cracking occur (Bertin et al., 2000). It has been established that fruit cracking occurs when there is a rapid net influx of water and solutes into the fruit, or when the strength and elasticity of the tomato skin is reduced (Peet, 1992; Ohta et al., 1997). Yet, the causes for these occurrences in fruit are not well understood. Peet (1992) reviewed many environmental influences, anatomical characteristics and cultural practices believed to cause fruit cracking.

Some research has suggested that plant xylem, phloem, and transpiration fluxes can show varying diurnal patterns depending on immediate greenhouse conditions, and that these flows can affect the diurnal growth of fruit, and in turn, affect the quality of the fruit. Whereas fruit dry matter growth is irreversible and rather stable on a short time scale, fruit volume growth is reversible and variable (Guichard et al., 2005). Guichard et al. (2005) observed changes in fruit volume growth due to plant water movements during high temperatures and high VPD environmental conditions. They reported a reduction in tomato fruit size when daytime VPD and temperature reached 2.7 kPa and 30 °C, respectively. These observations agreed with earlier results published by Lee et al. (1989), Johnson et al. (1992), Grange and Andrews (1995), and van de Sanden and Uittien (1995), all of which showed a decrease in fruit growth rate during daylight and an increase at night. Other authors (Ehret & Ho 1986; Pearce et al. 1993) reported a tomato growth rate higher during the day than at night, but as assumed by Pearce et al. (1993)

and demonstrated by Guichard et al. (2005), such results are likely due to experimental conditions with low diurnal stresses.

2.5 Environmental Sensing and Analytical Procedures

In order to properly measure the various components of the climate of the NVAC greenhouse, environmental sensing is required. The experiments listed in this research follow the guidelines presented in Both et al. (2015). Suggested precision and accuracy was respected or exceeded when possible and deemed necessary.

2.5.1 Temperature

Thermocouples, thermistors, resistance thermometers and radiation thermometers are some of the principal methods for measuring temperature in many industries. Their applications vary according to practicality and cost. Ultrasonic thermometry evolved as a new temperature measurement technology (Tsai et al., 2005). Although accurate, ultrasonic systems are not practical nor economical for many applications. Thermocouples, thermometers and other physical temperature measurement devices can be subject to significant error from radiation, even when shielded (Tanner et al., 1996; Lin et al., 2001; Richardson et al., 1999). Mechanically (fan) aspirated air sensors are therefore the recommended sensing device for air temperature in greenhouses (Both et al., 2015), and in many other industries (Nakamura & Mahrt, 2005). Such a device includes at least one temperature sensor such as a thermocouple, placed in an enclosure equipped with a downstream fan to provide a continuous air flow around the sensor, at a speed of approximately 3 $m \cdot s^{-1}$ (Both et al., 2015). These systems can be unpractical in some circumstances for their installation is more complex than other simple sensors. Therefore, air temperature sensors can be exposed or shielded from solar radiation and be subject to passive air movement, although their accuracy can be less than for aspirated air devices. Whiteman et al. (2000) considered the performance of HOBO data loggers and thermistors (Onset Computer Corporation, Bourne, MA) and found them to be adequate, practical and economical systems for long-term air temperature monitoring.

2.5.2 Relative Humidity

There exist many methods to measure relative humidity, including semi-conductor sensors (Eder et al., 2014), polymer capacitive sensors (Savage, 2010) and acoustic sensors (Schaik et al., 2010). The measurement of relative humidity, however, depends on several practical and environmental factors. Obtaining reliable, long-term stable, accurate and precise measurements of relative humidity remains a difficult practical issue (Zhang et al., 2016). With respect to greenhouse climate, it can be challenging to obtain accurate measurements of both inside and outside humidity conditions, for the sensors are subject to elements such as varying solar radiation, varying air movement and direct water from rain, irrigation or evaporative cooling equipment.

A psychrometer is a device used in many fields of research, including food engineering (Maskan et al., 2002; Tanaka et al., 2010), environmental control in building engineering (Schaik et al., 2010) and greenhouse engineering (Toida et al., 2006). It measures relative humidity indirectly from two temperature probes, one being wetted by a wick placed in a distilled water bath. Compared to modern electronic relative humidity sensors, the psychrometer is one of the relative humidity measurement devices that can be used in a dirty environment, can withstand direct water, and can provide a large range of measurement values (Zhang et al., 2016).

Using psychrometer measurements, relative humidity values can be calculated from dry bulb temperature, wet bulb temperature and barometric pressure. A methodology from Snyder and Shaw (1984) is described below:

The station barometric pressure (P) is calculated using the elevation (Z) in meters (m) of the study site:

$$P = 101.3\left[\frac{293-(0.0065Z)}{293}\right]^{5.26} \qquad \text{Equation 3}$$

Saturation vapor pressure E_w in millibars (mb) at the wet-bulb temperature is calculated from the recorded wet bulb temperature:

$$E_w = \frac{6.108e^{(17.27W)}}{(237.3+W)} \qquad \text{Equation 4}$$

Actual vapor pressure E is calculated from the saturation vapor pressure using the recorded wet bulb temperature, the recorded dry bulb temperature and the recorded station barometric pressure:

$$E = E_w - (0.00066(1 + 0.00115W)(T - W)P) \qquad \text{Equation 5}$$

Saturation vapor pressure E_s in millibars (mb) at the dry-bulb temperature is calculated from the recorded dry bulb temperature:

$$E_s = \frac{6.108e^{(17.27T)}}{(237.3+T)} \qquad \text{Equation 6}$$

Relative humidity RH (%) is calculated from actual vapor pressure and saturation vapor pressure using the dry bulb temperature:

$$RH = 100\left[\frac{E}{Es}\right] \qquad \text{Equation 7}$$

Vapor pressure deficit VPD (kPa), as defined previously in this proposal, is calculated from collected data as follows:

$$VPD = (1 - (RH/100))(100\,Es))/1000 \qquad \text{Equation 8}$$

where RH is relative humidity and E_s is the saturation vapor pressure (mb) at the dry bulb temperature.

2.5.3 Solar Radiation

In addition to temperature and relative humidity, solar radiation is of great importance to the greenhouse environment. Irradiance is the radiant energy flux per unit plane surface area, usually expressed in the units of $W \cdot m^{-2}$. The photon irradiance, is the incident photon flux per unit plane surface area, expressed in $\mu mol \cdot m^{-2} \cdot s^{-1}$. Photosynthetically active radiation, or PAR, is the part of the radiation spectrum that is, by definition, used by plants for photosynthesis, and is expressed in $\mu mol \cdot m^{-2} \cdot s^{-1}$. Net radiometers, pyranometers, quantum sensors and spectroradiometers are used for the measurement of solar radiation.

2.5.4 Air Movement

2.5.4.1 Anemometer

The experimental study of air movement in greenhouses is considered the ultimate test to clearly define air circulation (Wang et al. 1999). Several techniques have been developed, such as mechanical, hot-wire and sonic anemometry. A sonic anemometer is regarded as one of the most accurate devices for the measurement of air movement in large enclosures like greenhouses (Wang et al., 1999; Boulard et al., 1997). Greenhouse air velocity has been measured using three-dimensional sonic anemometers in several published papers including: Wang et al., (1997), Boulard et al. (1997), Boulard et al. (1998), Boulard et al. (2000), Tanny et al. (2006), Teitel et al. (2008), Kittas et al. (2008) and Katsoulas et al. (2010). The use of anemometer measurements in controlled environment research has been regarded as a highly precise way of measuring air movement velocity and direction. The high resolution, stability and proper frequency response of the system are well adapted for the study of the air velocity field in greenhouses (Wang et al., 1999).

2.5.4.2 Smoke Emitters

Smoke candles can be used to visualize the air movement in greenhouse designs. These comprise of 15-049 Tel Tru smoke sticks (E. Vernon Incorporated, Rohnert Park, CA) that emit various colored smoke (Regin HVAC Products, Inc., Oxford, CT). The colored smoke allows for visual separation of different air streams. Smoke can be added to the air in the greenhouse to see where the air is entering the greenhouse's main space and how it moves around the interior (Bartok & Grubinger, 2015; Albright, 1995; Wheeler & Both, 2002). A certain amount of creative license is needed when using airflow visualization methods (Wheeler & Both, 2002).

2.5.5 Transpiration

There are multiple methods available to measure plant transpiration both directly or indirectly. Several greenhouse researchers have used lysimeters to measure evapotranspiration (Kittas et al., 2001; Boulard & Wang, 2000). Other have conducted sap flow tests and performed measurements requiring gauges to be placed within the stems of plants (Nagler, et al., 2003). Weighing device such as a balance or a load cell can be used to measure the amount of water gained by irrigation or rain, and weight lost from the plant by mass differences (Sabeh 2007; Prenger et al., 2002; Simonneau et al., 2002; Jolliet & Bailey, 1992).

2.5.6 Photosynthesis and Fluorescence

Different devices are used by researchers to monitor photosynthesis in a plant. Over 95% of research involving measurements of photosynthetic CO_2 uptake in modern research use commercial systems (Long & Hällgren, 1993; Long et al., 1996), such as the LI-6400 by Li-Cor Inc. (Lincoln, Nebraska, USA), the CIRAS-II by PP Systems (Hitchin, UK) and the LCA4 by ADC-Biosciences (Hoddesdon, UK). The LI-COR LI-6400 XT portable photosynthesis system can measure the photosynthetic responses of plants to environmental variables such as light, CO_2, humidity and temperature (LI-COR, 2017). With the addition of the 6400-40 Leaf Chamber Fluorometer, the same device can take simultaneous measurements of gas exchange and fluorescence over the same leaf area.

2.5.7 Sensors Applied to Greenhouse Crop Monitoring

Measurement and control methodologies involving plant sensing go beyond the climate parameters of the greenhouse and environmental sensing, they can assess and adjust greenhouse settings based on the reactions observed in the crop. Direct plant measurement methods involve some form of physical contact with the plant. This is the typical means of gathering crop stress or growth information (Ehret et al., 2002). Special care must be taken to prevent the measurement equipment from influencing the measurements, as even the most delicate equipment can have a large impact on plant stem, leaves or organs.

With increasing access to technology, interest is growing in the development of methods to automatically and continuously detect stress, water use, growth and nutrition in greenhouse crops (Ehret et al., 2001). Table 1 summarizes the current technologies available to researchers and growers to monitor crops. Although direct methods have existed for decades, non-invasive, non-contact, and non-destructive methods are preferred and being developed for rapid and continuous measurement of various parts of the crop. A single leaf, fruit or a full crop canopy can be monitored with imaging devices, and a variety of analysis can be performed. Red-green-blue (RGB), multispectral and hyperspectral imaging devices each offer different possibilities in terms of image capture and analysis.

Table 1. Uses, advantages and disadvantages of various sensors applied to automated crop monitoring. Modified from Ehret et al. (2001).

Sensor	Used to Detect	Advantages	Disadvantages	Suggested Literature
Imaging camera	Plant growth, canopy temperature, water stress, fruit quality, mineral status	No interference with the plants, monitors many plants simultaneously, fully automated	Complicated equipment, affected by lighting conditions, expensive	Polder van der Heijden 2010; Katsoulas et al., 2016; Story and Kacira, 2015
Infrared thermometry	Canopy temperature, water stress, heat stress	No interference with the plants, monitors many plants simultaneously, fully automated instant response	Field of view must be precisely aligned, may not detect short time-scale changes	Clawson & Blad, 1982
Sap flow meter	Transpiration, water stress	Measures whole plant transpiration (compared to porometers which do not)	Small sample size (one plant), may interfere with the plant if not moved periodically, hence only semi-automated, requires consistently good fit around the stem	De Swaef et al., 2012; Nagler, et al., 2003
Weighing lysimeter	Transpiration, water stress	May be configured to monitor several plants simultaneously, no interference with the plants, no interference with the plants, fully automated, low maintenance requirements	Sensitive to perturbations, measurements should be corrected for plant growth or changes to the mass of the growing media over time	Corral et al., 2016; Kittas et al., 2001; Boulard & Wang, 2000

LVDT	Growth and water stress	Measures small increments in organ growth or contraction over short time periods instant response	Small sample size (one fruit, one stem or one plant) sensitive to perturbations and may require stabilizing superstructure	Guichard et al., 2005; Johnson et al., 1992
Load cells	Growth and water stress	May be configured to monitor many plants simultaneously, no interference with the plants, fully automated	Restricted to use on suspended vine crops such as tomatoes, sensitive to perturbations, hourly measurements may be confounded by simultaneous changes in water status and growth	Sabeh 2007; Prenger et al., 2002; Simonneau et al., 2002; Jolliet & Bailey, 1992
Photosynthesis meter or porometer	Photo-synthesis, transpiration, water stress	Measures gas exchange at precise locations within the canopy, instant response	Small sample size (part of one leaf), may interfere with the plant if not moved periodically, hence only semi-automated, expensive	Guichard et al., 2005
Stem hygrometer	Plant water status, water stress	Most direct measure of plant water potential instant response	Small sample size (one plant), may interfere with the plant if not moved periodically, hence only semi-automated, sensitive to mechanical damage, difficult to use; requires careful calibration	Dixon et al., 1984

Connecting Text

Chapter 3, *Protected Agriculture in Extreme Environments: A Review of Controlled Environment Agriculture in Tropical, Arid, Polar and Urban Locations* was authored by Lucas McCartney and Mark G. Lefsrud. Chapter 3 was submitted to the ASABE journal *Applied Engineering in Agriculture* on June 25, 2017.

Chapter 3 reviews the current status and future trends of protected agriculture technology in tropical, arid, polar and urban climates. This chapter goes beyond what is presented in the literature review of this thesis by presenting the issues faced by growers using greenhouse technology in extreme climates, and the solutions that are currently available to them. The review is based on previous literature on the subject, and on field experience by the authors. The four climates considered in this review, including urban, share many common setbacks in terms of protected agriculture, with energy efficiency and water efficiency at the center of most problems. Most greenhouse technology has been developed for North American or European climates. In other regions of the world, there is a lack of adapted greenhouse technology, tailored specifically for the local climates. This chapter provides a detailed account of the rationale behind the research and development of energy and water efficient, sustainable and locally available greenhouse technologies. The significance of novel greenhouse cooling technologies, such as the NVAC greenhouse design, becomes apparent with the information presented in Chapter 3.

3. Chapter 3: Protected Agriculture in Extreme Environments: A Review of Controlled Environment Agriculture in Tropical, Arid, Polar and Urban Locations.

Lucas McCartney and Mark G. Lefsrud

Additional index words. Protected agriculture; tropical climate greenhouse; arid climate greenhouse; evaporative cooling; natural ventilation; urban agriculture; vertical farming

3.1 Abstract

Many methods of protected agriculture are used to modify the growing environment of plants. Ideally, plant production would take place in regions that do not require protective structures, regions that present ideal temperatures, no harsh extremes, and sufficient but not excess precipitation. This is not the case however, as most countries, except for a select few, require various forms of controlled environment agriculture to protect crops against climatic and environmental extremes. Although the greenhouse industry has developed vast amounts of technology for the temperate climate regions of our planet, much remains to be improved in terms of protected agriculture in the more extreme climates. Tropical, arid, polar and urban locations offer contrasting environments that present various challenges for plant growth. Some challenges are specific to each location, while others are common across them. Tropical and arid climates offer high solar radiation, but present harsh temperature and relative humidity conditions. Most protected agriculture structures are relatively open in nature to ventilate and discharge heat, but are susceptible to pests and diseases. On the other hand, polar climates and urban environments often lack solar radiation and require a high level of control of the air quality. The structures used in these environments are relatively enclosed to entrap heat (polar) and to make efficient use of space. The sustainability of available technologies and energy efficiency are important themes present in all discussed climates and environments. Protected agriculture technologies offer solutions to growers in locations with extreme climates wishing to produce high yields of high quality crop, and this paper presents a review of the existing challenges and of the advancements made in this field.

3.2 Introduction

Protected agriculture is the modification of an environment to achieve improved conditions for plant growth. It allows for crop yields that are far greater than in field operations. It allows for successful crop production in locations, climates or during seasons that are otherwise unsuitable or even hostile to plant production (Wittwer & Castilla, 1995). Producers can thus extend their production season or accomplish year-round production (Jain & Tiwari, 2002). In recent times, protected agriculture has demonstrated the potential to address the growing concerns of food security with climate change and urbanization (Lawrence et al., 2014; Despommier, 2011; Jensen & Malter 1995). Techniques vary in complexity from the use of row covers to sophisticated controlled environment plant systems. In protected agriculture, control may be imposed on, but not limited to, air and root temperature, light intensity and quality, water and plant nutrition, growth substrates, air quality such as relative humidity and carbon dioxide levels, and protection from all exterior elements including pollution, pests and pathogens. Greenhouses are a widespread form of protected agriculture found worldwide that can offer control of the plant environment at different levels. When fully enclosed, the greenhouse becomes a form of controlled environment agriculture that pushes the limits of protected agriculture and offers complete control of the plant environment. Such systems are currently found in sophisticated space travel and urban agriculture systems. Now used worldwide in many ways at varying levels of control, the technology of controlled environment agriculture is rapidly evolving with systems now producing yields never before seen (Jensen, 2001).

The type of protected agriculture that is needed in any given region is conditional to the type of crop being grown, the level of environment control desired and the climate of the immediate area. To categorize extreme environments and their global significance, the climate classification developed by Köppen (Köppen-Geiger classification) is most frequently used. Table 2 presents the 30 possible climate types, and it includes the following zones: the equatorial or tropical zone (A), the arid zone (B), the temperate zone (C), the cold zone (D) and the polar zone (E) (Kottek et al., 2006; Peel et al., 2007). Globally the dominant climate zone by land area is arid B (30.2%) followed by cold D (24.6%), tropical A (19.0%), temperate C (13.4%) and polar E (12.8%). In Köppen's system, another series of letters are used subsequent to the zone letters to define certain climate types within these zones. More specifically, the most common climate type by land area is BWh (14.2%, hot desert) followed by Aw (11.5%, tropical savannah) (Peel et al., 2007). Tropical A is the most densely populated climate zone, while both tropical A and temperate C share most of the world's population (Small and Cohen, 2004; Cohen and Small, 1998). Additionally, developing countries, mostly in tropical and sub-tropical regions, contribute and are expected to continue contributing as high as 90% of the world's population increase (Shamshiri & Ismail, 2013).

Table 2. The Köppen climate classification is one of the most widely used climate classification systems. Description of Köppen climate symbols and defining criteria. Adapted from Peel et al. (2007).

Zone	Type abbreviation		Description		
A	f		Tropical	Rainforest	
	m			Monsoon	
	w, s			Steppe or Savanna or Wet and Dry	
B	W		Arid	Desert	
	S			Steppe	
		h			Mild
		k			Cold
		n			Hot
C	s		Temperate	Dry Summer	
	w			Dry Winter	
	f			Without Dry Season	
		a			Hot Summer
		b			Warm Summer
		c			Cold Summer
D	s		Cold (Continental)	Dry Summer	
	w			Dry Winter	
	f			Without Dry Season	
		a			Hot Summer
		b			Warm Summer
		c			Cold Summer
		d			Very Cold Winter
E	T		Polar	Tundra	
	F			Eternal Winter (icecap)	

Yet, the protected agriculture industry has not reacted to the growing need to develop solutions for the most important regions of the world in terms of land area, climate and population. With the ease of access to new technology, strong agricultural economies and relatively cheap energy, temperate climate regions have driven the industry and shown most of the progress in protected agriculture. Works by von Elsner et al., (2000a, b) and Critten and Bailey (2002) present a European and global overview of greenhouse design development. Temperate conditions with occasional extremes are the conditions for which most technology has been adapted (Abdel-Ghany at al., 2012; Sutar & Tiwari, 1995). In Europe, most greenhouses were initially located in the centre and the north, and consisted of high-cost, glass-covered structures with control systems (Orgaz et al., 2005). This situation is changing and, at present, greenhouse operations are emerging in new regions (Kumar et al., 2009; Briassoulis et al., 1997).

The present trend in greenhouse cultivation is to extend the crop production season in order to maximize the use of the equipment and increase annual productivity and profitability (Jain & Tiwari, 2002; Arbel et al., 1999). In recent times, other development in protected agriculture practices for tropical, arid and polar climates has allowed nations in these regions to expand their food production. However, many existing greenhouse operations lack proper adaptation to their respective environments, being merely borrowed from their temperate counterparts, and usually exhaust their lifespan prematurely or fail from the start. Some existing technologies are not economically feasible in regions other than that for which they have been designed. Furthermore, the structure and the shape of these shelters are often poorly adapted to the climatic conditions of the regions (Castilla & Lopez-Galvez, 1994), aggravating instead of alleviating the problems (Baille, 2000). Therefore, some of the sunniest countries in the world have become net importers of food due to unfavorable conditions for plant growth (Davies, 2005; Al-Jamal, 1994).

Although cities are expanding, an important challenge of the future will be the further development of rural areas (Eigenbrod & Gruda, 2015). Tilman et al. (2011) emphasize that the ‘attainment of high yields on existing croplands of under yielding nations is of great importance if global crop demand is to be met with minimal environmental impacts’. Food production in rural areas will remain an important activity, and developments in protected agriculture for extreme environments will allow for better, more effective and more widespread production within existing rural areas. However, in order to produce enough food for the future, vacant spaces in cities should be considered as possible agricultural locations. This can help reduce dependence on rural agriculture for certain foods, to cut back on deforestation for arable land (Eigenbrod & Gruda, 2015), and to reduce transport costs. Currently, urban, indoor and extraterrestrial agriculture advances have contributed to the world of protected agriculture by offering innovative solutions and demonstrating successful technology transfer. As presented in this chapter, many sites in tropical, arid and polar climates are home to various forms of protected agriculture, but lack adaptation and optimization. As worldwide protected agriculture technology develops, better solutions will be available to growers in many specific extreme environments and climates.

3.2.1 Tropical Environment Protected Agriculture

Many tropical nations rely heavily on agriculture for economic, social and food security motives (Lawrence et al., 2014; von Zabeltitz, 2011; von Zabeltitz and Baudoin, 2005; Barbier, 2004). However, many have deforested land with poor soils that cover large areas which makes much of the land unusable for agriculture (Mendelsohn and Dinar, 1999). These regions face climate change challenges such as sea level rise and decreased soil moisture (Battisti and Naylor, 2009). Shorter and more intense rainfall events and longer and more pronounced dry seasons are impacting agriculture in the tropics (Lawrence et al., 2014; Stocking, 2003). Sub-Saharan Africa and parts of Latin America, the Caribbean, and Central Asia are tropical regions suffering the worst from this decline in available local agriculture (Stocking, 2003). Constraints impacting the current use of protected agriculture technology in tropical regions such as the Caribbean are largely rooted in the designs of the structures being used (Lawrence et al., 2014, Lawrence et al., 2011). The development of adequate protected agriculture solutions will allow some tropical nations to counter some of these changes.

A tropical climate is defined to have an absolute minimum temperature of 18 °C, but is typically hot at midday year-round, nearing or surpassing 30 °C, with heavy precipitation (Af, tropical rainforest, and Am, tropical monsoon, Table 2) (Kottek et al., 2006). High relative humidity is therefore common in many tropical locations. In such environments, protected agriculture offers protection from high daytime temperatures, intense rain and winds, vast amounts of pests and diseases, and strong solar radiation (DeGannes et al., 2014; von Zabeltitz, 2011; Jensen, 2001; Kumar et al., 2009; Sethi & Sharma, 2007; von Zabeltitz & Baudoin, 2005).

A tropical climate can also be dry for varying lengths of time (As, tropical savannah and Aw, tropical wet and dry Table 2) (Kumar et al., 2009; Kottek et al., 2006). In very hot and dry tropical environments, the conditions can resemble that of an arid climate, and protected agriculture is used to limit plant evapotranspiration to reduce plant water stress (von Zabeltitz, 2011; von Zabeltitz & Baudoin, 2005). High relative humidity levels and ambient temperatures in tropical greenhouses create a complicated dynamic system that is influenced by varying external conditions, making it a challenging environment to control (Shamshiri & Ismail, 2013).

Considering the changing quality of the soils in tropical regions, protected agriculture offers improved growing substrates that are soilless (Basirat & Davoodi, 2014; Jensen, 2001). Worldwide, most of the hydroponic industry uses inorganic growing media such as rockwool, sand, perlite, vermiculite and others (Olle et al., 2012; Sawan et al., 1999; Böhme et al., 2008), while only about 12% use organic growing media such as peat, bark, sawdust and others (Olle et al., 2012). Table 3 summarizes many materials used as growth substrates around the world in varying climates and types of production, but the most popular growing media for greenhouse production of vegetables remains rockwool (Islam, 2008). Although rockwool dominates, due to its widespread use in temperate climates, the specific substrate to be used is entirely based on production type, cost, on-site performance and local availability (Albaho et al., 2013; Jensen, 2001). In fact, according to Islam (2008) substrates such as rice husk biochar and coconut coir gave similar or better yield in tomato production than rockwool under high temperature stress conditions (30 °C and 35 °C, when compared to 25 °C). This coincides with the availability and surplus of these materials in tropical and sub-tropical locations. The variety of growing systems that exist, namely hydroponic systems, such as nutrient film technique (NFT) systems (Resh, 2012), deep well or deep flow systems (Jensen, 2002) or ebb and flow systems can be used with soilless plant substrates successfully in tropical regions.

Table 3. Inorganic and organic growing substrates found worldwide in greenhouse vegetable production. Adapted from Olympios (1999) and Olle et al., (2012).

Inorganic Media		Organic Media
Natural Media	Synthetic Media	
Sand	Polyurethane Foam Mats	Coconut Coir
Gravel	Oasis Plastic Foam	Bark
Rockwool	Hydrogel	Sawdust
Glasswool	Expanded Polystyrene	Wood Chips
Perlite	Urea Formaldehydes	Peat
Vermiculite		Fleece
Pumice		Pomace or Marc
Expanded Clay		Rice Hull
Zeolite		Bagasse
Volcanic Tuff		Cotton
Sepiolite		Hemp

Greenhouse ventilation, air movement and temperature control is critical in tropical climates. In many developing countries, however, it is critical for greenhouse designs to remain low-cost and to consist of locally available materials. Passive ventilation and cooling measures are recommended over active ones as they are simple and economically viable (Rault, 1989). The inaccessibility to technology, rising cost of energy and the unreliability of power grids renders forced ventilation unfeasible in most tropical nations (Buffington et al., 2013; Sachs, 2001). If economically available, evaporative cooling solutions are useful during the very driest and hottest periods, which can be infrequent in many tropical locations (Kumar et al., 2009). Evaporative cooling is discussed in a later section of this paper. However, cooling methods in tropical climates must be used with caution to avoid the sanitary repercussions of increased relative humidity and airborne water droplets (Montero, 2006). One of the key challenges remains providing effective greenhouse cooling in high relative humidity environments. Alternative cooling solutions such as the geothermal horizontal earth tube system presented by Mongkon (2014), and improved systems such as variable fogging rate natural ventilation system suggested by Villarreal-Guerrero (2011) each offer added solutions, but require further development. McCartney (2017) developed a system called the natural ventilation augmented cooling (NVAC) greenhouse that provides over 5 °C of cooling in natural ventilation greenhouses in tropical climates during the dry season, and up to 12.1 °C of cooling in arid climates, with minimal energy and water requirements.

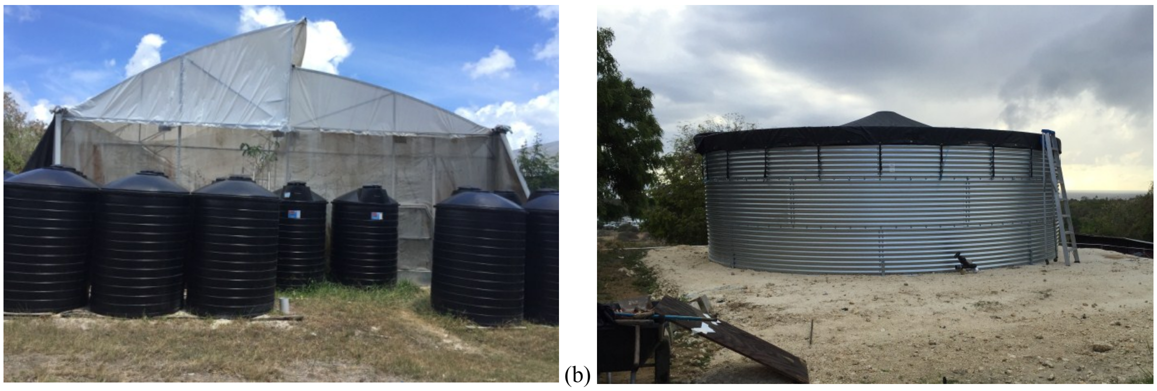

(a) (b)

Figure 3. Roof and sidewall vented natural ventilation greenhouse with structural balconies in (a). Multiple 1000-gallon (3785.4 L) water reservoirs seen in the foreground. In (b) a 50,000-gallon (189270.5 L) rainwater reservoir. Location: Barbados, West Indies.

Simple split roof designs with large roof vents (Figure 3a), single layer film cladding, tall screened sidewalls and natural ventilation are ideal for tropical environments (DeGannes et al., 2014; Kumar et al., 2009). Polyethylene film is widely used across the globe in greenhouse construction for its accessibility and ease of use, but many other cladding materials are available to growers. Table 4 summarizes many materials used for greenhouse cladding. The lifespan of greenhouse films varies between 6 to 45 months, depending on the photostabilizers used, the geographic location, the climate and the use of pesticides and other chemical products (Espi et al., 2006). Polyethylene film used for greenhouses ranges in thicknesses from 3 to 8 mil (0.08 mm to 0.22 mm) (Espi et al., 2006) and is the preferred cladding material for tropical climate protected agriculture (von Zabeltitz & Baudoin, 2005). It is a question of location, durability and economy whether a greenhouse is covered every year with a new thinner film (4 mil or 0.1 mm) or every other year with a thicker film (6 mil or 0.15 mm). Many tropical locations have high solar radiation which makes even thicker films brittle within months; in which case, yearly replacement is necessary regardless of the choice of film. Harsh weather conditions negatively impact cladding and other plastics in the greenhouse systems and rapidly degrade their optical and mechanical properties (Abdel-Ghany at al., 2012). During dry seasons, dust accumulates on the film and can cause important reduction in light transmission. Washing the film can prevent this. Some woven plastic films varying from 0.2 mm to 0.25 mm (8 mil and 10 mil) are available to some growers. Such films are durable and may last a few years even in strong solar radiation. However, these resistant films have poor light transmission and can therefore only be used with a crop that does not require high levels of light. More advanced but costly greenhouse film materials can contribute to the cooling of the greenhouse with proper material and additive choice. Added benefits can include certain reflective, absorptive and interference properties, as well as condensation and drip control (Hoffmann & Waaijenberg, 2001). However, these materials must remain resistant and economically available.

The height of the greenhouse up to the gutter should be in the range of 2.5 to 4.5 m instead of the traditional range of 1.5 to 2 m to allow for better airflow within, and air influx from the wind. The current trend in passive greenhouse technology is towards taller greenhouses (Kumar et al., 2009; Connellan, 2001), to reduce the peak greenhouse air temperatures at crop level. A screening mesh size of mesh 70 (0.21 mm) is able to thwart most insect pests (Ghidiu & Roberts, 2010; Murphy & Ferguson, 2000). More specifically, for control of greenhouse whitefly (*Trialeurodes vaporariorum*), a very common pest, the pore size should be a maximum of mesh 58 (0.29 mm) screen. This size screen would also exclude aphids (Hemiptera: *Aphididae*) and leaf miners and it is sometimes called an “anti-virus” screen (DeGannes et al., 2014). Although effective in preventing the entry of insects, sidewall and roof vent screening will cause a restriction in airflow (Tantau & Salokhe, 2006; Soni et al., 2005). Larger mesh sizes can be used or sections of mesh can be entirely removed from vents to enhance air movement, ventilation and cooling, at the expense of increased pest stress (DeGannes et al., 2014; Kumar et al., 2009). Studies by Soni et al. (2005) and Miguel et al. (1997) on the impact of thermal and insect screening on the airflow within the greenhouses offer details of these methodologies.

Shade cloth is used to reduce the solar radiation load reaching the crop (Al-Helal & Abdel-Ghany, 2011; Willits & Preet, 2000). The density is expressed as the percentage of light excluded. For example, 30% shade cloth has 30% light exclusion and allows 70% light to pass through. Shade cloth is also commonly used in greenhouses for hardening tissue culture planting material or for hardening of budded and grafted plants (DeGannes et al., 2014). In certain situations, it is used as an alternative to insect mesh or as thermal screens. A more expensive solution, reflective aluminized netting, is used as an effective ceiling above the crop to reduce solar radiation and aid in reducing greenhouse and plant leaf temperatures (Ferreira et al., 2014). Finally, some growers may rely on the application of whitewash on the greenhouse cladding to reduce the solar radiation reaching the plants and reduce the heat entering the greenhouse. All these methods reduce the photosynthetically active radiation (PAR) reaching the crop and can cause a reduction of quality and yield (Runkle et al., 2002). Near infrared (NIR) reflecting cladding film can reduce heat loads while allowing high transmittance of PAR, but are not recommended for use in tropical climates (von Zabeltitz, 2010). Better focus on ventilation will provide better quality and yield in tropical greenhouse operations.

Table 4. Characteristics of greenhouse cladding material available in tropical regions. Adapted from DeGannes et al. (2014), von Zabeltitz (2011) and, von Zabeltitz and Baudoin (2005).

Type of Plastic	Advantages	Disadvantages	Durability	Light Transmission
Anti-drop UV-stabilized Polyethylene Film	Wide and of variable sizes, relatively inexpensive, UV-resistant	Expensive, requires maintenance and can puncture and tear easily	Fair, 2-3 years	Very good when kept clean 89-91%
UV-stabilized Polyethylene Film	Wide and of variable sizes, relatively inexpensive, UV-resistant	Requires maintenance and can puncture and tear easily	Fair, 2-3 years	Very good when kept clean >90%
Polyethylene Film Non-Stabilized	Inexpensive, wide and of variable sizes.	Requires maintenance and can puncture and tear easily	Poor, 1 year	Very good when kept clean >90%
Acrylic	Weather-resistant and break-resistant	Flammable, expensive, easily scratched, not applicable to tropical or warm climates	Very good, >5 years	Very good, >90%
Polycarbonate	Impact-resistant, flexible, thin and relatively inexpensive	Easily scratched, reduced light transmission with ageing and expands/contracts, not applicable to tropical or warm climates	Good, 5 years	Fair to good, 80-90%
Fiberglass	Impact-resistant, moderately priced and easily cut	For smaller greenhouses, expensive in larger scale, reduced light transmission with ageing, collects dust easily	Very good, >5 years	Fair, 80%
Polyvinyl Chloride (PVC) and Ethylene-vinyl acetate (EVA) film	Allows UV through, heat retention properties	Not applicable to tropical or warm climates, short lifespan for rigid cladding	Fair, <5 years	Good when kept clean, 87-91%

Many locations, tropical or not, do not have sufficient groundwater supply for a greenhouse operation. Gutter systems with water reservoirs (Figure 3 a, b) provide irrigation water through rainwater harvesting (DeGannes et al., 2014; von Zabeltitz, 2011; von Zabeltitz & Baudoin, 2005). Oversized gutters provide rapid harvesting of rainwater for later use in irrigation during drier periods. The plumbing from the gutters to the reservoirs should include netting to remove debris, and the reservoirs should be light-blocking (black in colour), fully closed or covered with a roof system.

Although simple in design, greenhouse structures can be subject to significant loads from the environment, crop and maintenance routines. The minimum critical wind speed required to impair a typical single-span plastic greenhouse is as low as 52.2 $km \cdot h^{-1}$ (Yang et al., 2013). Tropical structures and their cladding material must be designed to withstand daily rain and wind loads, and the loads imposed by tropical storm winds: 63 to 118 $km \cdot h^{-1}$. Structural balconies provide added rigidity to the structure and supplement the floor space and air volume in natural ventilation greenhouses. The cladding and the sidewall screening can be designed to be removable in the event of an imminent storm, hurricane or typhoon, where the winds exceed 118 $km \cdot h^{-1}$. Wiggle-wire or groove-lock systems allow for plastic films to be installed taut and firmly, but also allow for the films to be dismounted and reinstalled post-storm.

In regions where wiggle wire is unavailable, a system of pipes and plastic or metal clips can be used to tighten and affix the plastic film, such as presented by von Zabeltitz and Baudoin (2005). Moreover, if the cladding is removed, the trellis systems can be descended and tall plants placed close to the ground or bundled onto each other as a form of protection. A greenhouse made from corrugated polycarbonate panels on a sturdy foundation presented by Resh (2012) was designed for the Caribbean to withstand winds in excess of 190 $km \cdot h^{-1}$, and proved to be suitable in winds up to 240 $km \cdot h^{-1}$ during a hurricane event. This sturdier structure located in Anguilla was costly however, and required active ventilation and cooling solutions to sustain proper crop conditions.

Live loads are loads that are temporarily imposed by the occupancy and use of the greenhouse (Hanan, 1997), and this can include the weight of workers maintaining the structure and cladding. The trellis systems in vegetable production can impose substantial additional loads depending on the crop, and therefore can be integrated into the design of the greenhouse or be considered as a separate system. An average pepper (*Capsicum annuum* L.) production in a natural ventilation greenhouse can impose a crop load of 8.5 $kg \cdot m^{-2}$ whereas tomato production can impose a load of 10 to 14 $kg \cdot m^{-2}$ when fruiting (Anderson, 1995), putting a large load on the trellis system. The Dutch standard for crop trellis load is 15.3 $kg \cdot m^{-2}$ (Hanan, 1997). It must be noted that many manufactured greenhouses need to be adapted for such loads as the initial designs may not account for crop or trellis loads.

With the research by DeGannes et al. (2014), von Zabeltitz (2011) and von Zabeltitz and Baudoin (2005), and with attention to local climate, design and material choice, properly protected agriculture can be adapted to the tropics. Still, growers in tropical regions are too often left unaided with greenhouse innovation. Growers frequently remain isolated with their own developments due to a lack of resources and inaccessibility to new technology.

3.2.2 Arid Environment Protected Agriculture

Due to fresh water scarcity, low relative humidity, high potential evapotranspiration and high temperatures, arid environments require protected agriculture to sustain crop production (Al-Ismaili & Jayasuriya, 2016; Al-Jamal, 1994; Gale, 1981). In many arid countries that suffer a chronic shortage of water, such as those of the Middle East and North Africa, over 80% of all fresh water consumed is used for agriculture (Mahmoudi et al., 2010). Increased water use efficiency is critical in arid climate protected agriculture (Mahmoudi et al., 2010; Castilla, 1993). With growing populations, food security concerns and increasing awareness of the declining freshwater availability, protected agriculture is a growing trend in arid regions such as the Middle East.

Arid and semi-arid regions account for approximately 30% of the world total area and are inhabited by approximately 20% of the total world population (Peel et al., 2007; Sivakumar et al., 2005). The arid and semi-arid regions of the world are home to roughly 24% of the total population in Africa, 17% in the Americas and the Caribbean, 23% in Asia, 6% in Australia and Oceania, and 11% in Europe (Sivakumar et al., 2005). An arid climate typically has very low annual precipitation and a large annual potential evapotranspiration. A steppe arid climate (BS, Table 2) receives annual precipitation below annual potential evapotranspiration, but not extremely, whereas a desert arid climate (BW, Table 2) receives very little annual precipitation, sometimes none, and experiences high evapotranspiration (Kottek et al., 2006; Sivakumar et al., 2005).

Reduction of heat stress and control over evapotranspiration is required in arid and semi-arid climates. In desert conditions where temperatures are high and relative humidity is very low, increasing the relative humidity inside the greenhouse causes a desirable reduction in crop evapotranspiration by almost 60 to 80% (Al-Ismaili & Jayasuriya, 2016). In many regions of the Middle East and Northern Africa, the average summer daytime temperatures inside a greenhouse structure can reach 46°C, with the average outside temperature over 38 °C, with very little to no fresh water supply (Al-Ismaili & Jayasuriya, 2016; Mattara et al., 2015; Al-Helal & Alhamdan, 2009; Ali et al., 1990). In Al-Jamal (1994) the maximum temperature in an unvented greenhouse in south-east Jordan, was measured at 75 °C when the outside ambient temperature was about 37 °C. Due to infrared radiation exchange with interactions with the greenhouse cover, the inside temperature was in fact a few degrees below the outside ambient air temperature during late night and early morning hours. In a study by Al-Helal (2007) in Al-Muzahmyah, Saudi Arabia, the average outside temperature and relative humidity varied from 31.7 to 38.7 °C and 11.2 to 16.7%, respectively, from nighttime to daytime. An interesting observation from this study is that the average inside temperature, with crop, dropped to 23.3 °C overnight.

Indeed, arid and semi-arid climates protected agriculture must deal with greatly varying seasonal and diurnal temperatures (Gale, 1981). During hot periods, active ventilation and cooling is required if year-round crop production occurs. Fogging systems and pad and fan systems are the most widespread (Al-Ismaili & Jayasuriya, 2016; Jensen, 2001; Montero, 2006). Evaporative cooling coupled with active ventilation and shading can reduce greenhouse air temperature by up to 8 °C, though some reports show cooling up to 12 °C is possible in hot arid regions (Kittas et al., 2003; Arbel et al., 1999; Al-Jamal, 1994; Singh et al., 1989; Landsberg et al., 1979). Pad and fan systems are effective at cooling the air, but create temperature and humidity gradients from inlet to outlet (López et al., 2012). Whilst fog cooled greenhouse may not be as cool as a pad and fan cooled greenhouse, the conditions will be more uniform. For this reason, fogging systems are sometimes preferred over pad and fan systems (Connellan, 2001; Arbel et al., 1999). Moreover, active ventilation must be limited to avoid stressing the crop through increased transpiration (Kittas et al., 2003).

Although effective at cooling greenhouse temperatures, it is reported that the water used in greenhouse evaporative cooling represents as high as 67% of the greenhouse gross water demand (Al-Mulla, 2006). A study by Sabeh et al. (2007) suggests that pad and fan systems can use up to 18 kg (18 L or 4.8 gal) of water per cubic meter of air with a ventilation rate of 0.053 $ft^3 \cdot ft^{-2} \cdot s^{-1}$ (0.016 $m^3 \cdot m^{-2} \cdot s^{-1}$), and fog systems can use up to 12 kg (12 L or 3.2 gal) with a ventilation rate of 0.036 $ft^3 \cdot ft^{-2} \cdot s^{-1}$ (0.011 $m^3 \cdot m^{-2} \cdot s^{-1}$). To aid in reducing this amount, passive ventilation is utilized as the first stage of cooling followed by pad and fan evaporative cooling which takes over when the passive system is not providing the needed cooling. As previously suggested, the trend in passive greenhouse technology is towards taller greenhouses to reduce the peak greenhouse air temperatures. This technique is most applicable in tropical climate protected agriculture where active ventilation and cooling systems may not be used. This design consideration reduces the efficiency of active ventilation and cooling as the volume of the greenhouse is increased and control over air inlets and outlets is reduced. In order to make a design consisting of a combination of passive and active systems of cooling and ventilation functional, retractable roof systems and closable side and roof vents are necessary. Considering the importance of water use efficiency, there is growing interest in building structures combining both passive and active systems of ventilation to reduce energy and water needs (Kittas et al., 2003; Jensen, 2001).

Evaporative cooling with forced ventilation provides cooling when in optimal working conditions, but presents certain limitations in arid climates. A literature review by Abdel-Ghany at al. (2012) revealed that neither ventilation nor evaporative cooling is sufficient for adequately cooling greenhouses in hot arid regions. The lack of water resources and the salinity of the available water cause a fast deterioration in the cooling performance of the pad and fan systems due to clogging of the pad. The ever-presence of airborne dust and salt accumulation restricts the air flow. Clogged pads were found to reduce the efficiency of the cooling system performances significantly. The electric energy consumed by the fan motors increased by about 22%, while the inside greenhouse air temperature rose to over 52 °C and the relative humidity crashed to below 10%, from 33.6 °C and 33.5% with well operating pads (Al-Helal et al., 2004). It is therefore suggested that preventing heat from entering the greenhouse is the most appropriate technique for cooling greenhouses.

Table 5. The importance of properties of cladding material for use in protected agriculture in arid, subtropical and tropical climates. Adapted from von Zabeltitz (2010).

Property	Arid Climate	Subtropical Climate	Tropical Climate
Anti-dust	High	High	Low
Scattering of direct radiation	High	Medium	Low
No-drip	Low	High	Medium
High *PAR*[a] transmittance	Medium	High	High
FIR[b] blocking	High	High	Low
NIR[c] blocking	High	High in summer low in winter	High

[a] *PAR* Photosynthetically Active Radiation

[b] FIR Far-Infrared Radiation

[c] NIR Near-Infrared Radiation

To reduce the amount of heat entering the greenhouse, various cladding materials are considered. However, similar to tropical climates, arid climates present a harsh environment for plastics. Resistant cladding that is ultraviolet light-stabilized must be utilized. Table 5 presents various roof cladding material properties and their importance for arid, subtropical and tropical climates. NIR reducing cladding material can have advantages under very high solar radiation conditions, such as is found in arid climates and certain tropical regions. These films reduce the undesired NIR reaching the inside of the greenhouse, thereby reducing the inside temperature, while not reducing the amount of PAR reaching the crop (von Zabeltitz, 2010). High temperatures, high solar radiation, aging and accumulation of dust and dirt on the material can be major factors in the degradation of transmittance of polyethylene films. Several undesirable effects can result from arid conditions including rapid deterioration of mechanical resistance and light transmission (Alhamdan & Al-Helal, 2009; Al-Helal & Alhamdan, 2009). Regular cleaning of the film will reduce the accumulation of dust on the film, and regular replacement of the film is required depending on the environmental conditions and financial availability. Some co-extruded and multilayer extruded polyethylene films offer dust prevention, amongst other available properties, but most reduce overall transmittance by roughly 10% (von Zabeltitz, 2010; Giacomelli & Roberts, 1993). Other films provide drip prevention during condensation periods.

It is important to prevent water droplets from accumulating and dripping from the inside of greenhouse cladding and reaching the crop canopy, to reduce disease infestation and water spots (von Zabeltitz, 2010). The accumulation of drops on the underside of cladding reduces transmittance of light, by as much as 21% in some circumstances (Pollet, 2002). No-drip material with film-condensation behavior, instead of drop condensation, combined with a minimum roof inclination will prevent some of the drawbacks of condensation in greenhouses.

Under some arid, semi-arid conditions and subtropical climates, crop damage can occur during clear nights when the inside greenhouse temperature can drop below the outside temperature, caused by far-infrared radiation (FIR) losses through the cladding material (Jensen, 2001; Hoffmann & Waaijenberg, 2001). The temperature drops caused by this effect can cause recurring condensation on the crop leaves, which can lead to various foliar diseases. Retractable thermal screens can be used, but many cladding films are commercially available with a thermicity varying between 15% and 35%, which gives the cladding material the ability to trap only FIR, keeping the crop warm during clear and cold nights (Hoffmann & Waaijenberg, 2001). Photochromic and thermochromic materials are being considered for application in greenhouse cladding films as they are able to keep out NIR only during periods with high irradiation, and trap FIR during cold nights. Other applications may include adaptive shading of the cladding in response to very high solar radiation. The current use of such advanced cladding materials is however limited by high costs (Hoffmann & Waaijenberg, 2001). In any climate and with the use of a variety of cladding materials, the transmittance of PAR should remain high, particularly for vegetable crops (von Zabeltitz, 2010)

By limiting high greenhouse temperatures, using irrigation techniques such as timed or sensor driven drip irrigation and controlling for relative humidity and ventilation, water efficiency can be improved (Dukes & Scho, 2005; von Zabeltitz, 2011). Hydroponic greenhouse crop production in its various forms greatly reduces irrigation water use compared to field growth (Sabeh et al., 2007). Crop quality and crop productivity can be increased by use of hydroponic systems, not only in extreme climates, but in all forms of protected agriculture. In a deep well or deep flow hydroponic system, chilling of the nutrient solutions was shown to reduce bolting and tip burn incidents in lettuce (*Lactuca sativa* L.), which is especially important in tropical and desert regions (Jensen, 2002). Alternatively, studies by Fereres and Soriano (2007), Tüzel et al. (2013) and Alomran et al. (2013) present deficit irrigation methods as an important tool to achieve the goal of reducing the use of irrigation water. Although many options are available to growers, rockwool is currently still the main growth substrate used, as presented in the previous section. There are however an increasing number of growers who are considering the drawbacks of rockwool such as the harmful effects on human health, problem of disposal after use and the susceptibility of crops to root diseases (Benoit & Ceustermans, 1995; Os Van, 1995; Yu & Komada, 1999). The same organic substrates presented in the previous sections for tropical climates can be considered for use in arid climates. Szmidt and Graham (1989) reported the use of polyethylene oxide as a hydrogel substrate for plant growth under the use of highly saline irrigation water. In fact, salinities of up to 32 000 ppm sodium chloride, which nears that of most seawater, were applied and it was shown that plants in the presence of the hydrogel were tolerant to all levels of salinity tested. The development of such technology would allow growers in arid regions to be less dependent on vast amounts of freshwater irrigation.

Many solutions are available for greenhouse growers in hot arid climates in order to control the environment of the greenhouse. Most involve the use of active measures to reduce the air temperature and evapotranspiration, which makes them electricity-intensive. The focus of the current work is to combine passive solutions with active solutions to make greenhouse cooling more efficient in arid climates. Work by Sethi and Sharma (2007) offers a comprehensive review of greenhouse cooling technologies. Some characteristics that make arid and semi-arid regions harsh, also offer positive benefits. For example, the annual solar radiation in most arid areas can easily double that of temperate climate regions (Gale, 1981). This is an advantage for increased crop yield, and if properly harnessed, can be a technical benefit. The seawater greenhouse is a technology that uses seawater and solar energy to humidify and cool the greenhouse air, and through solar heating, condense fresh water (Figure 4). Two growing areas in a seawater greenhouse are cooled in this process, and condensing water from the humidified greenhouse air, using a web of tubing, results in a freshwater supply. The maximum air temperature drop was 9.8 °C when the ambient air temperature and relative humidity were 38.5 °C and 25.4%, respectively (Al-Ismaili & Jayasuriya, 2016). Some drawbacks such as high construction costs for sizeable operations and low efficiencies are challenging this technology (Zurigat & Abu-Arabi, 2004; Chaibi, 2000). Seawater greenhouses have been built in Tenerife, Spain; Abu

Dhabi, United Arab Emirates; near Muscat, Oman (Figure 4) and most recently in Port Augusta, South Australia (Al-Ismaili & Jayasuriya, 2016).

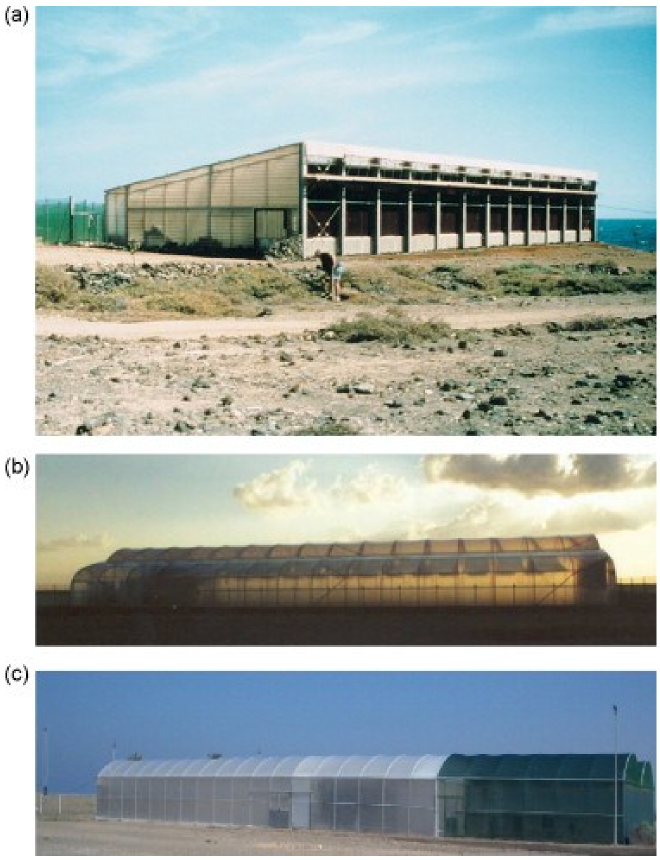

Figure 4. Illustrations of seawater greenhouses. (a) The seawater greenhouse in Tenerife, Canary Island 1992. (b) Seawater greenhouse constructed on Al-Aryam Island, Abu Dhabi, United Arab Emirates, 2000. (c) The seawater greenhouse at Al-Hail, Muscat in the Sultanate of Oman, 2004. Reprinted from Mahmoudi et al., (2010) with permission from Elsevier. See Appendix F for license.

In some semi-arid regions, the greenhouse industry has grown tremendously by profiting from the near constant solar radiation. The arid climate region of Almería, Spain has a large greenhouse industry, with now over 55 000 ha of production, mostly natural ventilation structures, making it one of the largest greenhouse concentrations in the world (Franco et al., 2014; Soto et al., 2014). Summer conditions for crops in these greenhouses remain far from optimal, especially with regards to temperature and vapor pressure deficit (Meca et al., 2013). In Almeria and other Mediterranean regions, high temperatures (>35 °C) and high vapor pressure deficit (>1 kPa) are common in greenhouses during the summer months (Katsoulas et al., 2001). These conditions are responsible for the decrease in yield and quality of greenhouse production. Recent work on protected agriculture in this region suggests that passive evaporative cooling through fogging coupled with shading is the most effective at creating an improved plant environment (Meca et al., 2013). Other research has reported alternative evaporative cooling techniques for arid climate greenhouses that use less forced ventilation than typical pad and fan systems (Franco et al., 2014). Nonetheless, natural ventilation remains the most practical and economical, and therefore the most used method to lower greenhouse temperatures (Meca et al., 2013). However, there is still a lack of control of the plant environment, as these passive systems are oftentimes open to the environment leaving the crop exposed to the natural environment. Increased adjustability, to deal with diurnal and seasonal changes, is needed (Castilla & Montero, 2008). Throughout arid climate protected agriculture, many challenges remain with regards to cladding material choice, energy and water use efficiency and proper control of the plant environment.

3.2.3 Polar Environment Protected Agriculture

The major difficulties with growing food in polar regions are the very short production season, typically less than 60 days between frosts; very long summer days with up to 24-h daylight; and cold, dark winters with up to 24-h nighttime periods (Humphries and Landry-Cuerrier, 2013). Outdoor field production is limited to crops that can handle the very short growing season and long days, and not be impacted by the winters (Dearborn, 1979). Very few plants can handle this production stress, and very few fruits or vegetables can be produced during this time. Most vegetable production is impossible without protected agriculture, even during clement periods, permafrost and ice cover prevent any traditional form of agriculture. The high costs of transportation to these regions are embodied in all goods and materials used in northern retail logistics, including fruit and vegetable production and retail. Access to market foods is currently very difficult due to a lack of accessibility given the high transport costs and lack of availability due to an absence of in situ production. The evidence from many reports indicate that far-northern Canadian populations, for instance, face poor quality along with high prices and periodic unavailability of fruits and vegetables (Chan et al., 2006).

A polar climate is usually found north or south of respective 60° latitude and is characterized by cool summers and very cold winters. A tundra polar climate (ET, Table 2) has an average maximum summer temperature of 10°C, whereas a frost polar climate, or icecap climate (EF, Table 2), has an average maximum monthly temperature that never surpasses 0 °C (Kottek et al., 2006). Some northern polar regions experience mean high daily temperatures of -37.4 °C (Eureka, Canada, 79°59′N, 85°56′W) during the winter months, whereas regions in the interior of Antarctica can experience mean daily temperatures that never surpass -29.9 °C year-round (Vostok Station, Princess Elizabeth Land, Antarctica, 78°27′S, 106°50′E) (Environment Canada, 2016; Keller et al., 2010). In most polar regions and some continental regions, daily minimums can reach below these values. Many cold or continental climates (D, Table 2) can show characteristics of extreme climates, with cold summers or very cold winters. Polar-like climates can be found sporadically within other climate zones, namely at high altitudes. They can be referred to as alpine, montane or highland climates, usually found at altitudes above the tree line, and are also abbreviated as polar ET.

The most common reported passive systems in the Arctic and Antarctica consist of mostly plastic covered greenhouses, with a variety of other materials sparsely in use (Chapin & Shaver 1986; McCurdy & Svoboda 1989; Coulson et al. 1993; Debevec & MacLean 1993; Havström et al. 1993; Strathdee & Bale 1993; Wookey et al. 1993; Kennedy, 1995). Many of these studies, however, did not focus on protected agriculture of food crops, but rather on related issues such as biomass growth. Chapin and Shaver (1986) in Brooke Range, Alaska (68°38'N, 149°34'W) reported the use of a glasshouse for growth of fern (*Eriophorum vaginatum*). McCurdy and Svoboda (1989) described radish production in a temporary hemispherical solar heated greenhouse in Alexandra Fiord, Nunavut, Canada (78°54′N, 76°00′W). Coulson et al. (1993) and Wookey et al. (1993) studied artic and subarctic plant species using small polythene tents to simulate microclimates on vegetation in polar-desert and tundra climates in Ny Ålesund, Svalbard, Norway (78°56'N, 11°49'E). Havström et al. (1993) studied a shrub species in Abisko, Sweden (68°21′N, 18°49′E) and Ny Ålesund, Svalbard, Norway and used PVC tubing and polyethylene sheeting to simulate microclimate changes in CO_2 concentrations and temperature. Clear acrylic and polystyrene sheeting with Agrofleece was used in a study by Strathdee and Bale (1993) to elevate temperatures in global warming modelling experiments in Ny Ålesund, Svalbard, Norway. Finally, Kennedy (1995) offers a review of various passive greenhouse designs in high-latitude climate change experiments. Although informative for protected agriculture development, the structures used in these studies were all temporary and for experimental use and not food production.

Although severely extreme, extraterrestrial conditions are comparable to terrestrial polar climates in terms of cold temperatures, low light levels and remoteness (Bucklin et al., 2001). In fact, space-based advanced life support systems, which provide fully controlled environments, benefit significantly from ground-based experience in greenhouse production. Development of extraterrestrial technology is routinely tested in polar conditions on Earth. Reciprocally, advanced life support systems have and continue to demonstrate significant technology transfer to terrestrial greenhouse production (Bamsey et al., 2009). The Haughton Mars Project's Arthur Clarke Mars Greenhouse (ACMG) in the Canadian High Arctic (75°26′N, 89°52′W) has supported extreme environment related research for many years (Giroux et al., 2006). A group at the German Aerospace Center is currently developing a shipping container-style closed system named the Eden ISS that will be deployed at the Neumayer III station in Antarctica in late 2017 (Zabel et al., 2015). A container-style plant production unit named the Canadian Integrated Northern Greenhouse (CING) is currently being developed for use in far-northern regions of Canada by Gaudet et al. (2014) (Figure 5). With the growing trend of modular indoor agriculture solutions in urban centers, researchers are combining many indoor controlled environment technologies and adapting them for use in harsh northern climates. Other systems, such as that presented by Guo et al. (2008) and Bucklin et al. (2001), show solutions for plant growth in extreme environments based on extraterrestrial plant growth requirements. The controlled ecological life support system, or CELSS, presented by Guo et al. (2008) contains a volume of 40.0 m^3 and a cultivating area of 8.4 m^2 with a growing structure that allows the vertical distance of each growing bed to be adjusted automatically and independently. The system controls and logs parameters such as temperature, relative humidity, oxygen concentration, carbon dioxide concentration, total pressure, lighting intensity, photoperiod, water content in the growing-matrix, and ethylene concentration. An extensive review by Zabel et al. (2016) presents decades' worth of progress in this field.

Figure 5. Canadian Integrated Northern Greenhouse (CING) being developed for applications in the far-northern communities of Canada. Seen here at the Macdonald Campus of McGill University in Ste-Anne-de-Bellevue, QC, Canada (45°24′N, 73°57′W).

There are currently many greenhouse projects in the far northern regions of Canada, for example a pilot project community greenhouse in Inuvik, Canada (68°21′N, 133°43′W) (Public Health Agency of Canada, 2009). These regions show varying intensity of the cold harsh climate. Some pilot projects for far-northern protected agriculture in Canada look to link industry related waste heat with greenhouse operations to overcome the high heating needs (Humphries & Landry-Cuerrier, 2013). This can be sometimes referred to as a waste-to-energy scheme, and has been studied in Northern Italy by Chinese et al. (2005). Other projects are focusing on adapting passive, or sometimes called Chinese-style solar greenhouses, and deep winter greenhouses, for far-northern or far-southern climates. These greenhouses, already in use during winter seasons in temperate climates, have a variety of designs, but are typically oriented east-west and have a solar-facing glazed side with a solid northern side. The glazed side is angled according to the local latitude, plus 15°, to maximize absorption of solar radiation (Tiwari, 1985). Such designs rely on direct solar energy to heat the greenhouse during the day, and store energy in large thermal masses for use during the colder night periods. The Chinese-style solar greenhouse stores the thermal energy in the north facing wall, whereas the deep winter greenhouse stores energy in an underground rock bed. Waaijenberg et al. (2004) have studied the design of a highly insulated solar greenhouse using inflated structural cladding. Supplemental lighting and heating is still required in such designs for effective year-round production. It was found by Van Ooteghem (2010) that in an optimally controlled solar greenhouse with heating, the use of an aquifer as a thermal mass can reduce natural gas use by 52%, while the resulting crop production can be increased by 39%, as compared to an optimally controlled conventional greenhouse without the solar greenhouse design. Beshada et al. (2006) designed a greenhouse in Eli, Manitoba (49°54′N, 97°45′W) with an insulated solid north wall and a thermal blanket system. On the coldest day, the lowest nighttime temperature recorded inside the greenhouse was 1.6 °C when the outdoor temperature was -29.2 °C. The mean night indoor temperature was 2.4 °C while the mean outdoor temperature was -13.1 °C in the month of February. It was found in the study that solar radiation had more influence on the greenhouse temperature than did the outdoor temperature, and that supplemental heating is required to maintain adequate greenhouse temperatures. Debevec and MacLean (1993) studied the effects of clear polyethylene plastic film, polyester fabric, and rigid fiberglass panels on light transmission, photosynthesis of plants, air and soil temperature, and thaw depth, at a location 165 km north of Fairbanks, Alaska (64°50′N, 147°43’W). They reported that greenhouses covered with plastic elevated daily maximum and daily mean air temperatures by an average of 7.8 and 2.0 °C, respectively. The use of fabric had very little effect. Soil temperature at a 10-cm depth was elevated in all greenhouses, but no effect on depth of thaw was detected.

The extremely cold conditions, lack of sunlight, and inaccessibility are some of the challenges that need to be overcome in polar and polar-like conditions. Heating and lighting energy requirements can be very high in these colder climates, especially during cold and dark seasons. In large glass-covered heated greenhouses, in far less severe conditions, the heating requirements accounts for 30 to 50% of the total production cost (Wang et al., 1999). Various ground-source heating systems, such as those suggested above and by Hepbasli (2011), are not feasible in true polar protected agriculture due to the presence of permafrost or continuous ice cover. A review of passive greenhouse heating for milder climates is presented by Sethi and Sharma (2008), but only considers cold locations from 28 to 52.5 °N latitude. Natural gas, oil and biomass heating using water boilers and networks of piping are widespread in colder climate protected agriculture (Chau et al., 2009; Teitel et al., 1996). Biomass heating is in fact developing quickly in subarctic off-the-grid communities (Exner-Pirot, 2012). Hepbasli (2011) compares efficiencies of various water boiler systems, including natural gas and biomass boilers. Currently, condensing boilers and retractable thermal screens are very common solutions used for heating and conserving heat in greenhouses in Southern Canada, which can experience polar-like conditions during winter months. However, many polar regions, such as most of the Arctic and Antarctic regions, do not have access to biomass. Without access to natural gas, other energy sources such as wind and micro-nuclear power may provide cost effective sources of energy in the future (Exner-Pirot, 2012). Exner-Pirot (2012) published a report on the Chena Hot Springs greenhouse in Alaska (64°50′N, 146°25′W) that uses geothermal energy to sustain 12-month plant production (Figure 6).

Figure 6. A view of the LED lighting fixtures and natural lighting in the Chena Hot Springs Greenhouse, Alaska (64° 50′ N, 146° 25′ W) (Exner-Pirot, 2012).

In cold but not polar climates, many forms of greenhouse double-walled cladding have been proposed, including double-wall rigid sheets of acrylic or polycarbonate materials, and the use of two polythene sheets with a pressurised air space between them (Roberts et al., 1989). Some even suggest a triple layer to collect condensation during the spring months (Giacomelli &

Roberts, 1993). Thermal screens have yielded valuable energy savings for many growers in cold regions, but show certain limitations such as increased relative humidity during overnight use and restrictions of daytime sunlight even when retracted (O'Flaherty & Maher, 1987). During clement periods, dehumidification can be accomplished by ventilation with heat recovery at times of heat demand, and by using the windows at times of heat surplus, as in normal greenhouse practice (Van Ooteghem, 2010). Comparisons of energy conserving capabilities of greenhouse covering systems in combination with movable nighttime insulation systems have been documented extensively, with a summary reported by Roberts et al. (1989). Due to large snow loads and high winds, cladding choice and structural strength of polar climate protected agriculture systems become yet additional challenges. Typical glass and film greenhouse materials, as they are currently used, do not have structural and thermal resistances suited for extreme cold temperatures or large snow loads. In the study by Beshada et al. (2006), the solar greenhouse built in Manitoba had an insulated solid north wall with a thermal resistance of 3.6 $m^2 \cdot °C \cdot W^{-1}$, to store solar energy in the daytime and to release thermal energy in the nighttime. It also integrated a cotton thermal blanket of resistance 1.2 $m^2 \cdot K \cdot W^{-1}$ over the glazed surface during nighttime, to minimize heat loss. The glazed plastic cover was a single layer of 6-mil polyethylene, which has a solar radiation transmissivity of 0.90. The RSI value for typical 6-mil polyethylene film is 0.15 $m^2 \cdot K \cdot W^{-1}$ and common 3-mm glass panels have an RSI value of 0.17 $m^2 \cdot K \cdot W^{-1}$. The structural live load specifications for typical greenhouses can range from 58.6 to 73.2 $kg \cdot m^{-2}$ and is typically for loads applied by workers for construction and repair (Bucklin, 2015), but can be suitable for environmental loads such as snow loads in temperate climates. This is because the low thermal resistance of these materials allows heat from the greenhouse to melt the snow as it accumulates. High winds, low temperatures and large snowfalls render such a system unfeasible in more extreme climates. To adapt to extreme conditions, the cover of the Arthur Clarke Mars Greenhouse was made of 6 mm Twin Wall Lexan polycarbonate sheets, with an RSI value of 1.55 $m^2 \cdot °C \cdot W^{-1}$, supported by 1.2-m spaced steel struts complying with a 163-$kg \cdot m^{-2}$ live load specification and resisting up to 144-$km \cdot h^{-1}$ wind speeds (Giroux et al., 2006). The trellis load must be considered when dense crop production is occurring. Some greenhouse manufacturers have designed for live loads beyond 450 $kg \cdot m^{-2}$. Such structures, including the ACMG, are small however, and designing commercial sized greenhouses with good light transmittance in extreme polar conditions remains a challenge.

With such focus on heat retention structural soundness, the structures built for protected agriculture in polar regions can overheat during the short summer seasons, and require significant ventilation. Instead of designing for two very contrasting sets of conditions, some growers will dismiss their greenhouses during summer months as the ventilation requirements are too great.

Multilayered rigid cladding and reinforced frames provide thermal insulation and structural strength, but can reduce the already low levels of solar radiation. Thermal insulation prevents snow from rapidly melting on the greenhouse cladding, which is the preferred method for snow removal on greenhouse structures. The significant snow accumulation provides another cause of shading. This introduces the design trade-off between light transmission, snow melt and thermal insulation. Some may choose to allow snow to accumulate over the course of a season and supply artificial lighting, or snow removal can be performed if logistics allow for it. With the increasing efficiencies of artificial lighting for crop growth, some fully closed systems may be developed to be more efficient than greenhouse-style systems, for insulation issues are lessened if light transmission is entirely ignored. Modern rigidly structured plastic coverings, such as fiberglass, polycarbonate, acrylic, and polyvinyl carbonate are normally corrugated or have multilayered cross-sections for strength. They are strong, have a long life, and double-walled panels improve heat retention in the greenhouse. An extensive review of greenhouse structural cladding is presented by Briassoulis et al. (1997). A potentially practical insulation solution presented by Valerio et al. (2014) offers as a low power variable insulation system combining sunlight-concentrating structures and low cost thermal insulation. Experimental devices have achieved thermal resistance values exceeding RSI 3.33 $m^2 \cdot K \cdot W^{-1}$ while also maintaining light transmittance values greater than 70% (compared to RSI 0.42 $m^2 \cdot K \cdot W^{-1}$ for triple layer polycarbonate and RSI 0.30 $m^2 \cdot K \cdot W^{-1}$ for polyethylene double 6-mil film).

In response to dark natural conditions and structural shading, supplemental electrical lighting is required (Figure 6) to achieve satisfactory plant growth (Bucklin at al., 2001). Light emitting diodes (LEDs) are one of the most promising technologies for controlled agriculture plant lighting systems (Massa et al., 2008), especially for extraterrestrial crop growth applications (Barta et al., 1992; Massa et al., 2007; Morrow, 2008; Mitchell, 2012; Poulet et al., 2014). Techniques such as intercanopy lighting can improve light distribution and thus increase crop yield and light use efficiency in enclosed or low light circumstances such as polar climates, indoor agriculture and vertical farming (Hao et al., 2012; Jokinen et al., 2012). Even with efficient LED technologies, the energy requirements for supplemental lighting remain relatively high. Recent assessments show that an enclosed system providing 1500 $\mu mol \cdot m^{-2} \cdot s^{-1}$ of artificial light requires 2.175 $kW \cdot m^{-2}$ (Anderson et al., 2015). In contrast to other forms of protected agriculture however, in polar protected agriculture the waste heat from lighting can be directly used to heat the plant space (Hao et al., 2012; Bucklin et al., 2001). To reduce energy requirements and the overall cost, it is suggested to maximize the use of solar radiation when it is available, even indirectly via solar collectors and concentrators (Bamsey et al., 2009; Bucklin et al., 2001). Combining natural light with electrical sources in challenging environments can decrease the equivalent system mass of a closed plant production chamber by 45% (Drysdale et al., 1999). This may seem like a specific parameter to only extraterrestrial technologies, but this can be particularly beneficial for technologies needed in remote and polar regions. A vast portion of Canada is not served by all-weather roads or railways (Council of Canadian Academies, 2014) and less bulky systems are easier to transport.

According to Humphries and Landry-Cuerrier (2013), pilot greenhouse projects such as that in Inuvik, Canada, other northern Canadian regions, and in Northern Europe demonstrate that high latitude production of quality vegetables is possible. But the major challenge is to increase the scale, efficiency, and sustainability of these projects. Achieving such goals requires greenhouse production designed specifically for each local polar climate. The technology developments for extraterrestrial plant production can provide countless terrestrial benefits in the fields of food safety and security for communities, and overall plant production efficiency (Bamsey et al., 2009). In combination with existing protected agriculture solutions, such as biomass and passive heating methods, this innovative technology can be a promising solution for the harsh conditions of polar climates.

3.2.4 Urban Protected Agriculture

Although not perceived as an extreme environment to humans, urban protected agriculture is an expanding form of extreme environment plant production that combines a variety of technologies from all types of protected agriculture, from arid to extraterrestrial. Known under multiple aliases such as cubic farming, vertical farming, Zfarming, plant factories with artificial lighting (PFAL), closed plant production system (CPPS) or simply indoor agriculture. Urban protected agriculture is combining technologies from all types of controlled environment agriculture. Some examples of work on urban farming techniques include vertically suspended grow bags for lettuce and strawberry (Neocleous et al. 2010), the use of vertical columns for strawberry production (Linsley-Noakes et al. 2006), conveyor-driven stacked growth systems (Mahdavi et al. 2012), A-frame designs for medicinal herb, rhizome, and root crops (Hayden, 2006), cable and tray systems with intercanopy lighting for a variety of crops (McCartney, 2015), and plant factory approaches for a variety of crops (Kozai et al., 2015). Although current trends are putting urban indoor agriculture in the spotlight, it is not a novel technique. The U.S. and Japan have worked on fully controlled vegetable factories using only artificial light, with the aim of year-round planned production since the 1970's, and Japan is now leading in the field of plant factories (Watanabe, 2009; Newbean Capital, 2016). Moreover, besides indoor agriculture, urban protected agriculture includes semi-closed systems such as rooftop greenhouses (Specht et al., 2014), though the former will not be discussed in this paper. For a review of North American rooftop agriculture and a presentation of initial European work, see Dvorak and Volder (2010).

The rationale behind urban protected agriculture can be vast. As increasing urbanization and population growth continues, new agricultural approaches are expected to contribute to delivering fresh and local food for cities (Kozai et al., 2015; Mok et al., 2014; Specht et al., 2014; Wimberley et al., 2007). Currently, over 6,000 tons of food is imported every day in a large city with a population of 10 million or more (Eigenbrod & Gruda, 2015). In a city such as London, England, the equivalent of 40 % of Britain's entire productive land is required for meeting its food needs, even if only 12% of the population live in the city (Deelstra and Girardet, 2000). With a global population expected to reach 9 billion by 2050, with more than half of the population living in cities, an estimated 70 to 80% increase in agricultural production will be required (Corvalan et al. 2005). This increase will be met with many challenges, including the toll that such production will have on the environment. Currently, retailing and food distribution systems, relying on lengthy storage techniques and motorised transport, impose a heavy environmental toll (Kulak et al., 2013; Eigenbrod & Gruda, 2015). It is stated that eventually, cities that heavily rely on food imports may need to consider reviving agricultural production in urban areas or in the urban fringe to reduce the demand for land surfaces elsewhere (Deelstra and Girardet, 2000). The significance of urban agriculture around the world has been stated by many, and a review by Mok et al. (2014) offers noteworthy insight on a) the impacts of continued urban sprawl and loss of peri-urban agricultural land; b) appropriate government and institutional support; c) the role of urban agriculture in self-sufficiency of cities; d) the risks posed by pollutants to and from agriculture to urban ecosystems; and e) the carbon footprint of urban agriculture. Kulak et al. (2013) presents an integral assessment of the advantages urban agriculture presents in terms of greenhouse gas emission reductions, with respect to many types of crops. Besides food production, fully controlled plant factories provide suitable systems for the production of medicinal plants and genetically modified crops for pharmaceutical use (Goto, 2012).

As with polar and extraterrestrial protected agriculture, due to factors such as limited space and unavailability of soil or natural light, urban protected agriculture can require a high level of control, and therefore some of the same technologies are found across these types of production. As previously mentioned, high levels of control of the plant growth environment can be quite resource-demanding and technically challenging. However, the advantages of a high level of control are many, the most important being the capacity to optimize the environmental conditions necessary to achieve ideal growth of nearly any crop. This ensures maximum yield per area of growing space (Despommier, 2013). Combined with ideal conditions, the use of multilayer growth shelves has contributed to increasing productivity. Productivity is often expressed as yield per unit area, and depends on the crop being grown. From four to 10-layer shelf systems are currently used in commercial plant factories in Japan (Goto, 2012). Other methods such as rotating track multilayer systems are being developed for increased crop uniformity and ease of harvest (Figure 7). Fischetti (2008) proposes yields in indoor agriculture four times that of field operations, whereas McCartney (2015) and Kozai et al. (2015) suggest lettuce yields hundreds of times that of field based systems. In another recent study, a vertical agriculture system produced 13.8 times more crop compared to a typical horizontal hydroponic system, calculated as the ratio of yield (fresh mass) to occupied growing floor area (Touliatos et al., 2016).

Figure 7. Stainless steel tray and cable system used in an indoor farming system. The modular nature of the growth units can be seen. The growth units are placed side-by-each in the fully closed warehouse space. Copyright 2015 ASABE, used with permission.

The modifications that growers can bring to the growing environment are endless, and the plant responses to these alterations are countless. Stapleton and Hochmuth, (2001) investigated 12 vegetable varieties, including arugula (*Eruca vesicaria*), basil (*Ocimum basilicum*), and oregano (*Origanum vulgare*) in a vertical growth system and reported excellent plant vigor and growth. Increased productivity is not the only positive outcome of indoor agriculture. Given the level of control of parameters such as light quality and nutrient delivery, plant morphology can be altered (Massa et al., 2008; Morrow, 2008) and nutritionally important components in the crops can be improved if desired, such as pigments, glucosinolates and mineral elements (Kopsell et al., 2015). For example, in a study by Lefsrud et al. (2008), chlorophyll *a* and *b* concentrations in kale seedlings (*Brassica oleracea* var. acephala) were highest when exposed to LED wavelengths of 640 and 440 nm, which established a positive correlation between wavelength and chlorophyll accumulation. Others showed that white light supplemented with blue light (476 nm) resulted in significantly higher lettuce leaf tissue β-carotene and total xanthophyll carotenoids (Li & Kubota, 2009).

The modularity of many urban agriculture systems is a growing trend that offers many advantages, such as easy transport and mobility of the structures. Cubic farming, or container-style plant production, is based on plant factory technology but is modular, standardized, easily expandable and can adapt to nearly any climate or environment, beyond that of an urban setting. Moreover, with increasing system automation, the rising potential plant density in vertical farming operations contributes to increased resource and energy efficiency. The use efficiencies of water, CO_2 and light energy are considerably higher in fully controlled plant production systems when compared to conventional greenhouses (Kozai et al., 2013). Kozai et al. (2013) reported a water use efficiency in the range of 0.95 to 0.98 in the studied vertical agriculture plant production system, and compared these values to 0.02 to 0.03 in typical greenhouse systems. Their findings suggest that controlled environment plant production systems can be 30 to 50 times more efficient in terms of water usage compared to greenhouses. Additionally, impressive investment and development is being made in the agricultural lighting sector (Newbean Capital, 2016), which suggests continuous improvements and even better efficiencies in the future.

Although a booming sector of agriculture, the world of urban controlled environment vertical agriculture faces important challenges in improving and developing the technology (Kozai et al., 2013). For instance, airflow becomes a challenging matter due to the very high density of the crops. The improper design of air conditioning and air distribution systems in an indoor plant factory can cause non-uniform environmental condition and airflow patterns, leading to non-uniform crop growth, uneven quality and crop disorders (Zhang et al., 2016). A study by Zhang et al. (2016) offers some recommendations in terms of air flow in vertical controlled environment plant production systems, such as the use of perforated air tubes able to provide an average air velocity of $0.42\ m \cdot s^{-1}$. Other issues such as plant size restrictions in vertical plant systems are forcing researchers to focus on highly productive dwarf varieties of certain crops, such as the ‘Micro-Tina’ tomato (Scott et al., 2000). This same issue is shared with extraterrestrial plant production systems. The ‘Micro-Tina’ variety is used by researchers in the field of extraterrestrial plant production (Schulze et al., 2016).

With the correct technology, indoor agriculture in an urban setting can offer rapid plant growth and unparalleled consistency without the use of fungicides, herbicides and pesticides. The result is a resource-efficient and fully traceable operation compared to soil-based agriculture

(McCartney, 2015). The advantages, however, come at a cost. Estimates based on high-pressure sodium lamps and fluorescent light systems indicate that lighting accounts for approximately 40% of the total running cost for vegetable production (Watanabe, 2009). Ventilation, air circulation, air quality control, heating and cooling are energy intensive in an enclosed system. At present, is it estimated that 10 kWh of electrical energy is consumed to produce 1 kg of lettuce in a plant factory setting (Kozai et al., 2015). As with other forms of protected agriculture that incorporate supplemental lighting technology, improvements in LED lighting quality and efficiency, as well as techniques such as intercanopy lighting, can improve light use efficiency (Hao et al., 2012; Jokinen et al., 2012). Kozai et al. (2015) offers detail with regards to resource savings, amongst other topics, in indoor farming with electrical lighting.

Technology-intensive indoor agriculture operations with artificial light in urban areas are steadily increasing in number (Kozai et al., 2014). Such operations are a potential driving force for the development of resource-efficient technology to enhance the sustainability of protected agriculture. The number of urban, indoor and warehouse agricultural operations in the U.S. has grown from 15 to 56, from 2015 to 2017 (Newbean Capital, 2017). In Japan, the number of plant factories with artificial lighting for commercial production of leaf vegetables, such as lettuce and spinach, has increased from 35 in December 2009 to 106 in December 2011 (Kozai et al., 2013). In the whole of Asia, it is reported that there are over 518 plant factories, as of the end of 2016, and three operating commercial container-style farms, with four to five others in the process of commercializing (Newbean Capital, 2016).

Several countries with widely varying climates, such as South Korea, China, Italy, Holland, Jordan, Saudi Arabia, and Canada, amongst other, are developing various forms of vertical farming projects (Besthorn, 2013). In areas where available, alternative energy sources like geothermal, wind and sun driven energy supplies can help counter a strong reliance on energy (Kozai et al., 2015; Despommier, 2011). Waste-to-energy schemes, such as suggested in polar region, could be incorporated in urban vertical farming project. Regions of the world that offer relatively affordable electricity can serve as testbeds for novel vertical farming technologies. For the moment being, upfront investment costs are high, as designers learn how to best integrate the various systems needed. Smaller prototypes must be built, as they are needed for the integration of the required technologies (Despommier, 2009). It is evident and suggested by many that further research should consider innovative means for improving energy efficiency

(Kozai et al., 2016; Wheeler, 2015). As other types of protected agriculture develop alongside urban agriculture, new technology will be available and will be adapted for use by growers in urban centers.

3.3 Concluding remarks

Protected agriculture offers technology of varying complexity to suit the immediate needs of the growers, depending on the local climate. It allows for high quality and quantity plant growth during off seasons, or in adverse environments to traditional plant production. Work remains to be done in the fields of plant science and engineering as many systems require proper adaptation and improvements, especially in terms of energy use efficiency.

In tropical and arid climate protected agriculture, work still remains with regards to:

- Sustainable and energy efficient cooling and ventilation technologies
- Sustainable and efficient water use methods
- Properly adapted materials for high temperatures and strong solar radiation
- Accessibility of technologies
- Automation of systems

In polar protected agriculture:

- Sustainable and energy efficient heating technologies
- Cladding materials that offer high light transmission and high insulation properties
- Energy efficient electrical lighting
- Accessibility of technologies and ease of transport of material

In urban protected agriculture:

- Energy efficient electrical lighting
- Energy efficient air quality control, heating and cooling
- Automation and control technologies
- Affordability of technologies

With the outcomes of climate change and a growing world population, protected agriculture will undoubtedly adapt to extreme environments. As we develop sustainable living for space, we will also learn more about sustainable living on Earth (Wheeler, 2015).

Connecting Text

Chapter 4, *Field Trial of The Natural Ventilation Augmented Cooling (NVAC) Greenhouse*, was authored by Lucas McCartney and Mark. G. Lefsrud. Chapter 4 was submitted to the journal *HortTechnology* on June 7, 2017 and is currently in under review.

Chapter 4 embodies the development of the NVAC greenhouse design in field trials. The first NVAC greenhouse was built in 2012 at McGill University in Ste-Anne-de-Bellevue, QC, Canada under summer conditions to test the concept. Subsequent builds and testing in Ste-Anne-de-Bellevue and in Trents, Barbados allowed for further design refinement and data collection under field conditions. Following the knowledgebase of Chapter 3, Chapter 4 explains the various design considerations that were taken into account to make this greenhouse successful in arid and tropical climates. The climate in Barbados is a wet and dry (savanna) tropical climate that oftentimes borders on arid during the dry season, with strong solar radiation year-round. This type of environment was suitable for field development of the NVAC greenhouse. This chapter defines the requirements for automation of the system and the overall performance and efficiency of the NVAC greenhouse under field conditions. In Appendix B, a detailed account of the construction process of an entire NVAC greenhouse in Holetown, Barbados, including the greenhouse structure, is presented in text, figures and via video media.

4. Chapter 4: Field Trials of The Natural Ventilation Augmented Cooling (NVAC) Greenhouse.

Lucas McCartney and Mark G. Lefsrud

Additional index words. evaporative cooling, arid climate greenhouse, subtropical climate greenhouse, tropical climate greenhouse, natural ventilation

4.1 Abstract

Greenhouses create an optimal growing environment for crops through control of environmental parameters including temperature, relative humidity, light conditions and through protection from harsh weather and pests. Traditional greenhouse designs use ventilation systems and evaporative cooling to decrease inside air temperature and provide fresh air to the crop. Such systems are energy intensive, require maintenance and are not available to all markets, making them unsuitable for certain regions. Other locations such as regions with arid and hot climates may have access to the newest technology but may wish to reduce the energy input required to provide an adequate greenhouse environment. Some greenhouse designs rely solely on natural ventilation, which makes them suitable for use in milder climates or for the production of heat-tolerant crops. For warmer climates, we propose a natural ventilation augmented cooling (NVAC) greenhouse. The NVAC greenhouse is naturally ventilated and improved by augmenting the thermal buoyancy and wind effects with a strategically placed misting system. The greenhouse structure is comprised of tall sidewalls, oversized side vents, a roof vent, and an additional inside roof. The misting system is located above the gutters of the greenhouse and sprays a mist of water horizontally between the top roof and the added inside roof. The added roof guides the cooled air to the plant space and prevents water droplets from reaching the crop foliage. Prototypes were built at the Macdonald Campus of McGill University in Ste-Anne-de-Bellevue, QC, Canada where tests were performed during hot summer days in a temperate climate. A large prototype was built in Trents, Barbados where the design was improved and tests were performed in a tropical wet and dry climate. In its final design, the NVAC greenhouse design provided cooling ranging from 1.3 to 3.6 °C in comparison to outside temperatures, while

increasing relative humidity by 5.7 to 17.7%. The temperature response was rapid, dropping by 3.3 °C within 120 s after activation of the system. The NVAC greenhouse is a simple and affordable design that uses 5.6% of the electricity required to run a pad and fan system in a comparably sized greenhouse. The NVAC misting system can be used both intermittently or continuously, as needed, to cool greenhouse temperatures year-round or to extend the growing season. Site-specific conditions such as wind gusts and natural variations in daily temperature and relative humidity must be considered as they play a large role in the design and performance of the NVAC greenhouse, and an automation system can help improve usage.

4.2 Introduction

Although many active greenhouse cooling and ventilation methods exist, there remains widespread commercial use of natural ventilation in greenhouse operations worldwide (Lee et al., 2003; Parra et al., 2004). Moreover, many existing greenhouse operations in warmer climates lack proper adaptation to their respective environments; their design and operating strategies borrowed from operations located in temperate regions, and usually complete their lifespan prematurely or fail from the start. For example, a 4.5-acre (1.82-ha) greenhouse complex sits abandoned in Barbados, only a few years after its construction, due to design flaws such as poor material and roof design choice, rapid clogging of the cooling pads and high energy costs for the pad and fan cooling system.

Yields and quality of many common vegetable crops reduce at temperatures above 26 °C, even with specialized cultivars (Heuvelink, 2008; Kittas et al., 1996; Sato et al., 2006). Natural ventilation alone can be sufficient for very few select crops, but for those plant species that require air temperatures lower than typical outside temperatures, evaporative cooling is the most common solution in the greenhouse industry (Buffington et al., 2013). In fact, in arid and semi-arid areas, evaporative cooling is a pre-requisite for extending the growing season (Montero, 2006). Evaporative cooling solutions are useful in warm climates and a review of existing methods and many other cooling measures is presented by Sethi and Sharma (2007).

Generally, pad and fan cooling is an effective method of lowering the air temperature of the greenhouse by 4 to 6 °C if used alone, and 4 to 12 °C if used with shading (Jain & Tiwari, 2002; Kittas et al., 2003; Sethi & Sharma, 2007). The main disadvantage of pad and fan systems is the creation of large temperature gradients (up to 8 °C) inside the greenhouse (Kittas et al., 2003), the high energy cost of running the fan and pump systems, and the water use in the system. It is reported that evaporative cooling in arid climates can use up to 67% of the greenhouse gross water demand, well beyond the amount used for irrigation (Al-Ismaili and Jayasuriya, 2016). Arbel et al. (1999) showed that the cooling performance of a fog system varied from 8.5 to 12.0 °C, and that the corresponding increase in relative humidity varied from 35 to 68%. However, the efficiency of fog systems is often limited by insufficient natural air convection, in the absence of wind, and by the risk of wetting the plants when water droplet evaporation is not complete (Kittas et al., 2003). Moreover, high-pressure fog systems come at high costs relative to natural ventilation alone (Shen and Yu, 2002). Therefore, natural ventilation and shading are still used in many regions of the world with warm climates as they are simple and economically viable (Meca et al., 2013; Rault, 1989). For instance, natural ventilation is still the main means of climate control in the greenhouses of the Spanish province of Almería, which cover tens of thousands of hectares (Molina-Aiz et al., 2009). In this region and other locations using this technology such as Mexico, China, Colombia and Morocco, summer conditions exceed ideal greenhouse temperatures (Guichard et al., 2001; Molina-Aiz et al., 2009) and therefore cooling is often desired to extend the growing season (Kittas et al., 2003; Luo et al., 2005). In fact, under Mediterranean summer conditions, the high radiation and air temperature coupled with low relative humidity cause serious problems for climate control inside greenhouses, and the production of crops such as tomato (*Solanum lycopersicum*) decreases in terms of yield and quality (Guichard et al., 2001). Similarly, greenhouse production facilities in Australia are located in regions which include temperate, subtropical and tropical climate zones with high temperatures over 35 °C, putting many crops at risk (Connellan, 2001).

There is a resurgence in protected agriculture in tropical areas such as the Caribbean (DeGannes et al., 2014; Lawrence et al., 2014), and Southeast Asia (Kamaruddin et al., 2001). These areas have a growing greenhouse industry. Although relative humidity can be very high in tropical climates, some tropical regions with drier daytime conditions or dry seasons (Kottek et al., 2006; Kumar et al., 2009; von Zabeltitz, 2011), such as Barbados, can benefit from new evaporative cooling strategies, provided they are financially accessible. The West Indies report an increasing number of protected agriculture structures. Jamaica, St-Lucia and Dominica each report over 200 individual protected structures, however, less than 40% of them are in operation due to design flaws making the inside conditions too warm (DeGannes, et al., 2014). The inaccessibility to technology, rising cost of energy and the unreliability of power grids results in forced ventilation having limited feasibility in most tropical nations (Buffington et al., 2013; Sachs, 2001). Therefore, both pad and fan systems and fog cooling systems are not used, even if the climatic conditions permit their use.

Considerable research has been devoted to improvements in naturally ventilated greenhouses, however, in most cases, the results are informative but not always applicable (Bakker et al., 1995; Mutwiwa et al., 2008). Many authors have discussed solar refrigeration systems of which there are several types (Grossman, 2002). The seawater greenhouse (Davies & Paton, 2005) successfully uses seawater for cooling, instead of freshwater, in a greenhouse providing both cooling and desalination. Cooling of over 10 °C was possible in the hot and arid climates in which the design is intended for. Some systems combine desiccation with evaporative cooling. For example, Jain et al. (1994) compared different types of systems that use liquid desiccants and solid desiccants (Jain et al., 1995), focusing on hot and humid climates. Davies (2005) proposed a desiccation method combined with evaporative cooling to provide up to 15 °C of cooling, but the concept still presented several practical challenges. Although innovative, these systems, including the seawater greenhouse, remain energy intensive.

Another innovative system, the Watergy greenhouse, is a concept developed by Buchholz et al. (2006). It is a closed greenhouse with a passive cooling and dehumidification strategy, allowing for a reduction of water consumption by 75% and continuous plant production even during hot summer conditions in Southern Spain. The greenhouse temperature during daytime ranged from 20 to 35 °C. During the daytime, hot air rises from the vegetation area, through the roof area into the tower (Buchholz et al., 2005). To increase the energy and water content of the rising air, it is further humidified in the roof area by sprinklers on an inner roof. This design relies on a tall water tower, water condensation, heat exchange and energy storage.

Hemming et al. (2004) worked on a greenhouse design for the tropical lowlands of Indonesia. The design incorporated existing technologies to provide resistance against local wind loads using natural ventilation and insect netting for pests control. 8 mil (~200 μm or 0.2 mm) polyethylene film with a lifetime of about 3 years in Indonesia was developed. The film contains an ultraviolet-blocking pigments and has highly light diffusing properties. Other film prototypes were developed that selectively reflect near infrared radiation (NIR) to reduce greenhouse temperatures. No supplemental cooling beyond that of the shading was provided.

Other alternative cooling solutions such as the horizontal earth tube system presented by Mongkon et al., (2014) offer some new means of passive greenhouse climate control, but are not in widespread use because further development is still required. Lastly, improved high-pressure fogging systems suggested by Villarreal-Guerrero (2011) and Hayashi and Kozai (2005), that do not rely on active ventilation, offer good cooling performance, but remain costly.

Growers in a variety of climates who rely on natural ventilation or who are already using active ventilation systems may seek to rely on efficient cooling methods during certain periods increase production and to reduce energy costs (Jensen, 2010). It is apparent that there is a need to develop more water and energy efficient cooling systems to reduce dependency on high energy inputs for greenhouse operations. An alternative greenhouse design, such as the NVAC greenhouse, that makes use of evaporative cooling in an innovative way, can be used with natural ventilation greenhouse designs to provide cooling in a simple and cost-effective manner.

4.3 Materials and Methods

The natural ventilation augmented cooling (NVAC) greenhouse was built as a natural ventilation design with large side vents and a roof vent (Figure 8-10). The misting system was installed above the gutters in the rafters of the greenhouse and the spray was directed horizontally in one direction over an added roof, named the NVAC roof (Figure 8). The misting system operated at relatively low pressures ranging from 60 psi to 160 psi (414 to 1103 kPa) to reduce the design's complexity and energy consumption. A misting channel (Figure 8) is created by the added NVAC roof and the uppermost roof of the greenhouse, and this channel contain the mist, allowing the water droplets to evaporate or to drop onto an added roof if not fully evaporated. The NVAC roof channels the cooled air into the main area of the greenhouse and prevents any unevaporated water droplets from reaching the plant foliage. The NVAC roof also allows for unused water to be collected by gutters, and reused in the irrigation system. The unused water is collected in a gutter running the length of the bottom of the NVAC roof. A variety of structural designs and configurations of the misting line were tested in the study (Figure 8) to optimize the cooling performance of the NVAC greenhouse.

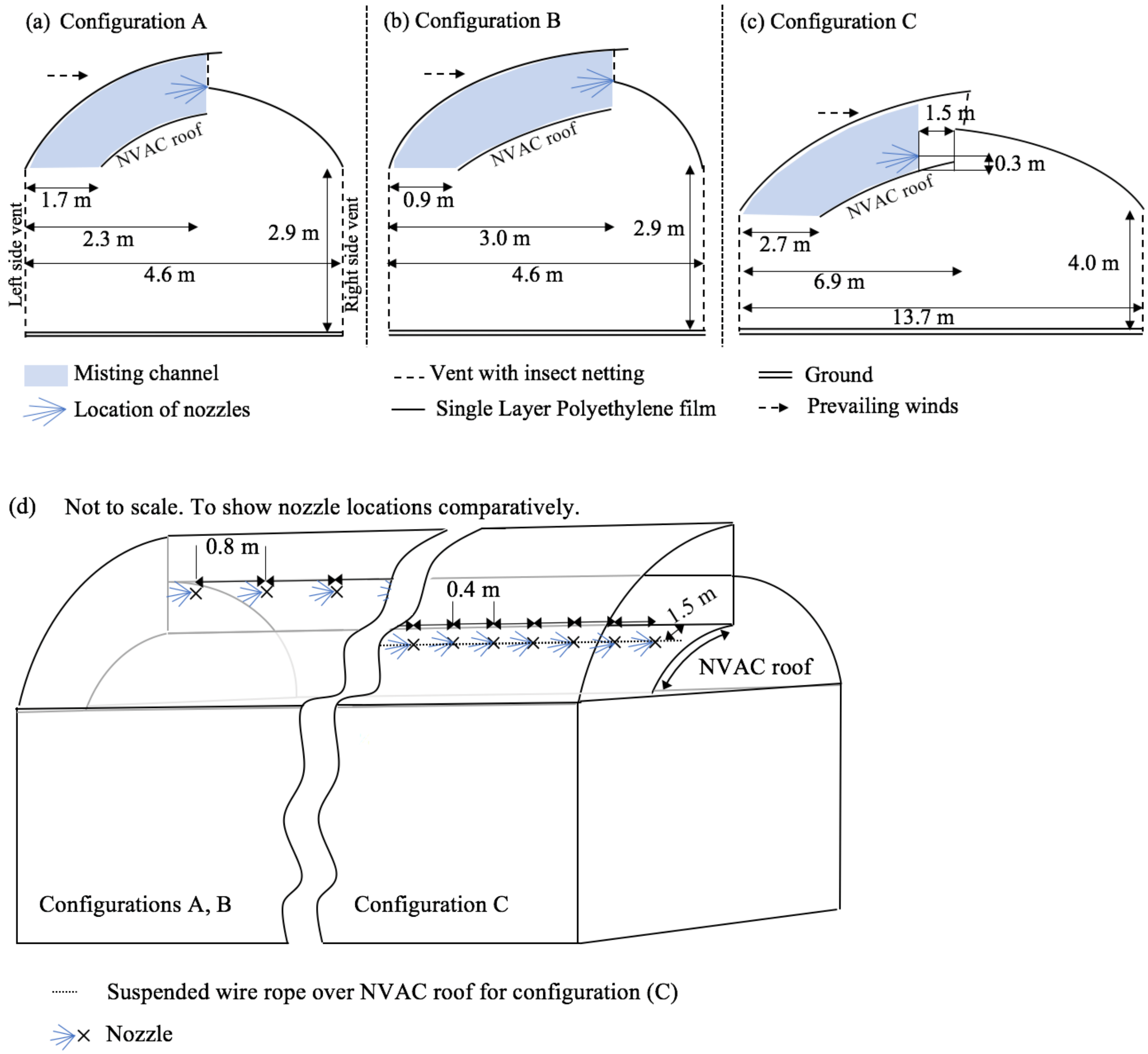

Figure 8. Geometries of the three different configurations tested for the natural ventilation augmented cooling (NVAC) greenhouse design. In all configurations, the mist direction is horizontal over the NVAC roof and the shaded area is the mist channel. In (a) the NVAC roof covers half of the width of the greenhouse and the misting line runs along the ridge of the lower outer roof; (b) the NVAC roof is enlarged to cover two-thirds of the width of the greenhouse and the misting line runs along the top ridge of the lower outer roof; (c) the NVAC roof covers half of the width of the greenhouse and the misting line is suspended over the NVAC roof; (d) a side view showing the 2.5-ft (0.4-m) nozzle configuration for configurations (A) and (B) and the 1.25-ft (0.4-m) nozzle configuration for configuration (C).

4.3.1 Experimental Greenhouses

Prototypes were built at the Macdonald Campus in Ste-Anne-de-Bellevue, QC, Canada (45°24′N, 73°57′W) in the summer of 2012 and 2013 (Figure 9). The 4.6-m wide by 6.1-m long and 4.3-m height prototype greenhouses tested configuration (A) which had a 1.4-m mist channel width (not shown) with an NVAC roof with an ellipticity *e* of 6.17 (not shown), and tested configuration (B) which had a 2.14-m mist channel width with an ellipticity *e* of 8.94 (Figure 9). The gutter height of the greenhouse was at 2.4 m. The floor space of the greenhouse was 27.9 m^2 and the volume was 68 m^3 not including the volume above the gutter. The greenhouse was built in-house as a natural ventilation design with a roof vent using ¾-inch diameter (19-mm) galvanized steel structural members that were bent using a handmade bending jig. The NVAC roof curvature followed the curvature of the roof under which it was built (Figure 8). The four sidewalls of the greenhouses were covered in insect screening (Mesh 40, 20-23%, black high-density polypropylene, ShadeLogic Canada, Brampton, ON). The roofs were covered with 6-mil polyethylene film (PlastiTech, Saint-Remi, QC, Canada), clamped to the structural members with plastic snap-clamps (Circo Innovations, Grass Valley, CA) on edges and fastened with wiggle wire along the roof edges (Harnois Industries, Saint-Thomas, QC, Canada). The misting system was a modified 3/8-inch o.d. (9.5 mm) beige-colored misting line (Professional 12-ft mist cooling system, Model 20090, Orbit Irrigation Products Inc. Bountiful, UT). Brass ‘Slip Lok’ fittings (Model 10121W, Orbit Irrigation Products Inc.) were used to install brass body and stainless steel insert 0.3-mm orifice nozzles (Model 10106H, Orbit Irrigation Products Inc.). In both configurations (A) and (B), the misting line was installed along the edge of the lower outside roof (Figure 8) with eight nozzles installed at 2.5-ft (0.76 m) intervals. This resulted in a water usage of 15.1 $L \cdot h^{-1}$ and one nozzle per 3.3 m^2 of greenhouse floor area. The water supply for the misting system was from a municipal water source, at a line pressure of 60 psi (414 kPa). No filtration or pressure regulation was used. The greenhouse was kept empty for this study and the floor was covered with non-porous white polyethylene tarpaulin (Uberhaus Rona, Boucherville, QC, Canada).

(a)

(b)

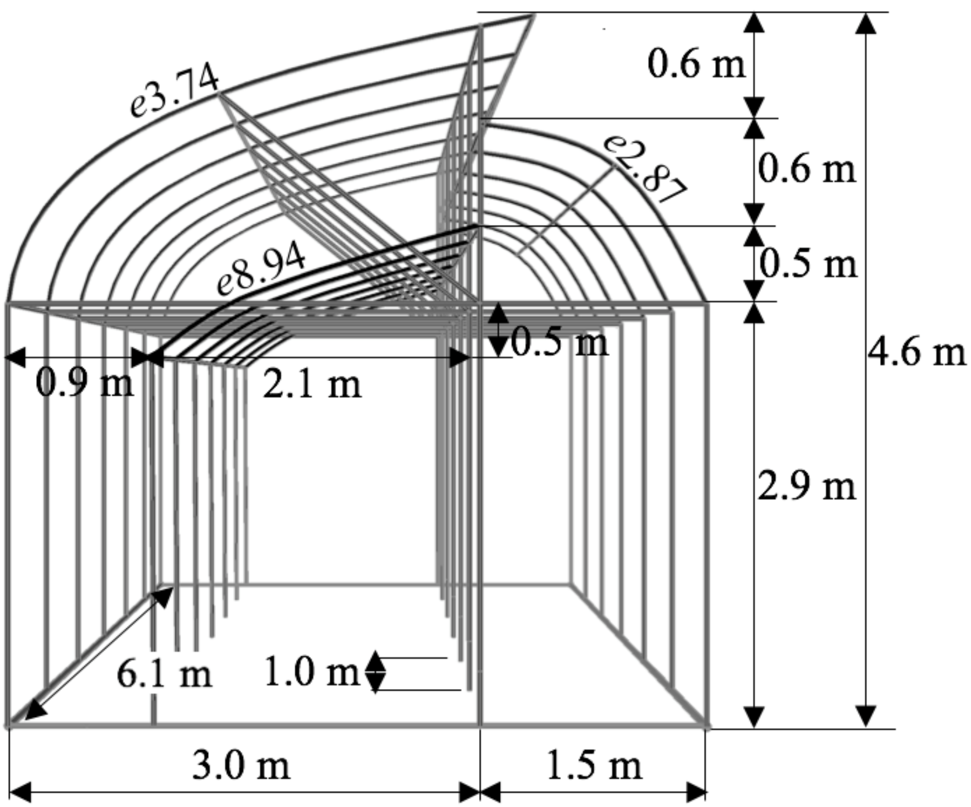

Figure 9. The natural ventilation augmented cooling (NVAC) greenhouse design in 2013 at McGill University, Macdonald Campus, Ste-Anne-de-Bellevue, QC, Canada. In (a) the NVAC greenhouse prototype under configuration (B), and in (b) the geometry and dimensions of configuration (B).

A 13.7-m by 32-m commercial greenhouse using the NVAC system was built in 2014 in Trents, Barbados (13°11'N, 59°37'W) (Figure 10). The sidewalls of the greenhouse were 4.0 m up to the gutter. This greenhouse had a floor space of 439 m^2 and a volume of 1753.6 m^3 not including the volume above the gutters. The climate of Barbados is a tropical wet and dry climate. The design was a modified natural ventilation Coral Amber® manufactured greenhouse, covered with an 8-mil (~200 µm or 0.2 mm) polyethylene film on the roofs and mesh 58 white insect netting covering the four sidewalls (Jamaica Drip Irrigation, Mandeville, Jamaica). The two lengthwise sidewalls of the greenhouses were covered in shade cloth (Mesh 18, black high-density polypropylene, ShadeLogic Canada, Brampton, ON). Aluminet thermal reflective cloth was installed at the gutter height (Isratech Ltd., Mandeville, Jamaica). The exact installation method of the Aluminet varied according to the experiment and is discussed below.

(a) 

(b) 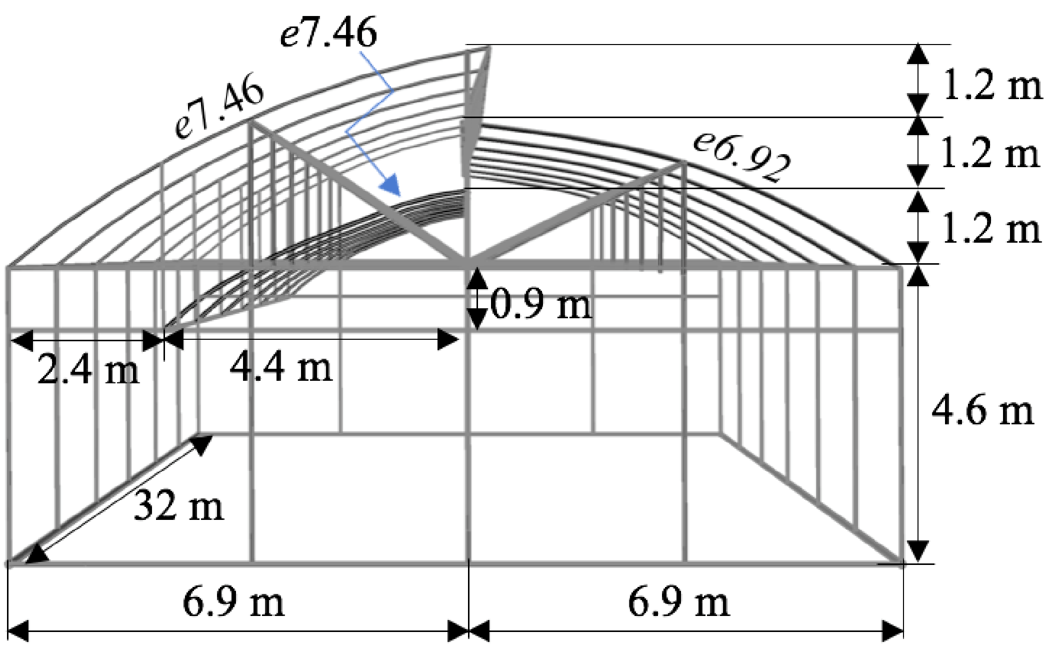

Figure 10. The natural ventilation augmented cooling (NVAC) greenhouse design in Trents, Barbados under configuration (C) from 2014 to 2016. In (a), the NVAC greenhouse with rainwater harvesting tanks seen in the foreground, and in (b) the geometry and dimensions of configuration (C).

Configuration (A) was initially selected for the design of the NVAC greenhouse study in Trents, Barbados. During preliminary tests in 2014 and 2015, the NVAC misting system did not provide noticeable cooling nor increased relative humidity. Therefore, an improved design was developed. In 2016, the misting line was reinstalled in suspension, 1.5 m into the mist channel, protecting the mist stream from any drafts or turbulence (Figures 8 and 11). This configuration, identified herein as configuration (C), is the final configuration used for the study in Trents, Barbados. The greenhouse was kept empty except for the low profile growing benches, growbags and RollerPlast trellising (Jamaica Drip Irrigation). In this study, it was assumed that these items had a negligible effect on the temperature and relative humidity. The floor of the greenhouse was hard-packed coarse stone dust over a buried non-porous white polyethylene tarpaulin (True Value Manufacturing, Cary, IL).

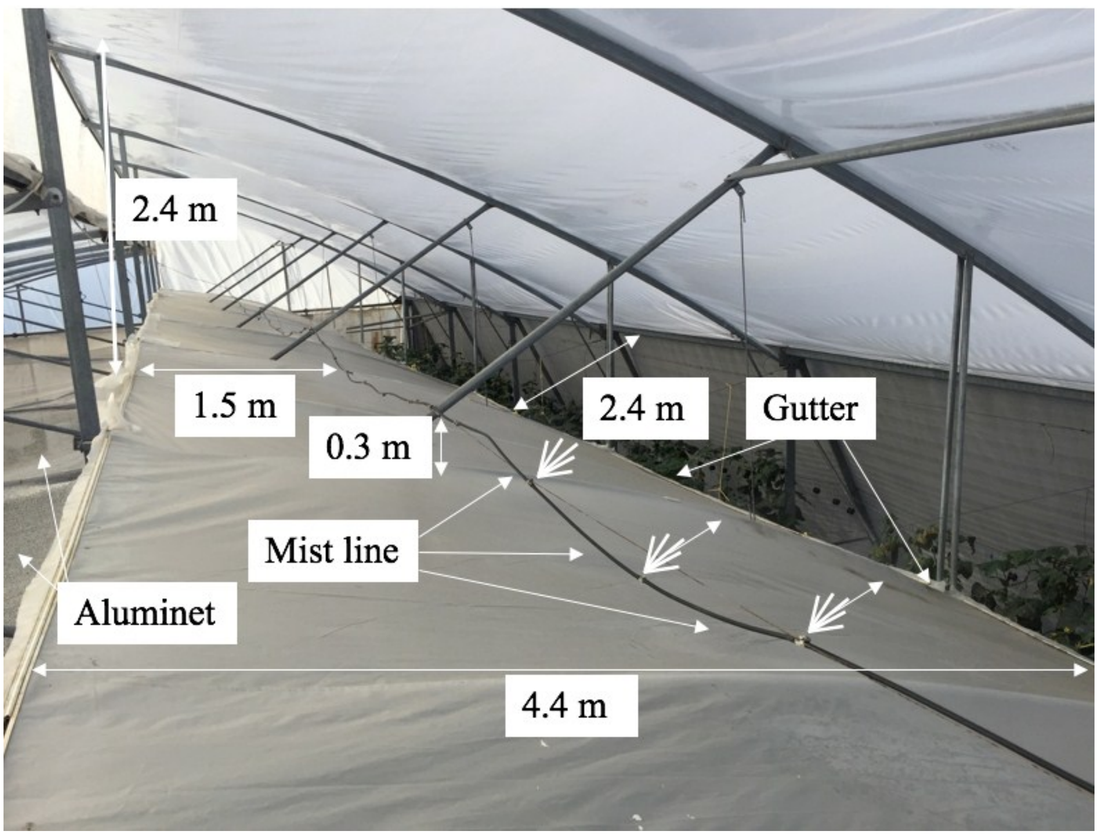

Figure 11. View of the misting channel in the natural ventilation augment cooling (NVAC) greenhouse located in Trents, Barbados in 2016 under configuration (C). The view of the mist channel shows the suspended misting line located above the NVAC roof.

The misting line was a polyamide 12 nylon tubing that was heat stabilized, ultraviolet stabilized, plasticized, and semi-flexible with a 3/8-inch o.d. and 0.075-inch wall thickness. The tubing was installed onto a stainless-steel wire rope (1/8-in diameter) that was taught and ran the entire length of the greenhouse. Stainless-steel 0.3-mm orifice nozzles without filters (AmFog Nozzle Technol., Inc. Casa Grande, AZ) were used in the final design. The nozzles were installed in barbed T-connectors (Misting and Cooling Barbed T Connector Brass, AmFog Nozzle Technol., Inc.) that were connected to the tubing with hose clamps to prevent leaks. The hose clamps also connected the tubing to the cable. The tubing was fastened to the frame of the greenhouse using rubberized mounting clamps (Mounting clamps for tubing, stainless steel with rubber, 3/8-in i.d., AmFog Nozzle Technol., Inc.) that prevented the tubing from rotating from the position in which it was installed. In preliminary tests, the nozzle configuration was one nozzle per 8.8 m^2 of greenhouse floor area, or one nozzle per 35.0 m^3 of greenhouse volume, not considering the volume above the gutter. In the final design of the NVAC greenhouse in 2016, the nozzle configuration was increased to one nozzle per 4.2 m^2 of greenhouse floor area, or one nozzle per 17.5 m^3 of greenhouse volume, not considering the volume above the gutter. With these nozzle configurations for configurations (A) and (C), 42.9 $L \cdot h^{-1}$ and 84.0 $L \cdot h^{-1}$ of water were used in the misting system during misting, respectively.

Due to an unusually high content in calcium carbonate, local aquifer water was not used for the NVAC misting system in Barbados. An advanced filtration system or water softening system were not financially available for testing, nor for commercial applications. A rainwater harvesting system was used to collect water from the greenhouse roof using two 1000-gal (3785-L) black tanks (Rotoplastics, Bridgetown, Barbados). Other similar tanks collected rainwater for irrigation purposes. All components and devices used for the NVAC misting system were grouped together in one area of the greenhouse (Figure 12). The water was pumped from the tanks to the greenhouse using a 0.5-horsepower (0.37 kW) water pump (Goulds Pumps, Seneca Falls, NY). Once on site, the water was pressurized to 45 psi (310 kPa) and kept in a 20-gal (75.7-L) water pressure tank (Goulds Pumps) before passing through two separate filtration units, a 100-µm filtration grade filter (Netafim DF100-140, Amiad Water Systems Ltd., Ami'ad, Israel) and a 20-µm filtration grade filter (Model S1A, Culligan Water, Rosemont, IL). The water was then sent to the rafters where it was further pressurized to 160 psi (1103 kPa) using a secondary pump (Professional 160 psi misting booster pump, Model 92100, Orbit Irrigation

Products Inc.). A polypropylene ultraviolet-light water purifier (1/4-inch inlet, 2 gal/min, McMaster-Carr, Aurora, OH) was added to the line and much of the white polyvinyl chloride (PVC) piping for the pumping and filtration system was painted matte black or buried shallow in the ground to reduce algal growth. Solenoid valves were used to control the supply of water in the misting line and to bleed the line (3/4-inch electric solenoid valve, 24 V with flow control, Irrigation Direct, Inc. Livermore, CA). The bleed valve was added to the end of the misting line to allow for daily bleeding when the misting system was shut off. A control system incorporating temperature sensors, relative humidity sensors, rain sensors and a timing option provided automation (Figure 13). The misting automation allowed for the system to shut itself off in the event of cool temperatures, rain or unusually high relative humidity. The automation system incorporated a TORO® Evolution series irrigation controller and timer (The Toro Company, Bloomington, MN) that ran on 120 V and provided a 24-V relay for the solenoid valves for activating the misting line and bleed valve. The controller used a backup 9-V battery in case of grid power failure.

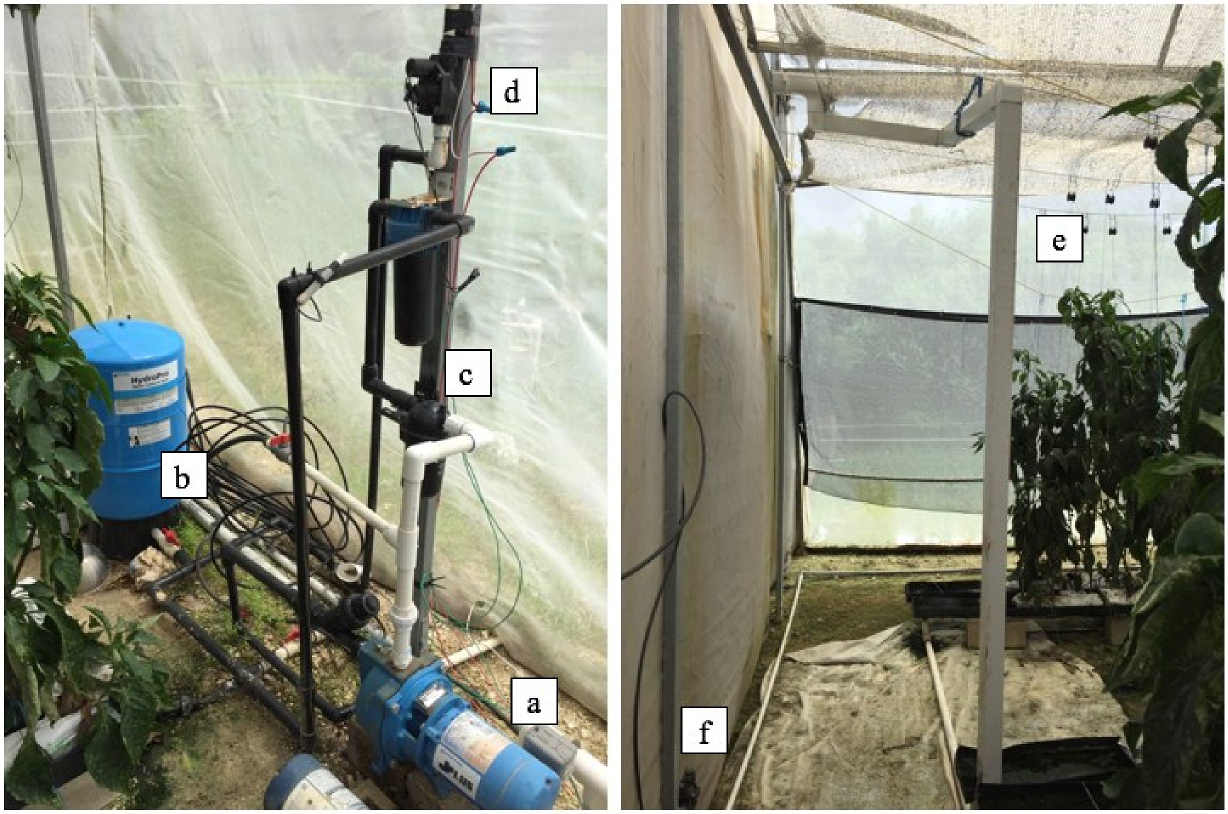

Figure 12. The water supply system for the natural ventilation augmented cooling (NVAC) greenhouse in Trents, Barbados. In (a) the water supply pump; (b) the pressure tank; (c) the filters; (d) the water supply solenoid valve; (e) the spout to drain unused mist water from the gutters; (f) the misting line bleeding solenoid valve. Plants are shown in images but the greenhouse was plant-free during experiments. Photo taken before testing.

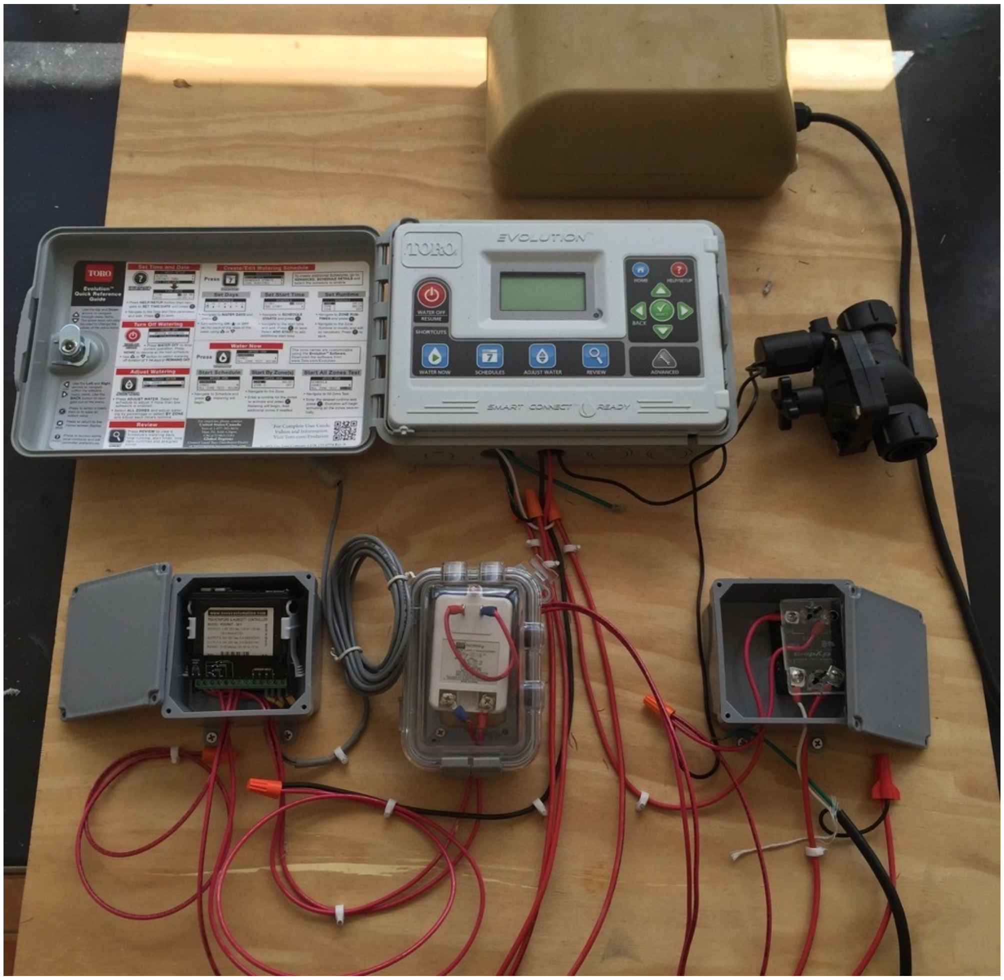

Figure 13. The automation and control system for the natural ventilation augmented cooling (NVAC) greenhouse in Trents, Barbados. In (a) a TORO® Evolution Series irrigation controller; (b) the misting line secondary pressure pump usually located in the rafters; (c) the misting line bleed valve; (d) and (e) the transformers; (f) the misting temperature sensor, relative humidity sensor, rain sensor (unseen) and timing device.

4.3.2 Data Collection

At both locations, two Onset data loggers were used (Onset Computer Corp., Bourne, MA) with temperature, relative humidity and solar radiation sensors calibrated as recommended by Both et al. (2015). Laboratory calibration of the temperature sensors was accomplished using a large ice bath and distilled water. The temperature sensors (model S-TMB-M006, Onset Computer Corp.) provided < ± 0.2 °C total accuracy and resolution of < ± 0.03 °C, over the range of 0 to 50 °C. The humidity sensors (model S-THB-M008, Onset Computer Corp.)

provided an accuracy and resolution of ± 2.5% from 10% to 90% relative humidity and 0.1% relative humidity at 25 °C, and below 10% and above 90%, ± 5%. The temperature and relative humidity sensors were shielded using perforated white Styrofoam cups or solar radiation shields (RS3 Solar Radiation Shield, Onset Computer Corp.) when available. At the Ste-Anne-de-Bellevue, QC, Canada location, a weather station (HOBO U30-NRC weather station starter kit, U30-NRC-SYS-C, Onset Computer Corp.) provided additional data such as wind direction and speed. The measurement range of the wind speed sensor (S-WSB-M003, Onset Computer Corp.) was 0 to 76 $m \cdot s^{-1}$ over -40 to 75 °C, with an accuracy of ± 1.1 $m \cdot s^{-1}$ or ± 4% of reading whichever is greater. Its resolution was 0.5 $m \cdot s^{-1}$ with a starting threshold of 1 $m \cdot s^{-1}$. The wind direction sensor had a measurement range of 0 to 355 degrees, with a 5-degree dead band, accuracy of ± 5 degrees, resolution of 1.4 degrees and starting threshold of 1.0 $m \cdot s^{-1}$. Wind speed and direction were not measured at the Trent, Barbados location due to limited availability of sensor equipment. Prevailing wind data was obtained from the National Oceanic and Atmospheric Administration (National Oceanic and Atmospheric Administration, 2016).

The photosynthetically active radiation (PAR) (Onset Computer Corp.) sensors had an accuracy of ± 5 $\mu mol \cdot m^{-2} \cdot s^{-1}$, and a resolution of 2.5 $\mu mol \cdot m^{-2} \cdot s^{-1}$, with an additional temperature-induced error ±0.75 $\mu mol \cdot m^{-2} \cdot s^{-1}$ °C^{-1} from 25 °C. Other PAR readings were done at all indoor sensor locations (Figure 14) and additional indoor locations with a LI-193 spherical quantum sensor (LI-COR, Inc., Lincoln, NE) to measure the effect of the added NVAC roof on the PAR reaching the plant space at the Trents, Barbados greenhouse. These measurements were taken during periods with no cloud cover at 15 location following the empty crop rows, at a height of 1.5 m, at four occasions, on 31 July, 01 August, 03 August and 04 August 2014 at 13:00 HR, and were averaged.

Wet-bulb and dry-bulb temperatures were measured at three indoor and three outdoor locations using aspirated air sensors and recorded using an Agilent 34972A LXI data logger (Keysight Technology Canada Inc. Mississauga, ON). Wet-bulb sensors were fabricated using thermocouples, a distilled water reservoir and wicking cotton. The wet-bulb and dry-bulb sensors were made from type-T thermocouple wire (Spectris Canada, Omega Environmental, Laval, QC, Canada) and were placed in an enclosure with fans providing 3 $m \cdot s^{-1}$ air velocity across the thermocouples (Both et al., 2015; Langhans & Tibbitts, 1997). The type-T thermocouples had a range of measurement of -270 to 370 °C with a standard accuracy of ± 1.0 °C or ± 0.75%, whichever is greater. The fans were supported by a 12-V power source or batteries. The thermocouples were calibrated as recommended by Both et al. (2015). The air velocity was measured using a hot-wire anemometer (TPI 565C1 digital anemometer with hot-wire probe, 0.2 to 20 $m \cdot s^{-1}$ velocity, -20 to 80 °C temperature, Test Products International Inc., Beaverton, OR). Each set of thermocouples was housed in a 6-inch diameter white PVC pipe to shield from solar radiation. Using wet-bulb and dry-bulb temperature data, relative humidity was calculated according to the method suggested by Snyder and Shaw (1984). The aspirated boxes were used to correct for potential errors in readings from the other temperature sensors.

The Onset Computer Corp. temperature and relative humidity sensors and the dry-bulb and wet-bulb aspirated air apparatuses were placed throughout the greenhouse at various locations a height of 1.5 m (Figure 14). Because the greenhouse was empty during tests, this height was arbitrarily selected as the location of the crop canopy (Both et al., 2015).

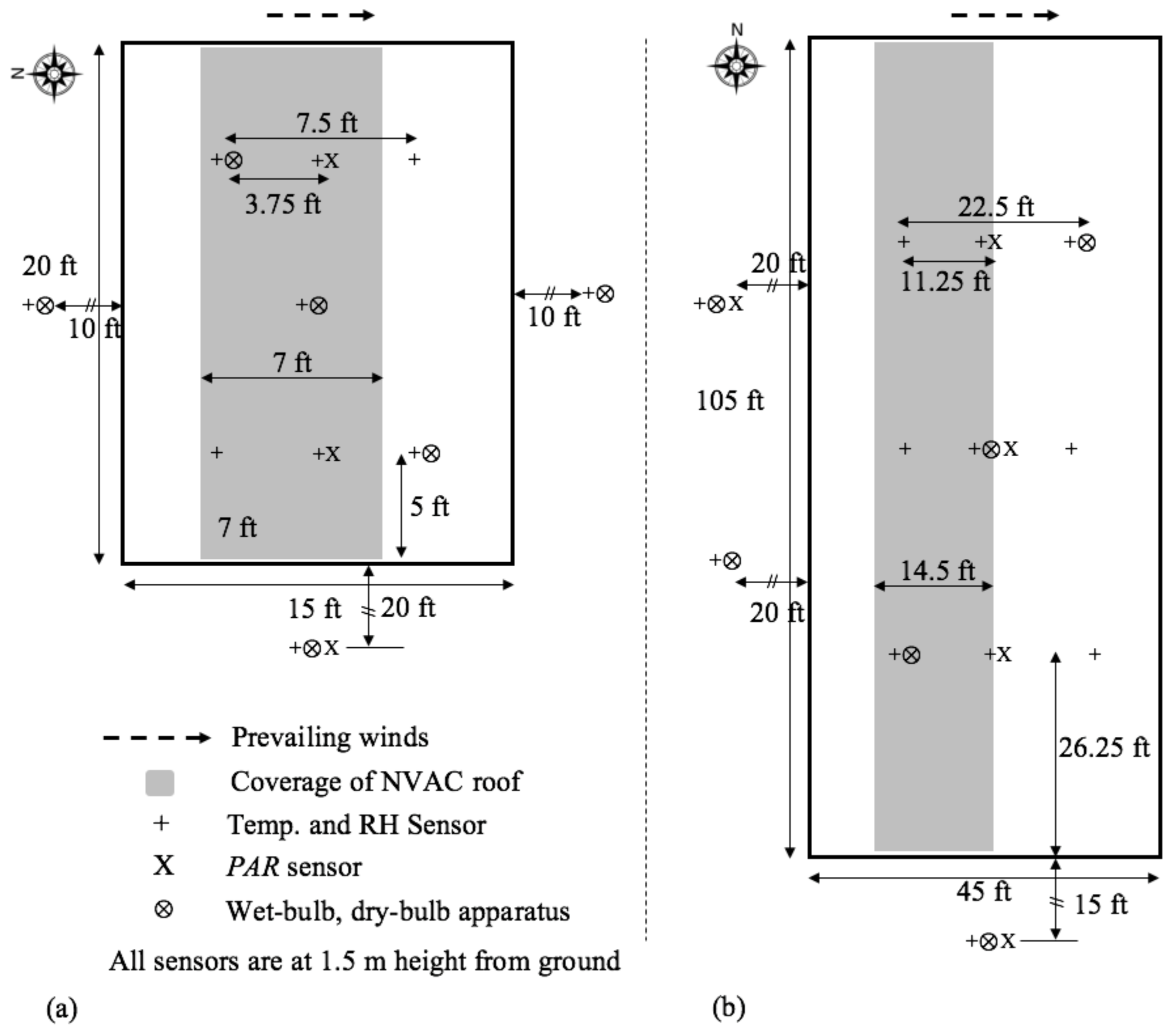

Figure 14. Location of the temperature and relative humidity sensors (+), aspirated wet-bulb and dry-bulb sensors (⊗) and PAR sensors (X) in the natural ventilation augmented cooling (NVAC) experimental greenhouses. Prevailing wind directions are shown. Experimental greenhouse (a) is at the Macdonald Campus, Ste-Anne-de-Bellevue, QC Canada, and (b) in Trents, Barbados experimental greenhouse. The shaded area is the area inside the greenhouse covered by the NVAC roof.

To properly observe and measure the effect that the NVAC misting system had on the conditions inside the greenhouse, the system was manually activated for at least 1 h once per day at the Ste-Anne-de-Bellevue, QC, Canada greenhouse, to obtain preliminary data, and three times per day for at least 1 h in Trents, Barbados greenhouse, by overriding the automation device. For analysis, the temperature and relative humidity measurements inside the greenhouse over the period of misting were averaged and compared to the average outside conditions over the same period. The inside averages were also compared to the average values of the measurements over 1 h immediately preceding the use of the NVAC misting system. This method was used to demonstrate the cooling potential of the NVAC misting system even if the amount of cooling was not sufficient to bring greenhouse temperatures below outside conditions.

All test days had no cloud cover during the day nor rain events. Weather occurrences that imitate the effect of the NVAC misting system (i.e., sudden short-term cloud cover or light rain) occurred during preliminary tests, but were highly unlikely. Conditions were monitored during final tests to avoid such circumstances.

4.4 Results and Discussion

4.4.1 2012-2013 Configurations (A) and (B) Small-Scale Greenhouse

During the 2012 and 2013 tests of the NVAC greenhouse in Ste-Anne-de-Bellevue, QC, Canada test were done on days that the weather conditions were considered warm and wind conditions were calm. The NVAC misting system was activated when the inside temperature reached 30 °C, except for one day in 2012 and two days in 2013. These relatively cooler days had very low wind conditions and were considered useful for testing the system. Although the greenhouse did not contain plants, the tall grass surrounding the greenhouse provided humid nighttime conditions. Prior to use of the NVAC system, inside temperatures were 1.6 to 7.2 °C warmer and inside relative humidity levels varied from 4.0% drier to 17.0% more humid in comparison to outside conditions. During the use of the NVAC misting system, inside temperatures varied from 0.7 °C warmer to 4.4 °C cooler than outside temperature (Table 6). Figure 15a illustrates the change in temperature and relative humidity inside and outside the greenhouse when the misting system was activated on August 23, 2012, a test that showed good cooling performance of the NVAC greenhouse misting system. The test conducted on August 16, 2012, a very warm day, also showed good cooling with respect to conditions prior to the use of the NVAC system (Table 6).

Table 6. Conditions measured inside the Natural Ventilation Augmented Cooling (NVAC) greenhouse in configurations (A) and (B) in 2012 and 2013 in Ste-Anne-de-Bellevue, QC, Canada: the average outside temperature (T_o) and relative humidity (RH_o) over a 1-h period prior to misting and ($T_{o'}$) and ($RH_{o'}$) over a 1-h period during the periods that the NVAC misting system was used; the average temperature and relative humidity inside the greenhouse over a 1-h period prior to misting (T_i and RH_i); the average temperature and relative humidity inside the greenhouse over a 1-h period with the use of the NVAC misting system (T_m and RH_m); and their respective differences Δ_{i-o} and Δ_{m-o}. Standard deviations are also given (n = 210 for inside averages and n = 90 for outside averages).

Date	Conditions	T_o and RH_o	T_i and RH_i	$T_{o'}$ and $RH_{o'}$	T_m and RH_m	Δ_{i-o}	Δ_{m-o}
2012 Configuration (A), Ste-Anne-de-Bellevue, QC, Canada							
16 Aug.	T (°C)	30.1 ± 0.9	37.3 ± 1.5	32.0 ± 0.6	32.7 ± 0.9	7.2	-0.7
2012	RH (%)	42.7 ± 4.0	38.7 ± 3.5	43.1 ± 3.6	46.5 ± 0.9	-4.0	3.4
22 Aug.	T (°C)	21.9 ± 0.4	23.5 ± 1.4	26.8 ± 0.4	22.5 ± 1.5	1.6	-4.3
2012	RH (%)	55.4 ± 0.5	61.4 ± 1.4	39.8 ± 2.0	64.1 ± 1.5	6.0	24.3
23 Aug.	T (°C)	26.9 ± 1.1	30.7 ± 0.8	30.9 ± 0.3	26.5 ± 1.3	3.8	-4.4
2012	RH (%)	42.3 ± 2.1	56.3 ± 1.1	43.0 ± 1.4	68.4 ± 3.4	14.0	25.4
24 Aug.	T (°C)	27.3 ± 0.7	31.3 ± 0.5	27.5 ± 0.8	28.2 ± 0.9	4.0	0.7
2012	RH (%)	39.8 ± 1.1	49.1 ± 1.5	37.0 ± 1.6	52.1 ± 1.0	9.3	15.1
2013 Configuration (B), Ste-Anne-de-Bellevue, QC, Canada							
22 Jul.	T (°C)	28.1± 0.5	29.2 ± 0.6	27.4 ± 0.5	30.1 ± 1.1	1.1	2.7
2013	RH (%)	57.9 ± 2.1	59.4 ± 1.9	45.6 ± 1.6	46.2 ± 2.1	1.5	0.6
07 Aug.	T (°C)	24.6 ± 0.6	26.4 ± 1.2	26.6 ± 0.5	27.0 ± 0.8	1.8	0.4
2013	RH (%)	52.8 ± 1.2	59.2 ± 3.4	53.4 ± 1.6	57.7 ± 1.7	6.4	4.3
	T (°C)	24.9 ± 0.4	27.2 ± 0.5	30.2 ± 0.5	28.3 ± 0.8	2.3	-1.9

08 Aug. 2013	RH (%)	59.2 ± 1.1	59.9 ± 1.2	59.6 ± 1.7	57.8 ± 2.0	0.7	-1.8
19 Aug.	T (°C)	25.0 ± 0.4	28.1 ± 0.6	31.7 ± 0.5	29.0 ± 0.9	3.1	-2.7
2013	RH (%)	68.1 ± 1.4	63.2 ± 1.8	65.0 ± 3.4	61.9 ± 1.0	-5.9	-3.1

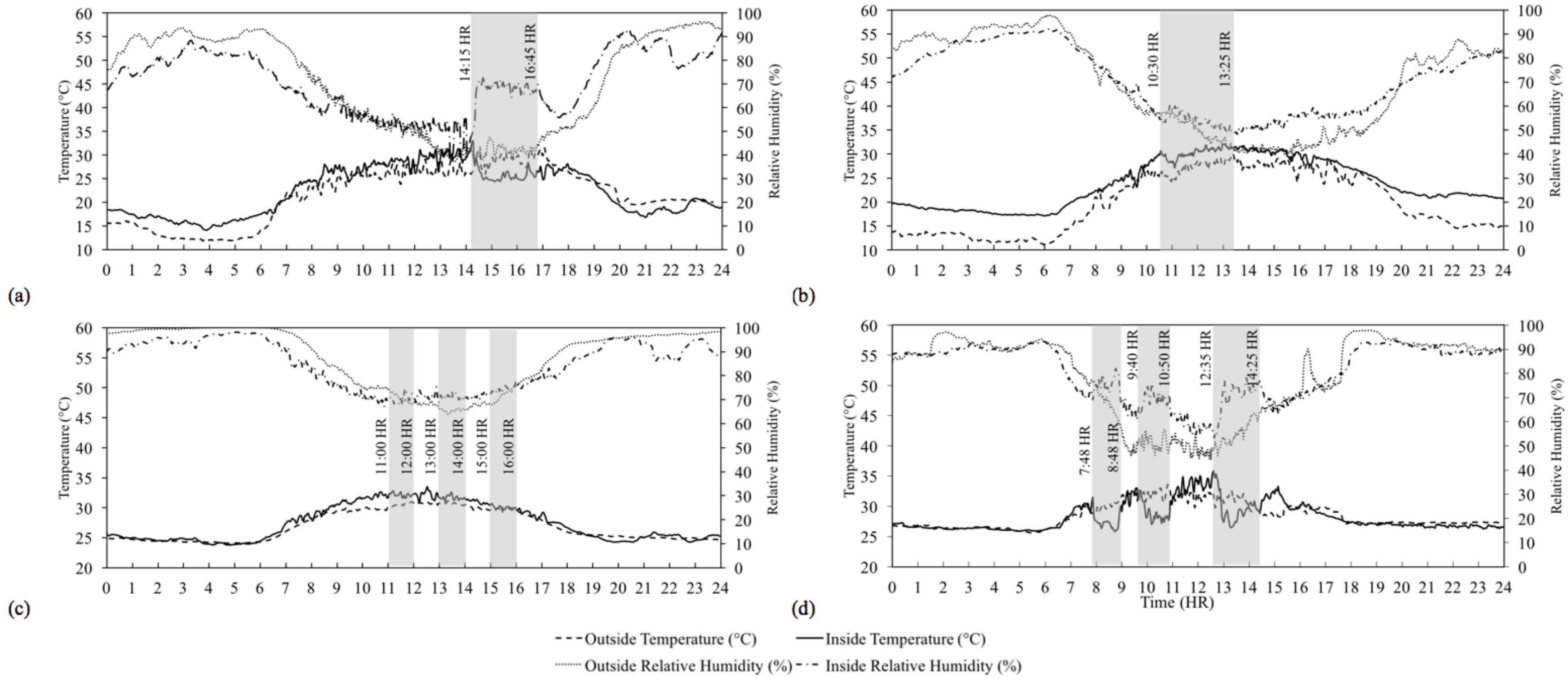

Figure 15. Graphical representation of the recorded temperatures and relative humidity of (a) 16 August 2012, (b) 22 July 2013, (c) 06 August 2014 and (c) 11 June 2016 inside and outside the natural ventilation augment cooling (NVAC) experimental greenhouses. Graphs (a) and (b) are from experiments at the Macdonald Campus location in Ste-Anne-de-Bellevue, QC, Canada, where the NVAC misting system was used for the period of the day that temperatures exceeded 30 °C. Graphs (c) and (d) are from experiments at the Trent, Barbados location, where shorter misting periods were imposed throughout the day to study the greenhouse climate response. The periods when the NVAC system was functional with misting are shaded.

The sharpness of the decrease in temperature or of the increase in relative humidity was affected by the immediate weather conditions such as wind velocity. Because the NVAC greenhouse design relies on natural ventilation, days with wind gusts larger than 2 $m \cdot s^{-1}$ provided ample air movement inside the greenhouse and therefore reduced the effect of the NVAC design. Such windy days were not considered in the present study, even if the outside and greenhouse temperatures were high. This is because winds stronger than 1.8 to 2.0 $m \cdot s^{-1}$ dominate the ventilation process and in this case thermal buoyancy is negligible (Bot, 1983; Papadakis et al., 1996). Buoyancy driven ventilation is more important if the wind velocity is lower than 0.5 $m \cdot s^{-1}$. In the intermediate cases where wind velocity is between 0.5 $m \cdot s^{-1}$ and 2 $m \cdot s^{-1}$, the ventilation is driven mostly by the wind effect and some influence of the buoyancy can be observed (Kacira et al., 2004).

The amount of PAR reaching the crop was reduced with the NVAC greenhouse design. The comparison of outside to inside PAR throughout the day (Figure 16) shows that transmission of *PAR* agrees with transmittance of 6-mil polyethylene film (53 to 90% depending on angle of incidence, Pollet and Pieters, 2000). The average PAR reaching the inside of the greenhouse from 12:00 HR to 14:00 HR was in fact 69.2% of the outside PAR over the same period. The average PAR inside the greenhouse from 12:00 HR to 14:00 HR during the study days peaked at 1300.1 $\mu mol \cdot m^{-2} \cdot s^{-1,}$ with an average of 1218.2 $\mu mol \cdot m^{-2} \cdot s^{-1}$, while the average outside PAR during the same period peaked at 1945.0 $\mu mol \cdot m^{-2} \cdot s^{-1}$, with an average of 1759.7 $\mu mol \cdot m^{-2} \cdot s^{-1}$.

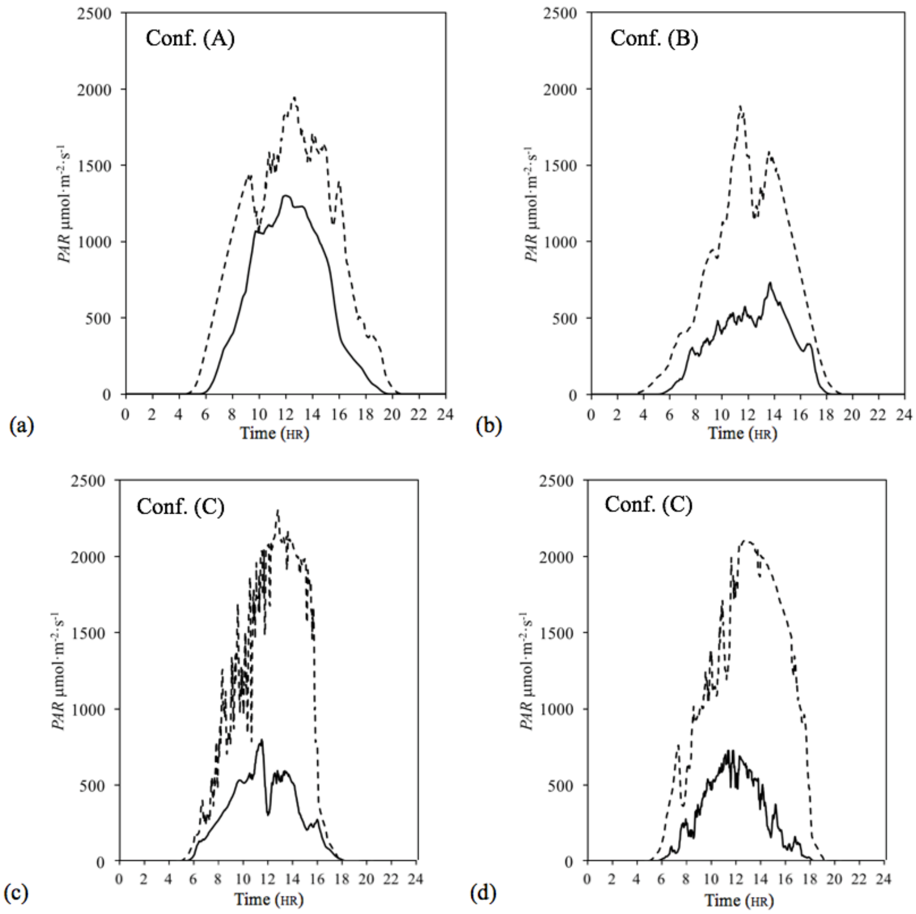

Figure 16. Graphical representation of the average PAR recorded outside (----) and inside (—) the natural ventilation augmented cooling (NVAC) experimental greenhouses. The averages are calculated over the four respective test days of each year. In (a), the PAR in 2012 at the Ste-Anne-de-Belleuve, QC, Canada location; (b) in 2013 at the Ste-Anne-de-Belleuve, QC, Canada location; (c) in 2014 at the Trents, Barbados location; (d) in 2016 at the Trents, Barbados location.

In 2013, configuration (B) was tested. It was assumed that a larger misting channel (Figure 8b) would increase the cooling potential of the design. The larger NVAC roof of configuration (B) had a larger ellipticity compared to configuration (A) (i.e. a greater degree of flattening), and caused more shading in the greenhouse (Figure 16b), thus reducing the PAR reaching the crop, and reducing solar warming of the plant space. In fact, the transmissivity of the greenhouse structure was reduced to 40.8%, in comparison to 69.2% in configuration (A) in

2012, when comparing the average PAR reaching the inside of the greenhouse from 12:00 HR to 14:00 HR to the outside PAR over the same period. The average PAR inside the greenhouse during the study days peaked at only 574.2 $\mu mol \cdot m^{-2} \cdot s^{-1,}$ with an average of 564.7 $\mu mol \cdot m^{-2} \cdot s^{-1}$, while the average outside PAR peaked at 1885.0 $\mu mol \cdot m^{-2} \cdot s^{-1}$, with an average of 1382.8 $\mu mol \cdot m^{-2} \cdot s^{-1}$. In addition to added shading from a greater NVAC roof, the greater ellipticity of the roof of configuration (B) caused a greater water accumulation from the misting. The water droplets from the misting line had less airborne time to evaporate and were more likely to land on the polyethylene film surface of the NVAC roof. This created areas with thin films of water on the NVAC roof. Pollet and Pieters (2000) reported that presence of water droplets on regular 6-mil polyethylene film can further reduce transmittance by up to 23%. Due to the lower curvature of the NVAC roof in configuration (B), air movement was also hindered, and much of the mist and cooled air stagnated or flowed in undesired directions such as out from the left side vent (Figure 8) of the greenhouse. Configuration (A), a lower ellipticity (a steeper roof pitch), allowed the cooled air to flow down into the plant space more effectively.

Although the design of configuration (B) of the NVAC greenhouse may have contributed to cooler temperatures through shading, configuration (B) did not provide as much cooling as observed in configuration (A) (Table 6 and Figure 15). In fact, inside conditions were warmer during the periods when the NVAC misting system was used during two of the test days (Table 6). We determined that the NVAC system under configuration (B) did not perform adequately as the design was not able to reduce inside greenhouse temperatures. The ineffectiveness of the NVAC greenhouse in configuration (B) was attributed to the lack of curvature in the NVAC roof. Follow-up research in our laboratory has thoroughly investigated the air movement in the NVAC greenhouse design in a model unit under controlled conditions.

4.4.2 2014 configuration (A) large-scale greenhouse

The NVAC greenhouse was built in Trents, Barbados in 2014 according to configuration (A). Given the location of Trents, Barbados (13°11'N, 59°37'W), except for a lengthy dry season, the seasonal climate and daily weather conditions vary very little throughout the year. This consistency provided us with consistent conditions during testing. Windy days were avoided and this was determined by observation. Although rare, days with rain events were dismissed as greenhouse temperatures remained low during rain and long-term cloud cover. The temperature, relative humidity and PAR inside the greenhouse without the use of the NVAC misting system averaged over 10 sunny days of July 2014 are presented in Figure 17. The conditions of the four test days presented (Table 6) were uniform in that the inside temperature of the greenhouse exceeded 30.0 °C without any cloud cover during the day nor rain events.

Table 7. Conditions measured inside the Natural Ventilation Augmented Cooling (NVAC) greenhouse in configuration (C) in 2014 and 2016 in Trents, Barbados: the average outside temperature (T_o) and relative humidity (RH_o) over a 1-h period prior to misting and ($T_{o'}$) and ($RH_{o'}$) over a 1-h period during the periods that the NVAC misting system was used; the average temperature and relative humidity inside the greenhouse over a 1-h period prior to misting (T_i and RH_i); the average temperature and relative humidity inside the greenhouse over a 1-h period with the use of the NVAC misting system (T_m and RH_m); and their respective differences $\Delta_{i\text{-}o}$ and $\Delta_{m\text{-}o}$. Standard deviations are also given (n = 270 for inside averages and n = 90 for outside averages).

Date	Conditions	T_o and RH_o	T_i and RH_i	$T_{o'}$ and $RH_{o'}$	T_m and RH_m	$\Delta_{i\text{-}o}$	$\Delta_{m\text{-}o}$
2014 Configuration (A), Trents, Barbados							
06 Aug.	T (°C)	30.6 ± 0.6	32.0 ± 1.1	31.3 ± 0.8	31.0 ± 0.9	1.4	-0.3
2014	RH (%)	68.2 ± 0.4	72.6 ± 2.9	65.9 ± 0.4	70.9 ± 2.2	5	4.4
07 Aug.	T (°C)	28.1 ± 0.9	29.9 ± 0.5	31.5 ± 1.0	31.0 ± 1.3	1.8	-0.5
2014	RH (%)	69.3 ± 2.0	76.9 ± 2.1	69.9 ± 5.2	75.8 ± 1.9	7.6	5.9
09 Aug.	T (°C)	30.0 ± 0.6	31.5 ± 1.1	31.5 ± 1.0	31.6 ± 1.1	1.5	0.1
2014	RH (%)	69.8 ± 3.8	74.9 ± 1.1	61.9 ± 4.6	71.1 ± 2.3	5.1	9.2
10 Aug.	T (°C)	29.3 ± 0.9	31.5 ± 1.1	32.0 ± 1.1	32.0 ± 1.3	2.2	0.0
2014	RH (%)	73.3 ± 2.2	78.0 ± 1.3	68.2 ± 3.5	76.1 ± 4.9	4.7	7.9

2016 Configuration (C), Trents, Barbados							
09 June	T (°C)	31.8 ± 0.3	34.7 ± 0.8	32.9 ± 0.3	30.6 ± 0.4	2.9	-2.3
2016	RH (%)	56.1 ± 1.6	57.4 ± 2.4	53.5 ± 2.2	64.3 ± 2.0	1.3	10.8
10 June	T (°C)	29.0 ± 0.2	32.9 ± 0.4	32.6 ± 1.0	31.3 ± 0.8	3.9	-1.3
2016	RH (%)	65.1 ± 1.4	56.7 ± 1.9	60.2 ± 5.7	67.6 ± 2.7	-8.4	7.4
11 June	T (°C)	31.9 ± 0.7	34.3 ± 0.9	31.1 ± 0.5	27.5 ± 0.8	2.4	-3.6
2016	RH (%)	51.3 ± 1.8	66.2 ± 1.7	52.4 ± 3.8	70.1 ± 2.6	14.9	17.7
12 June	T (°C)	30.4 ± 0.6	33.7 ± 0.5	31.9 ± 1.3	29.3 ± 0.5	3.3	-2.6
2016	RH (%)	54.9 ± 1.5	58.5 ± 1.1	68.8 ± 2.6	74.5 ± 2.3	3.6	5.7

After preliminary tests, configuration (A) of the NVAC greenhouse design was deemed unsuitable for the larger greenhouse size and environmental conditions of the region. A recurring draft created by the negative pressure of the prevailing wind gusts (Figure 14) over the roof ridge occasionally pulled the mist from the rafters. Analysis of measurements showed that the system did not provide any significant cooling nor any change in relative humidity (Table 7). The average inside temperatures with the NVAC misting system varied from -0.5 °C cooler to 0.1 °C warmer than outside conditions. When compared to outside conditions, the average temperatures inside the greenhouse varied from -0.3 to -0.5 °C cooler than outside. This may suggest a small amount of cooling occurred. However, with consideration of the standard deviations of the temperature measurements, this amount of cooling is not significant (Table 7). Upon examination of the temperature and relative humidity profiles of the 2014 test days, no significant drops in temperature nor increases in relative humidity could be noticed during periods when the NVAC misting system was used. The profiles corresponding to the test performed on 06 August 2014 are presented in Figure 8c and show very little change in conditions during misting periods. The relative humidity inside the greenhouse is seen to be greater than outside relative humidity however. This differs from the average conditions inside the greenhouse without the use of the NVAC misting system, where relative humidity drops over the course of the day (Figure 17). Although the outside conditions of the test days presented higher relative humidity compared to previous days in July 2014 (Figure 17) the fact that the relative humidity increased beyond outside conditions suggests that the NVAC misting system influenced the conditions inside the greenhouse, only not enough to provide cooling. An increase in relative humidity may have been due to added surfaces of water such as in the gutters of the NVAC roof, on the surface of the NVAC roof, and from leaks in the misting line. It was deemed that the type of mist nozzle should be changed to reduce clogging and dripping, that the number of nozzles should be increased, and that the location of the misting line should be changed.

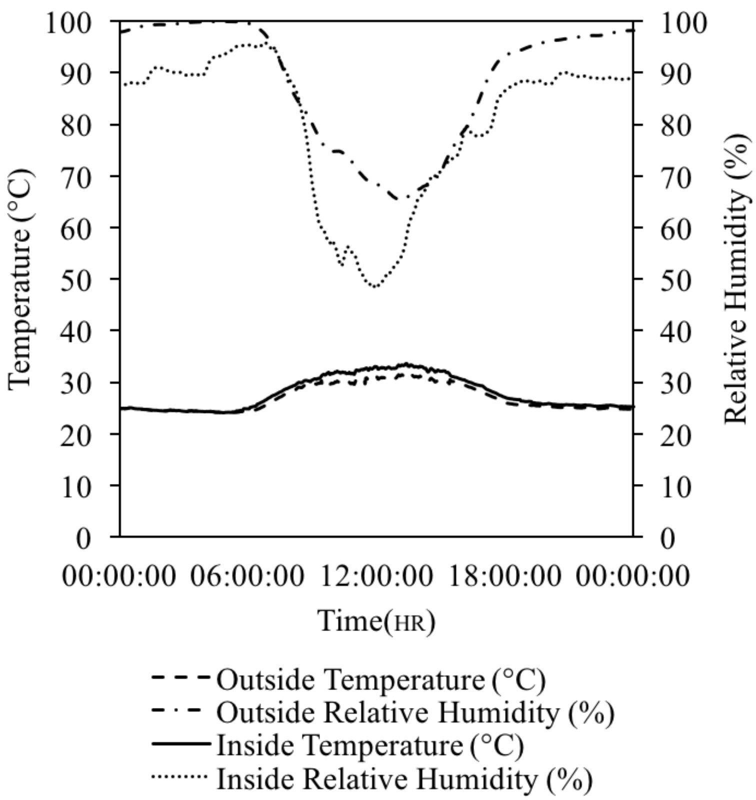

Figure 17. Graphical representation of the average recorded temperatures and relative humidity inside and outside the natural ventilation augmented cooling (NVAC) experimental greenhouse in Trents, Barbados. The averages are over 10 sunny days in July 2014. The NVAC misting system was not used during this period.

In a similar way to in the experimental greenhouse in Ste-Anne-de-Belleuve, QC, Canada, the amount of PAR reaching the crop in the Trent, Barbados location was reduced with the NVAC greenhouse design. The comparison of outside to inside PAR throughout the day

(Figure 16) shows the average PAR reaching the inside of the greenhouse from 12:00 HR to 14:00 HR was 25.3% of the outside PAR over the same period. This large reduction in PAR is due to the use of Aluminet thermal reflective cloth (Isratech Ltd.) to reduce the thermal load entering the greenhouse. The Aluminet was kept in place during tests.

4.4.3 2016 Configuration (C) Large-Scale Greenhouse

In preparation for the 2016 tests, the misting line was reinstalled 4 ft into the mist channel, protecting the mist stream from drafts or turbulence from the roof vent (Figure 8). The number of nozzles per area of greenhouse was doubled. The final nozzle arrangement was one nozzle per 4.2 m^2 of greenhouse floor area, or one nozzle per 17.5 m^3 of greenhouse volume, not considering the volume above the gutter.

The NVAC greenhouse under configuration (C) was tested in 2016 in Trents, Barbados. The temperature and relative humidity profiles of August 2016 in Trents, Barbados were similar to the July 2014 profiles (Figure 17) and are not presented. However, during the test days, outside temperatures were warmer than in August 2014 and this is presented in Table 7. The average PAR profiles are shown for the 2016 tests and validate that configuration (C) impacted the PAR reaching the plant space in a similar way as configuration (A) (Figure 16). The drop in average PAR in the afternoon in 2016 is due to a shadow cast onto the sensors by a structural member in the greenhouse not part of the NVAC design.

The response in the greenhouse conditions to the NVAC misting system were evident (Fig. 15d). It was seen that under configuration (C), the NVAC misting system provided cooling varying from 1.3 to 3.6 °C and a relative humidity increase varying from 1.3 to 14.9%, when comparing to outside conditions (Table 7). During all four tests, the average temperatures prior to the use of the NVAC system were higher than outside temperatures, and temperatures during the use of the NVAC system were lower than outside temperatures.

During daytime high temperatures, the response to the NVAC system is in fact quite rapid. Upon closer examination of the data collected on 11 June 2016, the greenhouse temperature went from 31.5 ± 0.3 °C to 28.2 ± 0.2 °C, a drop of 3.3 °C, during the first 120 s of activation of the NVAC system of the first misting event of the day (Figure 15d). A more gradual drop in temperature of an additional few degrees was noticed in the subsequent minutes, reaching a low of 25.8 ± 0.4 °C. When the NVAC misting system was stopped, a reverse effect was seen where the temperature rapidly increased. Subsequently, and before the second use of the NVAC system, the temperature inside the greenhouse eventually reached a maximum of 35.3 ± 0.5 °C. The relative humidity followed similar but opposite response patterns. In all tests, the NVAC system altered the conditions inside the greenhouse by providing cooling and an increase in relative humidity, but conditions nonetheless followed daily trends, as the conditions inside the NVAC greenhouse are subject to the conditions outside. This comes as no surprise as the greenhouse is naturally ventilated. This is noticeable during the test on 11 June 2016 (Figure 15d) where the first use of the NVAC system early in the day provided cooling and a relative humidity increase, but the curves of these alterations followed the daily trend, which is increasing temperature and decreasing relative humidity, as the time of day approached peak-heat. During the last misting event, the temperature inside the greenhouse was already dropping and conditions after the misting event did not return to the warmer and drier conditions that preceded the event. Considering that the evening and nighttime relative humidity conditions were naturally high (Figure 17), such cooling and increase in relative humidity before sundown may not be necessary. For this reason, the NVAC misting system is best used during the hours of the day straddling peak-heat.

Although seen as a drawback of most evaporative cooling systems, an increase in relative humidity may be desirable in dry climates, such as arid climates, or during certain dry periods of the day in other climates to reduce transpiration and crop stress. Katsoulas et al. (2001) confirmed that a crop in a greenhouse with a misting system was less stressed under such conditions. The influence of relative humidity on the expansion and water relations of young tomato fruits has been studied, and using misting to reduce air vapor pressure deficit alleviated the reduction in fruit volume increase during dry periods and led to better fruit quality (Guichard et al., 2005). Based on the performance of the NVAC greenhouse in this study, the NVAC greenhouse could also be used to reduce crop stress through manipulation of the relative humidity.

Despite the fact that the NVAC greenhouse is different in design compared to traditional evaporative cooling systems, it relies on the evaporative cooling process to provide cooling. It is expected that the NVAC greenhouse design will show similar or better cooling performance in hot arid climates, because a larger cooling performance is possible under drier conditions. Follow-up research in our laboratory is investigating both the cooling performance of the NVAC greenhouse design in a variety of climate types, and the impact that the NVAC misting system has on tomato fruit growth.

4.4.4 Nozzles

The characteristics of the misting nozzles were studied during preliminary tests in Trents, Barbados in July and August of 2014 and 2015. To improve the reliability of the system, three types of commonly available misting nozzles were tested: 1) brass body with stainless steel inserts and a 0.3-mm orifice (Model 10106H, Orbit Irrigation Products Inc.), 2) entirely stainless steel 0.3-mm orifice with built-in micro filters (MT with filter-long 10/24 thread, low-med-high pressure nozzle, AmFog Nozzle Technology, Inc), and 3) entirely stainless steel 0.3 mm orifice with no filters or removable internal pin (MT 10/24 thread, low-med-high pressure nozzle, AmFog Nozzle Technology, Inc). The entirely stainless steel nozzles without filters or pins lasted for months without clogging, whereas the two other types showed clogging within days. The entirely stainless steel 0.3 mm orifice nozzles with no filters were selected for final system testing in Trents, Barbados in 2016.

Unlike the effectiveness of the mist tubing in the NVAC greenhouse at the Ste-Anne-de-Bellevue, QC, Canada location, the mist tubing at the Trents, Barbados location required improvements to mitigate algae and biofilm clogging. The tubing was changed from a beige 3/8-inch o.d. tube (Orbit Irrigation Products Inc.) to a black polyamide 12 nylon 3/8-inch o.d. and 0.075-inch wall-thickness tube (AmFog Nozzle Technology Inc.). An ultraviolet-light water purifier was used to reduce algae and biofilm growth. Metal tubing such as copper or stainless steel were avoided to keep the design affordable and accessible to growers in any region.

4.4.5 Light transmission

Measurements were taken during test days in August 2014 at 1300 HR in Trents, Barbados NVAC greenhouse with the LI-193 spherical quantum sensor. These measurements were used to make the light conditions inside the NVAC greenhouse uniform. Aluminet was either entirely removed or reduced to one layer on the side of the greenhouse under which the NVAC roof was built. A double layer of Aluminet was kept over the area unaffected by the shading of the NVAC roof. The amount of light reaching the plants at a height from the ground of 1.5 m under the newly installed NVAC roof with one layer of Aluminet was no different than under the pre-existing conditions with the double layer of Aluminet (Table 8). However, in later studies, it was observed that without rainfall on this inner roof, dust and dirt accumulation was more pronounced compared to typical greenhouse roofs, and reduction in light transmission eventually occurred (Al-Helal and Alhamdan, 2009). In this case, the growers chose to eventually remove the Aluminet all together under the NVAC roof. Washing the surface of the roof with a spray of water can help prevent such a circumstance. At Row 3, lower levels of light were due to the structural components of the greenhouse, not related to the NVAC design (Table 3). At no point over the course of this research project, under all configurations, did algae develop on the NVAC roof surface or in the NVAC roof gutter.

Table 8. The average photosynthetically active radiation (PAR) in $\mu mol \cdot m^{-2} \cdot s^{-1}$ in the natural ventilation augmented cooling (NVAC) greenhouse in Trents, Barbados. Hand-held measurements were taken throughout the greenhouse, following the five empty crop rows, running lengthwise in the greenhouse, at three locations per row at a height of 1.5 m. Measurements were taken at four occasions, on July 31, August 1, August 3 and August 4, 2014 at 13:00 HR, and were averaged.

Under NVAC roof		Middle	Under usual roof	
Row 1	Row 2	Row 3	Row 4	Row 5
Average PAR ($\mu mol \cdot m^{-2} \cdot s^{-1}$) ± standard deviation (n=4)				
696 ± 20	732 ± 25	532 ± 22	672 ± 25	747 ± 25
733 ± 40	539 ± 23	484 ± 45	765 ± 31	743 ± 46
756 ± 39	647 ± 44	493 ± 56	766 ± 46	713 ± 21

4.4.6 Cost and Water Use

The NVAC greenhouse design can be built as an integrated system into a new structure, or can be retrofitted to an existing structure. The costs involved in constructing an NVAC greenhouse are the costs related to acquiring a typical natural ventilation greenhouse in addition to the costs for the NVAC system's components (Table 9). A detailed account of the materials required for the construction of a 4.5-m by 9-m NVAC greenhouse, including both the greenhouse structure and NVAC system, is presented in Appendix C with local costs. The costs of procuring an NVAC system for the smaller greenhouse (4.6 m by 6.1 m) used in this project is $3.05 per square meter of growing area, which is more than for a larger structure, such as the 13.7-m by 32.0-m NVAC greenhouse at $2.76 per square foot. This is because the greenhouse is very small in scale and any addition to the cost of the structure represents a large cost per growing area. Although significant structural work, automation devices, greater water pressure and water supply volume are required in the larger structure, the scale of the greenhouse is large enough to reduce the cost per growing area (Table 9b).

Table 9. The cost analysis for construction elements of a natural ventilation augmented cooling (NVAC) system installed in (a) a small scale NVAC greenhouse and (b) a large scale NVAC greenhouse. Cost of the greenhouse or labor not included. Shipping costs or sales taxes not included. Values are in Canadian Dollars. A detailed account of the materials required for construction of the NVAC system and of the greenhouse structure is presented in Appendix C with local costs.

Item	Cost	Cost·m^{-2}
(a) 4.6-m by 6.1-m NVAC greenhouse, 2.9-m gutter height		
12-ft (3.66 m), 3/8-inch (9.53 mm) o.d., ultraviolet light stabilized tubing, set of eight brass fittings with 0.3-mm orifice nozzles, hose adapter and end plug (Professional 12-ft mist cooling system, Model 20090, Orbit Irrigation Products Inc. Bountiful, UT)	$90	$0.98
Added roof structure and sheeting	$150	$2.72
On/Off ball-valve	$10	$0.10
Gutter and required fittings	$30	$0.33
Total	$280	$3.05
(b) 13.7-m by 32.0-m NVAC greenhouse, 4.6-m gutter height		
45.7 m of 3/8-inch (9.53 mm) polyamide 12 nylon tubing (heat stabilized, ultraviolet light stabilized and plasticized)	$159	$0.33
120 stainless-steel 0.3-mm orifice nozzles (AmFog Nozzle Technol., Inc.	$389	$0.26

Casa Grande, AZ)		
50 misting line mounting clamps with rubberized fitting (AmFog Nozzle Technol., Inc.)	$45	$0.03
Ultraviolet light water purifier (1/4-inch (6.35 mm) inlet, 2 gal/min (7.6 $L \cdot min^{-1}$), McMaster-Carr, Aurora, OH)	$200	$0.13
100-micron filtration grade filter (Netafim DF100-140, Amiad Water Systems Ltd., Ami'ad, Israel)	$115	$0.07
20-µm filtration grade filter (Model S1A, Culligan Water, Rosemont, IL)	$40	$0.03
3/8-inch (9.53 mm) 160 psi (1103 kPa) booster pump (Model 92100, Orbit Irrigation Products Inc.)	$150	$0.10
Added structure and sheeting	$1200	$0.82
Automation device including temperature and weather sensing[x]	$350	$0.23
Two solenoid valves (3/4-inch Electric Solenoid Valve, 24 V with flow control, Irrigation Direct, Inc. Livermore, CA) – A minimum of 1 ball-valve required if no automation is used	$100	$0.07
40 ft (12.2 m) of 3/4-in (19.05 mm) polyvinyl chloride (PVC) piping	$50	$0.03
20-gal (75.7 L) water pressure tank (Goulds Pumps, Seneca Falls, NY)	$175	$0.13
0.5-horsepower (0.37 kW) water supply pump (Goulds Pumps)[y]	$185	$0.13
Gutter and required fittings	$200	$0.13
Two 1000-gal water tanks	$1000	$0.69
Total	$3969	$2.76

[x] amount of control and automation can vary depending on grower's requirements

[y] not required, greenhouse irrigation pump can supply NVAC system if plumbed accordingly

The nozzle water usage for the stainless-steel nozzles used in 2014 and 2016 was rated by the manufacturer at 2.7 $L \cdot h^{-1}$ at 150 psi (1034 kPa), but was measured to be 2.5 $L \cdot h^{-1}$ per nozzle at 160 psi (1103 kPa). This represented a consumption of 0.58 $L \cdot h^{-1} \cdot m^{-2}$ for the configuration of the NVAC greenhouse providing the most cooling performance, in Trents, Barbados (one nozzle per 4.2 m^2 of greenhouse floor area). In smaller greenhouses, such as the experimental greenhouse in Ste-Anne-de-Bellevue used in the present study, a water usage of 0.54 $L \cdot h^{-1} \cdot m^{-2}$ at a lower pressure of 60 psi (414 kPa) was adequate. In previous studies on a pad and fan evaporative cooling system, it was observed that the average water usage for cooling varied from 0.65 to 1.08 $L \cdot h^{-1} \cdot m^{-2}$ of floor area, respectively (Al-Helal, 2007), making the NVAC system less water-intensive. Flow rates reported in fog evaporative cooling systems vary greatly depending on the design, but in the literature, ranges from 0.13 to 1.22 $L \cdot h^{-1} \cdot m^{-2}$ (Öztürk, 2003), 0.23 to 0.64 $L \cdot h^{-1} \cdot m^{-2}$ (Hayashi & Kozai, 2005) and 1.23 to 1.63 $L \cdot h^{-1} \cdot m^{-2}$ (Arbel et al., 1999) are reported. The water use in the NVAC greenhouse evaporative cooling system is comparable to that reported in studies on fog cooling systems. The water use in the NVAC greenhouse evaporative cooling system is comparable to that reported in studies on fog cooling systems with similar cooling performances. In natural ventilation greenhouses, Öztürk (2003) reported an average of 3.8 °C and a maximum of 6.6 °C of cooling with respect to outside temperatures and Hayashi and Kozai (2005) reported up to 6 °C of cooling with respect to outside temperatures. On the other hand, in a forced ventilation greenhouse with a greater water usage per growing area, Arbel et al. (1999) observed cooling ranging from 8.5 to 12.0 °C.

In the Netherlands, it has been reported that water consumption for mature tomato plants is estimated at 1.9 to 2.5 $L \cdot m^{-2} \cdot day^{-1}$ (Papadopoulos, 1991). At maturity on sunny days, however, plants may need up to 6.8 $L \cdot m^{-2} \cdot day^{-1}$ (Snyder, 1992). The exact irrigation demand in arid climate greenhouses is not well reported, and therefore the value 6.8 $L \cdot m^{-2} \cdot day^{-1}$ will be used to provide an estimate for comparison purposes. In comparison to the normal amount of water used in greenhouse irrigation (1.9 to 2.5 $L \cdot m^{-2} \cdot day^{-1}$) and to the amount needed in arid climate greenhouse irrigation (most likely greater than 6.8 $L \cdot m^{-2} \cdot day^{-1}$), the amount of water used in the NVAC misting system water demand represents 25% and 8%, respectively, of the irrigation water demand.

4.4.7 Electricity Use

The NVAC greenhouse design consumed less electricity than other conventional greenhouse cooling systems, such as pad and fan systems. No electricity was required to power the small NVAC greenhouse in Ste-Anne-de-Bellevue, QC, Canada as a pressurized municipal water line was available and was sufficient for its size. The larger NVAC greenhouse in Trents, Barbados serves as a good example for the study of the electricity usage. Most of the electricity was required for driving the water supply pump (Goulds Pumps) and the secondary high-pressure water pump (Orbit Irrigation Products Inc.). The electricity required for the control system is negligible. The water supply pump draws 4.3 amps when operating on 220 V, and the secondary pump draws 1 amps on 115 V. The polypropylene ultraviolet-light water purifier draws 0.13 amps on 115 V. Typically, the supply pump ran intermittently three to four times per hour, for 2 to 3 min, to supply the water pressure tank. The secondary pump ran continuously for the periods during which the NVAC misting system was required. Using configuration (C) and providing cooling continuously for an experimental 8-h day, 2.2 kWh of electricity was required. A greenhouse of the same dimensions would require three to four 48-inch (1.2-m) belt driven exhaust fans (Galvanized Box Fans, Belt Drive, FarmTek, Dyersville, IA), each drawing 4.5 amps on 220 V continuously, to vent and provide cooling through a pad and fan system. A water pump similar to the supply pump used in the NVAC system would also be required to continuously supply water to the cooling pads. Such a system would require an estimated 39.2 kWh of electricity to provide cooling for an 8-h period (National Greenhouse Manufacturers Association). The NVAC greenhouse design, in this comparison, consumes only 5.6% of the electricity that a pad and fan system would consume for the same period of cooling. This greatly reduces the costs required to provide cooling in the greenhouse (Table 10).

Table 10. The cost of electricity required to operate the natural ventilation augmented cooling (NVAC) greenhouse as built in Trent, Barbados (1739 m^2) for an 8-h period per day. A comparison is made with a pad and fan cooling system for a greenhouse of the same dimensions over the same period per day. The cost is based on the Caribbean regional average cost of electricity of \$0.33·kWh (National Renewable Energy Laboratory, 2015).

	$kWh\cdot day^{-1}$	$kWh\cdot m^{-2}\cdot day^{-1}$	$\$\cdot h^{-1}\cdot m^{-2}$	$\$\cdot day^{-1}\cdot GH^{-1}$
NVAC Greenhouse	2.2	0.005	0.002	0.88
Pad and Fan System	39.2	0.089	0.029	12.7

Under warmer and drier conditions than those considered in this study, or in a greenhouse of larger scale, the number of nozzles per unit of greenhouse volume should be increased. The flowrate of the nozzles could also be increased by using alternate nozzles, or nozzle clusters

(Cluster head and adaptor, AmFog Nozzle Technology, Inc.). It is envisioned that the NVAC greenhouse design can be installed in gutter-connected multi-span greenhouses, provided each span has a roof vent of a similar design to the vents in the two greenhouses in this work. Alternatively, Lee and Short (2000) or Kacira et al. (1998) present a variety of different roof vent configurations that could also be well suited to accommodate the NVAC system. An NVAC roof and misting system would be installed under each span. Future work should consider the NVAC greenhouse system under alternative roof vent designs.

4.5 Conclusion

Many regions of the world with warm climates rely on natural ventilation greenhouse designs. To make crop production possible in arid climates, or to simply extend the growing season, growers rely on evaporative cooling solutions. The NVAC greenhouse was tested under three different configurations and provided cooling from 1.3 to 3.6 °C in its final iteration by means of a new evaporative cooling design that improved naturally ventilated greenhouses. The NVAC system comes at a low cost compared to pad and fan cooling systems and fog cooling systems, and is comprised of readily available materials. In comparison to such traditional greenhouse cooling methods, the system requires very little electricity to operate.

Connecting Text

Chapter 5, *An experimental study of the cooling performance and air movement in a Natural Ventilation Augmented Cooling (NVAC) greenhouse by means of direct measurement and tri-sonic anemometry*, was authored by Lucas McCartney, Valérie Orsat and Mark. G. Lefsrud. Chapter 5 was submitted to the journal *Biosystems Engineering* on June 19, 2017 and is currently under review.

Following five summer seasons of field development and testing of the NVAC greenhouse in Ste-Anne-de-Bellevue and Trents, a scaled-down physical model was built in a research greenhouse at the Macdonald Campus of McGill University. Chapter 5 presents the results of an extensive study of the performance of the NVAC greenhouse under varying climatic conditions, without the influence of external factors such as wind and rain. This chapter presents the findings of our investigation into the air movement inside the NVAC greenhouse brought about by the NVAC system. The performance of the system varied according to the climate types, and this allowed us to calculate a variety of efficiencies. From the performance and air movement results that we obtained, we were able to compare the NVAC greenhouse system to traditional evaporative cooling systems such as pad and fan systems and high-pressure fog systems. The results obtained in this study lay a foundation for future computational fluid dynamics studies on the novel greenhouse design.

5. Chapter 5: An Experimental Study of the Cooling Performance and Air Movement in a Natural Ventilation Augmented Cooling (NVAC) Greenhouse by Means of Direct Measurement and Tri-Sonic Anemometry.

Lucas McCartney, Valérie Orsat and Mark G. Lefsrud

Additional index words. Greenhouse cooling; Ventilation; Air Movement; Natural Ventilation

5.1 Abstract

A Natural Ventilation Augmented Cooling (NVAC) greenhouse is a natural ventilation greenhouse that is improved by coupling natural ventilation with a non-conventional misting system. Previous work on the cooling performance of the NVAC greenhouse design investigated temperature and relative humidity within the greenhouse under field conditions. To further investigate the cooling capabilities and the nature of the airflow in the NVAC greenhouse, a network of thermocouples and a three-dimensional sonic anemometer were used for the measurement of temperature, relative humidity and air velocities inside a model 1:4 scale NVAC greenhouse. The cooling performance of the NVAC greenhouse design varied from 1.9 to 12.6 °C and relative humidity increased by 1.4 to 31.2% depending on the ambient conditions. The NVAC greenhouse reduced vapor pressure deficit by 0.3 to 4.9 kPa. Although temperature distributions were more uniform under natural ventilation, the amount of cooling was significantly greater with the use of the NVAC design, compared to none. It was shown that the NVAC greenhouse can provide air movement in the plant space of the greenhouse at velocities up to 0.40 $m \cdot s^{-1}$ without the use of fans. The average turbulence intensity of the air inside the greenhouse was increased to 0.32 with the use of the NVAC design, compared to 0.19 under natural ventilation. The performance of the NVAC greenhouse is comparable to that of pad and fan and fogging systems, and offers advantages over these traditional systems such as better water use efficiency and prevention of foliage wetting.

5.2 Introduction

Natural ventilation is a passive greenhouse design that requires less energy input and equipment compared to active ventilation, and is the cheapest method of cooling a greenhouse.

Although natural ventilation designs remain widespread (Muñoz et al., 1999), natural ventilation offers limited control of airflow in the greenhouse.

In hot climates such as arid and tropical climates, protected agriculture is used to control temperature, relative humidity and airflow. Other elements such as carbon dioxide concentration, light intensity and pest control are also considered. Yields from many common vegetable crops reduce at temperatures above 26 °C even with specialized cultivars (Heuvelink, 2008; Sato et al, 2006). The climate found in arid regions is characterized as hot with long summer seasons that have ambient temperatures exceeding 45 °C around midday, and dry with ambient relative humidity dropping below 10% at midday (Abdel-Ghany et al., 2012). In tropical climates, the ambient temperature during the day can easily exceed 30 °C year-round, and midday relative humidity can vary from very dry conditions to very humid conditions, depending on the region (Kottek et al., 2006). Under such conditions, inside greenhouse temperatures can soar well beyond these values, and relative humidity can vary greatly throughout the course of a day.

Proper air circulation decreases temperature, decreases relative humidity, improves carbon dioxide uniformity in the greenhouse, and reduces the incidence of stagnant air. The ASHRAE (1985) Fundamentals Handbook states that greenhouse air velocities in the range of 0.5 to 0.7 $m \cdot s^{-1}$ are optimal (Kittas et al., 2003). Furthermore, in terms of plant productivity and quality, the velocity of the air movement in a greenhouse is suggested to not exceed 1 $m \cdot s^{-1}$ across the plants (ASHRAE, 1985).

5.2.1 Natural Ventilation

The main driving forces of ventilation for a greenhouse equipped with both roof and side openings are caused by a combination of pressure differences induced by a multitude of effects (Boulard & Baille, 1995; Kittas et al., 1997; Baptista et al., 1999). The buoyancy effect (chimney effect) induces pressure differences between the side and the roof openings (Bruce, 1978; Bruce, 1982). The wind effect induces pressure differences around the greenhouse, mainly between the windward and the leeward parts of the greenhouse (Boulard et al., 1996; Kittas et al., 1997). The turbulent effect of the wind seen across the greenhouse openings and into the plant space affects ventilation (Boulard et al., 1996). These effects generate a vertical ventilation flux due to the chimney effect and a horizontal ventilation flux due to the side wall and turbulent wind effects (Kittas et al., 1997). However, in the absence of any of these influences, such as in low wind conditions, these fluxes may be altered, minimized or eliminated entirely. It is reported that winds stronger than 1.8 to 2.0 $m \cdot s^{-1}$ dominate the ventilation process and that in this case buoyancy can be neglected (Bot, 1983; Papadakis et al., 1996). Buoyancy driven ventilation is more important if the wind velocity is lower than 0.5 $m \cdot s^{-1}$. In the intermediate cases where wind velocity is between 0.5 $m \cdot s^{-1}$ and 2 $m \cdot s^{-1}$, the ventilation is driven mostly by the wind effect and some influence of the buoyancy is observed (Kacira et al., 2004).

In the naturally ventilated greenhouses widely used in the Mediterranean region, the air velocity typically observed in the plant space varies from 0.1 to 0.5 $m \cdot s^{-1}$, which includes the wind effect (Molina-Aiz et al., 2003, Molina-Aiz et al., 2004, Jiménez-Hornero et al., 2005; Teitel et al., 2005). It is important to note that such airflow can vary depending on the weather and the season, and that in many regions, such airflow cannot be sustained by natural ventilation alone (Latimer, 2009). The necessity of installing insect netting in order to prevent proliferation of diseases and pests induces a pressure loss, thereby reducing the ventilation efficiency by up to 50% (Miguel et al., 1997; Kittas et al., 2002; Bailey et al., 2003). In certain weather conditions, the air inside the greenhouse can stagnate for several minutes at a time, causing local peaks in temperature that may cause harm to the crop. Natural ventilation systems currently in use are not considered as dependable or satisfactory as a mechanical ventilation system in terms of providing continuous, uniform greenhouse ventilation (Buffington et al, 2013). Moreover, no cooling beyond that of ambient conditions is possible in solely natural ventilation designs (Giacomelli et al., 1985).

5.2.2 Fan Systems

Systems comprised of vents, exhaust fans and circulating fans can supply immediate air movement and high air exchange rates whenever needed, at the expense of electricity consumption. When used without evaporative cooling, these systems are limited as they allow maintenance of inside greenhouses temperatures to a level equal or slightly higher than the outside ambient temperature (Sethi & Sharma, 2007). In a study by Fernandez and Bailey (1994), air velocity was measured inside an empty greenhouse with side vents (no cooling pads), with and without circulation fans, which showed that the fan provided significantly greater velocities (Table 11).

Table 11. Minimum (u_{min}) and average (u_{avg}) recorded air velocity in a Venlo-style test greenhouse without crop, with and without circulation fans. Circulation fans were used at their respective maximum velocity. Data from Fernandez and Bailey (1994).

Conditions	Without Crop	
	u_{min} ($m \cdot s^{-1}$)	u_{avg} ($m \cdot s^{-1}$)
Without Fans (Still)	0.11	0.12
With Fans	0.48	0.64

5.2.3 Pad and fan Systems

Pad and fan systems rely on evaporative cooling and forced ventilation, and are effective at providing cooling. Pad and fan cooling is an effective method of lowering the air temperature of the greenhouse by 4 to 6 °C if used alone, and 4 to 12 °C if used with shading (Jain & Tiwari, 2002; Kittas et al., 2003; Sethi & Sharma, 2007). In Al-Helal (2007), the averages of air temperature and relative humidity inside a greenhouse cooled with a fan and pad system, with and without shading, varied from 30.2 to 33.6°C, and 33.5 to 37.5%, respectively. The outside temperature and relative humidity were 38.7°C and 11%.

López et al. (2010) studied the airflow and distribution of temperature and humidity in a multi-span greenhouse equipped with a pad and fan cooling system operating both with a tomato crop and without a crop. The air movement data in this study (Table 12) was collected with a three-dimensional sonic anemometer.

Table 12. The minimum (u_{min}), maximum (u_{max}) and average (u_{avg}) recorded air velocity in a multi-span greenhouse equipped with an evaporative cooling fan and pad system, with and without tomato crop. Data from López et al. (2010).

Conditions	u_{min} ($m \cdot s^{-1}$)	u_{max} ($m \cdot s^{-1}$)	u_{avg} ($m \cdot s^{-1}$)
With Crop			
	0.13	0.75	0.21
u_x	0.13	0.70	
u_y	0.00	0.15	
u_z	0.00	-0.24	
Without Crop			
	0.10	0.58	0.26
u_x	0.09	0.55	
u_y	0.00	0.17	
u_z	0.00	-0.23	

In the study by López et al. (2010), it was shown that the flow of air that passed through the evaporative pads underwent a sharp drop in velocity when it encountered the dry, warm air inside. The main disadvantage of cooling pad systems is therefore the creation of large temperature gradients inside the greenhouse, from the pads on one side to the extracting fans on the opposite side. Kittas et al. (2003) reported temperature gradients up to 8 °C from the cooling pads to the fans.

5.2.4 Mist and Fog Systems

Both high (fog) and low-pressure (mist) systems are used in greenhouses to maintain high humidity, prevent excessive water loss from leaf surfaces and provide cooling (Jackson & Darby, 2010). However, without proper consideration of structural design and local climate, mist and fog systems often involve excess humidity in stagnant air. Arbel et al. (1999) studied a fog system operating at varying pressure to cool an actively vented greenhouse and found that the fog system provided more uniform temperature and humidity conditions compared to a pad and fan system, under similar conditions. The study, however, was on an actively ventilated greenhouse which provided forced air exchange and air movement. The cooling performance varied from 8.5 to 12 °C, and the increase in relative humidity varied from 35 to 68% (Table 13).

Table 13. Initial and experimental conditions in a greenhouse operated by a fog system, under various conditions. Modified from Arbel et al. (1999).

		Ambient Conditions		Experimental Conditions	
Trial	Nozzle Pressure (kPa)	$T_{db,o}$ (°C)	RH_o (%)	$T_{db,c}$ (°C)	RH_c (%)
1	45	35	30	24.5	90
2	35	36.5	25	26	60
3	25	37	24	28.5	80
4	45	38.5	22	26.5	90

The efficiency of fog or mist systems in natural ventilation greenhouses is often limited by insufficient natural air movement, the absence of wind, and the risk of wetting the plants when water droplet evaporation is not complete (Kittas et al., 2003). The range of wetness duration requirements for plant infection from fungal parasites vary from 0.5 to more than 100 h (Huber & Gillespie, 1992). Short term leaf wetness may be no different from rainfall, but prolonged or continuous leaf wetness can lead to increased disease incidence. Pathogens often require a water film on the leaf to develop and infect (Prenger & Ling, 2000). Even the presence of minute droplets or a thin film of water such as condensation provide an environment in which fungi and bacteria can germinate and grow (Wei et al., 1995). Diseases such as *Botrytis obstusa* can germinate in water droplets within 4 h at 24 °C (Jarvis, 1992).

5.2.5 The NVAC Greenhouse Design

In many regions of the world, financial limitations due to high electricity costs and inaccessibility to technology prevent the use of fans and typical evaporative cooling systems for greenhouse ventilation and cooling (von Zabeltitz & Baudoin, 2005). An alternative greenhouse design, the NVAC greenhouse, provides cooling and relative humidity control without the use of typical systems such as cooling pads and fans. The passive design is presented in McCartney (2017). It is a natural ventilation greenhouse with side and roof vents, and houses a non-conventional misting system in the rafters of the greenhouse. In field trials, the NVAC greenhouse design provided cooling between 1.6 to 6.8 °C, while increasing relative humidity by 6.9 to 17.1% (McCartney, 2017). During field trials, it was observed that the evaporative cooling effect of the NVAC system coupled with the roof design provided improved air movement at the plant level, but this has not yet been studied. The present paper is to further examine the cooling capabilities and relative humidity control of the design, and to accurately study the air movement. Comparisons with traditional evaporative cooling techniques is therefore possible.

5.2.6 The Study of Air Movement

The experimental study of air movement in real greenhouses is considered the ultimate test to clearly define the air circulation (Wang et al. 1999). Several techniques have been developed, such as mechanical, hot-wire and sonic anemometry. A sonic anemometer is regarded as one of the best devices for the measurement of air movement in large enclosures like greenhouses (Wang et al., 1999; Boulard et al., 1997b). Greenhouse air velocity has been measured using three-dimensional sonic anemometers in several published papers including: Wang & Deltour, (1997), Boulard et al., (1997b), Boulard et al. (1998), Boulard et al. (2000), Tanny et al. (2006), Teitel et al. (2008), Kittas et al. (2008) and Katsoulas et al. (2010). In the present study, the NVAC greenhouse design was tested under windless conditions in order to identify the air movement potential, along with the cooling potential, of the misting system and roof design of the NVAC greenhouse concept.

5.3 Materials and Methods

5.3.1 Experimental Setup

A model NVAC greenhouse was built in 2016 in one bay of the research greenhouse at the Macdonald Campus of McGill University in St-Anne-de-Bellevue, QC, Canada (45°24′N, 73°57′W). The climate within the research greenhouse bay was modified to suit the variety of tests performed in this study. During tests, the controlled environment allowed for the wind effect to be eliminated to isolate the effects of the use of the NVAC system. A combination of solar radiation, hot water heating and control of the research greenhouse ventilation provided the required control of the test environment conditions leading up to the tests. During tests, greenhouse bay conditions were maintained using solar radiation and hot water heating, but all ventilation was ceased to not induce artificial wind. At this point, all vents of the research greenhouse bay were closed and sealed with polyethylene film and duct tape to prevent seeping of outside air into the bay.

The model NVAC greenhouse was a 1:4 design 6.10 by 6.10 m, and 3.05 m in height, based off of a 1:4 NVAC greenhouse used for field testing. The fully screened sidewalls had a height to the gutter of 1.75 m. The upper vent (roof) had a screened opening of 0.6 m, running the full length of the greenhouse. The upper ridge of the NVAC roof was 0.6 m below the roof vent, and the bottom ridge of the NVAC roof is at the level of the greenhouse gutter height (Figure 18). The structure was built from galvanized steel, insect screening (Mesh 40, 20-23% high density polypropylene, ShadeLogic Canada, Brampton, ON) and 6-mil polyethylene sheeting (Plastitech, Saint-Rémi, QC). The misting line was a 9.5-mm beige tube (Orbit® Irrigation Products Inc. Bountiful, UT). Brass push-to-connect fittings (Orbit® Irrigation Products Inc.) were used to install brass 0.3-mm orifice nozzles (Orbit® Irrigation Products Inc.). A 120-V and 1 amp booster pump (Orbit® Irrigation Products Inc.) was used to pressurize the misting line. Temperate water was used for the misting system. The water supply pressure and temperature for the misting system was monitored during all tests, and remained at 1103.16 kPa and varied from 28 to 32 °C, respectively. Three or six nozzles, depending on the trial, were evenly spaced along the edge of the second roof. The greenhouse had a floor space of 37.2 m^2 and a volume of 56.6 m^3 not including the rafter volume. The rafter volume is the volume of the greenhouse above the gutter. The nozzle configuration was therefore one nozzle per 12.4 m^2 of greenhouse floor area, or one nozzle per 18.9 m^3 of greenhouse volume, not considering the rafter volume, for the three-nozzle trials. The configuration was one nozzle per 6.2 m^2 of greenhouse floor area, or one nozzle per 9.4 m^3 of greenhouse volume, not considering the rafter volume, for the six-nozzle trials. The nozzle water usage was rated by the manufacturer at 1.89 $L \cdot h^{-1}$ at 413.7 kPa, but was measured to be 3.47 $L \cdot h^{-1}$ per nozzle at 1103.2 kPa. This represented a consumption of 0.28 $L \cdot h^{-1} \cdot m^{-2}$ and 0.56 $L \cdot h^{-1} \cdot m^{-2}$ for the three and six-nozzle configuration, respectively. A gutter was installed along the bottom ridge of the NVAC roof to collect the unevaporated misting water.

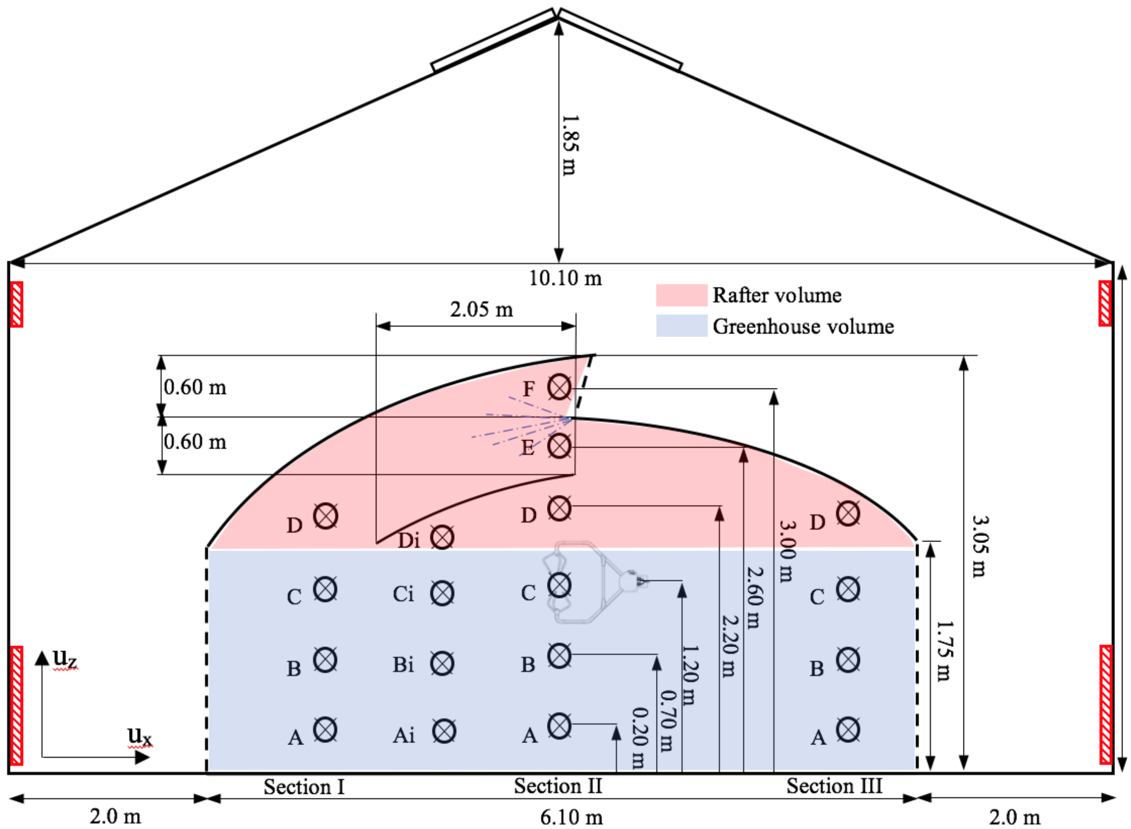

Figure 18. Dimensions of the natural ventilation augmented cooling (NVAC) model greenhouse seen inside a research greenhouse. The locations of the sonic anemometer measurements are indicated with crossed circles and identified with letters per section. The greenhouse was separated into three sections, each having three measurement locations at three heights. The positioning of the sonic anemometer can be seen, as an example, at Section II height C. Measurements performed in the rafters of the NVAC greenhouse are identified by letters D, E and F. The measurements taken under the inside roof (between Sections I and II) at heights A, B, C and D are denoted by an i preceding the identifying letter. Dashed lines indicate vents covered with insect screening. Red and patterned boxes indicate location of the heaters in the research greenhouse. The location and direction of spray of the mist nozzles are seen between measurement heights E and F.

5.3.2 Equipment and Instrumentation

Temperature and relative humidity were measured inside and outside the NVAC greenhouse. Wet-bulb (T_w) and dry-bulb (T_s) temperatures were recorded at six locations inside the greenhouse and three locations outside (in the greenhouse bay) (Figure 19). During air movement tests, T_w and T_s temperatures were recorded at three indoor locations of varying height in the middle of the greenhouse (Figure 19). Wet-bulb sensors were fabricated using thermocouples, a distilled water reservoir and wicking cotton. The wet-bulb and dry-bulb sensors were made from type-T thermocouple wire (Spectris Canada, Omega Environmental, Laval, QC, Canada) and were placed in an enclosure with fans providing 3 $m \cdot s^{-1}$ air velocity across the thermocouples (Both et al., 2015). The type-T thermocouples had a range of measurement of -270 to 370 °C with a standard accuracy of ± 1.0 °C or ± 0.75%, whichever is greater. The air velocity of the aspirated sensors was measured using a hot-wire anemometer (TPI 565C1 digital anemometer with hot-wire probe, 0.2 to 20 $m \cdot s^{-1}$ velocity, -20 to 80 °C temperature, Test Products International Inc., Beaverton, OR). Each station was housed in a white PVC channel (diameter 0.15 m) to shield from solar radiation. An Agilent 34972A LXI data logger (Keysight Technologies Canada Inc. Mississauga, ON, Canada) was used to record measurements.

The air velocities in directions x, y and z in this study were measured with a three-dimensional sonic anemometer (model CSAT3, Campbell Scientific Canada, Edmonton, Canada). Data was recorded by a data logger (model CR5000, Campbell Scientific Canada) and instantaneous measurements were programmable from 1 to 60 Hz. The analog velocity output range of the device is ± 30 $m \cdot s^{-1}$, ± 60 $m \cdot s^{-1}$ in x and y, ± 8 $m \cdot s^{-1}$ in z and 300 to 366 $m \cdot s^{-1}$ or -50 to 60 °C in temperature. The resolution of the device is 1 $mm \cdot s^{-1}$ rms in x and y, 0.5 $mm \cdot s^{-1}$ rms in y and 15 $mm \cdot s^{-1}$ or 0.025 °C rms in temperature.

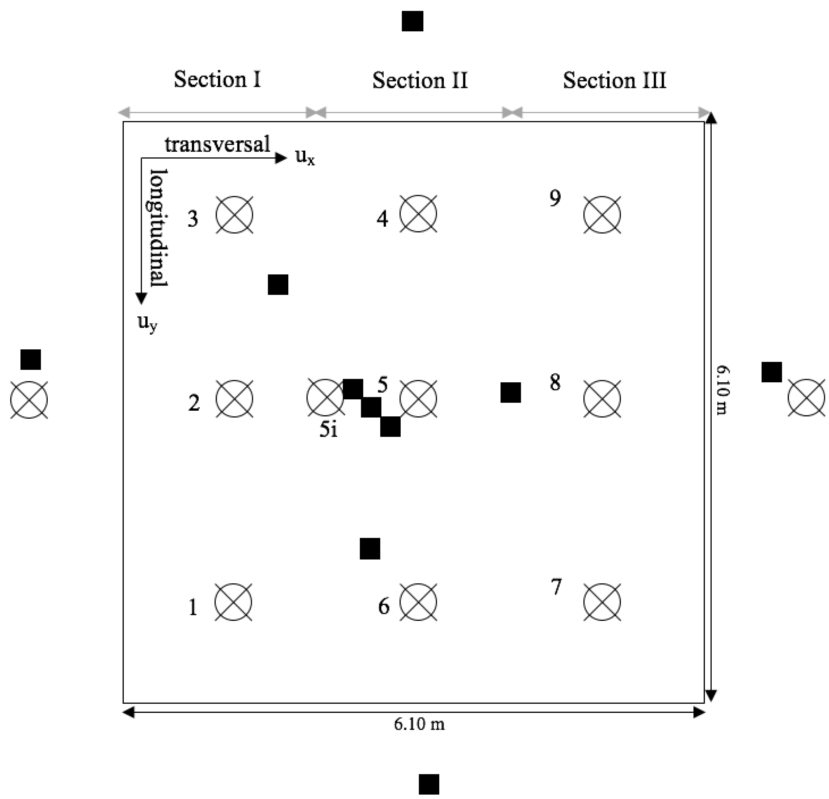

Figure 19. The distribution of the wet-bulb and dry-bulb temperature aspirated sensors and of the measurement locations for the sonic anemometer measurements in the natural ventilation augmented cooling (NVAC) model greenhouse. Temperature measurement locations are identified with dark squares. Anemometer measurement locations are identified with crossed circles. Measurements were also done outside the model greenhouse, in the research greenhouse bay.

Figures 18 and 19 show the location of the airflow and temperature measurements locations in the model NVAC greenhouse. Measurements were done at three heights, 0.20 m, 0.70 m and 1.20 m, at nine locations in the plant space of the greenhouse. Other measurements were done at three heights (D, E, F) at point 2, 5 and 8 in the rafters of the greenhouse to obtain a cross-sectional assessment of the greenhouse air movement. The measurement locations were split transversally into three sections (Sections I, II and III) to facilitate analysis. During cross-sectional measurements, four more measurements were made at point 5, but slightly skewed to the location between points 2 and 5, which is the area beneath the inside roof. This point was identified as point 5i, and measurement height D is slightly lower than other height-D measurements (Figure 18). The influence of the crop or structure inside the greenhouse was disregarded in the determination of the airflow (Jiménez-Hornero et al., 2005). The scope of this study was limited to an empty greenhouse and therefore, the main area of the greenhouse was kept open, except for the anemometer apparatus, temperature sensors and greenhouse structure.

From the relative humidity data recorded by the stationary sensors, the specific humidity (q) was obtained and the sonic anemometer temperature (T_s) used for analysis was corrected for humidity using the method suggested by Burns et al. (2012):

$$T_{s_{air}} = \frac{T_s}{1+0.51q} \qquad \text{Equation 9}$$

The corrected temperature measurements obtained from the sonic anemometer (T^s_{air}) allowed for comparison with thermocouple measurements and thus for the analysis of temperature gradients in the NVAC greenhouse.

Smoke was used to visualize the air movement in the NVAC design using smoke emitting sticks (15-049 Tel Tru, E. Vernon Incorporated, Rohnert Park, CA). White smoke with a thin black cardboard backdrop worked best to visualize the air as it moved in the plant space (Albright, 1995). Measurements for temperature and relative humidity were carried out during sunny days in the month of March and April 2016. Anemometer measurements were carried out on December 12, 2016 and December 18, 2016, during which temperature and relative humidity were also measured. All vents in the greenhouse bay where the experiment took place were closed and sealed with polyethylene film and duct tape to prevent seeping of outside air into the bay. A combination of solar radiation, hot water heating and control of the research greenhouse ventilation provided the required control of the test environment conditions.

5.4 Analyses

5.4.1 Temperature, Relative Humidity and Vapor Pressure Deficit

The relative humidity values were calculated from dry bulb temperature, wet bulb temperature and barometric pressure (Snyder & Shaw, 1984). The station barometric pressure was calculated using the elevation Z in meters (m) of the study site (Snyder & Shaw, 1984) as:

$$P = 101.3 \cdot \left[\frac{293-(0.0065 \cdot Z)}{293}\right]^{5.26} \qquad \text{Equation 3}$$

Saturation vapor pressure E_w in millibars (mb) at the wet bulb temperature was calculated from the recorded wet bulb temperature T_w (Snyder & Shaw, 1984) as:

$$E_w = \frac{6.108 \cdot e^{(17.27 T_w)}}{(237.3 + T_w)} \qquad \text{Equation 4}$$

Actual vapor pressure E was calculated from the saturation vapor pressure at the wet bulb temperature, the recorded wet bulb temperature T_w, the recorded dry bulb temperature T_s and the recorded station barometric pressure P (Snyder & Shaw, 1984) as:

$$E = E_w - (0.00066 \cdot (1 + 0.00115 \cdot T_w)(T_s - T_w) \cdot P) \qquad \text{Equation 5}$$

Saturation vapor pressure E_s in millibars (mb) at the dry bulb temperature was calculated from the recorded dry bulb temperature T_s (Snyder & Shaw, 1984) as:

$$E_s = \frac{6.108 \cdot e^{(17.27 T_s)}}{(237.3 + T_s)} \qquad \text{Equation 6}$$

Finally, relative humidity RH (%) was calculated from actual vapor pressure E and saturation vapor pressure at dry bulb temperature E_s (Snyder & Shaw, 1984) as:

$$RH = 100 \cdot \left[\frac{E}{Es}\right] \qquad \text{Equation 7}$$

Vapor pressure deficit VPD (kPa) was calculated from collected data as (Murray, 1967):

$$VPD = (1 - (\frac{RH}{100})) \cdot (100 \cdot Es))/1000 \qquad \text{Equation 8}$$

5.4.2 Mean and Turbulent Air Velocities

For air velocity u and its components (transversal u_x, longitudinal u_y and vertical u_z), the mean air velocity measured over a period Δt is (López et al., 2010):

$$u_{avg} = \frac{1}{\Delta t}\int_t^{1+\Delta t} u\,dt \qquad \text{Equation 10}$$

We calculated the average value of the two-dimensional horizontal resultant of air velocity in the XZ-plane and the respective direction of the relative air movement, tilted away from the x-axis, through angle ϕ, which was given by:

$$\phi = \arctan(\frac{u_z}{u_x}) \qquad \text{Equation 11}$$

The variance in air velocity over a period of time Δt is defined as (Heber et al., 1996):

$$\sigma^2 = \frac{1}{\Delta t}\int_t^{1+\Delta t} (u - \bar{u})^2 dt \qquad \text{Equation 12}$$

where u is the instantaneous air velocity and $\bar{u}$ is the mean local air velocity. Turbulence intensity i_u is the standard deviation σ divided by the mean local velocity $\bar{u}$, so (López et al., 2010):

$$i_u = \frac{\sigma}{\bar{u}} \qquad \text{Equation 13}$$

At each of the measurement points in the present study, data was recorded for 2 min at a sampling frequency of 5 Hz. This time period is shorter than that found in previous studies of air movement in various greenhouse designs (Wang et al., 1999; Teitel et al., 2005), but similar to that used in López et al., (2011). The time interval used for calculating the average velocity and any ensuing analyses must be longer than any significant fluctuation and short enough for the transitory real-time effects not to affect the integration (Wang et al., 1999; Teitel et al., 2005; López et al., 2010). The constraints imposed by the time of day and position of the sun, along with the limited buffer capability of the ambient air of the research greenhouse, enforced a compromise between accuracy and variation with regards to outside conditions. The negligible outside air movement, due to the controlled environment of the research greenhouse in this study, meant less relative variance in the data, and allowed us to use a shorter sampling time of 2 min without sacrificing accuracy. In comparison, Molina-Aiz et al. (2009), periods of 6 and 3 min were used during a study on an Almería-type greenhouse with insect screens under field conditions.

5.5 Greenhouse Climate

The temperature and relative humidity tests were carried out during specific days clear-sky days of the months of March, April and December 2016 to test the NVAC system in varying artificial climates. The 'outside' conditions of the artificial climates (conditions of the research greenhouse) were varied from 25.0 to 45.6 °C and from 6.9 to 57.7% relative humidity (Table 14). Measurements for temperature, relative humidity and VPD were taken under NVAC system conditions i.e. the conditions found within the NVAC model greenhouse with the NVAC misting system active. In separate tests, air movement and temperature measurements were taken under both NVAC system conditions and natural ventilation conditions. Natural ventilation conditions are the conditions inside the NVAC greenhouse without the NVAC misting system. These conditions are typical natural ventilation conditions without the use of cooling methods.

Sase et al. (1984) were some of the first to experiment with greenhouse structures placed within wind tunnels, to examine the effects of wind on the inside climate of the greenhouse. More recently, Kacira et al. (2008), amongst others, have also done the same. The present study examines windless conditions but under multiple climates. Therefore, the volume of a closed research greenhouse, without active or passive ventilation but with solar radiation and heating, provides the required environment to accomplish this. The controlled environment area of the research greenhouse in which the NVAC greenhouse prototype was built was fully closed during testing. This provided us with an environment with minimal ambient air movement, except for the natural movement of air from the buoyancy effect and from the bay's heating system. This removed the wind effect from our study and allowed the focus to remain on the effect provided by the NVAC greenhouse system. The air found around the NVAC greenhouse prototype simulated field conditions without wind. However, the volume was not infinite. The volume of the greenhouse bay was 453.1 m^3 which is significantly larger than the NVAC greenhouse prototype volume (56.6 m^3). This larger volume of air was nonetheless limited in its ability to act as an outside infinite environment. For this reason, the tests on the NVAC greenhouse were kept between 1 and 2-h in length. This prevented the ambient environment of the research greenhouse bay from becoming saturated in water vapor as the NVAC greenhouse system operated from within the model.

5.6 Results and Discussion

5.6.1 Temperature, Relative Humidity and Vapor Pressure Deficit

The data collected in this study showed similar trends in all performed tests. The NVAC system decreased inside greenhouse air temperature and increased relative humidity. This is no different from conventional evaporative cooling solutions (Arbel et al., 1999). Compared to greenhouse fog systems, where conditions vary greatly when cooling occurs (Hayashi et al., 2005), the NVAC greenhouse system tests showed that inside greenhouse conditions remained stable for the entirety of the operation period. The magnitude of these changes depended on the initial inside greenhouse conditions and the misting nozzle configuration. In trials with identification (a) to (f), cooling varied from 1.9 to 4.0 °C, and the increase in relative humidity ranged from 1.4 to 29.6%. The greenhouse initial inside conditions, prior to testing, ranged from

25.0 to 35.8 °C and 6.9 to 57.7% under a three-nozzle configuration with a water consumption of 0.28 $L \cdot h^{-1} \cdot m^{-2}$. As seen in Figure 20 and Table 14, the warmer and drier the initial conditions were, the greater the cooling, but this was not true for all trials. Trial (f), which was the warmest and driest of all three-nozzle trials, did not show the greatest cooling performance, nor the greatest increase in relative humidity. However, trial (a), which was the coolest and most humid trial of all, showed a small decrease in temperature, which was anticipated, but showed a large increase in relative humidity.

Table 14. Outside conditions and initial and experimental greenhouse conditions in the NVAC model greenhouse on test days of March, April and May 2016. Dry-bulb temperature (T_{db}) and relative humidity (RH) are presented for outside, initial inside conditions, and NVAC system inside conditions. Vapor pressure deficit (VPD) is presented for initial inside conditions and NVAC system inside conditions. Differences in temperature (ΔT) and relative humidity (ΔRH), and efficiencies (Eff.) are presented.

		Outside Conditions		Initial Conditions			NVAC Test Conditions			Differences	
Test Date 2016	Graph ID	T_{db} (°C)	RH_o (%)	$T_{db,i}$ (°C)	RH_i (%)	VPD_i (kPa)	$T_{db,c}$ (°C)	RH_c (%)	VPD_c (kPa)	ΔT	ΔRH
March 10	a	24.6	57.2	25.0	57.7	1.3	23.1	78.0	0.6	-1.9	20.3
March 19	b	28.6	37.1	28.8	43.6	2.2	26.1	45.1	1.9	-2.7	1.4
March 21	c	27.7	37.6	29.3	40.5	2.4	26.3	45.4	1.9	-3.0	4.9
March 18	d	30.1	43.1	30.7	33.3	2.9	26.9	37.2	2.2	-3.8	3.9
March 9	e	22.8	31.6	31.9	25.1	3.5	27.9	54.7	1.7	-4.0	29.6
March 4	f	31.7	7.72	35.8	6.9	5.5	32.6	28.1	3.5	-3.1	21.2
April 18	g	25.3	52.4	27.5	43.8	2.1	23.6	72.4	0.8	-3.9	28.6
April 13	h	26.1	47.0	27.4	56.3	1.6	24.3	78.8	0.6	-3.1	22.5
May 10	i	27.0	18.0	29.2	17.4	3.3	23.7	33.9	1.9	-5.5	16.5
April 19	j	38.0	10.0	41.8	9.5	7.3	29.2	40.7	2.4	-12.6	31.2
April 17	k	37.7	9.5	42.7	8.4	7.8	31.5	31.5	3.2	-11.2	23.1
May 11	l	41.7	7.7	45.6	7.4	9.1	36.1	28.7	4.3	-9.5	21.3

In order to meet the need of more cooling at higher temperatures, trials were conducted at higher temperatures with a greater water supply using a six-nozzle configuration with a combined water consumption of 0.56 $L \cdot h^{-1} \cdot m^{-2}$, as opposed to the three-nozzle configuration in the first set of trials. As expected, the temperature of the air decreased and the relative humidity increased as the water supply was increased. The same was reported by Arbel et al. (2003) in a fog cooled greenhouse. Trials (g) through (l) were performed with six nozzles. The initial temperatures ranged from 27.5 to 45.6 °C and were higher than in the previous trials (25.0 to 35.8 °C). The nozzle configuration was one nozzle per 9.4 m^3 of greenhouse volume, not considering the rafter volume. Accordingly, the cooling was greater and varied from 3.1 to 12.6 °C, and the increase in relative humidity ranged from 16.5 to 31.2%. The trial with the greatest cooling performance coincided with the greatest increase in relative humidity, which was observed on April 19th, 2016 during trial (j). The initial conditions for this trial were 41.8 °C and 9.5% relative humidity. Trials (g) and (h), which had initial temperatures less than 29 °C (27.5 and 27.4 °C respectively), showed a higher resulting relative humidity when the NVAC system was used, 72.4% and 78.8%, respectively.

During trials with initial temperatures greater than 29 °C, the amount of cooling was greater (5.5 to 12.6 °C) and the resulting increases in relative humidity (from 28.7% to 40.7%) were less than in trials (g) and (h). The cooling performance of the NVAC system under the six-nozzle configuration (0.56 $L \cdot h^{-1} \cdot m^{-2}$) was comparable to the cooling performances of a fog system reported by Arbel et al. (1999) and Hayashi et al. (2005). These cooling performances were achieved without the irregular profiles of inside conditions caused by momentary drops in inside dry bulb temperature and surges in relative humidity, typical of fog cooling systems in natural ventilation greenhouses (Hayashi et al., 2005). In comparison to fog evaporative cooling systems, the NVAC greenhouse system was used uninterruptedly and was able to provide relatively stable cooling and relative humidity control over the periods of use of the NVAC system in this study (2 to 4 h, Figure 20), and during several hours (> 4 h) when used under field conditions (McCartney, 2017). This capability is comparable that of a fogging system used with forced ventilation reported by Arbel et al. (2003).

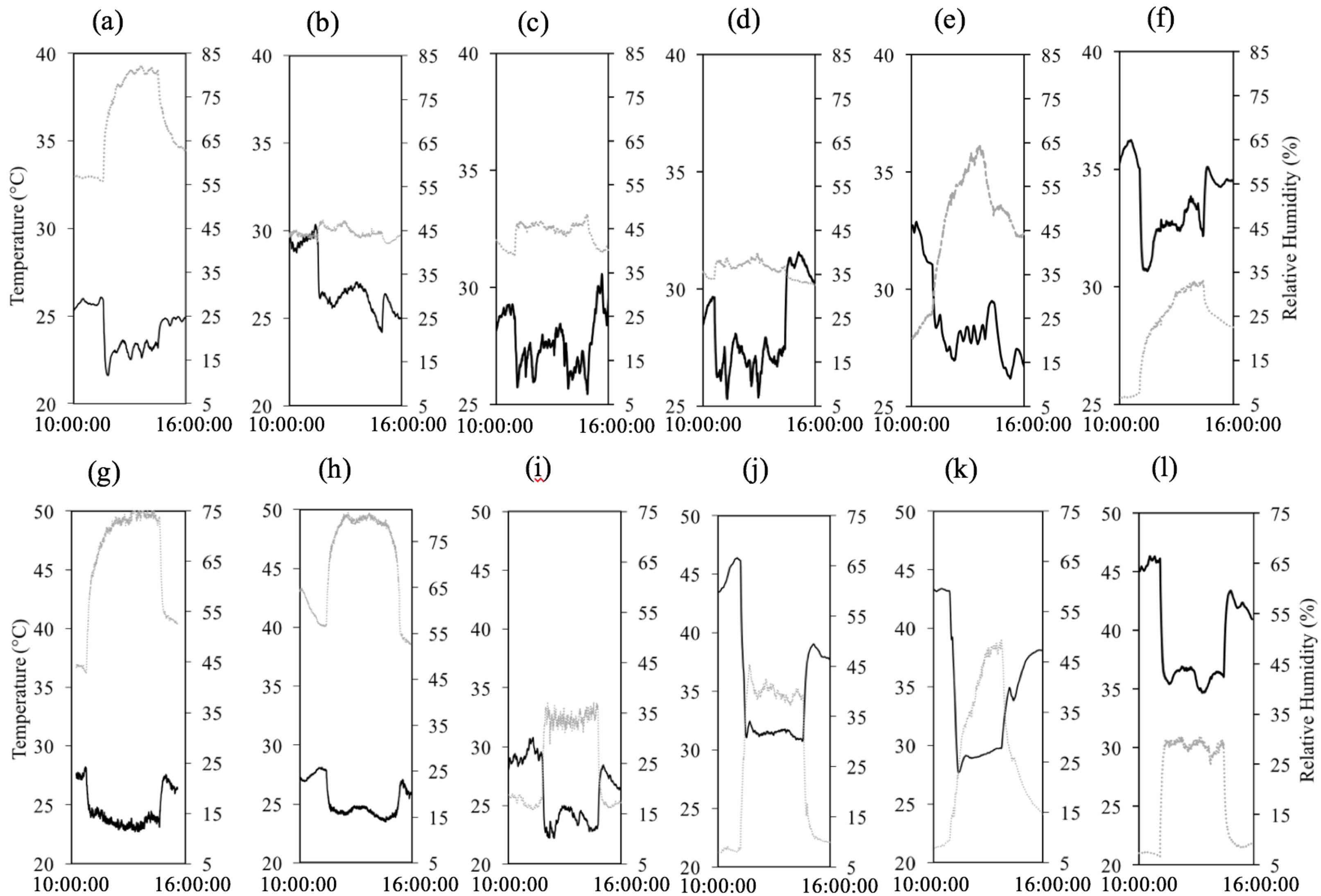

Figure 20. Graphical representation of the temperature (—) and relative humidity (·····) measurements made in the natural ventilation augmented cooling (NVAC) model greenhouse. The test days were in March, April 2016 and May 2016. (a) to (f) are the results of tests under the three-nozzle configuration and mist rate 0.28 $L \cdot h^{-1} \cdot m^{-2}$, with initial inside temperatures ranging from 25.0 to 35.8 °C and initial inside relative humidity ranging from 6.9 to 57.7%. (g) to (l) are the results of tests under the six-nozzle configuration and mist rate 0.56 $L \cdot h^{-1} \cdot m^{-2}$ with initial inside temperatures ranging from 27.5 to 45.6 °C, and initial inside relative humidity ranging from 7.4 to 43.8%.

During the air movement tests, a horizontal distribution in temperature was observed at the various measurement locations and heights by means of sonic anemometry corrected for inside humidity. In order to compare the values of temperature measured at different moments in time, we compared the difference between sonic anemometry temperature and average instantaneous inside greenhouse temperature, obtained from the thermocouple measurements. During the test under natural ventilation, the average outside temperature was 27.1 °C. The average inside temperatures at heights A, B and C were 26.7, 26.8 and 27.1 °C, respectively, which showed a characteristic vertical temperature gradient and gave an average greenhouse temperature of 26.9 °C. When under NVAC system conditions, the average outside temperature was 29.8°C. The average inside temperature was 25.6 °C. The vertical temperature gradient, 25.5, 25.5, 25.8 °C, from the ground-up respectively, was less obvious under NVAC system conditions because a greater amount of mixing of the air in the plant space occurs from the current of cooled air.

Figure 21 depicts the horizontal temperature distribution inside the greenhouse plant space with respect to instantaneous average greenhouse temperature, under both natural ventilation and NVAC system conditions. The horizontal temperature distribution inside the greenhouse was more uniform under natural ventilation conditions compared to under NVAC system conditions (Figure 21a). The largest difference in temperature was 0.5 °C, at location 5, height B, which coincided with the area in the greenhouse farthest from the side vents (i.e. middlemost location). Boulard et al. (1998) carried out a similar study in a natural ventilation greenhouse without plants and found that most of the temperature gradients occurred within small distances above the floor and below the roof. They observed strong temperature gradients in those thin layers, while the temperature inside the plant space remained constant, with a uniform and steady temperature distribution. The temperature distribution was less uniform under the NVAC system conditions and the magnitude of the temperature differences under NVAC system conditions was greater, compared to natural ventilation. The largest difference in temperature in this case was -1.0 °C, at location 2, height A, under the downdraft of air, in the space of measurement locations 1, 2 and 3.

The temperature distribution analyses allowed us to visualize the way in which temperature inside the greenhouse was altered when under NVAC system conditions. In Figure 21b, at height A, a large amount of cooling can be seen at measurement locations 1, 2 and 3

(Section I). This pattern in cooling agrees with the design concept of the NVAC greenhouse where a current of cooled air is initiated in the rafters, flows down the added inside roof and falls onto the ground of the plant space. The added inside roof acts as a baffle to restrain the flow of the air into the plant space until the water droplets have fully evaporated or have reached the surface of the roof at which point they are collected by a gutter system. In Figure 21b, at height C, a certain amount of warmer air can be seen at locations 8 and 9. This agrees with the air velocity and air direction analyses discussed below. It is no surprise that the location of lowest temperature in the greenhouse was located where the flow of cooled air enters the plant space. Kittas et al. (2003) and López et al. (2010) reported that the air temperature in a greenhouse equipped with a pad and fan cooling system gradually rises with distance in the greenhouse away from the cooling pads.

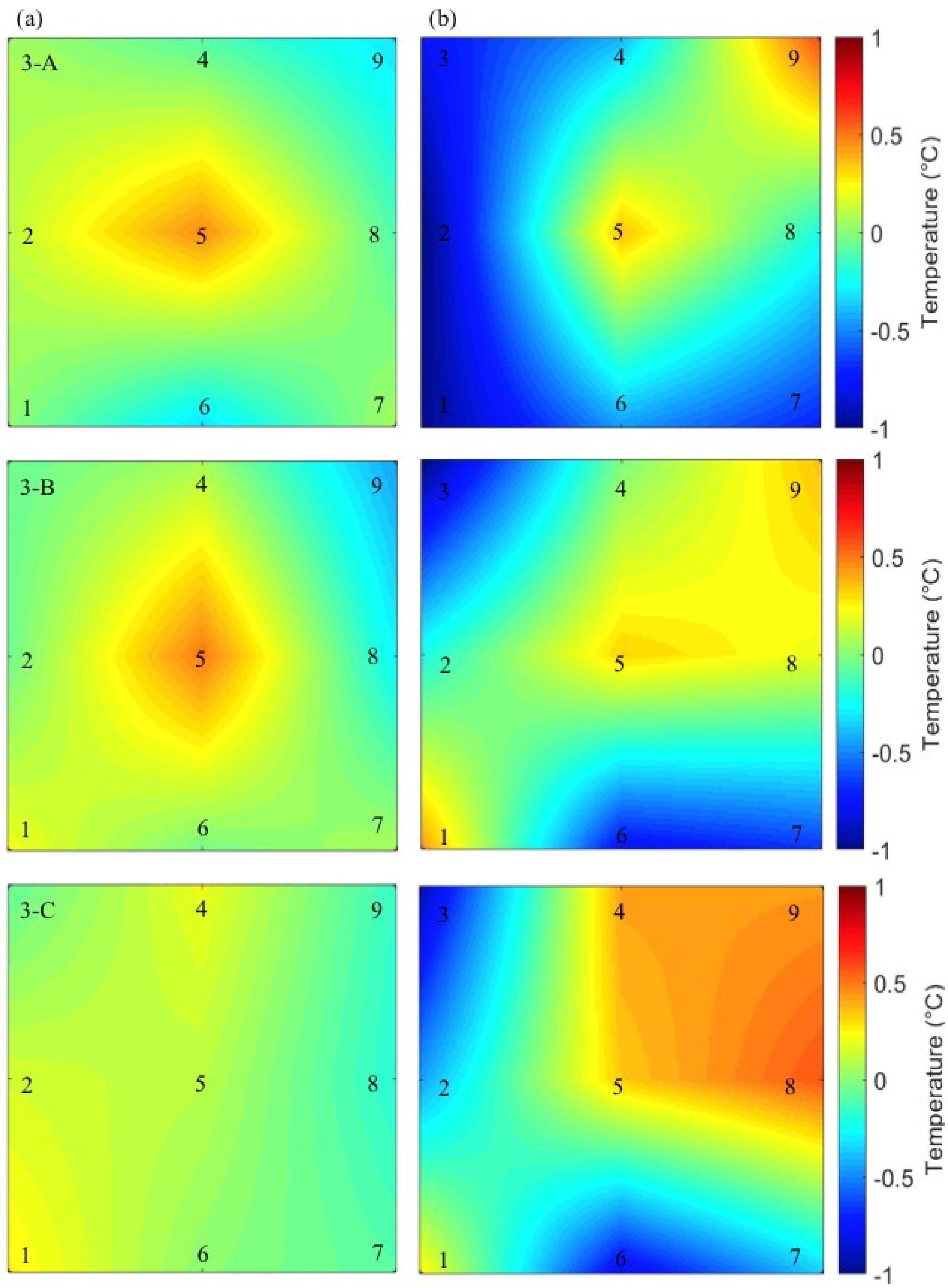

Figure 21. Horizontal distribution of differences between corrected sonic and instantaneous average greenhouse temperatures at all locations for heights A, B and C in the natural ventilation augmented cooling (NVAC) model greenhouse. Test in (a) under natural ventilation conditions on December 12, 2016, and in (b) under NVAC system conditions on December 18, 2016.

Figure 22 shows the horizontal temperature distribution inside the greenhouse plant space with respect to instantaneous average outside temperature, under both tests. Although similar in pattern to Figure 21, this analysis allows for better illustration of the cooling capabilities of the NVAC system. It is important to remember that natural ventilation alone is unable to provide conditions cooler than outside conditions (Sethi & Sharma, 2007). Figure 21a shows the average inside temperature profile of the greenhouse under natural ventilation conditions at heights A, B and C, which ranged from 1.8 to 2.8 °C greater than outside temperatures. Figure 21b shows the same analysis but for cooling, as the NVAC system provided inside temperatures ranging from 1.5 to 4.6 °C cooler than outside temperatures during the test on December 12th, 2016. At no point was the temperature warmer than outside conditions under this NVAC system test. When temperatures inside the greenhouse rise beyond a certain threshold, set by the growers and type of crop, the cooling provided by the NVAC greenhouse can outweighed the importance of temperature uniformity. At measurement location 8, height C a warm spot can be seen, which coincided with the location of an updraft of air that is particularly strong during NVAC system conditions, potentially drawing outside air into the greenhouse through the side vent.

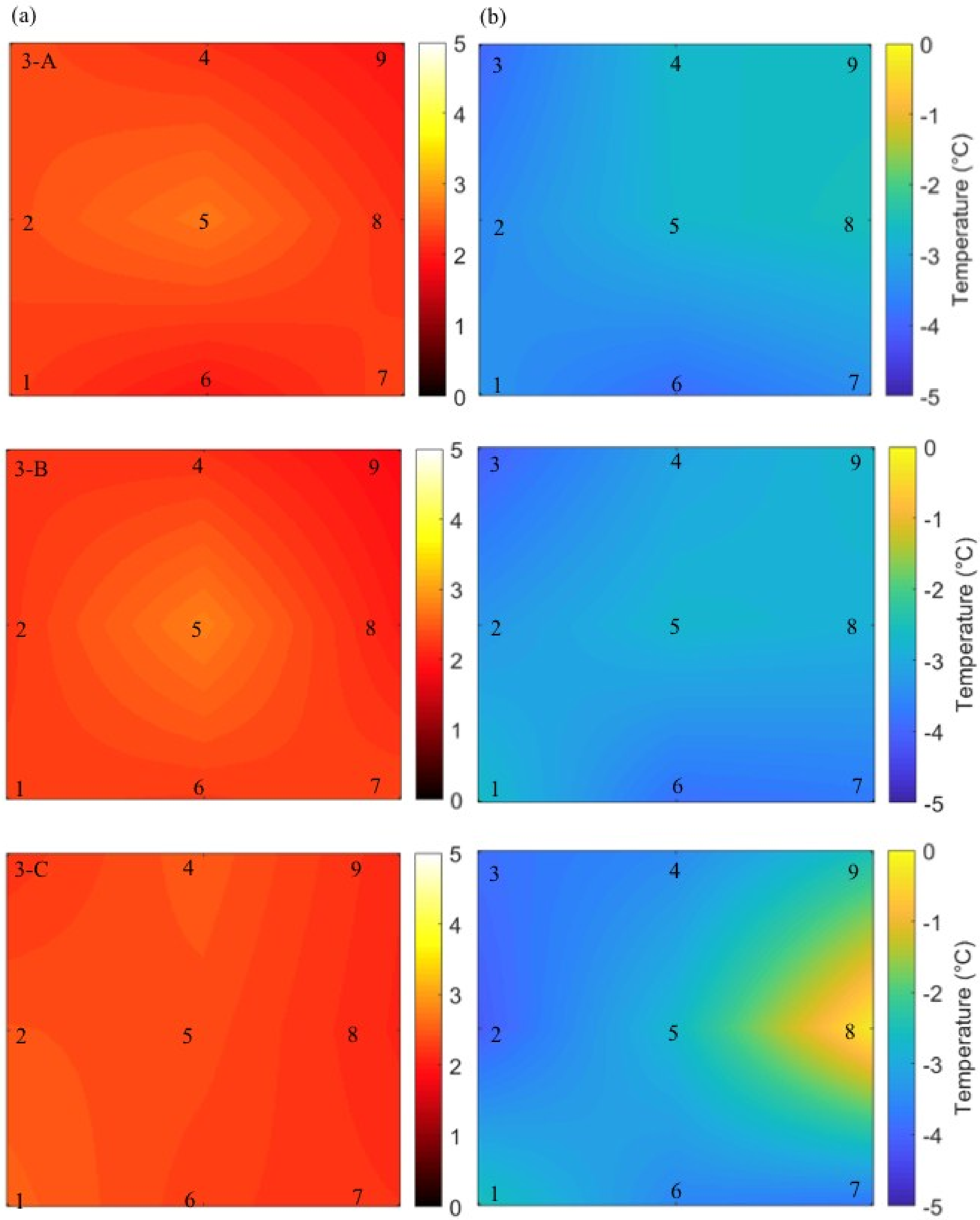

Figure 22. Horizontal distribution of differences between corrected sonic and average outside temperatures at all locations for heights A, B and C in the natural ventilation augmented cooling (NVAC) model greenhouse. Test in (a) under natural ventilation conditions on December 12, 2016 (color range from 0 to 5 °C), and in (b) under NVAC system conditions on December 18, 2016 (color range from -5 to 0 °C).

The difference between the inside initial temperature ($T_{db,i}$) and the test NVAC system temperature ($T_{db,c}$) determined the cooling performance (ΔT). The cooling performance of the NVAC greenhouse system depended on the initial inside conditions preceding the use of the NVAC system, which in turn are dependent on the outside conditions. Variations in temperature and relative humidity have an impact on the performance of the evaporative cooling process. The vapor pressure deficit, VPD, is tightly related to temperature and relative humidity and therefore the analysis of VPD was used as a tool for monitoring the cooling performance of the NVAC system. VPD was plotted against cooling performance and it was observed that the cooling performance under both misting rates increases with increasing VPD, but eventually decreased after an initial VPD (VPD_i) of 3.5 kPa for the mist rate of 0.28 $L{\cdot}h^{-1}{\cdot}m^{-2}$ and VPD_i of 7.5 kPa for the mist rate of 0.56 $L{\cdot}h^{-1}{\cdot}m^{-2}$, at which point the misting rate should be increased to suit the conditions of the air (Figure 23).

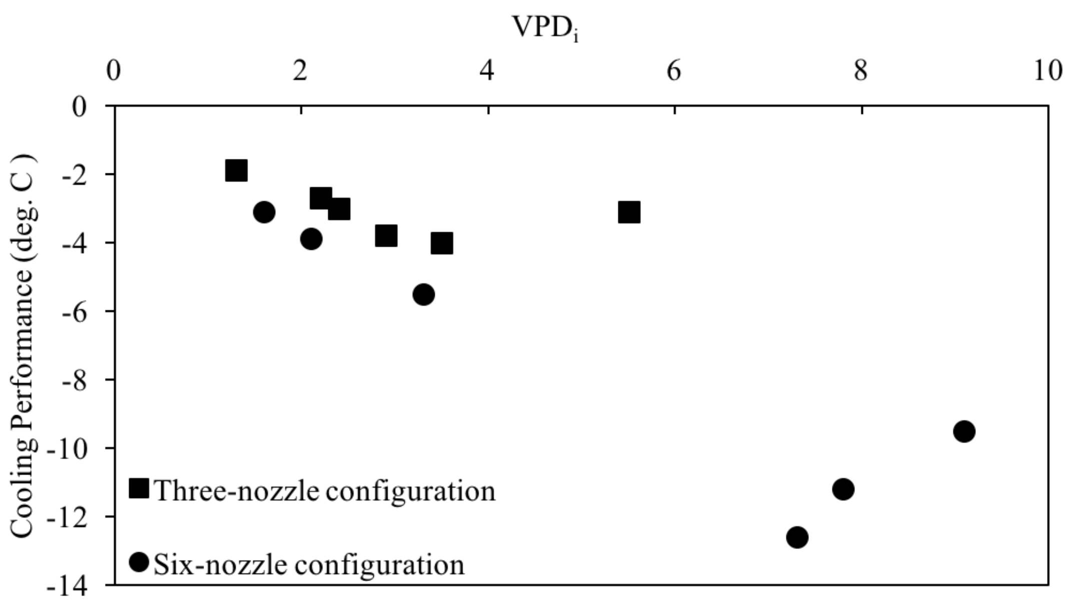

Figure 23. The cooling performance of the natural ventilation augmented cooling (NVAC) model greenhouse plotted against the initial vapor pressure deficit (VPD_i). Both the three-nozzle configuration and mist rate of 0.28 $L{\cdot}hr^{-1}{\cdot}m^{-2}$ and the six-nozzle configuration and mist rate of 0.56 $L{\cdot}hr^{-1}{\cdot}m^{-2}$ data are presented.

VPD is the difference (deficit) between the amount of moisture in the air and how much moisture the air can hold when it is saturated. It is a parameter that is closely studied in greenhouses crop environments because it can relate to various other parameters such as condensation threat, crop transpiration, temperature and relative humidity. For these reasons, VPD is a valuable climate control measurement (Prenger & Ling, 2000; Wollaeger & Runkle, 2015). A VPD between 0.3 and 1.0 kPa is considered ideal for most greenhouse crops (Hand, 1988). The analysis of VPD of each trial shows that the NVAC system provided VPD control by lowering it by 0.3 to 4.9 kPa, to within acceptable levels, when initial conditions were considered harsh (Table 4 trials on March 10, 2016, April 13, 2016 and April 18, 2016). During trials with a very high initial temperature and a very low relative humidity (extremely high VPD), the NVAC greenhouse system was unable to lower the VPD to within recommended levels (0.3 to 1 kPa), but nonetheless provided some relief by significantly lowering the VPD (Table 14, trials on April 17, 2016 and May 11, 2016). In no case did the NVAC greenhouse system lower the VPD below acceptable levels, and therefore the misting system can be, and was used continuously. In a greenhouse with plants, low VPD conditions would be easier to meet due to the plant transpiration contributing to the humidity levels. This feature offers an advantage over fog evaporative cooling systems as such systems can only be used intermittently to avoid wetting the foliage and bringing the VPD to very low levels, which limits their performance (Montero, 2006; Toida et al., 2006).

All cooling methods for greenhouses must be used with caution to avoid the sanitary repercussions of increased relative humidity and airborne water droplets (Montero, 2006). Fan and pad and fog cooling systems based on the combination of pressurised air and water are both expensive systems, sometimes costing as much as the greenhouse structures themselves (Kittas et al., 2000; Albright, 2001; Montero, 2006; Lit & Willits, 2008). Low-cost and low-pressure misting nozzles, such as that used in the NVAC greenhouse, can be useful for cooling simple greenhouses such as the “parral” type common in Almeria, or the screen houses that are found in warm climates like Mexico or the Canary Islands (Montero, 2006). Low pressure nozzles generate bigger droplets than the high-pressure nozzles of fogging systems and can therefore wet foliage (Arbel et al., 1999; Montero, 2006). In the NVAC greenhouse, the protection provided by the added roof and the distance that the air must travel, once cooled, to reach the crop prevent water droplets from reaching the foliage. The water droplets either evaporate, or fall onto the added roof where the unevaporated water is collected before the cooled air enters the plant space.

Although by its design the incidences of water droplets reaching the foliage are minimized, as with other evaporative cooling techniques, the use of the NVAC greenhouse system in an already very humid environment would be advised against. At 30 °C, for instance, if a VPD between 0.3 and 1 kPa is maintained, the relative humidity can vary from 77 to 93%, respectively. The NVAC system could therefore be used until the inside relative humidity reaches the threshold set by the grower. It was reported by Arbel et al. (2003) that air temperature and relative humidity of 28 °C and 80% were maintained during the summer at midday in a greenhouse with the combination of forced ventilation and fogging.

5.6.2 Velocity

Tables 15 and 16 present the air velocity (mean) and its components (u_x, u_y and u_z) over the 2-min period of measurements made in the plant area of the greenhouse. The average air velocity (u_{avg}) calculated as the average of air velocities from all points and heights in the plant space with natural ventilation alone, was 0.11 ± 0.02 $m \cdot s^{-1}$ (Table 15). This is comparable to still conditions reported by Fernandez and Baily (1994). The average air velocity (u_{avg}) measured in the plant space with the NVAC system was 0.20 ± 0.06 $m \cdot s^{-1}$ (Table 15), which is much greater than under natural ventilation conditions. This value is slightly less than that reported in the plant space of an empty greenhouse equipped with a pad and fan system (0.26 $m \cdot s^{-1}$) in a study by López et al. (2010). It is also less than in a greenhouse equipped with circulating fans (0.64 $m \cdot s^{-1}$), as reported by Fernandez and Baily (1994).

Table 15. The average air velocity ($m \cdot s^{-1}$) across all measurement locations of each section and height of the greenhouse under both natural ventilation conditions and NVAC system conditions.

Average air velocity ($m \cdot s^{-1}$)						
	Natural Ventilation			NVAC System		
Height/Section	I	II	III	I	II	III
A	0.11	0.09	0.08	0.29	0.31	0.08
B	0.09	0.11	0.11	0.20	0.24	0.07
C	0.12	0.14	0.12	0.24	0.23	0.10
Average	0.11	0.11	0.10	0.24	0.26	0.08
Average	0.11			0.20		

The airflow in the plant space of the greenhouse under both natural ventilation conditions and under NVAC system conditions was mainly in the XZ plane. The resultant air velocities were calculated for the XZ-plane, as the Y component had little influence on the overall air velocity. The maximum resultant air velocity in the XZ-plane in the greenhouse with the NVAC system was 0.38 $m \cdot s^{-1}$ at location 4 height A in Section II. In comparison, under natural ventilation conditions, the resultant air velocities never exceeded 0.14 $m \cdot s^{-1}$.

Table 16. The mean air velocity u ($m \cdot s^{-1}$) ± standard deviation, the mean air velocity components u_x, u_y and u_z ($m \cdot s^{-1}$) ± standard deviation, the turbulence intensity i_u and the resultant velocity in the XZ-plane ($m \cdot s^{-1}$) over the measurement period at the different locations and heights in the plant space of the greenhouse under natural ventilation conditions.

Point	u	u_x	u_y	u_z	i_u	XZ
Section I						
1A	0.08±0.03	0.08±0.03	-0.01±0.02	-0.02±0.03	0.15	0.08
1B	0.06±0.02	0.01±0.02	-0.02±0.01	-0.05±0.01	0.15	0.05
1C	0.12±0.02	0.10±0.02	-0.04±0.01	-0.04±0.02	0.14	0.11
2A	0.14±0.02	0.13±0.02	0.04±0.03	-0.05±0.02	0.15	0.14
2B	0.10±0.03	0.07±0.04	0.04±0.02	-0.06±0.02	0.28	0.09
2C	0.12±0.02	0.11±0.02	0.01±0.02	-0.05±0.02	0.17	0.12
3A	0.10±0.02	0.07±0.02	0.04±0.02	-0.05±0.02	0.16	0.09
3B	0.10±0.02	0.09±0.02	0.01±0.02	-0.05±0.02	0.19	0.10
3C	0.13±0.02	0.12±0.02	-0.03±0.02	-0.05±0.01	0.12	0.13
Section II						
4A	0.08±0.02	0.05±0.02	0.04±0.02	-0.04±0.02	0.21	0.07
4B	0.11±0.02	0.10±0.02	0.02±0.02	-0.05±0.02	0.15	0.11
4C	0.14±0.02	0.13±0.02	-0.02±0.02	-0.05±0.01	0.13	0.14

5A	0.07±0.03	0.05±0.03	0.04±0.02	0.01±0.01	0.38	0.07
5B	0.12±0.02	0.12±0.02	0.01±0.01	0.01±0.02	0.16	0.13
5C	0.14±0.01	0.13±0.01	0.00±0.02	-0.05±0.02	0.10	0.14
6A	0.11±0.02	0.09±0.03	-0.03±0.01	-0.04±0.02	0.21	0.10
6B	0.11±0.02	0.10±0.02	-0.03±0.02	-0.04±0.03	0.18	0.11
6C	0.13±0.02	0.11±0.02	-0.03±0.01	-0.05±0.01	0.12	0.12
Section III						
7A	0.07±0.02	0.02±0.02	-0.02±0.02	-0.05±0.02	0.23	0.06
7B	0.09±0.02	0.06±0.02	-0.02±0.02	-0.05±0.01	0.20	0.08
7C	0.12±0.03	0.11±0.03	-0.02±0.02	-0.05±0.01	0.21	0.12
8A	0.07±0.01	0.02±0.02	0.01±0.01	-0.07±0.01	0.12	0.07
8B	0.11±0.02	0.09±0.02	0.01±0.01	-0.06±0.01	0.21	0.11
8C	0.13±0.01	0.11±0.01	-0.01±0.02	-0.06±0.01	0.09	0.13
9A	0.10±0.04	0.08±0.06	0.01±0.02	-0.06±0.02	0.34	0.10
9B	0.13±0.02	0.12±0.02	-0.01±0.03	-0.05±0.02	0.16	0.13
9C	0.12±0.02	0.11±0.02	0.00±0.02	-0.03±0.02	0.20	0.12

The average value of the transversal velocity component (u_x) inside the greenhouse, calculated as the average of the air velocity in X (u_x) at all locations, heights A, B and C, was 0.09 ± 0.02 $m \cdot s^{-1}$ under natural ventilation and 0.13 ± 0.07 $m \cdot s^{-1}$ with the NVAC system. The average value for the vertical component u_z was 0.05 ± 0.02 $m \cdot s^{-1}$ under natural ventilation conditions and 0.10 ± 0.07 $m \cdot s^{-1}$ with the NVAC system. Both the vertical and transversal components of the air velocity were greater with the NVAC greenhouse system.

The air velocity (u) in Section I of the greenhouse was greatly influenced by the vertical velocity component (u_z), notably at location 2 heights B and C, where air velocity (u) was 0.31 ± 0.09 and 0.36 ± 0.10 $m \cdot s^{-1}$, respectively, with their vertical velocity components (u_z) being -0.27 ± 0.11 and -0.36 ± 0.12 $m \cdot s^{-1}$. Accordingly, Figures 26 and 28 show a strong downward flow of air in Section 1 of the greenhouse. Section II was mostly influenced by the transversal velocity component (u_x). The airflow at this point was collapsed onto the floor of the greenhouse, losing most of its downward direction and gaining in the transversal direction. At location 5 height A, u is 0.39 ± 0.08 $m \cdot s^{-1}$ with u_x being 0.38 ± 0.08 $m \cdot s^{-1}$. Correspondingly, the smoke test showed a strong transversal u_x current of air at location 5 height A. The turbulence intensity at location 5 height A was i_u = 0.21, contrary to that seen under natural ventilation conditions which was greater (i_u = 0.38). A lower turbulence intensity is typical of forced air movement, when compared to natural ventilation conditions. Such is the case in systems with extractor fans, such as a pad and fan system, where velocity and direction is increased but turbulence (mixing) is reduced (Tanny et al., 2008; López et al. 2010). However, this is a local phenomenon at measurement location 5 in the NVAC greenhouse, as overall turbulence intensity was increased with the use of the NVAC system.

Table 17. The mean air velocity u ($m \cdot s^{-1}$) ± standard deviation, the mean air velocity components u_x, u_y and u_z ($m \cdot s^{-1}$) ± standard deviation and the turbulence intensity i_u and the resultant velocity in the XZ-plane ($m \cdot s^{-1}$) over the measurement period at the different locations and heights in the plant space of the greenhouse under the NVAC system conditions.

Point	u	ux	uy	uz	i_u	XZ
Section I						
1A	0.23±0.06	0.15±0.06	-0.02±0.07	-0.17±0.06	0.25	0.23
1B	0.13±0.07	0.08±0.05	-0.02±0.05	-0.10±0.07	0.48	0.13
1C	0.15±0.11	0.01±0.08	-0.01±0.07	-0.15±0.11	0.57	0.15
2A	0.34±0.08	0.31±0.09	0.00±0.09	-0.14±0.08	0.23	0.34
2B	0.15±0.08	0.09±0.08	0.01±0.07	-0.11±0.07	0.43	0.15
2C	0.21±0.09	-0.03±0.11	0.04±0.07	-0.21±0.10	0.40	0.21
3A	0.32±0.08	0.23±0.09	0.04±0.11	-0.24±0.12	0.26	0.31
3B	0.31±0.09	0.13±0.09	0.03±0.08	-0.27±0.11	0.26	0.31

3C	0.36±0.10	-0.03±0.11	0.0±0.09	-0.36±0.12	0.26	0.36
Section II						
4A	0.31±0.06	0.27±0.07	0.01±0.07	-0.06±0.05	0.18	0.27
4B	0.29±0.11	0.25±0.09	-0.13±0.18	-0.04±0.11	0.32	0.26
4C	0.16±0.05	0.16±0.05	-0.01±0.04	-0.01±0.05	0.14	0.23
5A	0.39±0.08	0.38±0.08	0.06±0.07	-0.05±0.05	0.21	0.38
5B	0.25±0.06	0.12±0.05	-0.07±0.07	-0.06±0.04	0.25	0.14
5C	0.15±0.04	0.05±0.04	-0.11±0.04	-0.08±0.03	0.23	0.10
6A	0.24±0.07	0.21±0.08	-0.10±0.07	-0.03±0.06	0.29	0.22
6B	0.18±0.06	0.16±0.08	-0.06±0.06	-0.06±0.08	0.27	0.17
6C	0.17±0.05	0.14±0.06	0.02±0.04	-0.09±0.05	0.25	0.17
Section III						
7A	0.08±0.10	0.05±0.11	0.03±0.06	-0.06±0.06	0.74	0.08
7B	0.06±0.03	0.01±0.04	0.04±0.04	-0.04±0.04	0.34	0.05
7C	0.07±0.03	-0.06±0.07	0.02±0.05	-0.02±0.05	0.29	0.07
8A	0.11±0.04	0.04±0.06	0.08±0.05	-0.06±0.04	0.30	0.07
8B	0.11±0.03	-0.10±0.04	0.01±0.03	-0.05±0.02	0.23	0.11
8C	0.11±0.01	-0.10±0.02	0.02±0.02	-0.05±0.03	0.13	0.11
9A	0.05±0.07	0.03±0.07	-0.02±0.06	-0.04±0.08	0.62	0.05
9B	0.04±0.04	-0.04±0.05	-0.02±0.05	-0.01±0.04	0.40	0.04
9C	0.12±0.04	-0.12±0.04	-0.03±0.05	-0.02±0.03	0.28	0.12

Beyond that of the plant space, the air velocity in the rafters of the greenhouse was studied at a few select locations (heights D, E and F). The location of the greatest air velocity measured in the greenhouse under NVAC system conditions was 0.48 ± 0.11 $m \cdot s^{-1}$ in the mist channel, above the inside roof and downstream from the misting line, at location 2, height D. The air at this point was rapidly travelling down the inside roof, eventually falling into the top of the plant space in Section I (Figure 28). Both the transversal velocity component (u_x) and the vertical velocity component (u_z) play a large role in the velocity of the air at location 2, height D. In Section III at location 5, heights D, F and iD (Figure 18), and location 8 height D, the air is travelling upwards under NVAC system conditions. The greatest upward velocity (u_z) was at location 5 height F where the vertical velocity component (u_z) was 0.03 ± 0.09 $m \cdot s^{-1}$ (Figure 28). This agrees with the temperature differences seen in Figure 5b, where warmer air is seen at height C in Section III of the greenhouse. Some upward movement was found under natural ventilation conditions, namely at location 5, height A, but it is of much smaller magnitude (0.01 $m \cdot s^{-1}$).

Figure 24 shows the transition time between natural ventilation conditions and NVAC system conditions. From the 2-min interval before activation of the NVAC system to the first 2-min during which the system is active, there was a drastic change in air velocity (u) and its components (u_x, u_y and u_z). Larger velocities with greater variation was observed once the system was active. Moreover, the NVAC system presented rapid and sharp changes in air movement upon activation, occurring in a few seconds only (Figure 24).

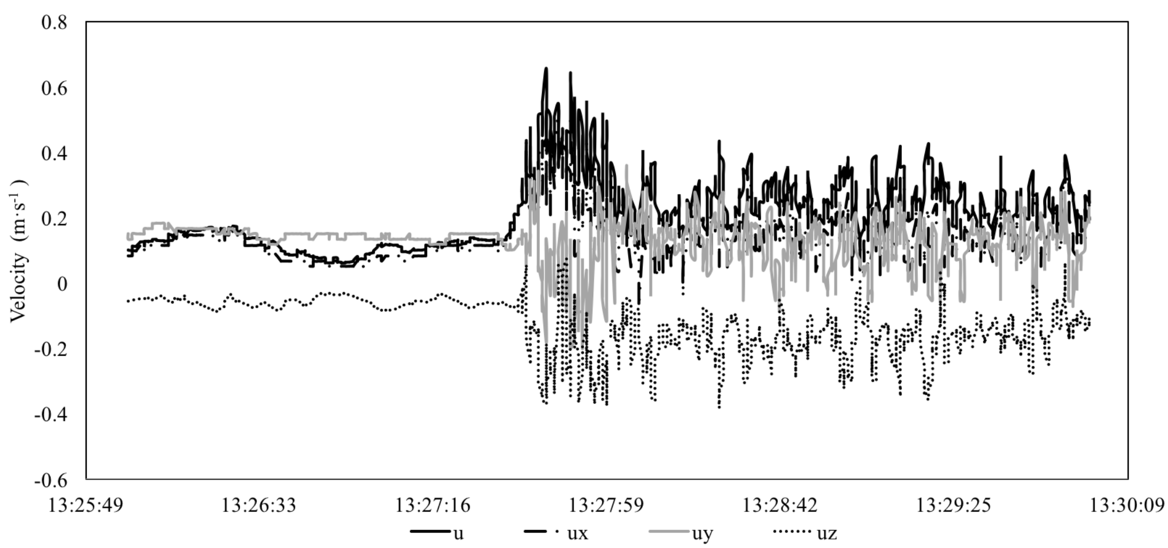

Figure 24. The velocity (u) and components u_x, u_y, and u_z in the natural ventilation augmented cooling (NVAC) model greenhouse 2 min before and 2 min after the NVAC system is activated at point 2, height A (0.2 m), in Section 1.

5.6.3 Airflow direction

The direction of the airflow under the NVAC system was more pronounced when compared to natural ventilation. A clearer pattern of airflow can be seen under the NVAC system when assessing the entire space (Figure 25, 26), and a clear direction of airflow can be seen when studying single locations (Figure 27, 28). Both natural ventilation alone and the NVAC greenhouse system provided transversal flow, u_x. The values of air velocity measured throughout the main floor space of the NVAC greenhouse show that the principal component of airflow, the transversal component (u_x), accounted for 54.4% and 75.6% of the air velocity (u) for the measurements under both natural ventilation and NVAC system conditions, respectively (Tables 4 and 5). These percentages are calculated as the average of the u_x/u ratio for the measurement points inside the greenhouse (López et al., 2010). The NVAC system, however, provided greater transversal flow (u_x) and much greater vertical flow (u_z), with u_z accounting for 42.7% of u. Longitudinal flow (u_y) in both scenarios was minimal. The flow from the side vents, in combination with the downdraft of cooled air from the misting, allowed for air movement in the plant space beyond what is possible under natural ventilation. Figures 8 and 9 show the two-dimensional resultants of air velocity in the XZ-plane with their respective angles of direction (ϕ). These cross-sectional representations of the NVAC greenhouse provide an overview of the direction and velocity of the air across all measurement locations in this study.

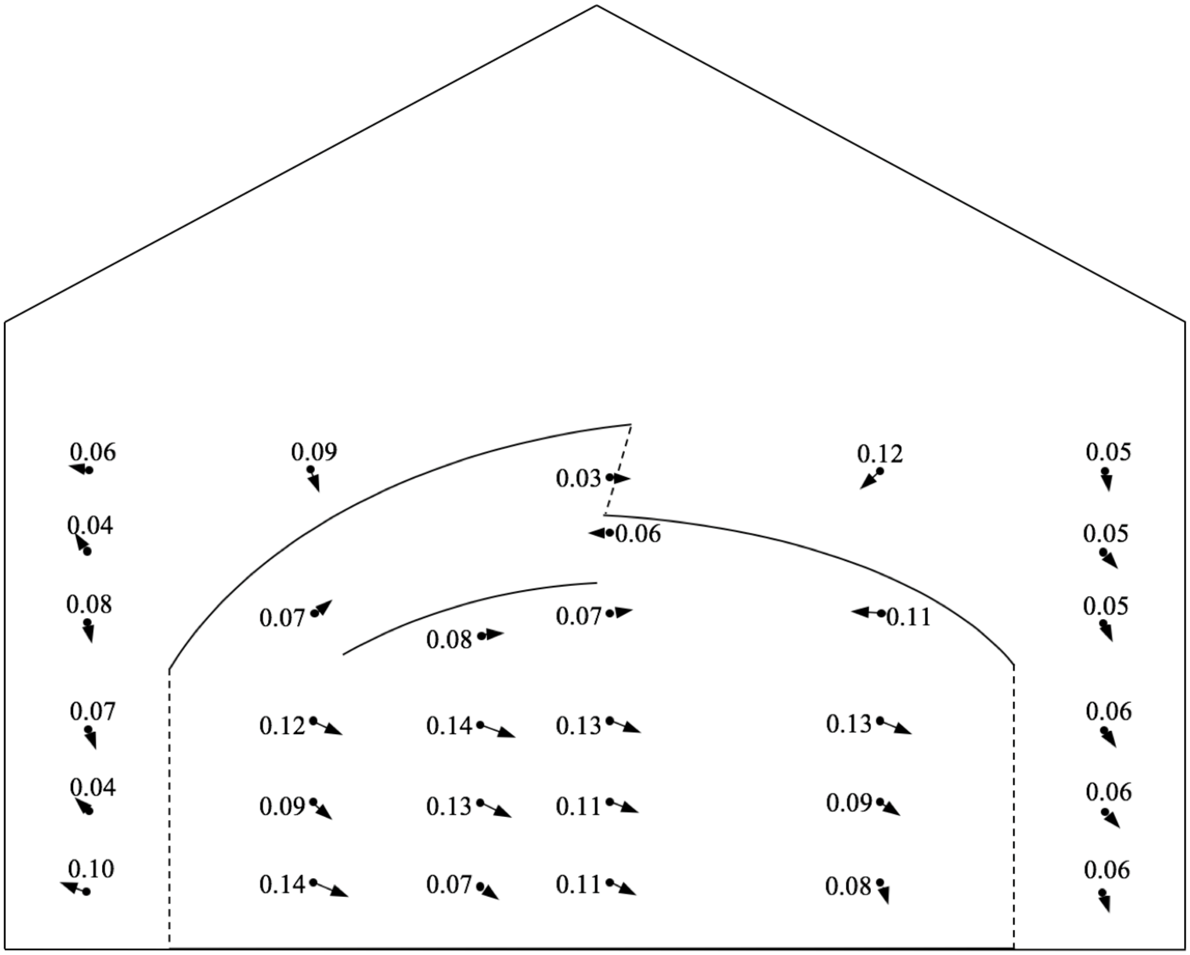

Figure 25. A cross sectional representation of the natural ventilation augmented cooling (NVAC) greenhouse model showing the average two dimensional resultants of air velocity in the XZ-plane and their respective direction angle (ϕ) under natural ventilation operation.

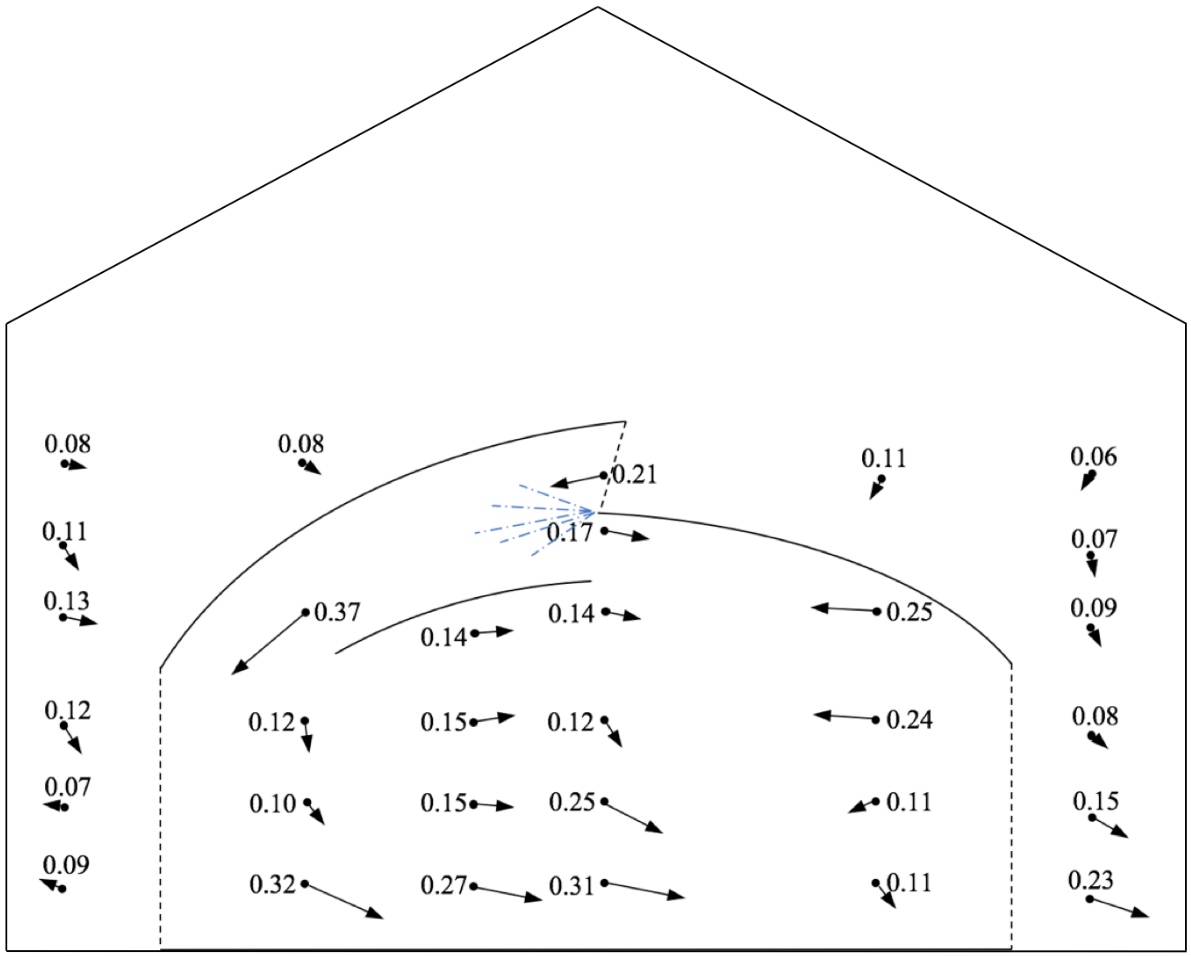

Figure 26. A cross sectional representation of the natural ventilation augmented cooling (NVAC) greenhouse model showing the average two dimensional resultants of air velocity in the XZ-plane and their respective direction angle (ϕ) with the NVAC system operation.

Under natural ventilation conditions, the transversal component influenced the direction, as the average values of the transversal components (u_x) and the air velocities (u) were similar, while the longitudinal and vertical components, u_y and u_z, were less influential (Table 16). The vertical flow (u_z) was downwards at all measurement locations and heights A, B and C, except for location 5 heights A and B, which agrees with the notion that natural ventilation alone provides a flow of fresh (cooler) air in from the sides, to replace the rising air in the middlemost section and flow out from the roof vent (Figure 25). The heat absorbed and emitted by the floor of the greenhouse was not sufficient to produce significant upward air movement (buoyancy) throughout the plant space. In a similar study by Sabeh (2007), buoyancy did not significantly affect air movement inside the greenhouse model either. Location 5 heights A and B were the only measurement points in the plant space where upward movement was present. In the rafters, however, the air flowed out from the roof vent (Figure 25). Moreover, the vertical component (u_z) at heights D, E and F were positive, yet small, indicating upward movement, agreeing with the concept of displacement natural ventilation.

Under the conditions provided by the NVAC greenhouse, the average values of the transversal velocity component (u_x) and the air velocity (u) were similar but larger, and the vertical velocity component (u_z) was in this case influential in the air velocity (u) in the plant space, compared to natural ventilation (Table 17). The longitudinal velocity component (u_y) was slightly larger under the NVAC system, but remained the least important of the three axes. The increase is most likely due to overall increased air velocity (Table 15). The vertical flow (u_z) was consistently downwards at all measurement locations at heights A, B and C, but was of greater magnitude in Section I, being closest to the bottom ridge of the added roof where the downdraft occurs (Figure 26). The vertical component at heights C and D at locations 5i and 8 were positive indicating upward movement. The airflow generated by the NVAC system in Sections I and II of the greenhouse appears to displace the air in Section III, causing warm air to rise at and around location 8 and drawing in outside warm air (Figure 26). The vertical velocity components (u_z) of Section II, including heights D, E, and F were negative indicating downward flow. However, the turbulence intensities at these heights (i_u = 0.21, 0.44 and 0.45 respectively) indicate turbulence and that the flow is very variable. In an analysis of airflow velocity and direction by Sabeh (2007), on a similar natural ventilation greenhouse (without the added NVAC inside roof) under wind conditions, a comparable cross-sectional profile was described under low wind ($\bar{u} = 2.65\ m \cdot s^{-1}$). From this comparison, the NVAC greenhouse can provide conditions similar to that of a natural ventilation greenhouse under wind conditions, without the presence of wind, and that, without fans.

The roof vent design in the NVAC greenhouse allowed airflow of both warm air out and fresh air in. This resulted in some airflow out, some airflow into the greenhouse from the roof vent, and airflow of mist cooled air backtracking to fall into Section II of the greenhouse. This combination of effects was supported by the very high turbulence intensities measured along the roof vent. The rising warm air from heights C and D in Sections II and III, combined with the turbulent flow at the roof ridges, may have contributed to the downward flow found in Sections I and II.

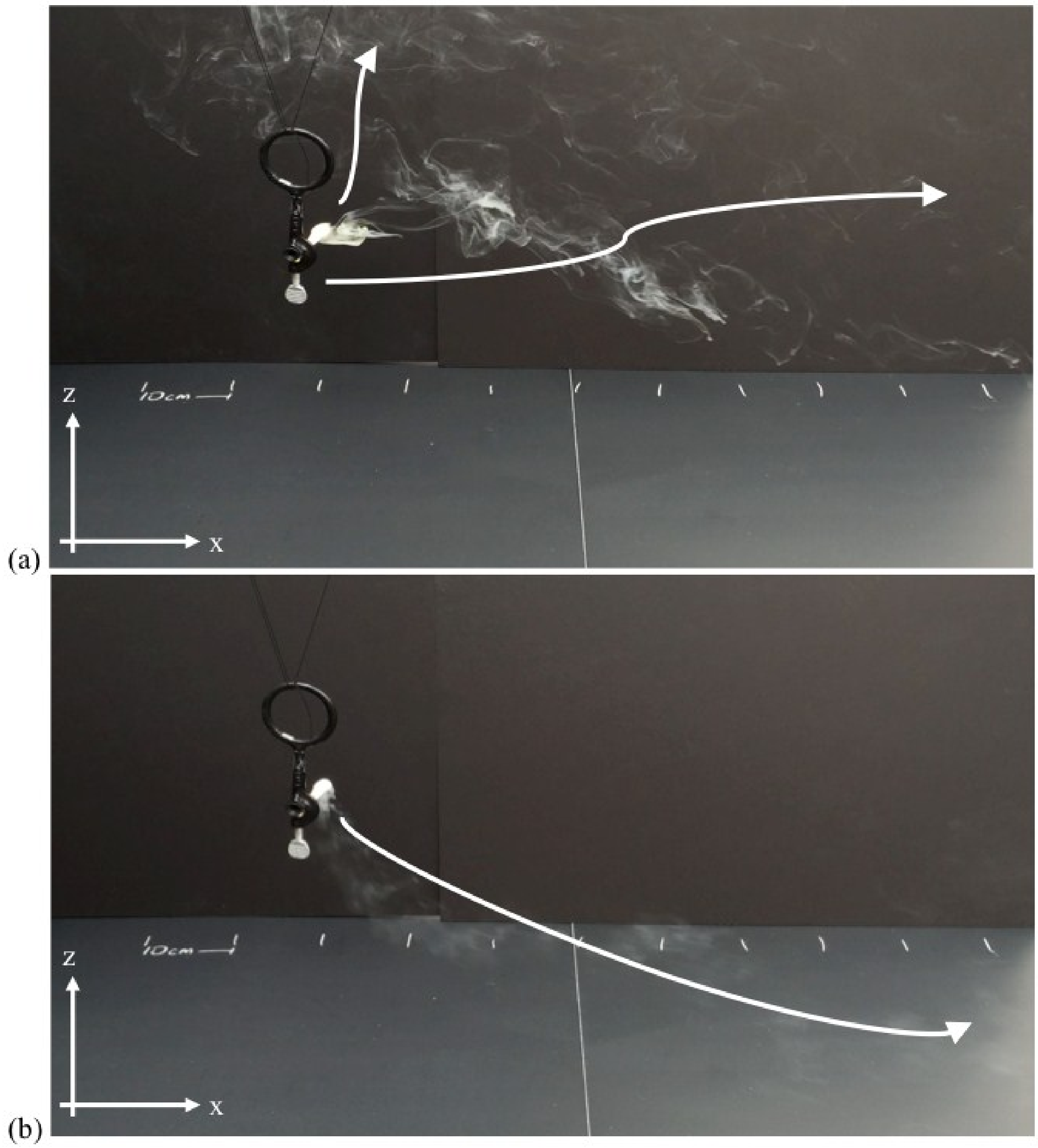

Figure 27. Smoke test still image from location 5 height A (0.2 m) in Section II in the natural ventilation augmented cooling (NVAC) model greenhouse. The greenhouse in (a) was under natural ventilation conditions, and in (b) was under the NVAC system. White arrows illustrate the main air movement.

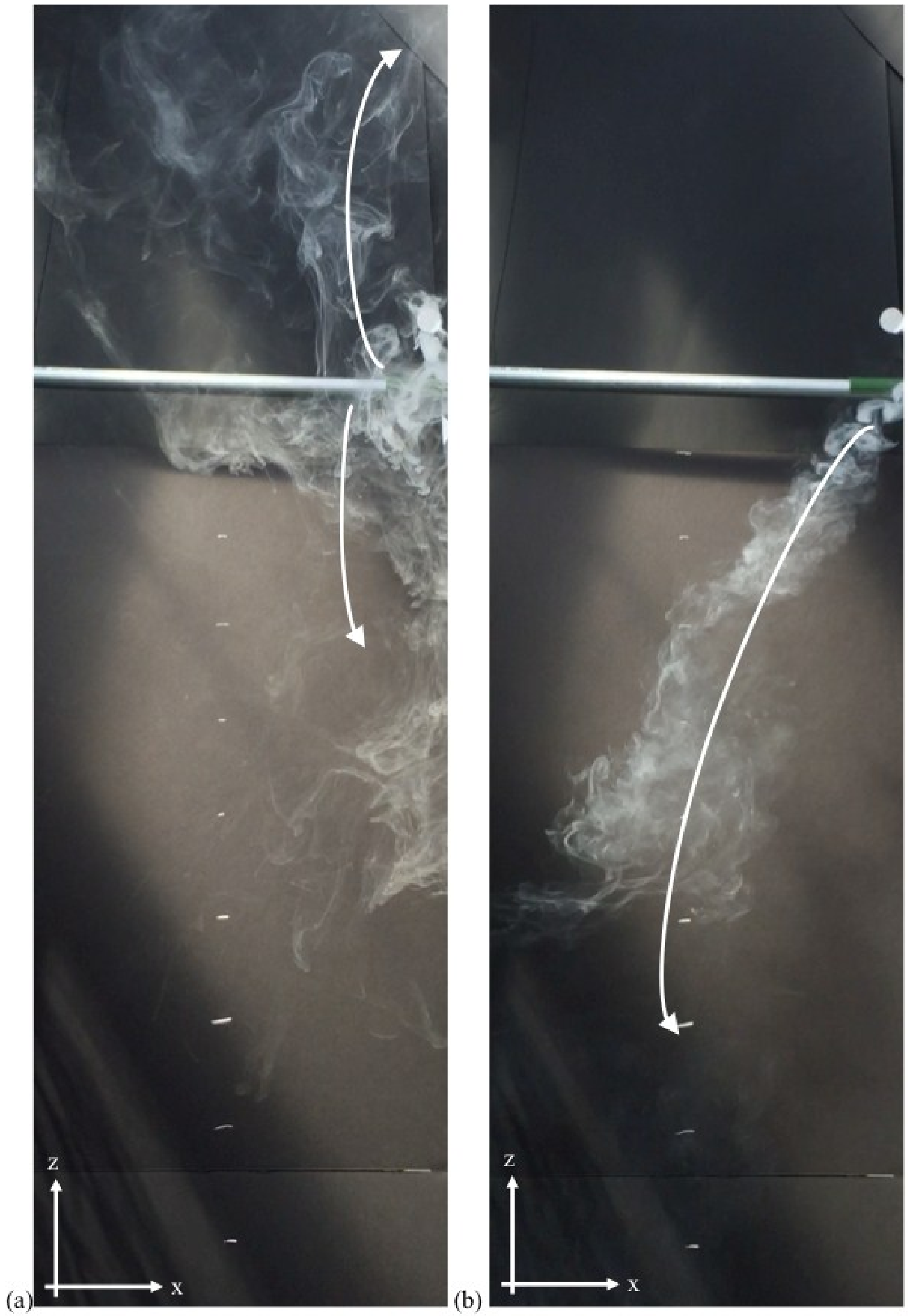

Figure 28. Smoke test still image from location 2 height C, (1.2 m) in Section I of the natural ventilation augmented cooling (NVAC) model greenhouse. The greenhouse in (a) was under natural ventilation conditions, and in (b) under the NVAC system. White arrows illustrate the main air movement.

Still images from videos of the smoke tests show the air movement at location 2, height C and location 5 height A, respectively (Figure 27 and 28). Location 2 height C was chosen for being under the downdraft of the inside roof, and location 5 height A was chosen for being in the center of the greenhouse: two locations of interest as these points were locations of high air velocity (u) under NVAC system conditions. The air velocities at these points under natural ventilation ($u = 0.12 \pm 0.02$ and 0.07 ± 0.03 $m \cdot s^{-1}$, respectively) were clearly smaller than under NVAC system conditions ($u = 0.21 \pm 0.09$ and 0.31 ± 0.08 $m \cdot s^{-1}$, respectively). Under natural ventilation, at both points, the air flowed slowly and moved in a mixing manner in all directions of the XZ-plane (transversally and vertically). Figures 27a and 28a show the rising warm air plumes in the greenhouse with colder drafts falling in from the sides. This provided turbulent movement both transversally and vertically, particularly noticeable in Figure 27a. Accordingly, the turbulence intensity at location 5 height A was the largest recorded under natural ventilation conditions ($i_u = 0.38$). Location 2 height C showed a relatively high turbulence intensity ($i_u = 0.28$), compared to other locations in the greenhouse under these conditions. Under NVAC system conditions, the turbulence intensity was $i_u = 0.40$ at location 2 height C and 0.25 at location 5 height A. The turbulence intensity was less at location 5 height A under NVAC conditions, which can be typical of more pronounced air currents (Ouyang et al., 2006).

5.6.4 Turbulence

An estimate of the temporal stability of the airflow can be obtained from the standard deviation (σ) of the air velocity, which remained constantly small (±0.01 to ±0.04) throughout all sections and measurement points under natural ventilation. The small standard deviation indicated that the velocity during the measurement time period of 2 min was close to the mean value. The properties of airflow, such as turbulence intensity (i_u), have a significant effect on the way in which thermal energy is transferred from one area of a structure to another, or to the outside, and thus on the indoor climate and air quality (Tanny et al., 2008). In this study, the turbulence intensity (i_u) was calculated at all measurement points from the air velocity measurements. In simple plastic greenhouse tunnels subject to significant wind, less heterogeneous and turbulent conditions were found to contribute to better plant growth, and it is suggested to reduce the mean air velocity and the turbulence within the greenhouse (Boulard et al., 2000). The NVAC greenhouse is however designed to provide cooling and added air movement in still conditions where a natural ventilation design does not suffice. Increased air velocity and turbulence is preferred in this case.

5.6.4.1 Turbulence Intensity

Tables 15 and 16 show the turbulence intensity (i_u) of the air velocity at each measurement point, across all locations and heights in the plant space. Table 17 shows the average turbulence intensity $i_{u\ avg}$ obtained in the different sections and heights in the plant space of the greenhouse. The levels of turbulence throughout the plant space varied differently under natural ventilation and NVAC system conditions (Table 18).

Table 18. Average turbulence intensity of the air velocity ($i_{u\ avg}$) corresponding to the measurement points in the plant space of the NVAC greenhouse.

Average Turbulence Intensity ($i_{u\ avg}$)						
	Natural Ventilation			NVAC System		
Height/Section	I	II	III	I	II	III
A	0.30	0.38	0.12	0.25	0.22	0.56
B	0.21	0.16	0.21	0.39	0.28	0.32
C	0.14	0.10	0.09	0.41	0.20	0.24
Average	0.22	0.21	0.14	0.35	0.24	0.37
Average	0.19			0.32		

Under natural ventilation, Section III is the area of least turbulence (Table 18, Figure 29a). Under NVAC system conditions, Section II shows the least turbulence (Table 18). This is likely because the air at Section II flowed uniformly in the transversal axis (Figure 27b), and was not affected by the side vents and the downward current of air in Section I. The highest average turbulence intensity was observed at height C in Section I ($i_{u\ avg}$ = 0.41). This is where the cooled and humidified air from the mist system interacts with the air in the plant space. Interaction between air masses with different density characteristics, caused by differing temperature and relative humidity, can cause an increase in turbulence (López et al., 2010). The greatest average turbulence intensity per section ($i_{u\ avg}$ = 0.37) is found in Section III under NVAC system conditions (Figure 29b). This turbulence intensity pattern is dissimilar to that observed in a study by López et al. (2010) on a greenhouse pad and fan system where the airflow entering through the pads showed little turbulence, becoming more turbulent inside the greenhouse before losing turbulence at the points closest to the extractor fans on the opposite side of the greenhouse. In fact, the observations made in the NVAC greenhouse showed differences, which are similar in some aspects to that reported by Boulard et al. (2000) in a tunnel greenhouse with side vents and no roof vent under field conditions (i.e. subject to wind). In the NVAC greenhouse and in the tunnel presented by Boulard et al. (2000) turbulence was at a minimum in the center of the greenhouse. Central locations in a greenhouse, especially low-lying, are perhaps the locations where the wind and buoyancy pressure gradients are the lowest, being farthest from the side and roof vents.

(a)

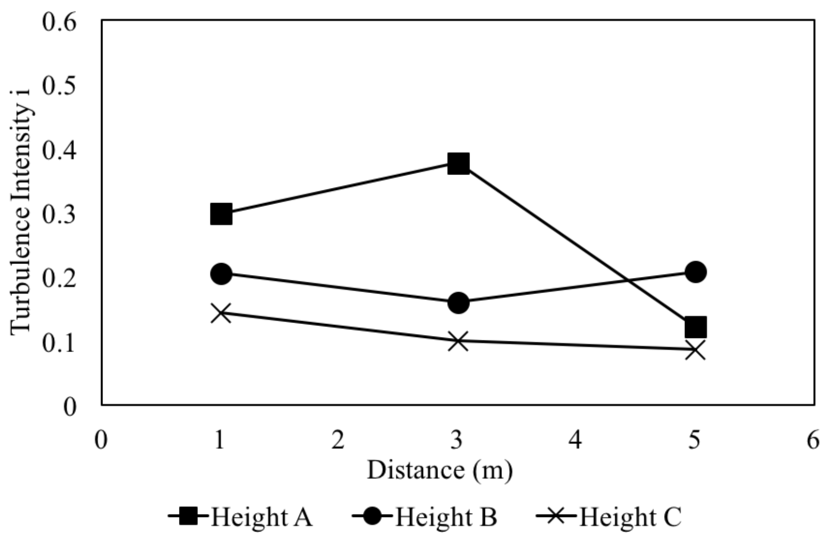

(b)

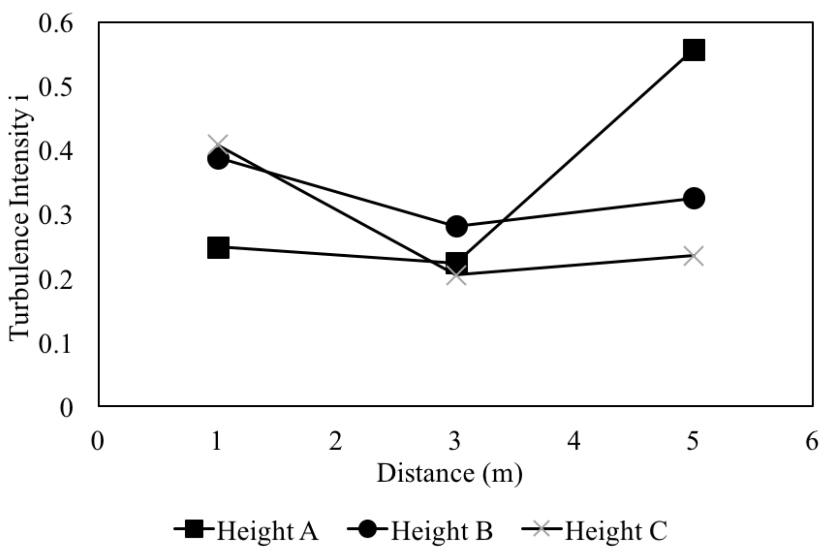

Figure 29. Profiles of turbulence intensity of the air velocity (i_u) in the natural ventilation augmented cooling (NVAC) model greenhouse in (a) under natural ventilation conditions and in (b) under NVAC system conditions. The heights A, B and C are 0.2 m, 0.6 m and 1.2 m from the ground, respectively. The distances (m) are transversal from the sidewall in Section I to the sidewall in Section III.

The NVAC greenhouse design provides greater overall turbulence intensity in the plant space, compared to natural ventilation. The average turbulence intensity ($i_{u\ avg}$) in the plant space was 0.19 under natural ventilation, and 0.32 under the NVAC system. This increase in turbulence agrees with the findings on vertical temperature gradients that suggested that more mixing of the air in the plant space causes a more uniform vertical temperature gradient. At heights F, in the upper vent, the turbulence intensity (i_u) was 0.45 under NVAC system conditions, higher than 0.32, the average inside turbulence in the plant space. This is due to the large variation in velocity of the air currents flowing around the mist nozzles and flowing in and out from the roof vent. Wang et al. (1999) recorded turbulence intensity values (i_u) ranging from 0.14 to 0.47 in the interior of a natural ventilation greenhouse with only a roof vent, under field conditions. It must be noted that the NVAC greenhouse design provided turbulence during perfectly still outside conditions. Tanny et al. (2006), recorded turbulence intensity values ranging from 0.1 to over 4.0 inside a natural ventilation greenhouse under different combinations of openings of side and roof vents, under field conditions (i.e. wind). In López et al. (2010), with mechanical ventilation and a pad and fan system, the average turbulence intensity in the interior of the greenhouse with a crop was 0.28, and 0.35 without a crop. López et al. (2012) reported that the average turbulence intensity was greater in a naturally ventilated greenhouse (0.42–0.82) than in an actively ventilated greenhouse (0.33–0.38), where extractor fans generated a less turbulent airflow. Without the effect of the wind on the inside space, lower turbulence of the airflow reduces the mixing of outside air entering the greenhouse through the vents, and contributes to greenhouse climate heterogeneity (López et al., 2010). This is the main disadvantage of active cooling systems such as pad and fan systems. Under this reasoning, the NVAC greenhouse design can provide a necessary increase in turbulence which contributes to added ventilation beyond that of the obvious current of air provided by the downdraft of evaporative cooled air

From the air velocity direction and turbulence intensity observations in the present study, we can deduce that under still environmental conditions, displacement ventilation (Tanny et al., 2008) most likely occurs in the NVAC greenhouse without the use of the misting system (i.e. under purely natural ventilation). The outside air enters through the lower vents and displaces warm air from the space through the opening of the higher-level vent (Haslavsky et al., 2006) (Figure 25). Inflow and outflow are in this case separate. From the measurements and observations made herein, a combination of displacement and mixing ventilation (Tanny et al., 2008) occurs when the NVAC greenhouse system is used. The high turbulence intensity found at the upper vent ($i_u = 0.45$) supports the notion that both inflow and outflow take place at different locations in the same vent. Incoming outside air mixes with the air at the mist nozzle area and further down within the plant space, while warmer air leaves through the same upper vent (Figure 25). Moreover, particularly high turbulence intensities were also found at Section III of the NVAC greenhouse, the two largest values $i_u = 0.62$ and $i_u = 0.74$ were found in this section. This indicates that relatively better mixing occurred at the side vents of Section III when the NVAC system is used, compared to under natural ventilation.

In the study by Tanny et al. (2008), results showed that turbulence in the opening of an upper vent caused mixing between the incoming and outgoing airstreams, and it was suggested that turbulent mixing between adjacent and opposite streams in a vent may reduce the rates of ventilation and change the characteristics of the air inflow, such as temperature and relative humidity, which may be undesired. However, in the present study, the NVAC greenhouse system may benefit from this effect. The high turbulence at the upper vent ($i_{u\ avg} = 0.45$) provided mixing of incoming air with the rising plant space air and the evaporative cooled air. This mixing would in fact be essential in providing fresh air with a lower water vapor content to allow the evaporative cooling effect, occurring in the rafters, to remain efficient.

5.6.5 Greenhouse Design

There are guidelines to optimize the performance of a natural ventilation structure based on the immediate environment in which the structure lies and based on the type of natural ventilation desired. The ratio (R) between surface areas of the roof vent openings (S_{VR}) and side vent openings (S_{VS}) affects the efficiency of buoyancy driven ventilation (Kittas et al., 1997). It was shown that when $0 < R < 0.27$, the mixing and displacement modes interact (Haslavsky et al., 2006). For $0.53 < R \leq 1$, the displacement mode prevails, whereas in the intermediate range, $0.27 \leq R \leq 0.53$, either the combined or the pure displacement mode takes place. In the present study on the NVAC greenhouse, the value of R was 0.17. According to Kittas et al. (1997), this value is below the appropriate range for maximization of the buoyancy ventilation flux ($0.5 < R < 2$). This value is outside the range $0.5 < R < 1$ where the displacement mode of buoyancy-driven natural ventilation prevails and outside air effectively enters through low-level vents and displaces warm air from the greenhouse through vents at higher levels (Haslavsky et al., 2006). Another important ratio to consider is the ratio of ventilator opening area A_V to greenhouse floor area A_G (von Zabeltitz, 2011), denoted here as R'. The recommended ratios take into consideration a variety of effects. For mild climates, an R' value ranging from 0.18 – 0.29 is recommended for sufficient ventilation in a natural ventilation design, but practical experience suggests a ratio from 0.18 to 0.25 (von Zabeltitz, 2011). The ANSI/ASAE EP 406.4 standard (2003), Kacira et al. (2004) and Sethi and Sharma (2007) give a range of 0.15 to 0.30. Overall, the higher the R' value, the greater the greenhouse ventilation rate. In the present study, R' was 0.6 which was far greater compared to the suggested values for mild climates. However, natural ventilation greenhouse design criteria for high temperature environments include enlarged side and roof vents, and greater greenhouse heights in order to maximize greenhouse volume (von Zabeltitz & Baudoin, 2005) and profit from wind driven ventilation. The NVAC greenhouse can be designed with a variety of R and R' ratios, but in this study, it was designed for hot climate use, as the NVAC system shows good performance under hot and arid conditions (Table 14, Figure 20). This introduces a design tradeoff: to maximize the wind effect, greenhouses in hot climates are being built taller with greater side vents having lower R values and R' values exceeding 1, which reduces the displacement ventilation effect. This explains how in this study, turbulence intensity was increased and was more uniformly distributed throughout the plant space with the use of the NVAC greenhouse system, compared to natural ventilation, and not vice-versa. Given low R values and high R' values, the NVAC greenhouse design would rely greatly on wind driven ventilation, under field conditions. During times of low wind, when buoyancy-driven ventilation predominates but is not sufficient for adequate ventilation, the NVAC greenhouse system can provide ventilation and cooling.

In multi-span greenhouses, regardless of the cooling measures, studies show an increase in air temperature from windward to leeward span since the air near the ground moves from a windward to leeward direction and accumulates heat that is released from the crop (Teitel et al., 2008). In Teitel et al. (2008), the leeward span was 8 to 9 °C warmer than ambient air, similar to values reported by Ould Khaoua et al. (2006) for their leeward compartment (6.2 to 7.5 °C). Hence, it is suggested growers need to operate mixing fans to obtain a more uniform climate in the greenhouse. It is anticipated that the NVAC system can be added to each span of a multi-span greenhouse to provide air movement and cooling, provided the design of the greenhouse includes roof vents on each span. Future studies will address this topic.

5.6.6 Water Usage

The NVAC greenhouse in the present study used 0.28 $L \cdot h^{-1} \cdot m^{-2}$ and 0.56 $L \cdot h^{-1} \cdot m^{-2}$ of water for the three and six-nozzle configurations, respectively. In a study on a pad and fan evaporative cooling system by Al-Helal (2007), it was observed that the average consumption of cooling water varied from 0.65 to 1.08 $L \cdot h^{-1} \cdot m^{-2}$ of floor area, making the NVAC system more efficient in terms of water use efficiency for a similar cooling performance. Flow rates reported in fog evaporative cooling systems vary greatly depending on the design, but can be found to range from 0.13 to 1.22 $L \cdot h^{-1} \cdot m^{-2}$ (Öztürk, 2003), 0.23 to 0.64 $L \cdot h^{-1} \cdot m^{-2}$ (Hayashi et al., 2005) and 1.23 to 1.63 $L \cdot h^{-1} \cdot m^{-2}$ (Arbel et al., 1999). The water use in the NVAC greenhouse evaporative cooling system is comparable to that reported in studies on fog cooling systems, with similar or greater cooling capabilities. Montero (2006) reported that under high temperatures and at low relative humidity, a fog cooling system should provide a water flow rate of 1 $L \cdot h^{-1} \cdot m^{-2}$ to supply enough water vapor during the early planting stages of the crops in Mediterranean climates. It was also stated that due to the high cost of implementing fogging systems, most facilities in the Mediterranean are designed to work at far below this value (Montero, 2006). In such a setting, the NVAC system could provide the required increase in relative humidity without the use of costly fogging systems.

5.6.7 Efficiency

There are two ways to address the efficiency (η) of an evaporative cooling design: the efficiency of the cooling process and the efficiency of the entire system. The equation commonly used for calculating the efficiency of a pad and fan evaporative cooling process is defined by ASHRAE (1985) as follows:

$$\eta = \frac{T_{db,o} - T_{db,c}}{T_{db,o} - T_{wb,o}} \qquad \text{Equation 14}$$

Equation 14 is valid only when the cooling process humidifies air at the outside dry and wet bulb temperatures and cools the outside relatively constant dry bulb temperature ($T_{db,o}$) to a cooled temperature ($T_{db,c}$) in the absence of sensible or latent heat affecting the value of the outside temperature ($T_{db,o}$) (Abdel-Ghani & Kozai, 2006). The temperature of the cooled air ($T_{db,c}$) is the temperature measured at the exit of the cooling pad, and therefore Equation 14 is an efficiency of the cooling process, and not of the greenhouse system (i.e. not representative of the conditions of the entire volume of air of the greenhouse). In a sense, this can also be referred to as the ideal efficiency of a cooling system. It is seen in the present study that in the NVAC greenhouse, there is a significant current of incoming outside air at the upper roof vent and therefore we are assuming that the NVAC evaporative cooling system, at this location, provides a similar process to that found at the cooling pads in a fan and pad system. However, the temperature of the cooled air ($T_{db,c}$) in the present study is the temperature of the cooling process at a variety of measurement points in the plant space in the NVAC greenhouse, and therefore Equation 11 becomes an expression of the efficiency (η) of the system. Moreover, it is not known, at this point, how much inside greenhouse air, which exchanges sensible and latent heat with various greenhouse elements including the cooling process itself, is mixed with the incoming outside air at the location of the evaporative cooling process. Therefore, using Equation 14 can result in unrealistic and even negative cooling efficiency values (Hayashi et al., 2005; Abdel-Ghani & Kozai, 2006). A modelling study by Abdel-Ghani and Kozai (2006) offers a cooling efficiency analysis specific to fog cooling systems by incorporating many elements of the energy system of a greenhouse, which offers insight into this issue.

When the NVAC system is used to cool the air, but not to temperatures lower than outside temperatures, which may be desirable in certain applications, such as in water-scarce situations, Equation 14 yields negative efficiencies (η), even if cooling occurs in the greenhouse (Table 19, for March 4, 2016). Hayashi et al. (2005) reported negative efficiencies in a fog cooling system. Therefore, a new equation of efficiency was developed. In the present study, the conditions in the research greenhouse bay were kept constant and therefore we can assume that the initial temperature ($T_{db,i}$) is the temperature at which the NVAC greenhouse would remain if the NVAC system was not used. This efficiency (η_c) is useful as it shows the cooling potential of the NVAC system, but it is only appropriate in unchanging conditions, such as in the controlled environment of the present study. The cooling efficiency of the NVAC greenhouse (η_c) is therefore:

$$\boldsymbol{\eta_c} = \frac{T_{db,i} - T_{db,c}}{T_{db,i} - T_{wb,i}} \qquad \text{Equation 15}$$

where $T_{db,i}$ and $T_{wb,i}$ are the initial wet bulb and dry bulb temperatures found in the greenhouse before the NVAC system is utilized. This type of efficiency is valuable as it incorporates the initial conditions, which are the conditions found within the greenhouse under natural ventilation conditions only. Li and Willits (2008) suggested a similar equation for cooling efficiency in a comparison study of two empty natural ventilation greenhouses, one of which was fog-cooled.

To give a measure of efficiency of the NVAC system, comparable to the methodologies used for pad and fan evaporative cooling systems, a modified version of Equation 15 was developed (η_c'):

$$\eta_c' = \frac{T_{db,mix} - T_{db,c}}{T_{db,mix} - T_{wb,mix}} \qquad \text{Equation 16}$$

where $T_{db,o}$ and $T_{wb,o}$ are replaced by $T_{db,mix}$ and $T_{wb,mix}$, which are the calculated values of the stabilized dry bulb and wet bulb temperatures of a hypothetical 50% mix of outside and inside air. This assumes that the evaporative cooling process in the rafters of the NVAC greenhouse uses a perfect mixture of inside and outside air. This assumption is drawn from the air movement and turbulence results from Section II, height E presented in previous sections of this study that suggest that a high level of turbulence is present in the rafters at the location of the mixing of inside air, outside air and misted air. This location is where the misting occurs and is the intersection of the ridges of the three roofs. The air direction analyses of Section II show that there are currents of air flowing into the greenhouse at height F, onto the inside roof at height E and into the plant space at height D, suggesting that a mixture of air occurs around height E. Lastly, a variety of supplemental smoke tests were performed in the NVAC plant space to visually asses the movement of the air in the entire volume of the greenhouse, including the rafters. Three smoke emitters placed on the ground at height A in Section II were triggered prior to activation of the NVAC system. Within seconds of activating the NVAC system, smoke was noticeable in the rafters of the greenhouse and into the volume of air above the inside roof, suggesting that plant space air is mixed into the cooling process at height E in Section II.

Table 19. The cooling performance, efficiency of the NVAC system evaporative cooling process (η), efficiency of the NVAC process considering initial greenhouse conditions (η_c) and efficiency of the NVAC system (η_c'). The performance and efficiencies are calculated based on tests of the NVAC model greenhouse in March, April and May 2016 and are presented in order of ascending cooling performance.

Test Date 2016	ΔT	η	η_c	η_c'
Three-nozzle configuration and mist rate 0.28 $L \cdot h^{-1} \cdot m^{-2}$				
March 10	-1.9	0.25	0.32	0.15
March 19	-2.7	0.25	0.30	0.15
March 21	-3.0	0.14	0.34	0.09
March 4	-3.1	-0.05	0.16	-0.03
March 18	-3.8	0.34	0.33	0.19
March 9	-4.0	0.12	0.29	0.08
Six-nozzle configuration and mist rate 0.56 $L \cdot h^{-1} \cdot m^{-2}$				
April 13	-3.1	0.23	0.48	0.16
April 18	-3.9	0.25	0.45	0.15
May 10	-5.5	0.24	0.38	0.15
May 11	-9.5	0.24	0.36	0.14
April 17	-11.2	0.30	0.48	0.19
April 19	-12.6	0.43	0.56	0.29

It is easier to compare the NVAC greenhouse design cooling efficiencies to that of fog system cooling efficiencies, than it is to compare with pad and fan systems efficiencies because previous work on greenhouse fog cooling systems analysed $T_{db,c}$ as the cooled inside greenhouse temperature measured at many points (Hayashi et al. 2005, Abdel-Ghani & Kozai, 2006). On the other hand, studies on pad and fan evaporative cooling efficiencies (Kittas et al. 2003; Ahmed et al., 2011) have defined $T_{db,c}$ as the air temperature found adjacent to the cooling pad, on the cool side , which is unrepresentative of the efficiency of the system at cooling the greenhouse space. In Table 19, we see that the conventional efficiency of the NVAC greenhouse process η varies from -0.05 to 0.43, depending on the outside conditions and the water flow rate. The efficiencies were greater when a higher flow rate was used. The cooling efficiency of the system (η_c) ranged from 0.16 to 0.56. When the mixing of air in the NVAC greenhouse design is considered, the efficiency of the system (η_c') ranges from -0.03 to 0.29. In a study on the efficiency of a fog cooling and natural ventilation system, efficiencies of -0.30 to 0.21 were reported when calculated using a multi-point measurement method and Equation 15 (Hayashi et al., 2005). In an alternative study on fog cooling, efficiencies ranged from 0.19 to 0.51, but were calculated using a non-conventional method (Abdel-Ghani & Kozai, 2006). In a study on the efficiency of a pad and fan system, Kittas et al. (2003) reported values ranging from 0.22 to 0.78, and Ahmed et al., (2011) reported values from 0.76 to 0.90. It remains difficult to compare evaporative cooling efficiencies of the NVAC greenhouse design to that of a pad and fan system because the types of data and methodologies used to calculate the efficiency differ greatly in the literature.

5.7 Conclusions

An experimental study of the air movement and cooling performance of a natural ventilation augmented cooling (NVAC) greenhouse was presented. The NVAC greenhouse design is a simple system that is capable of providing cooling, air movement and relative humidity control under high temperature conditions, without the use of active ventilation methods.

During times of low wind in a naturally ventilated greenhouse, in a greenhouse that does not provide a large vent area, or under hot conditions where outside temperatures are beyond acceptable inside temperatures, the NVAC system can provide up to 0.39 $m \cdot s^{-1}$ of air movement across the plant space.

The cooling performance varied from 1.9 to 12.6 °C, and relative humidity was increased from 1.4 to 31.2% depending on the initial conditions in the greenhouse. Accordingly, the vapor pressure deficit (VPD) conditions were improved with the NVAC greenhouse design. The VPD was lowered by 0.3 to 4.9 kPa, to within acceptable levels, when initial conditions were considered harsh (hot and low relative humidity). During very harsh trials with a very high initial temperature and a very low relative humidity (extremely high VPD), the system was unable to lower the VPD to within recommended levels, but nonetheless provided some relief by significantly lowering the VPD.

The choice of water usage, configuration of the misting nozzles and vent design of the NVAC greenhouse depend on the local conditions and on the needs of the grower. The water use efficiency of the NVAC greenhouse design varied from 0.28 to 0.56 $L \cdot h^{-1} \cdot m^{-2}$ and is comparable to that of traditional fog evaporative cooling systems.

The average turbulence intensity in the plant space of the greenhouse increased to 0.32 with the use of the NVAC system, compared to 0.19 in the same structure under natural ventilation. This helped provide better ventilation and cooling across the plant space. Increased turbulence intensity in the roof vent provided the required air movement to allow the NVAC system's process to function effectively in the rafters of the greenhouse. The temperature gradient was more pronounced under NVAC system conditions, but the cooling performance of the system outweighed possible drawbacks of temperature heterogeneity.

The efficiency of the NVAC system was assessed using various methodologies and it is comparable to that of fog cooling systems, but is difficult to directly compare with fan and pad cooling systems. The NVAC greenhouse design offers performance improvements over that of fog evaporative cooling methods, for it can be used continuously rather than intermittently, limits wetting of foliage, can be used without active ventilation, and offers air movement.

It is important to note that in the entirety of this experiment, all measurements were done without plants in the greenhouse. Generally, airflow is less uniform and more turbulent when there is no crop (López et al. 2010). Temperature and relative humidity is greatly affected by the presence of crop inside the greenhouse. Future studies should explore the microclimate and airflow characteristics of the NVAC greenhouse design with crop, and the impact that the design may have on the crop.

5.8 Acknowledgements

The authors would like to gratefully acknowledge support from Dr. Ian Strachan and Mrs. Kelly Nugent, Department of Natural Resources Sciences, McGill University. This work was supported by the Natural Sciences and Engineering Research Council of Canada (NSERC), Discovery Grant 355743-13.

Connecting Text

Chapter 6, *Photosynthesis, fluorescence and transpiration responses in bell pepper plants to high temperature and to the Natural Ventilation Augmented Cooling (NVAC) greenhouse design* was authored by Lucas McCartney and Mark. G. Lefsrud. Chapter 6 will be submitted to the journal *HortTechnology*.

A greenhouse creates an improved environment for plant cultivation. Chapter 6 studies the plant responses to the NVAC greenhouse design. Although many methods exist to measure and quantify crop growth, yield and quality, the focus of this work was on the measurement of plant stress and the alleviation of stress that the NVAC greenhouse can provide. The net photosynthetic rate, chlorophyll fluorescence and plant transpiration of pepper (*Capsicum annuum*) were studied under high temperature conditions and under conditions provided by the NVAC greenhouse. The high temperature conditions imposed on the plants were no different than the potential conditions to which greenhouse crop are subject to in greenhouses of regions such as the Caribbean and the Mediterranean. The greenhouse growers with whom we collaborated with for field tests in Barbados grew bell peppers as their main greenhouse crop, and were eager to test new cooling strategies to optimise production. Pepper is an important greenhouse crop in other areas of the world with significant greenhouse industries, including the coastal Mediterranean region. Compared to other greenhouse crops, such as certain tomato varieties, bell pepper is sensitive to high temperatures and growth, yield and quality of yield can easily be affected by supra-optimal temperatures. Therefore, bell pepper was chosen as a crop of study for our investigation into plant responses.

6. Chapter 6: Photosynthesis, Fluorescence and Transpiration Responses in Bell Pepper to High Temperature Greenhouse Conditions and to the Natural Ventilation Augmented Cooling (NVAC) Greenhouse Conditions.

Lucas McCartney and Mark G. Lefsrud

Additional Index Words. Greenhouse cooling; temperature stress; *Capsicum annumm*; crop sensing.

6.1 Abstract

Greenhouses in many regions of the world are subject to warm temperatures, either year-round or seasonally, causing non-optimal growing conditions. High temperature stress in many common greenhouse crops induces a variety of detrimental effects, causing significant reductions in yield and quality. The Natural Ventilation Augmented Cooling (NVAC) greenhouse is a new greenhouse design that provides cooling and increased humidity in naturally ventilated greenhouses. 'Bell Boy' pepper plants (*Capsicum annuum*) were studied under daytime high temperature conditions (>35 °C but <40 °C) that involved high vapor pressure deficit (VPD) (up to 3.9 kPa). The same plants were studied under improved conditions provided by the NVAC greenhouse. Under high temperature conditions, the net photosynthetic rate (P_n) and variable to maximum fluorescence ratio (F_v/F_m) in the pepper plants were significantly depressed compared to morning (11:00 HR) values. P_n at 11:00 HR was 10.5 ± 1.3 $\mu mol \cdot m^{-2} \cdot s^{-1}$, compared to 7.9 ± 2.1 $\mu mol \cdot m^{-2} \cdot s^{-1}$ at 15:00 HR, shortly after peak heat, representing a reduction of 33%. Transpiration rate followed a diurnal cycle, being at a minimum rate overnight, and reaching a maximum rate shortly after 12:00 HR. It was determined that the transpiration rate follows a linear relationship with temperature, relative humidity and VPD, but is most tightly related to relative humidity. The maximum transpiration rate coincided with peak temperature and VPD. The conditions provided by the NVAC greenhouse offered an improved greenhouse climate in terms of plant growth by means of cooling and an increase in relative humidity, which translated to a decrease in VPD. In contrast to conditions of high temperature, P_n was 8.0 ± 1.7 $\mu mol \cdot m^{-2} \cdot s^{-1}$ at 11:00 HR, while the average measurements at 15:00 HR reached

10.2 ± 1.8 $\mu mol \cdot m^{-2} \cdot s^{-1}$, an increase in 28%, under NVAC system conditions. Moreover, F_v/F_m was not depressed and transpiration rate of the plants was moderated, by an average of 31%, with the use of the NVAC greenhouse. From the results of this study, the NVAC greenhouse is able to provide an improved climate in terms of plant growth by reducing temperature stress, compared to the same greenhouse under natural ventilation and high temperature conditions.

6.2 Introduction

Plants can be subject to several stresses, including high or low temperature, water stress through a variety of factors, salinity, metal toxicity, and others. The response to stresses can vary amongst different species and amongst genotypes of a specific plant species, as reported by many authors including Camejo et al. (2005), Aprile et al. (2013) and Zandalinas et al. (2016). High temperature stress is one of the most studied plant stresses, as it provokes severe damage in the photosynthetic apparatus (Camejo et al., 2005). Photosynthesis is known to be one of the most heat-sensitive processes and it can be completely inhibited by high temperature before other symptoms of the stress are detected (Berry & Bjorkman, 1980). The inhibition of photosystem II activity (Quinn & Williams, 1985; Havaux et al., 1996), damage to the membrane (Shanahan et al., 1990) and inactivation of Rubisco (Weis, 1981; Feller et al., 1998) have all been linked to high temperature stress in plants. The inhibition of PSII has also been linked to a decrease in variable chlorophyll fluorescence (Camejo et al., 2005). Therefore, in vivo chlorophyll fluorescence has been reported to be a sensitive and reliable method for detection and quantification of temperature-induced changes in the photosynthetic apparatus (Krause & Weis, 1991), in addition to leaf gas exchange analysis. Larcher (1995) suggested that for monitoring heat stress, chlorophyll fluorescence may be a more reliable measurement of photosynthesis than gas exchange, which can be influenced by stomatal closure not induced primarily by high temperatures (Willits & Peet, 2001).

Changes in stomatal aperture are a primary and rapid response to environmental stresses aimed at regulating the flow of carbon dioxide (CO_2), leaf temperature (via transpiration) and water loss (Zandalinas et al., 2017). In most cases, heat causes an increase in stomatal conductance and transpiration. However, when high temperatures are combined with high VPD, an important water deficit within the plant can be induced and stomata can eventually close, reducing stomatal conductance (Grange & Hand, 1987).

These plant reactions to momentary or constant high temperatures cause a variety of morphological, physiological and biochemical changes in plants, which can affect plant growth and development and may lead to a drastic reduction in yield (Wahid et al., 2007). Yield potential in many common vegetable crops reduces at temperatures above 26.0 °C. Fruit set in important crops such as tomato (*Solanum lycopersicum*) and bell pepper (*Capsicum annuum*) is one of the first processes that is negatively influenced by daytime temperatures greater than 32.0 °C, even with specialized cultivars (Heuvelink, 2008; Sato et al, 2006). Poor fruit set is the most common issue noticed in bell pepper production under warm conditions (Erickson & Markhart, 2001). However, the reported optimal range for both reproductive development and vegetative growth of bell pepper plants is 21 to 33 °C, (Rylski & Spigelman 1982), although this can vary depending on the variety.

In Mediterranean countries where vast amounts of produce are grown in greenhouses, high temperatures and VPDs over 35 °C and 3.0 kPa, respectively, are commonly observed in natural ventilation greenhouses during summer months (Katsoulas et al., 2001). In regions of the Middle East and Northern Africa, the average summer daytime temperatures inside ventilated greenhouses can reach 46 °C without the use of evaporative cooling strategies (Al-Ismaili & Jayasuriya, 2016). It is no different in temperate climates, where outside summer temperatures can easily surpass 30 °C, which, combined with long days, causes greenhouse temperatures to easily exceed ideal conditions for many hours per day. Therefore, growers across the world rely on ventilation and evaporative cooling solutions to reduce greenhouse temperatures.

The cooling performance of the Natural Ventilation Augmented Cooling (NVAC) greenhouse in both field conditions and experimental conditions has been studied in previous work on the greenhouse design (Chapters 4-5). This improved natural ventilation design provides greenhouse cooling in warm climates, or during the summer seasons in other climates. To date, no work on the plant response to the novel greenhouse design has been carried out.

The present paper examines the response of ‘Bell Boy’ pepper plants to the evaporative cooling conditions brought about by the NVAC greenhouse design. The results are compared to that of the same plants subject to high temperature and high VPD conditions in the same greenhouse, under natural ventilation conditions only. Such conditions are no different from those under which the plants may be during warm summer seasons in some climates, or year-round in other high temperature climates, such as in the Mediterranean. In order to examine the plant responses to the NVAC greenhouse design, non-invasive methodologies were utilized. Pepper was chosen as it is an economically important greenhouse crop in many warm climates (Montero, 2006). Moreover, this species is regarded as relatively vulnerable to water stress as it has a relatively shallow root system (Dimitrov & Ovtcharrova, 1995), and a high stomatal density (Ben-Gal et al., 2008).

6.3 Methods and Materials

Experiments were conducted in an experimental NVAC greenhouse placed in one bay of a seven-bay research glass greenhouse at the Macdonald Campus of McGill University, in Ste-Anne-de-Bellevue, QC, Canada (45°24′N, 73°57′W). The NVAC greenhouse is a natural ventilation greenhouse that is improved using a non-conventional misting system installed above an added protective roof in the rafters of the greenhouse. More details on this greenhouse design can be found in Chapters 4 and 5. The environment of the research greenhouse bay was controlled to provide artificially high temperature field conditions, and the NVAC greenhouse misting system was activated to provide the NVAC system conditions. Twelve four-week-old bell pepper plants (*Capsicum annuum* var. Bell Boy) were transplanted into the NVAC greenhouse on June 20, 2016 into 5-gal containers (18.9 L) (2000 Series, 5-gallon, 11 7/8" top diameter, 11" height, International Greenhouse Company, Danville, IL) with commercial peat mix (Pro-Mix BX, Premier Horticulture Inc., Rivière-du-Loup, QC, Canada), and were daily irrigated and fertilized with full-strength Hoagland's nutrient solution (Hoagland & Arnon, 1950). Before conducting experiments and in between experiments, the plants were grown with a photoperiod of 16 h at 26 °C and a dark period of 8 h at 20 °C. Irradiance was 350 $\mu mol \cdot m^{-2} \cdot s^{-1}$ and daytime relative humidity was 60%.

Transpiration, photosynthesis and fluorescence experiments, were simultaneously conducted under both high temperature conditions (Figure 30) and NVAC greenhouse conditions (Figure 31) roughly two months after transplanting (August 2016), when all plants had flowered and most plants began fruiting. Each experiment was repeated at least three times. During high temperature experiments, greenhouse temperatures were >35 °C but <40 °C from 10:00 HR to 19:00 HR, and relative humidities were >80% before sunrise and dropped <50% after 12:00PM. This resulted in a daytime VPD varying from 0.5 to 3.9 kPa, the maximum being at peak temperature at 14:00 HR. The NVAC greenhouse conditions were the same as the heat stress conditions until 13:00 HR, but temperatures were dropped to <28 °C but >25 °C, and relative humidities were kept >60% but <75% by using the NVAC greenhouse system. The system was used from 13:00 HR to 16:00 HR. This resulted in daytime VPD varying from 0.2 to 3.1 kPa, the maximum being at 13:00 HR, just shy of the activation time of the NVAC system. However, the VPD during the period of use of the NVAC system ranged from 0.9 to 1.3 kPa. The temperatures and relative humidities were brought back to >30 °C and <50%, respectively at 16:00 HR. Each experiment was repeated three times.

Wet-bulb and dry-bulb temperatures were measured at three locations inside the model NVAC greenhouse using aspirated air sensors and recorded using an Agilent 34972A LXI data logger (Keysight Technology Canada Inc. Mississauga, ON). Wet-bulb sensors were fabricated using thermocouples, a distilled water reservoir and wicking cotton. The sensors were made from type-K thermocouple wire (Spectris Canada, Omega Environmental, Laval, QC, Canada) and were placed in an enclosure with fans providing 3 $m \cdot s^{-1}$ air velocity across the thermocouples (Both et al., 2015). The fans were supported by a 12-V power source. The thermocouples were calibrated as recommended by Both et al. (2015). The air velocity was measured using a hot-wire anemometer (TPI 565C1 digital anemometer with hot-wire probe, 0.2 to 20 $m \cdot s^{-1}$ velocity, -20 to 80 °C temperature, Test Products International Inc., Beaverton, OR). Each apparatus was housed in a 6-inch diameter white PVC pipe to shield from solar radiation. Using wet-bulb and dry-bulb temperature data, VPD and relative humidity were calculated according to the method suggested by Snyder and Shaw (1984).

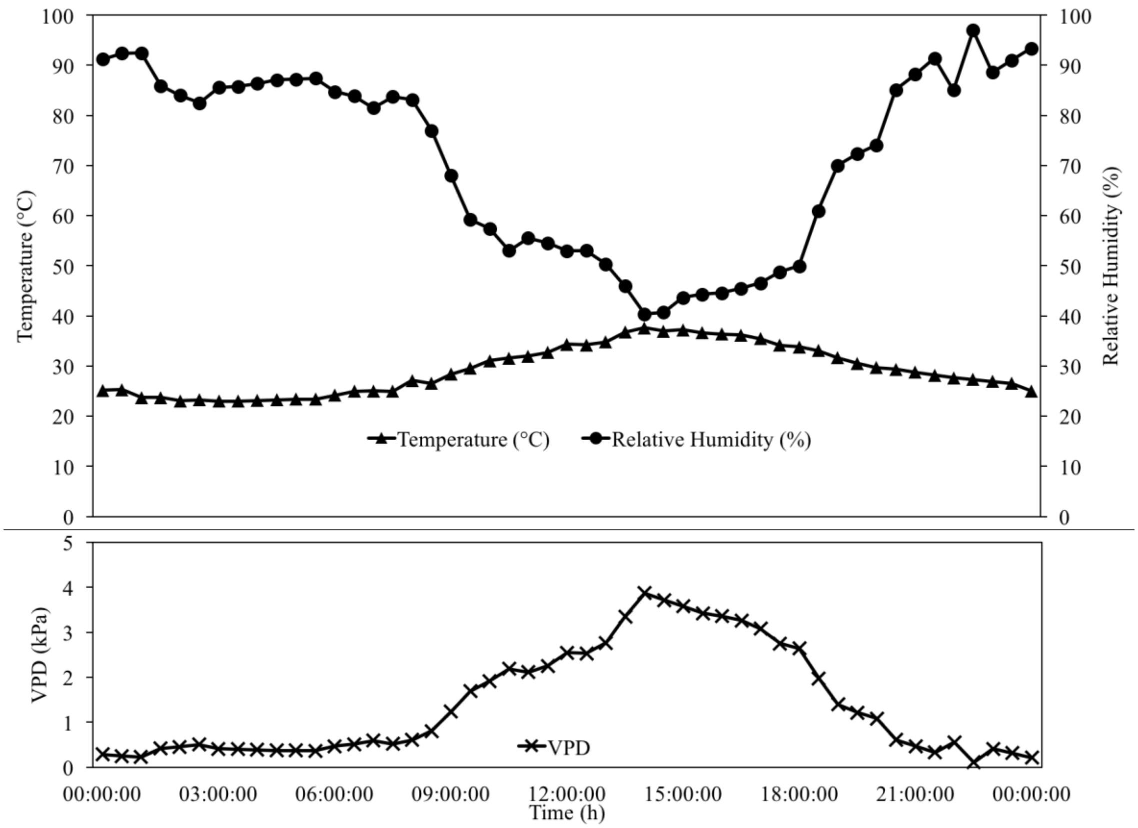

Figure 30. The temperature, relative humidity and vapor pressure deficit (VPD) inside the natural ventilation augmented cooling (NVAC) greenhouse during the high temperature experiments on August 18, 20 and 21, 2016. The data points presented are values averaged over the same 30-min periods on each day.

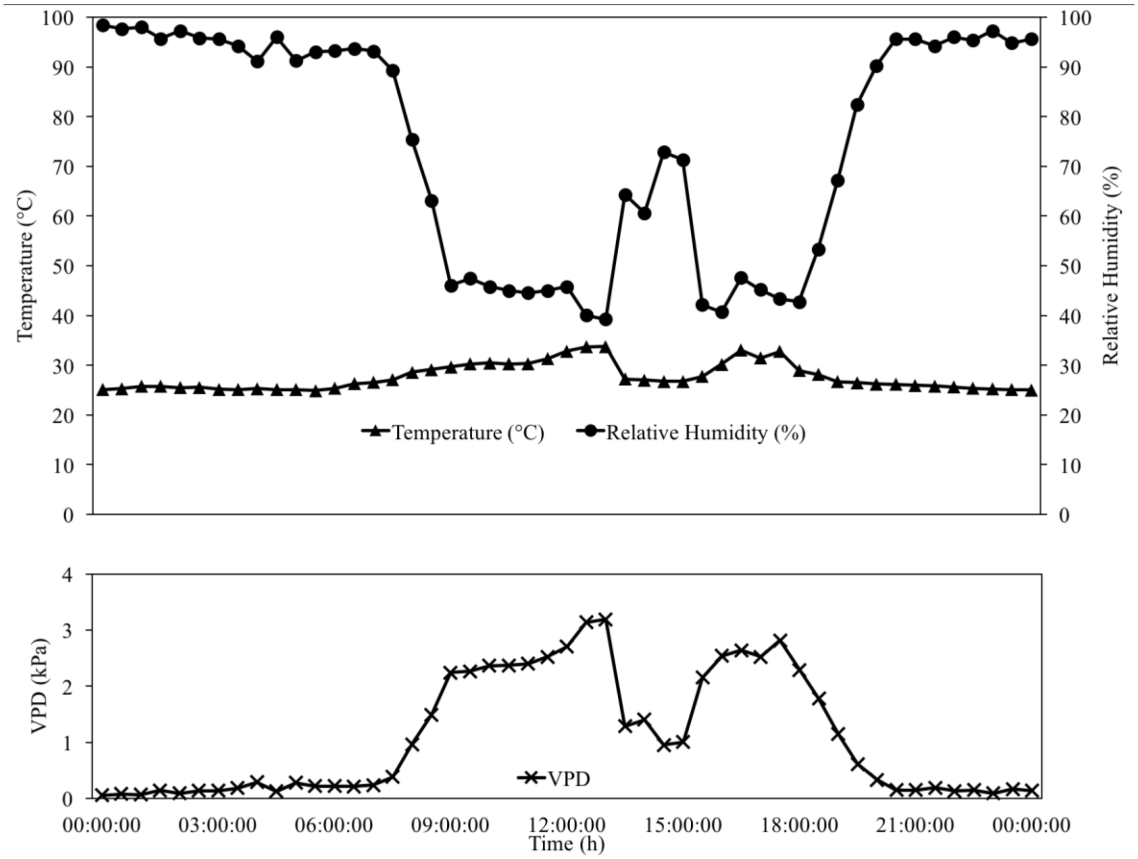

Figure 31. The temperature, relative humidity and vapor pressure deficit (VPD) inside the natural ventilation augmented cooling (NVAC) greenhouse during the NVAC system conditions experiments on August 23, 24 and 25, 2016. The data points presented are values averaged over the same 30-min periods on each day.

Net photosynthetic rate (gas exchange) and chlorophyll fluorescence measurements were taken on three fruiting bell pepper plants using a portable LI-COR Li-6400XT with the 6400-40 Leaf Chamber Fluorometer attachment (LI-COR Inc., Lincoln, NE). Measurements were taken over the same leaf area for each experiment, but different plants were selected for each of the three replicates. Relatively new yet large and well-developed leaves on the top of the plant were selected. Gas-exchange measurements were taken over a period of 30 min. The net photosynthetic rate measurements were taken starting at 11:00 HR, 15:00 HR and 19:00 HR. Measurement averaging on the device was set to 15 s, and measurements were recorded using a LI-COR AutoProgram. The measurement settings on the Li-6400XT were the following: 250 $\mu mol \cdot m^{-2} \cdot s^{-1}$ 50% blue and 50% red light at a block temperature of 25 °C and 60% relative humidity with a flow rate maintained between 100 and 400 µmol·s^{-1}. The LI-COR instrument settings were kept uniform regardless of the greenhouse experimental conditions to study the effect of the greenhouse climate on the plant, rather than the effect of the microclimate inside the LI-COR instrument measurement head. The instrument conditions were the same for the fluorescence measurements, but the leaves were darkened for 20 min before each measurement (Camejo et al., 2005), and measurements were taken at 10:40 HR, 14:40 HR and 18:40 HR, before the beginning of the gas-exchange measurements. The values of minimal fluorescence (F_o) and maximal fluorescence (F_m) from the dark-adapted leaves were determined after the 20-min dark period and were recorded using the LI-COR AutoProgram. Calculations for fluorescence parameters were based on the LI-6400/LI-6400XT Version 6.1 software program (LI- 6400/LI-6400XT 2008). The variable to maximum fluorescence ratio (F_v/F_m) was used to detect stress-induced issues in the photosynthetic apparatus (Baker and Rosenqvist, 2004).

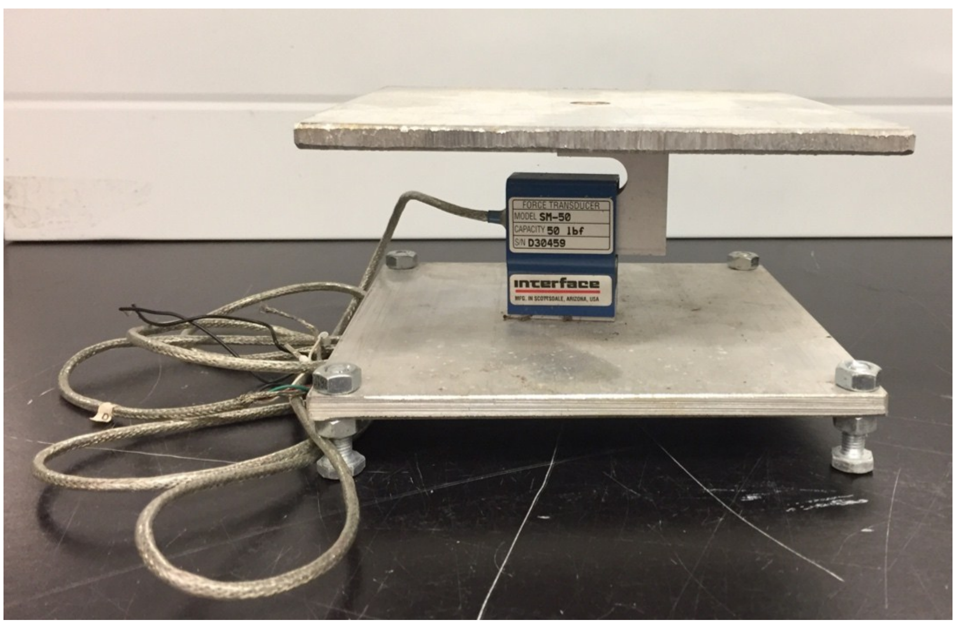

Figure 32. Load cell (SM50 S-Type load cell, Interface, Inc., Scottsdale, AZ) incorporated into aluminum apparatus. Four apparatuses were fabricated to measure changes in plant weight.

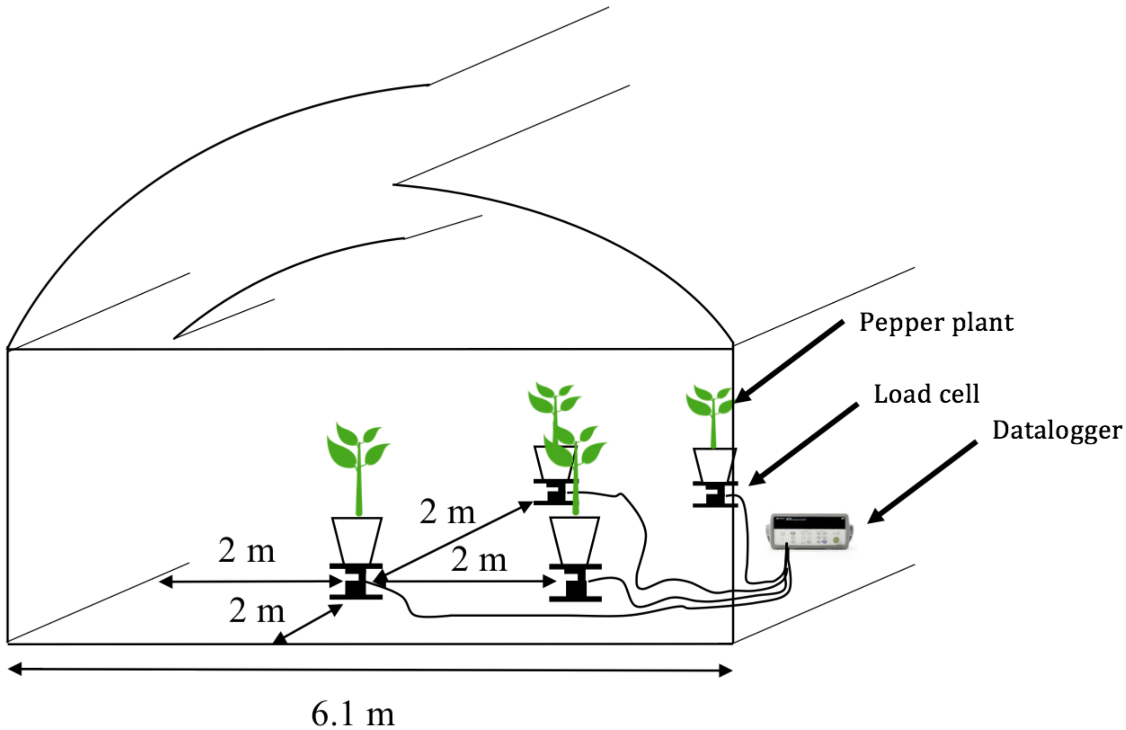

Figure 33. Schematic of the experimental Natural Ventilation Augmented Cooling (NVAC) greenhouse with the layout of the load cell transpiration monitoring apparatus. Four load cells were incorporated into aluminum structures designed to support the containers in which the plants were grown in, and wired to a data logger for measurement recording.

The transpiration of four mature and fruiting bell pepper plants was continuously measured using load cells. Four load cells (SM50 S-Type load cell, Interface Inc. Scottsdale, AZ) were incorporated into aluminum apparatuses (Figure 32) arranged according to Figure 33, from which measurement data was logged using an Agilent 34972A LXI data logger (Keysight Technologies Canada Inc. Mississauga, ON, Canada). The load cells were calibrated using calibration weights (Instron TTB-M TTB-C, Illinois Tool Works Inc., Norwood, MA). The custom-built weighing platforms were positioned 2.0 m from each other and from the sides of the greenhouse. Aluminum structures were designed to support the containers in which the bell pepper plants were being grown in. The load cells monitored the mass change of the plants due to transpirational water loss. During data collection, the containers were each wrapped in white plastic bags (Glad®, The Glad Products Company, Oakland, CA) up to the bottom of the stem of the plants, at which point the bags were closed snuggly but not tight against the stem of the plants using zip-ties (Cable-ties/Zip-ties, white, McMaster-Carr, Aurora, OH). This prevented water loss via evaporation from the surface of the peat in the containers. The bags were removed when experiments were not being conducted. The plants were irrigated before starting each experiment and were not irrigated during the experiments.

6.4 Statistical Analysis

All statistical analyses were done using RStudio version 1.0.143. Net photosynthetic rate (P_n) and variable to maximum fluorescence ratio (F_v/F_m) results are the means of three independent measurements on three different plants in each treatment. The significance of both high temperature stress conditions and of NVAC greenhouse conditions on the plants was analyzed using a *t* test.

6.5 Results

The pepper plants were subject to daytime high temperature stress which was revealed by the data collected on the plant parameters considered in this experiment. Net photosynthetic rate was at its highest at the 11:00 HR measurements (10.5 ± 1.3 μmol·m^{-2}·s^{-1}) compared to the 15:00 HR (7.9 ± 2.1 μmol·m^{-2}·s^{-1}) and 19:00 HR (6.0 ± 2.0 μmol·m^{-2}·s^{-1}) measurements (Figure 34). The same was true with the fluorescence measurements. A depression in F_v/F_m was observed throughout the day. F_v/F_m at 10:40 HR was 0.81 ± 0.009, while the readings at 14:40 HR and 18:40 HR were 0.80 ± 0.016 and 0.79 ± 0.014, respectively (Figure 35). The plant transpiration rate followed a diurnal cycle, being at a minimum overnight and a maximum shortly after 12:00 HR, when the daytime VPD reached a maximum. The transpiration rate surpassed 0.020 g·s^{-1} during the daytime on every test, including the days when the NVAC misting system was used. However, during high temperature experiments, the transpiration rate remained high throughout the afternoon, the peak rate coinciding with peak VPD, and decreased steadily into the evening, eventually reaching the low nighttime rate (Figure 36).

The plants reacted differently to the NVAC greenhouse conditions, compared to high temperature conditions. Again, net photosynthetic rate was at its highest at the earlier 11:00 HR measurements (8.0 ± 1.7 μmol·m^{-2}·s^{-1}). However, the 15:00 HR measurement was greater at 10.2 ± 1.8 μmol·m^{-2}·s^{-1}. When high temperature conditions resumed, measurements were lower than both previous measurements, at 7.8 ± 1.5 μmol·m^{-2}·s^{-1} (19:00 HR measurements) (Figure

34). The same was true with the fluorescence measurements. F_v/F_m at 10:40 HR was 0.80 ± 0.017, while the reading at 14:40 HR was 0.81 ± 0.013. The late reading at 18:40 HR was 0.79 ± 0.014 (Figure 35). No F_v/F_m depression was observed under NVAC greenhouse conditions. The transpiration rate decreased significantly with the use of the NVAC greenhouse misting system, but never to the lowest rates seen overnight (Figure 37). The average transpiration rate across all three experiments during the period when the NVAC misting was active was 0.013 $g{\cdot}s^{-1}$, compared to 0.022 $g{\cdot}s^{-1}$ during the same period on days without the use of the NVAC misting system. This represents a 31% decrease in average transpiration rate over this period.

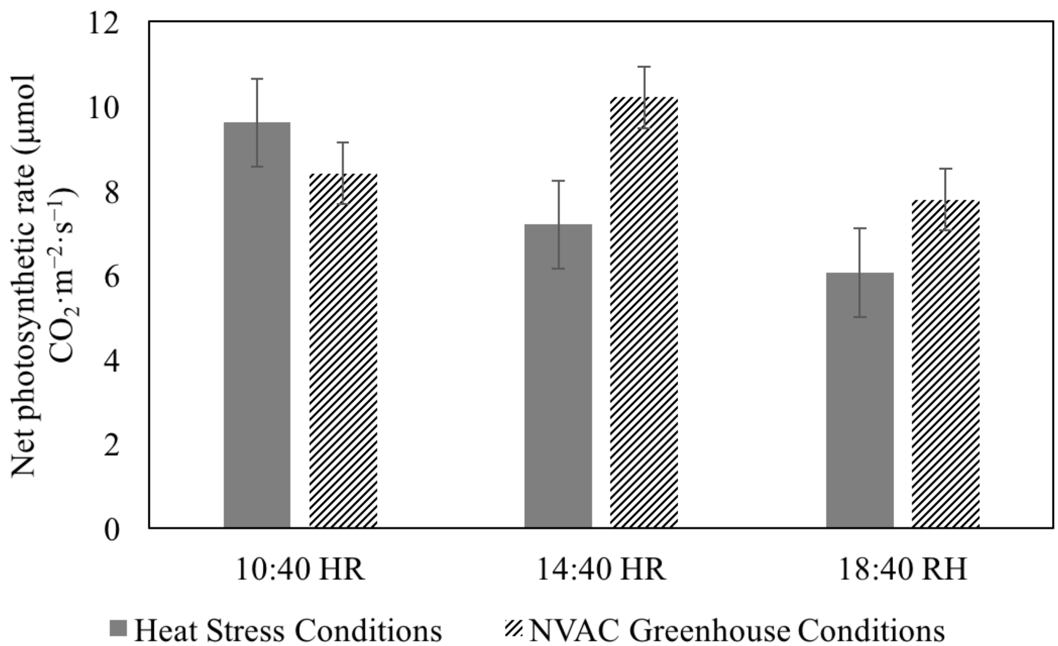

Figure 34. Net photosynthetic rate (μmol $CO_2{\cdot}m^{-2}{\cdot}s^{-1}$) measured over three 30-min periods, each starting at 11:00 HR, 15:00 HR and 19:00 HR, on the same leaf. A different plant was selected for each of the three replicates of the experiment. The photosynthetic rates shown represent the mean value over 30 min of measurements, averaged every 15 s by the LICOR Li-6400XT.

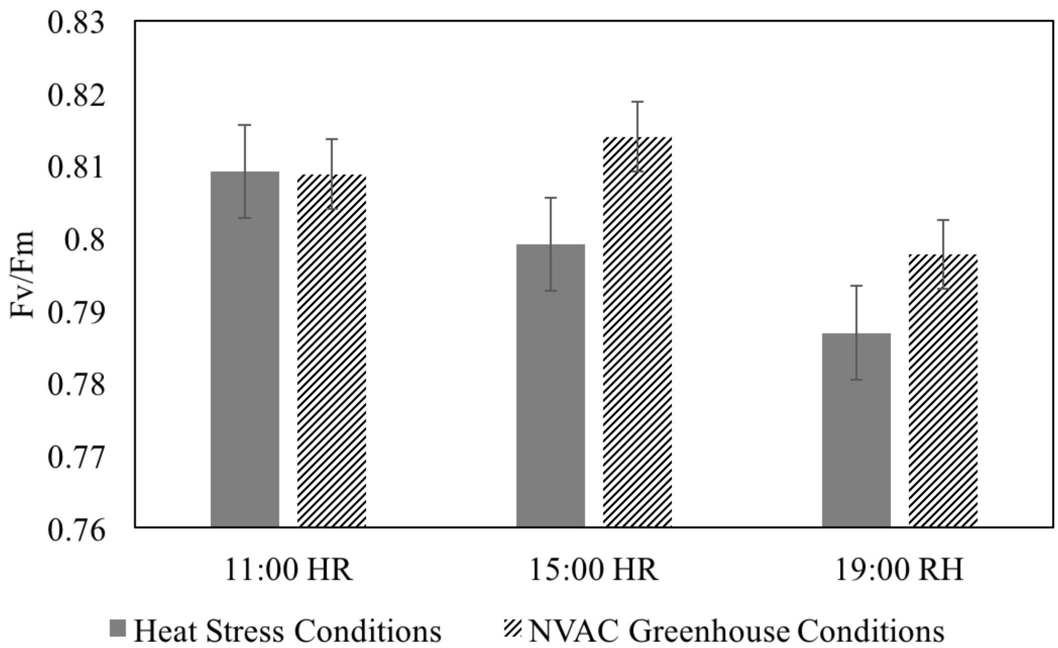

Figure 35. Mean F_v/F_m values measured at 10:40 HR, 14:40 HR and 18:40 HR on the same leaf. Values are the measurements made after leaves were darkened for 20 min. A different plant was selected for each of the three replicates of the experiment.

When considering the change in photosynthetic rate from the 11:00 HR to the 15:00 HR periods, and comparing these changes under the high temperature conditions to the changes under the NVAC greenhouse conditions, it was seen that the use of the NVAC greenhouse misting system allowed for a significant increase in net photosynthetic rate in the plants ($p<0.05$). The same was true when comparing the changes from the 15:00 HR period to the 19:00 HR period under both types of conditions ($p<0.05$). The same analysis was done on the fluorescence readings. It was seen that under the NVAC system conditions, the change in F_v/F_m from the 10:40 HR readings to the 14:40 HR readings was significant, in comparison to the high temperature conditions ($p<0.05$). However, when comparing the 14:40 HR readings to the 19:00 HR readings, the change was not considered significant ($p>0.05$).

The relation between the air VPD and plant transpiration rate showed that transpiration increased linearly with an increase in temperature, decrease in relative humidity and increase in VPD (Figure 38). Under heat stress conditions, the transpiration rate was most tightly related to relative humidity ($R^2 = 0.87$), although it was also related to temperature ($R^2 = 0.76$) and VPD

(R^2 = 0.86) (Figure 38a). Under NVAC conditions, the transpiration rate was most tightly related to VPD (R^2 = 0.86), but it was also related to temperature (R^2 = 0.81) and relative humidity (R^2 = 0.85) (Figure 38b). Medrano et al. (2003) demonstrated similar linear relations between the leaf transpiration rate and VPD for tomato plants grown in a Mediterranean climate with similar VPD ranges. Sase et al. (2007) showed similar results in tomato plants grown under cooler conditions and lower VPD. When comparing the VPD profile of the NVAC greenhouse conditions (Figure 31) and the transpiration rate profile of the plants under the NVAC conditions (Figure 37), it is clear that the decrease in canopy transpiration rate was driven by the decrease in temperature, increase in relative humidity, and decrease in air VPD.

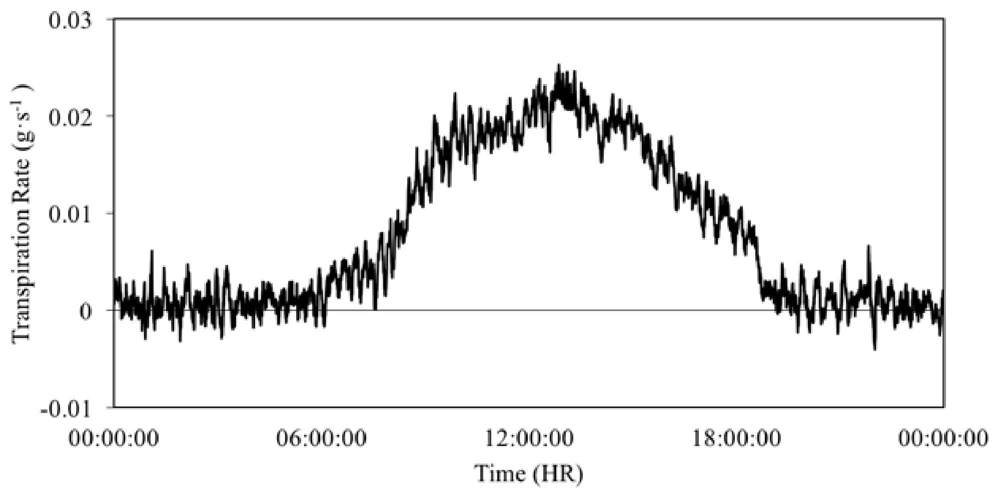

Figure 36. Average pepper plant transpiration rate in g·s^{-1}.

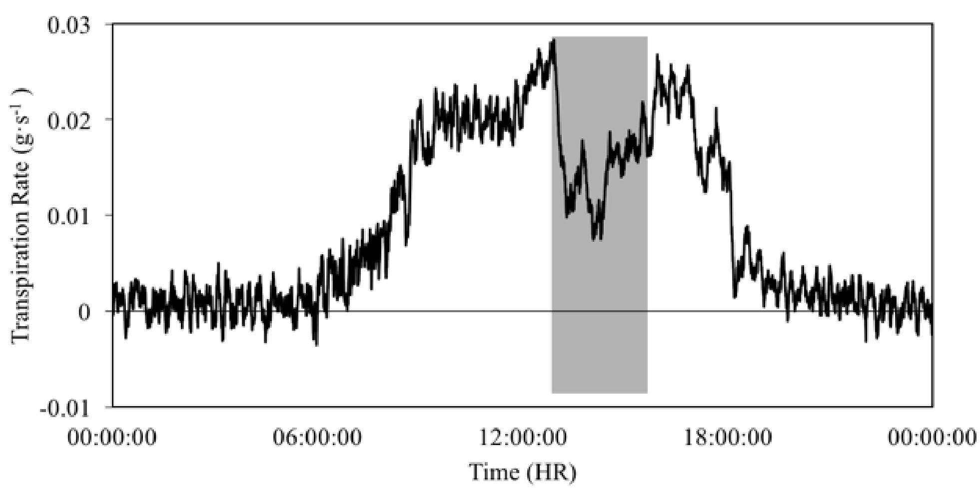

Figure 37. Average pepper plant transpiration rate in g·s^{-1}. Shaded areas are times when the NVAC greenhouse misting system was active.

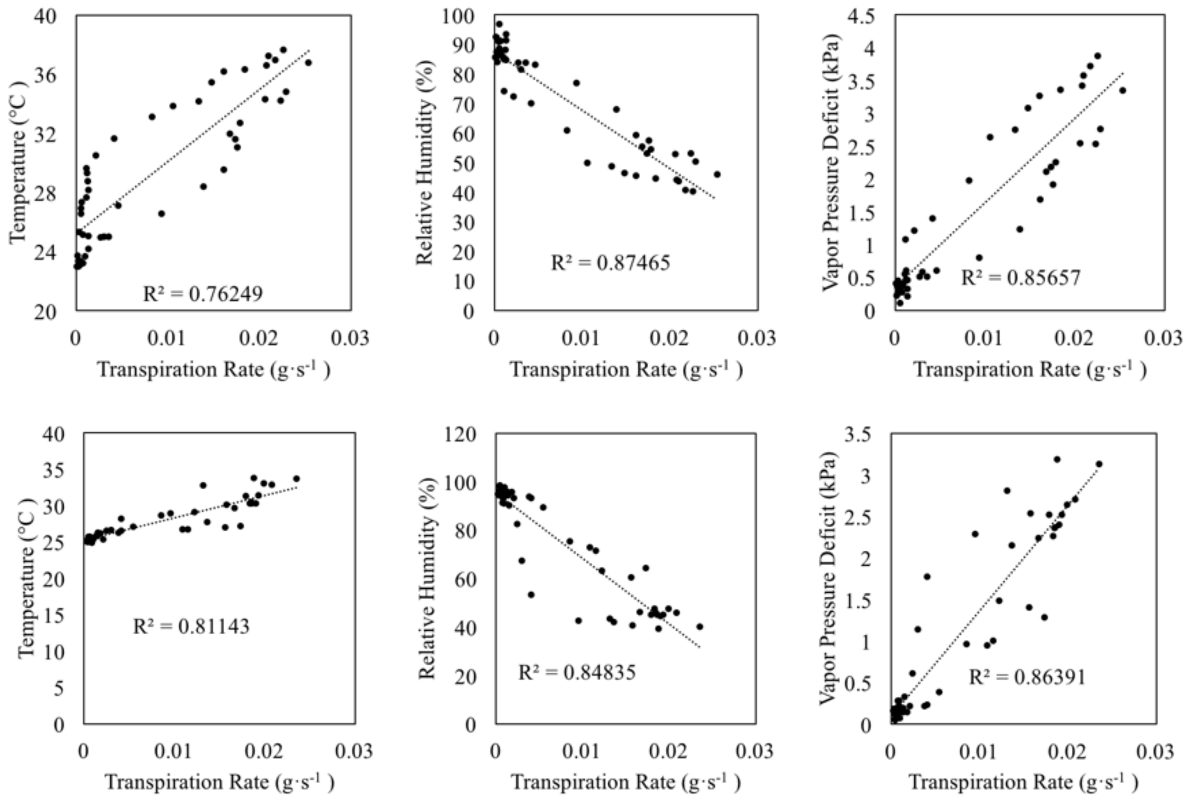

(a)

(b)

Figure 38. Relationship between the 30-min average temperature, relative humidity and VPD values, and plant transpiration rate under (a) heat stress conditions and (b) NVAC conditions.

6.6 Discussion

Our study demonstrated that the daytime conditions provided by the NVAC greenhouse improved photosynthesis and chlorophyll fluorescence in bell pepper plants, compared to high temperature stress conditions. From our results, the pepper plants were less stressed under the NVAC greenhouse conditions. Erickson and Markhart (2001) studied 'Ace' and 'Bell Boy' bell pepper plants at high temperatures. They found that the deleterious effects of high temperature, notably low fruit set, on pepper fruit set were not due to temperature induced water stress, but rather to direct temperature responses. Their gas exchange measurements showed that the photosynthetic rate increased in response to temperature, from 25 to 33 °C. They concluded that VPD was not a factor in affecting fruit set. It is important to note that our high temperature stresses involved higher temperatures and higher VPDs than in Erickson and Markhart (2001).

Our results compare well to those reported by Niu and Rodiguez (2006) on ornamental ‘Black Pearl’ pepper. They showed that leaf net photosynthetic rate of ornamental pepper declined as leaf temperature increased from 20 to 40 °C. They reported a depression in F_v/F_m over the course of the afternoon when pepper plants were subject to high temperatures nearing 40 °C. Based on our findings, the temperatures that lie in the range of 33 to 40 °C, and perhaps beyond, become critical to the vegetative growth of the plant, affecting net photosynthetic rate and chlorophyll fluorescence.

In studies on tomato (*Lycopersicon esculentum* Mill.), Sato et al. (2000) and Peet et al. (1997), showed that a moderate increase of average temperature never surpassing 32 °C did not affect photosynthesis, night respiration and vegetative growth, but impaired reproductive development such as fruit set. However, the work of Wahid et al. (2007) showed that when the ambient temperature exceeds 35 °C, tomato seed germination, seedling and vegetative growth, flowering and fruit set, and fruit ripening are all adversely affected.

It is therefore clear that greenhouse cooling, such as that provided by the NVAC greenhouse, can be critical for adequate cultivation in warm climates or during warm seasons of other climates. In the experiments herein, the NVAC system kept greenhouse temperatures well below 28 °C which reduced plant stress through improved photosynthesis compared to high temperature conditions.

During our experiments, plant transpiration increased throughout the day as temperature increased, and these results compare well with those presented by Niu and Rodiguez (2006). Transpiration and evaporation from plant leaves allow plants to cool themselves under high temperature conditions (Yang et al., 1990), induced either through elevated air temperatures or high solar radiation. Besides high temperatures, high VPD results in increased evaporation and transpiration from leaf surfaces (Larcher, 1995) which can result in plant water deficits (Erickson & Markhart, 2001). This can eventually induce leaf water stress when the uptake of water through the root system is inadequate to cope with high transpiration rates (Grange & Hand, 1987). According to Tibbitts (2012), even a slight increase in VPD from 1 to 1.8 kPa can cause a major reduction in plant growth on several crops. In fact, if the VPD creates a water deficit within the plant, the stomata can close reducing stomatal conductance (Grange & Hand, 1987), and the leaf water potential can decrease resulting in decreased photosynthesis (Nilsen & Orcutt, 1996; Xu et al., 1991). Under such conditions, improving the greenhouse climate by decreasing temperatures and increasing humidity (improved VPD conditions), using an evaporative cooling method such as the NVAC system can be beneficial. Our results show that the NVAC greenhouse can limit plant transpiration without eliminating it altogether, and this can be beneficial considering the aforementioned circumstances. Furthermore, even under moderate humidity conditions, increasing greenhouse humidity may be desirable to generate root pressure to avoid calcium deficiency in fruit or young leaves, or in the propagation of plants from leafy cuttings or in tissue culture (Grange & Hand, 1987).

Another potential application of the NVAC greenhouse design is revealed in saline cultivation. Irrigation water salinity has become a severe agricultural problem in many parts of the world (Ling Li, 2001), including the greenhouse-intensive Mediterranean coastal areas (Cuartero & Fernández-Muñoz, 1998). It has been reported that a more humid greenhouse climate may help control the effect of salinity (Sonneveld, 1988), thus improving greenhouse culture in certain regions of the world. Results by Montero (2006) show that high humidity through high-pressure greenhouse fogging improved yield in bell pepper by 14.0%. Fruit quality was improved by high humidity by greatly reducing blossom end rot compared to non-fogged conditions. Similarly, Romero-Aranda et al. (2002) reported positive results on the use of intermittent misting on greenhouse grown tomato plants in saline and non-saline conditions. In the misted treatment, air VPD was maintained at below 1.5 kPa, while in the non-misted treatment VPD was as high as 3.5 kPa at noon, with a maximum air temperature of 36 °C; conditions very similar to our experiment. In both salinized and non-salinized plants, leaf water potential, leaf turgor, total plant leaf area, dry matter and yield were all dramatically increased using the misting system. In the salinized plants, net photosynthetic rate was four times higher with the use of the misting system. They concluded that misted plants increased instantaneous water use efficiency by 84 to 100% compared to non-misted plants. Under such circumstances, the NVAC greenhouse can be an excellent design choice for increasing humidity and for providing cooling, at a reduced electricity and water cost compared to typical evaporative cooling systems such as pad and fan systems (Chapter 4). Furthermore, the NVAC greenhouse design protects the crop from direct contact by the fog or mist water droplets, thus providing the advantages of these evaporative cooling systems without the potential disease drawbacks of foliage wetting. Investigation into the use of the NVAC greenhouse for saline cultivation would be relevant future research.

Finally, from previous work on the novel greenhouse design, it was shown that the NVAC system provides air movement in addition to cooling and an increase in humidity (McCartney, 2017). Sabeh (2007) found that plant transpiration generally increased with increasing ventilation rate, though not necessarily with significant differences. This is because plant transpiration responds most directly to differences in temperature, relative humidity and ultimately VPD produced by the different ventilation rates, rather than the ventilation rates themselves (Prenger et al., 2002; Urban & Langelez, 2002; Jolliet & Bailey, 1992). The NVAC system provides improved air movement under natural ventilation conditions, but not in a manner that can further drive high transpiration rates, such as seen in forced ventilation systems. Rather, the added air currents provided by the NVAC greenhouse design are cooler and higher in humidity than the ambient greenhouse air, and therefore through improved VPD conditions, limit plant transpiration and reduce plant stress.

6.7 Acknowledgements

The authors would like to gratefully acknowledge help and support from Ms. Lara Hendry, undergraduate student in the Department of Bioresource Engineering at McGill University, Mr. Bo-Sen Wu, laboratory colleague and Ph.D. candidate in the Department of Bioresource Engineering, and Mr. Yvan Gariépy, research engineer in the Department of Bioresource Engineering.

Connecting Text

Chapter 7, *Measurement of diurnal fruit growth patterns in tomato using machine vision* was authored by Lucas McCartney and Mark. G. Lefsrud. To be submitted to the journal *Computers and Electronics in Agriculture*.

From field experience in the greenhouses in Barbados, and following the study of plant response to the NVAC greenhouse, it became apparent that the NVAC greenhouse provided an improved environment for the fruiting of greenhouse crops. Like plant responses, there are a multitude of methodologies used to measure and quantify fruit growth, yield and quality. From a survey of literature on the study of fruit growth in greenhouse crops, it came to our attention that the improved greenhouse climate provided by the NVAC system may have a significant impact on the diurnal fruit growth of certain fruit bearing crops. Although plant stress in pepper was studied in Chapter 6, tomato fruit (*Solanum lycopersicum*), a fruit sensitive to changes in plant water status with its large water content, was selected for this study. Moreover, literature on diurnal fruit growth mostly considers tomato fruit. An inexpensive and highly sensitive non-invasive and non-contact method of measuring real-time fruit growth was developed using machine vision. The script used for the image capturing, processing and data saving is provided in full in Appendix D. The precision of the response in the imaging method differs from the known linear voltage displacement (LVDT) method commonly used. The LVDT method involves clamping the device to the fruit and typically shows a response lag that is depend on the mechanics of the instruments. In order to validate the use of the imaging method, it was compared to the LVDT measurement method by running the experiments with both methodologies.

7. Chapter 7: Measurement of Diurnal Fruit Growth Patterns in Tomato Using Machine Vision

Lucas McCartney and Mark G. Lefsrud

Additional Word Index. Image thresholding; blob detection; blob measurement; linear voltage displacement transducer

7.1 Abstract

A fruit growth monitoring device was developed that makes use of automated red-green-blue (RGB) imaging with an inexpensive camera and MATLAB® processing. The image capture rate was variable, allowing for real-time and diurnal measurement of the fruit. To test the monitoring system, tomato fruit (*Solanum lycopersicum* var. Beefsteak) was analyzed using fruit area, diameter and perimeter measurements that were time-stamped and logged. This method of fruit growth measurement is comparable to the known linear voltage displacement transducer (LVDT) method, but does not require contact with the fruit. Therefore, this machine vision imaging method offered faster response and better precision when compared to the LVDT method. Both methodologies revealed responses to climate parameters including temperature, relative humidity, vapor pressure deficit (VPD) and solar radiation. The imaging methodology showed greater precision and could measure subtle changes in the tomato fruit that could not be measured by the LVDT method, allowing for monitoring of the irrigation schedule via the fruit.

7.2 Introduction

For better control of the environment in a greenhouse, the dynamics of both the greenhouse and the plants must be considered. Greenhouse climate parameters such as air temperature, humidity and light are easily measured and controlled using sensors placed within the plant space (Kacira et al., 2005). However, this is often inaccurate as the physical conditions surrounding the plants can vary differently per greenhouse area and can be different than the non-plant areas (Jones, 2013). Kittas et al. (2003) and López et al. (2012) have demonstrated that the climate across the greenhouse can be heterogeneous even with forced ventilation. The concept of plant response-based sensing can be valuable to provide a better understanding of the interactions between the greenhouse climate and the physical conditions of the plants (Kacira et al., 2005; Katsoulas et al., 2016). Current methods, such as measurement of soil water tension, leaf water potential, sap flow, and fruit diameter, have been widely used to assess plant and fruit water status (Wang & Gartung, 2010). However, these measurements require contact with the plant or destructive sampling, and often involve lag periods between initiation of plant stress, measurement and receipt of the required information (Johnson et al., 1992).

Noninvasive and nondestructive methods facilitate the study of the characteristics of fruits and plants without affecting their natural growth (Gastélum-Barrios et al., 2011). Considerable research has focused on the development of nondestructive and noninvasive techniques for measuring the quality attributes of fruits (Gómez et al., 2006). Sensing techniques through machine vision can continuously monitor plants and enable automated sensing and control capabilities (Ling et al., 1996). An assessment of uses, advantages and disadvantages of various sensors applied to automated crop monitoring is presented in Ehret et al. (2001). Image acquiring and analysis can be used to extract a vast amount of information from plants such as morphological (size, shape, texture), spectral (color, temperature, moisture), and temporal data (growth rate, development, dynamic change of spectral and morphological states) without contact with the fruit or plant (Story and Kacira, 2015). Previous efforts in machine vision and sensing have been successful in determining plant status by monitoring a single leaf (Seginer et al., 1992; Meyer et al., 1992; Shimizu and Heins, 1995), a whole plant (Hetzonri et al., 1994; Kacira et al., 2002), or a crop canopy (Sun et al., 2016; Story & Kacira, 2015). For example, Story et al. (2010) used machine vision for early detection of calcium deficiency in lettuce (*Lactuca sativa* cv. Buttercrunch). Machine vision and image analysis has been used to measure fruit characteristics such as color or volume. However, there is limited literature on machine vision used for fruit growth measurement and pattern detection. Monitoring fruit growth can help in predicting yield and assessing optimal levels of fertilization and irrigation (Koc, 2007). Koc (2007) used imaging and ellipsoid approximation and image processing to determine the final volume of harvested watermelon fruit (*Citrullus lanatus*). Choi et al. (1995) used RGB and hue, saturation, and intensity (HIS) values to identify six classes of tomato maturation. Hatou et al. (1994) used a two-camera video imaging system to analyze the growth rate, shape and color of greenhouse tomatoes. The system was able to detect the early stages of blossom end rot in the fruit, but results relating to growth rate with respect to water status or greenhouse climate were not studied.

Considering the existing relationship between diurnal fruit growth rate, greenhouse climate conditions and plant water relations, such as presented by Pearce et al. (1993a,b), Johnson et al. (1992) and Guichard et al. (2005), a device using imaging for continuous and automatic fruit growth measurement can provide valuable information in terms of overall plant health, plant stress, fruit yield and fruit quality. In their work, LVDTs were used to measure tomato fruit diameter in response to a variety of climate and irrigation conditions. Although valuable data was obtained from these devices, certain mechanical limitations influence the measurements. The arrangement of the LVDT apparatus must be carefully placed to clamp the fruit at its largest diameter. Determining the largest diameter is difficult to precisely accomplish and has to be visually approximated. Once in place, the fruit must counteract the holding force of the LVDT for the device to record any change. Therefore, although the fruit may in fact be continuously growing or swelling from water influx, the force of this growth may not be sufficient to be measured by the LVDT. The fruit may also contract throughout the day, and LVDTs can lag mechanically in response to fruit shrinkage (Johnson et al., 1992). In the present work, the fruit is not handled in any way and growth is monitored remotely through a camera to determine fruit area, perimeter and diameter measurements.

7.3 Methods and Materials

7.3.1 Apparatus

Machine vision was accomplished using a USB connected camera (Logitech Webcam HD Pro C920, Logitech® Inc., Newark, CA). The camera and a light source (5.5 W soft white LED 9290012036, Philips Lighting Canada Ltd., Markham, ON, Canada) were mounted onto one open end of an opaque polyvinyl chloride (PVC) cylinder 8 inches in diameter and 12 inches long (Figure 39). The light source, placed adjacent to the camera, was covered in a double layer of Kimwipes™ (KC34133, 11.8 x 11.8 inch, Kimberly-Clark™ Professional, Irving, TX) to provide diffuse light. The bottom half of the inside of the cylinder was covered in reflective aluminum foil to provide a shadowless environment. This apparatus blocked ambient greenhouse light and sunlight from reaching the studied fruit, but provided an unchanging light source. The other open end of the PVC cylinder was covered with a double layer of blue felt (Premiumfelt, Mold, Mildew, and Odor Resistant, 678 Royal Blue, Kunin Group, Hampton, NH). Offset slits down the middle of each felt piece allowed the fruit to be inserted into the cylinder with the stem protruding, while still blocking ambient light entry. 8-in hose-clamps fastened the felt and kept it taught. A universal stand with clamps held the light-blocking cylinder, camera and light source in place (Figure 39). An overreaching clamp fastened to the universal stand held the tomato fruit stem in place using a cable tie (zip-tie), affixed snuggly but not tight. This prevented movement of the fruit due to environmental disturbances unrelated to the experiments, or to human disturbances. Once a selected tomato fruit was inserted and the camera and light positions were adjusted, the remaining openings of the apparatus were covered in felt to block ambient light entry into the cylinder.

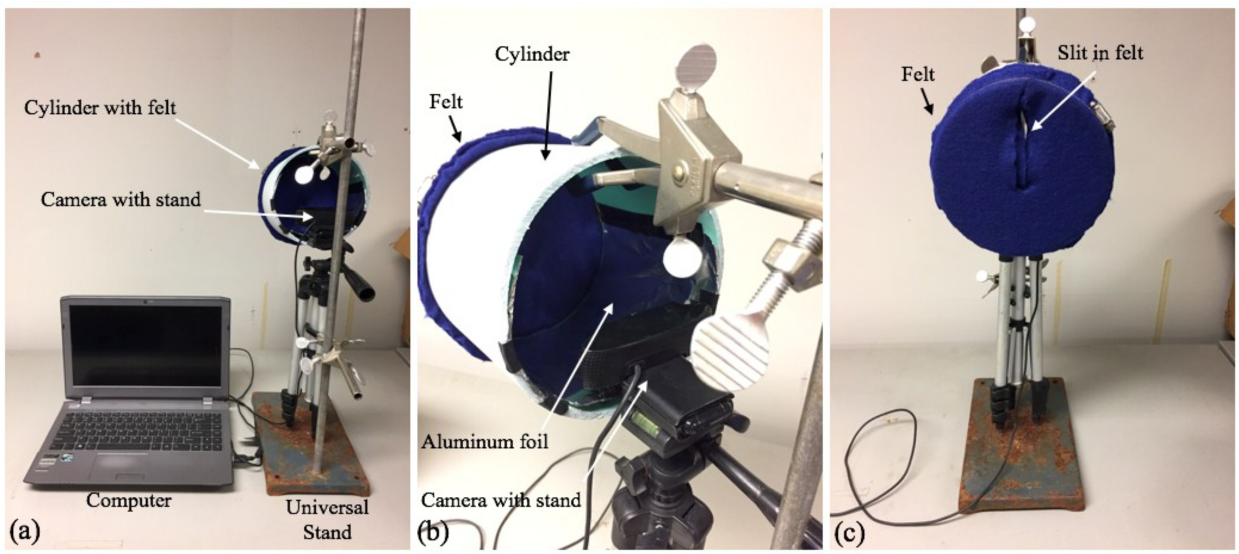

Figure 39. Device setup used for machine vision. In (a) an overview of the universal stand holding the components of the device together, with the computer for image capture, analysis and recording of data; in (b) a close-up of the cylinder showing the felt and the reflective aluminum foil inside the cylinder; and in (c) a front view of the device showing the slit in the double layer of felt to allow the tomato fruit to be inserted. The light source is not shown but would be placed adjacent to the camera.

A separate apparatus was assembled to mechanically measure the diameter of the tomato fruit. A Mitutoyo IDU25E digital indicator with a spring-loaded displacement sensor (resolution ± 0.0005”, Mitutoyo Corporation; Takatsu-ku, Kawasaki, Kanagawa, Japan) was appended to an aluminum frame. The rounded tip of the digital indicator was replaced by a flat aluminum plate.

A universal stand was utilized to hold the components of the apparatus together and onto the tomatoes. The resulting apparatus imitated the linear voltage displacement transducer systems used in previous work by Johnson et al. (1992) and Pearce et al. (1993a,b).

7.3.2 Image Acquisition and Processing

The camera settings were first manually adjusted and saved using the Logitech® Webcam Software (Version 2.40 Build 13.40.845, Logitech® Inc.) to suit the particular appearance of each tomato fruit. The manually set settings included image brightness, contrast, gain, backlight compensation, saturation and exposure. Subsequently, white balance, resolution, focus and zoom settings were overridden and set in the program script. Image processing was accomplished with a MATLAB® (MATLAB® R2017a, The MathWorks Inc., Natick, MA) script and the MATLAB® Image Processing Toolbox. RGB digital images were acquired by the camera at a resolution of 1024 × 576 pixels and temporarily saved in a PNG file format. The images were converted to HSV images. An HSV analysis revealed the respective pixel counts of hue, saturation and value and each was displayed in histograms. This step allowed for preliminary testing in order for the user to manually set the correct thresholds for the ensuing steps of the analysis. In this experiment, with green tomato fruit, the MATLAB® high and low thresholds for hue were from 0 to 0.3, for saturation were 0 to 0.7 and for value were from 0 to 0.8. It was seen that the main threshold of importance was hue, as the peak for green differs from the background blue peak (Figure 40). Including saturation and value thresholding was nonetheless required to account for brighter, darker or other color spots on the tomato fruit. Mature tomato fruit or other fruit of varying colors may require other combinations of hue, saturation and value thresholding. From the hue masked image, small objects seen in the image both in the tomato and in the background (small objects set to <500 pixels) were removed using the *bwareaopen* function. The border of the tomato was then smoothed using the *strel* disk morphological structuring element function. The area in the image representing the tomato was then filled using the *imfill* function based on the overriding assumption that this area fits in the HSV threshold values. This is necessary because even with ideal lighting, a certain amount of glare occurs on the tomato surface and renders the image of the tomato seen by the machine vision to be heterogeneous in HSV value where the brightest spots are. This may not be immediately obvious to the human eye. The masked bands from the various steps of the analysis were concatenated using the *cat* function and the RGB image was recreated with only the tomato fruit visible for the user to visually inspect. Once the processed image, showing just the tomato fruit, meets the users' definition criteria, the image file was processed for further analysis for measurement.

7.3.3 Image Analysis for Measurement

The processed image showing only the tomato fruit with a black background was converted to grayscale for measurement using the *rgb2gray* function. A normalized threshold of 0.4 was implemented to select the pixel area of the tomato in the image and ignore the black background. Another *imfill* hole filling step was used to remove any stray pixels in the image. At this point, the image of the tomato was processed as a blob for measurement. The *regionprops* function was used to extract the area (*PixelIdList*) and perimeter of the blob, in pixels. The equivalent circular diameter (ECD) of the blob, in pixels, was computed from the area output. In the event that multiple blobs were analyzed, the script ignored any data points beyond the largest blob. The area, perimeter and diameter data along with a time stamp were stored and the original and processed images were deleted. *tic* and *pause* functions were used to control the image acquisition rate. The number of iterations was set by the user prior to initiation of the image acquisition. Once the number of iterations was reached, the data was exported and saved as a Microsoft Excel .xlsx file. Image acquisition in the experiments herein was performed from midnight to midnight, at 30-second intervals, over the course of three days. Figure 40 illustrates the image capture, processing and analysis in logical steps and provides example images. For more detail, the MATLAB® scripts are provided in its entirety in Appendix D.

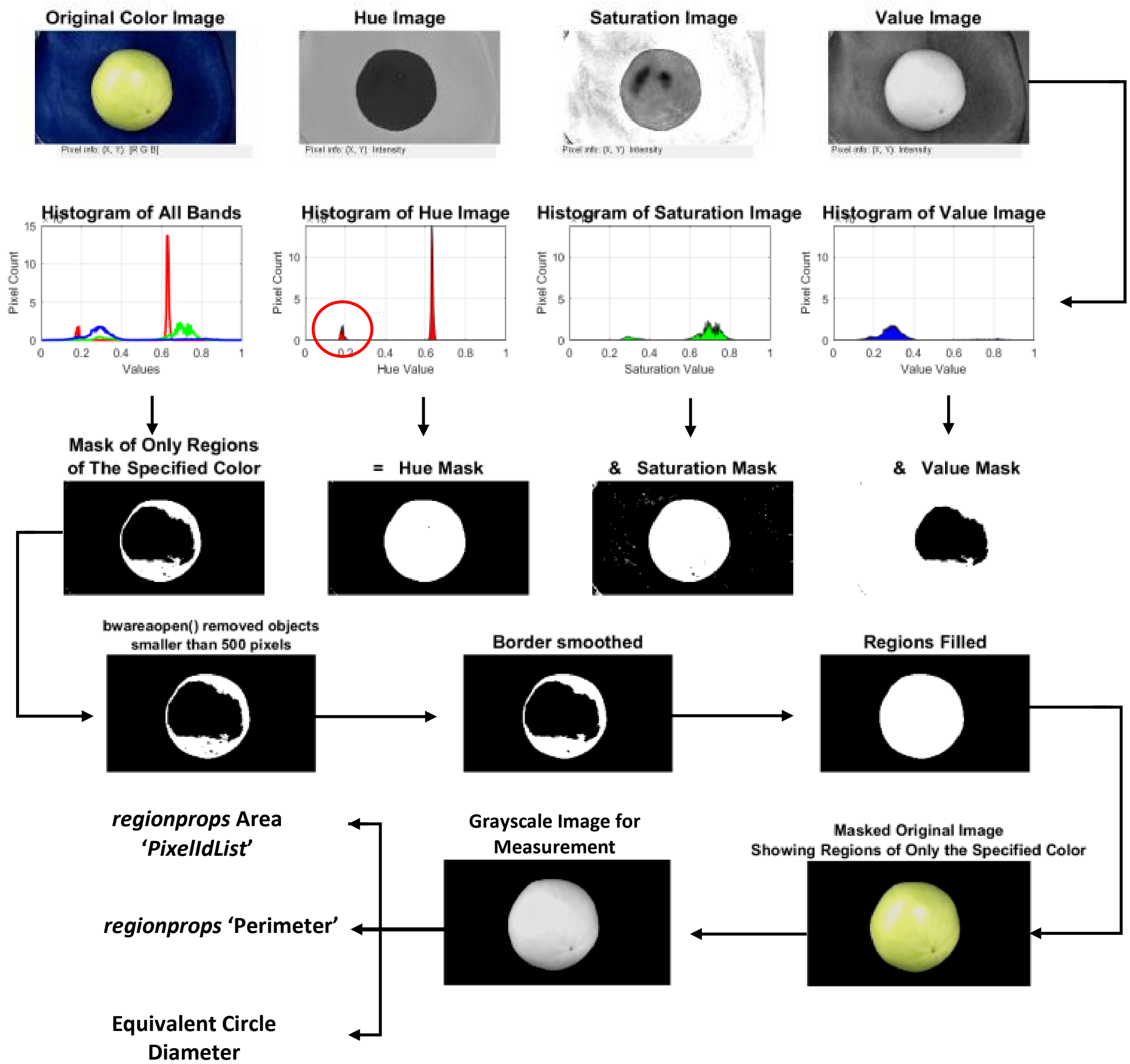

Figure 40. Flow diagram of the image capture, processing and analysis for fruit measurements done in MATLAB®. The original image is first broken down into hue, saturation and value images from which the user can set thresholding levels. With the resulting masks from the thresholding, the area of the image representing the fruit is kept. Any small areas in the image that are not related to the image of the fruit are removed and the border of the fruit is smoothed. The image of the fruit is filled and the original image of solely the fruit is reapplied. Finally, the image of the fruit is converted to grayscale for measurements of area, perimeter and calculation of diameter.

7.3.4 Experimental Conditions

Experiments were conducted in June and July of 2017 in a research greenhouse at the McGill University Macdonald Campus Research Greenhouses in Ste-Anne-de-Bellevue, QC, Canada. 25 'Beefsteak' tomato plants were germinated in 1.5-inch by 1.5-inch rockwool cubes (A-Ok Starter Plugs™, The ROCKWOOL Group, Hedehusene, Denmark) in a Conviron growth chamber (Controlled Environments Inc., Winnipeg, MB, Canada). Eight tomato plants were then grown to maturity in 4-inch by 4-inch rockwool cubes (Grodan cubes, The ROCKWOOL Group) in a nutrient-film technique (NFT) hydroponic system in the research greenhouse. A twine and tomato clip trellis system held the mature plants in place. The plants were irrigated and fertilized with full-strength Hoagland's nutrient solution (Hoagland & Arnon, 1950). The irrigation schedule provided 30 min of irrigation every 2 h. The greenhouse climate settings were set to 26 °C and 60% relative humidity daytime and 23 °C and 60% relative humidity nighttime. The photoperiod was set to 16 h, 6:00 HR to 22:00 HR, with high-pressure sodium (HPS) supplemental lighting. Once the plants were fruiting and during experiments, the greenhouse climate was altered to study the tomato fruit under varying conditions. Three different ranges of climate conditions were imposed on the tomato plants and the resulting diurnal fruit growth was measured using both the imaging methodology and the LVDT methodology. The experiments were repeated until three consecutive days of data were obtained under similar greenhouse climate conditions (Figures 41 and 42). For both the imaging and LVDT experiments, randomly chosen unripe tomato fruit of at least 4 cm in diameter were selected on healthy plants containing at least 2 other fruit, but no more than 4 other fruit. Experiments on the fruit were stopped when the fruit began to ripen i.e. when the image analysis detected hue consisting of mostly red bands as opposed to mostly green bands.

The climate parameters inside the greenhouse were recorded using a data logger (HOBO U30 USB Data Logger U30-NRC, Onset Computer Corp., Bourne, MA) with temperature, relative humidity and solar radiation sensors calibrated as recommended by Both et al. (2015). The logged data was time stamped. Temperature and relative humidity sensors were placed 1.5 m above the root zone of the tomato plants, whereas PAR sensors were placed atop the plant canopy. The temperature sensors (S-TMB-M006, Onset Computer Corp.) provided $< \pm 0.2$ °C total accuracy and resolution of $< \pm 0.03$ °C, over the range of 0 to 50 °C. The humidity sensors (S-THB-M008, Onset Computer Corp.) provided an accuracy and resolution of ± 2.5% from

10% to 90% relative humidity and 0.1% relative humidity at 25 °C, and below 10% and above 90%, ±5%. The temperature and relative humidity sensors were shielded using perforated white Styrofoam cups or solar radiation shields (RS3 Solar Radiation Shield, Onset Computer Corp.). The photosynthetically active radiation (PAR) (S-LIA-M003, Onset Computer Corp.) sensors had an accuracy of ± 5 $\mu mol \cdot m^{-2} \cdot s^{-1}$, and a resolution of 2.5 $\mu mol \cdot m^{-2} \cdot s^{-1}$, with an additional temperature-induced error ±0.75 $\mu mol \cdot m^{-2} \cdot s^{-1}$ $°C^{-1}$ from 25 °C.

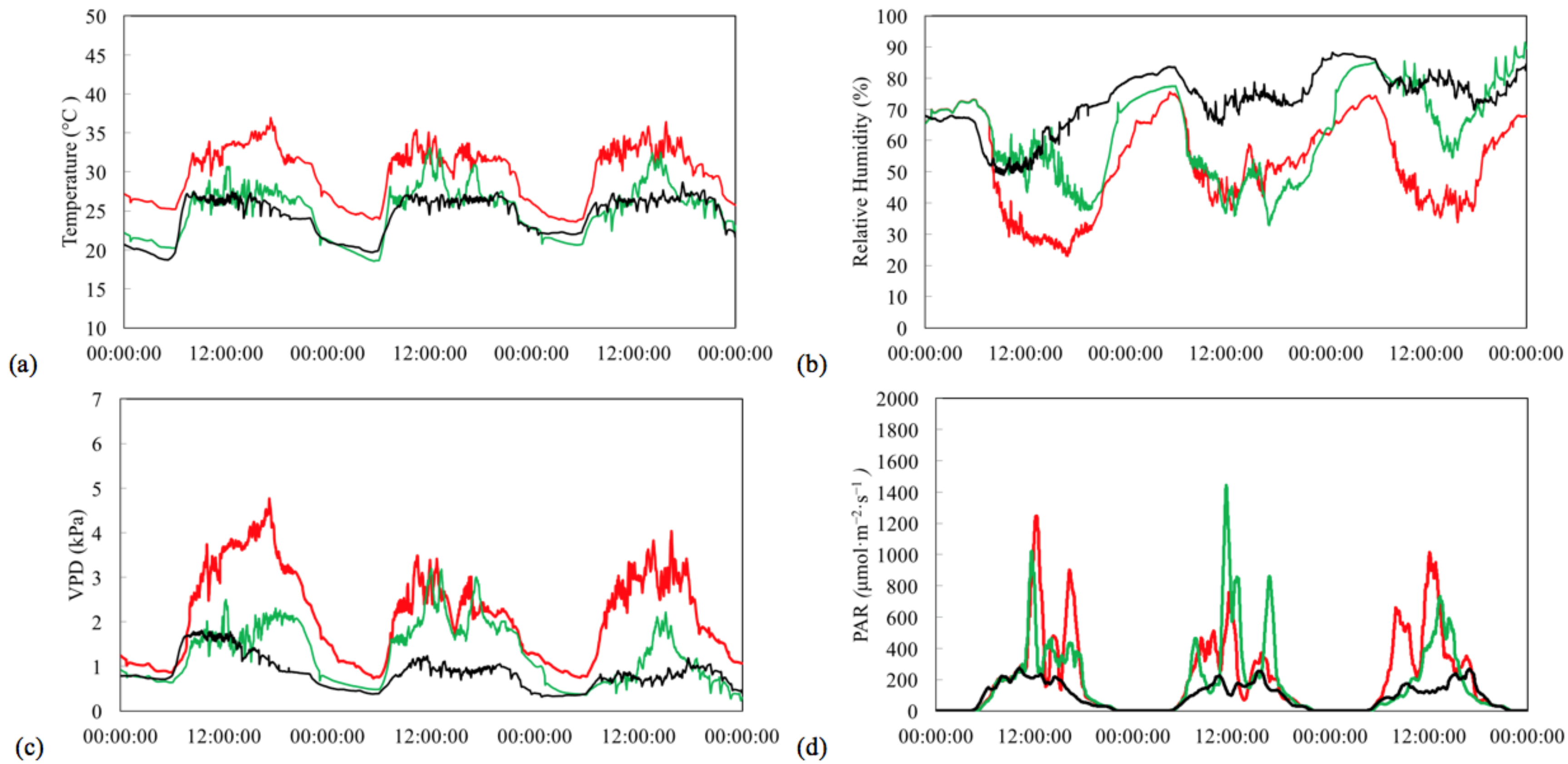

Figure 41. Graphical representations of the 3-day greenhouse climate under which the imaging experiments took place. In (a) temperature, (b) relative humidity, (c) vapor pressure deficit (VPD) and (d) photosynthetically active radiation (PAR) of the three experiments. Each experiment consisted of a set of three consecutive days. In black, relatively cool conditions, in green moderate conditions and in red hot conditions. Experiments were conducted at the Macdonald Campus of McGill University in Ste-Anne-de-Bellevue, QC, Canada.

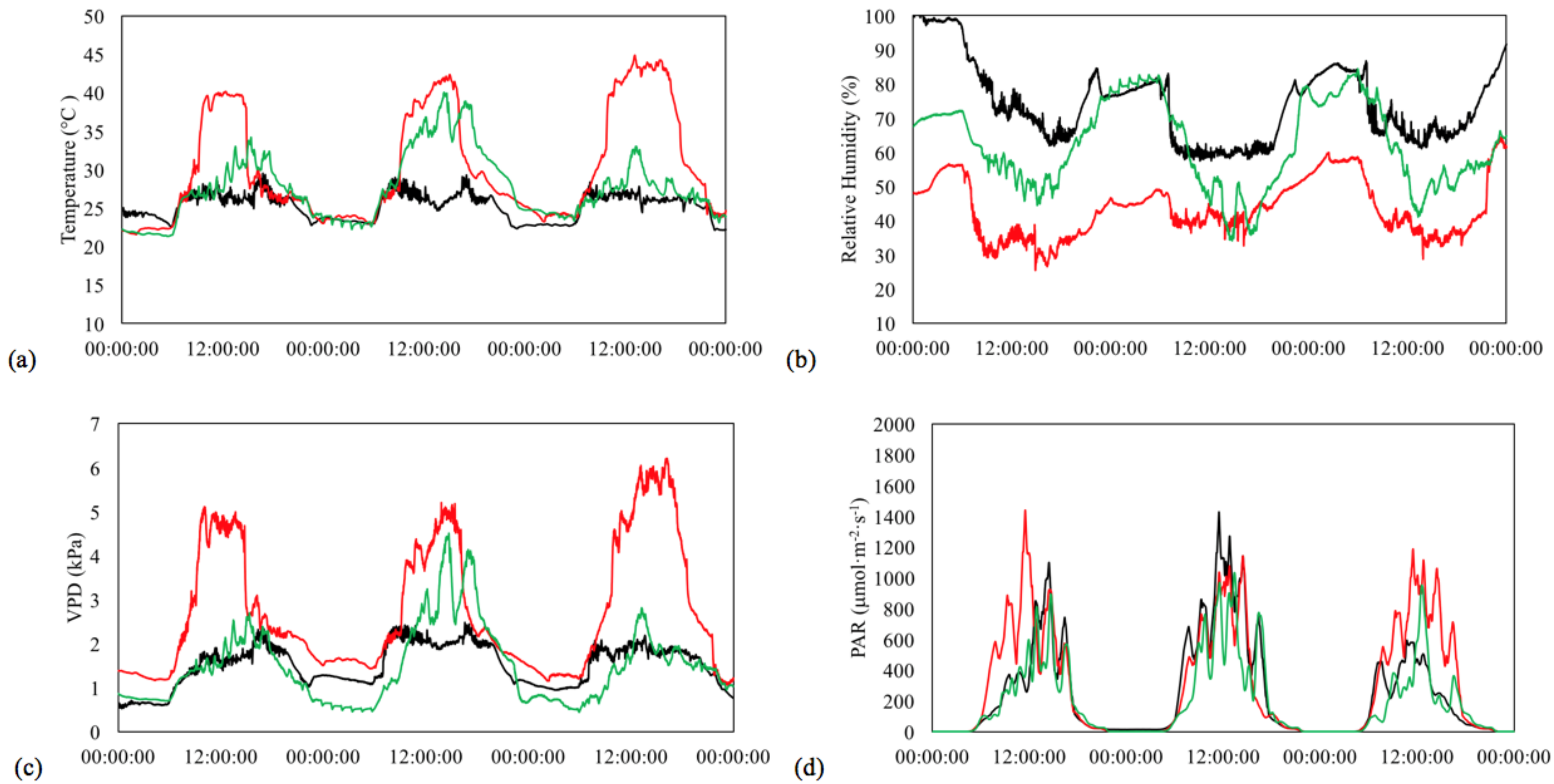

Figure 42. Graphical representations of the 3-day greenhouse climate under which the linear voltage displacement transducer (LVDT) experiments took place. In (a) temperature, (b) relative humidity, (c) vapor pressure deficit (VPD) and (d) photosynthetically active radiation (PAR) of the three. Each experiment consisted of a set of three consecutive days. In black, relatively cool conditions, in green moderate conditions and in red hot conditions. Experiments were conducted at the Macdonald Campus of McGill University in Ste-Anne-de-Bellevue, QC, Canada.

7.4 Results and Discussion

The goal of the image processing reported herein was to create a non-invasive and non-contact methodology of continuous measurement of relative fruit growth. The process needed to be automated and each step needed to be rapid enough to allow for real-time measurements. In the experiments presented here, images were acquired at 30-s intervals, over the course of three consecutive days. Depending on the processing time of the computer or device used for processing, this interval can range from a few seconds to any desired interval.

Measurements were kept in pixels, rather than converting to other units, to conserve precision. When comparing the measured parameters, it was evident in all experiments that the perimeter measurement obtained from this methodology was not as precise as the area and diameter measurements (Figures 43, 44 and 45). The variance of the perimeter measurements concealed the patterns in fruit growth in many cases, particularly in the experiment presented in Figure 46. The diameter measurement is the result of an equivalent circle diameter calculation using the area measurement. Therefore, its precision is the same as that of the area measurement.

Diurnal fruit growth experiments typically involve the study of fruiting plants or trees under a variety of stresses. The swelling, contracting and continuous growth profiles of the fruit can reveal plant response information to the investigator. According to previous work, the fruit is subject to a continuous and rather stable growth rate, with respect to 'true' growth, or dry matter accumulation (Johnson et al., 1992; Heuvelink, 1995). The fruit is also subject to a positive or negative swelling rate (water influx or efflux) related to the water relations of the plant (Johnson et al., 1992, Guichard et al., 2005). Climate parameters such as temperature, relative humidity, VPD and solar radiation all have a significant impact on the water relations of a plant, and therefore influence the immediate growth rate of the fruit of those plants (Adams et al., 2001; Pearce et al., 1993a; Peet, 1992). Under the six imposed climates in this work, different responses in fruit measurement were recorded by both the imaging and the LVDT methodologies. Generally, under high temperatures, low relative humidity, high VPD and high solar radiation, conditions that contribute to high plant transpiration, the area, diameter and perimeter of the tomato fruit plateaued or dropped, depending on the severity of the conditions. This was revealed in the imaging experiment presented in Figure 43, and in the LVDT experiment in Figure 46c. Under cooler temperatures, higher relative humidity, lower VPD and lower solar radiation, conditions that may reduce transpiration, the area, diameter and perimeter continued to increase steadily. Figure 44 and Figure 46a show the results of the imaging and LVDT experiments, respectively, under cooler conditions. Under moderate conditions, the measured parameters plateaued, but did not drop (Figures 45 and 46b). These results compare well with the results presented by Guichard et al. (2005) and Johnson et al. (1992), who performed similar experiments with LVDTs.

Although the LVDT experiments herein did not reveal different patterns in measurement in comparison to the imaging measurement patterns, the precision of the patterns is noticeably different. A lack of precision can be inferred due to the limitations in measurement imposed by the mechanical nature of the LVDT. Although the reading of the voltage output of the device may be very precise or the result of an amplification, the force required to provide movement to the rod of the device inherently reduces the precision of the method. Moreover, in order to account for swelling and shrinkage, the mechanical device used herein and in previous work incorporates a spring mechanism to the rod, which further reduces precision of the measurement.

Another drawback of mechanical measurement devices is the potential lag in measurement. Due to a minimum required force to move the spring-loaded rod of the device, the measured response in fruit diameter may be significantly delayed, as seen in Figure 46a and b. Figure 46a shows how the measurement of the diameter plateaued from the afternoon into the night of the second and third day of measurement. Based on the measurements data presented in Figure 46c, and in comparison, the multiple sets of measurement data from the imaging experiments, long plateaus in data are most likely the result of a lag in response of the mechanical device, rather than a true plateau in growth. Johnson et al. (1992) reported similar limitations during experiments using LVDTs on tomato fruit. Figure 46b shows severe lags in response, as seen by the drops in diameter over the night period in the first and second day of measurement. The orientation of the LVDT device was tilted to a near 90 degrees from the vertical plane in order to accommodate the largest diameter of the tomato. This introduces yet another drawback of mechanical measurement systems. In order to adequately measure the change in diameter of the fruit, the surface of contact of the measurement rod and of the clamping surface must be on perfectly placed opposing points of the diameter of the great circle of the tomato. A great circle (otherwise known as an orthodrome) is the largest circle that can be drawn on any given sphere. This task is done visually and the largest diameter (corresponding to the great circle) of the fruit is approximated. In most circumstances, such as in the experiment presented in Figure 46b, the diameter of the tomato is in a horizontal plane and the measurement device is placed in a horizontal position. Depending on the type of LVDT used, the precision of the device can be very limited under orientations other than in the vertical plane of measurement. The effects of friction and gravity on the components of the LVDT can vary from a vertical to a horizontal position. This was obvious in our work when comparing the results in Figure 46a, where the LVDT was in a vertical position, to the results in Figure 46b, where the device was in a horizontal position.

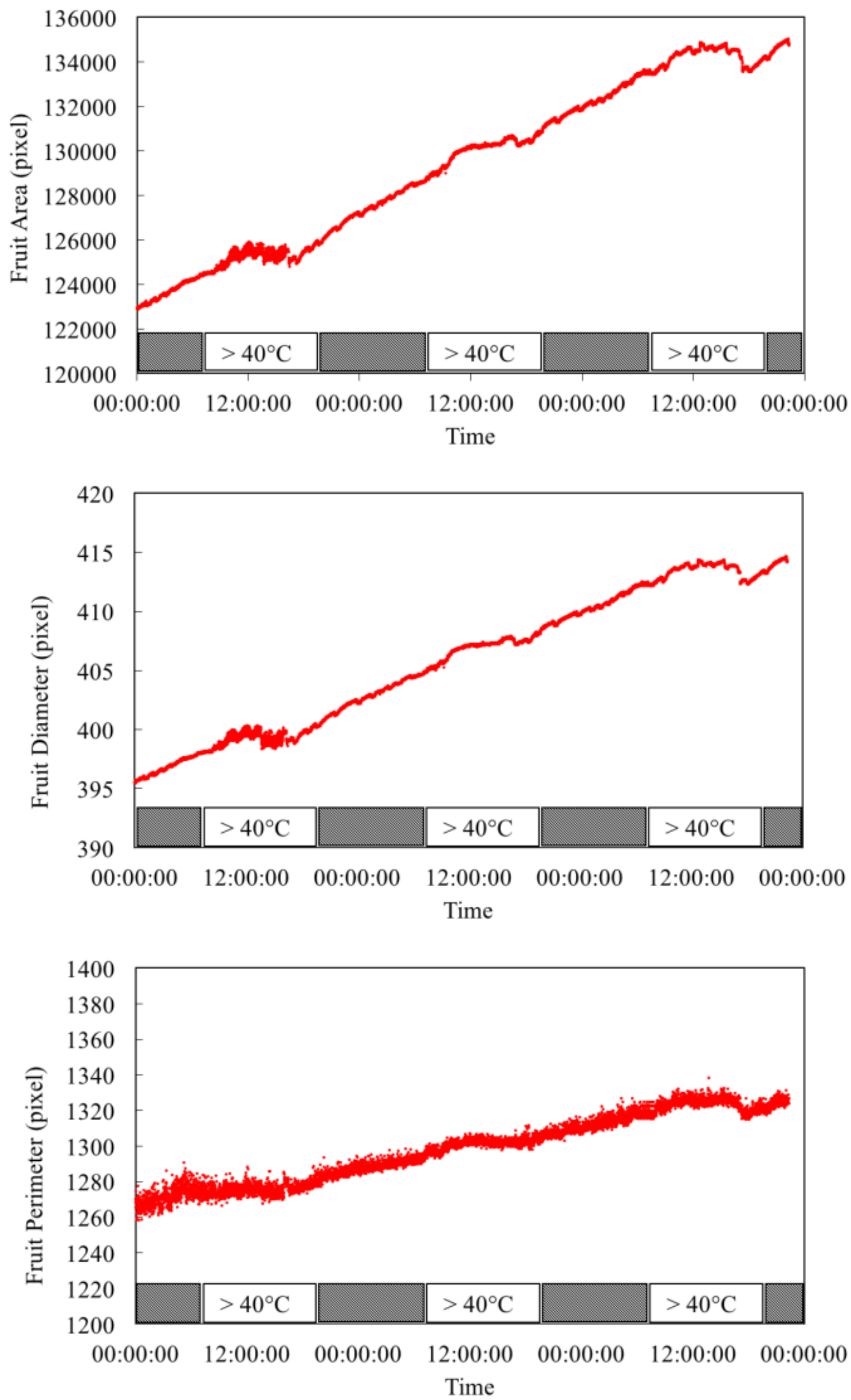

Figure 43. Diurnal area, diameter and perimeter patterns of the tomato fruit in pixels. The data presented is the result of an experiment conducted over three consecutive days under relatively high daytime temperatures (>40 °C), low daytime relative humidity (30-40%), high daytime VPD (4-6 kPa), and moderate solar radiation (1000 $\mu mol \cdot m^{-2} \cdot s^{-1}$ > PAR > 1500 $\mu mol \cdot m^{-2} \cdot s^{-1}$)

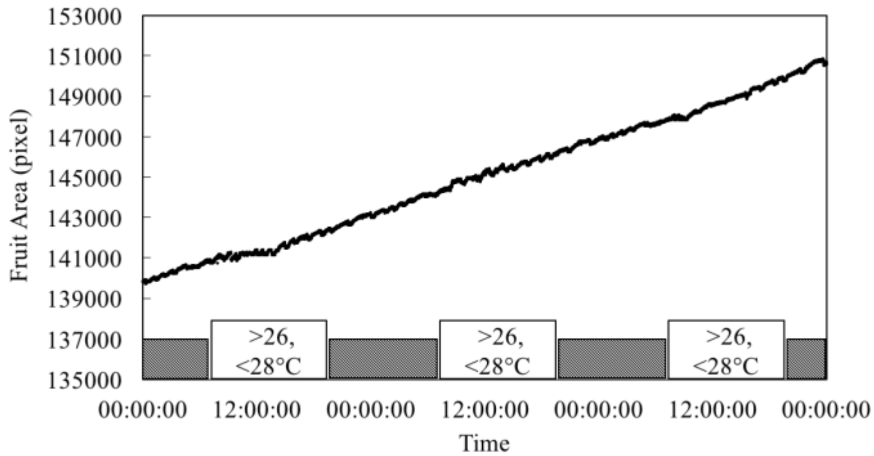

(a)

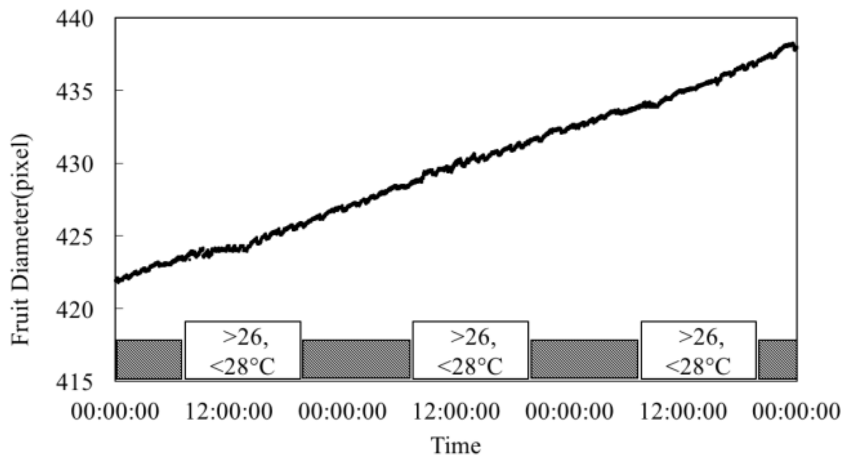

(b)

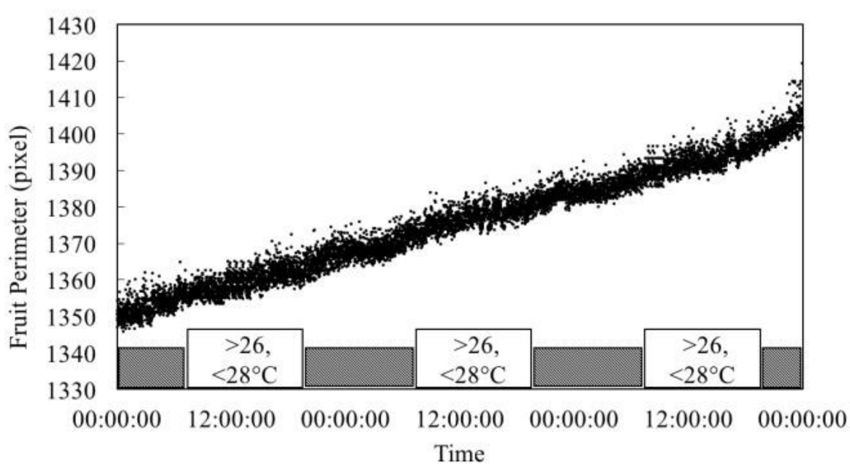

(c)

Figure 44. Diurnal area, diameter and perimeter patterns of the tomato fruit in pixels. The data presented is the result of an experiment conducted over three consecutive days under relatively low daytime temperatures (26-28 °C), high daytime relative humidity (60-70%), low daytime VPD (1-2 kPa), and moderate solar radiation 1000 $\mu mol \cdot m^{-2} \cdot s^{-1}$ > PAR > 1500 $\mu mol \cdot m^{-2} \cdot s^{-1}$).

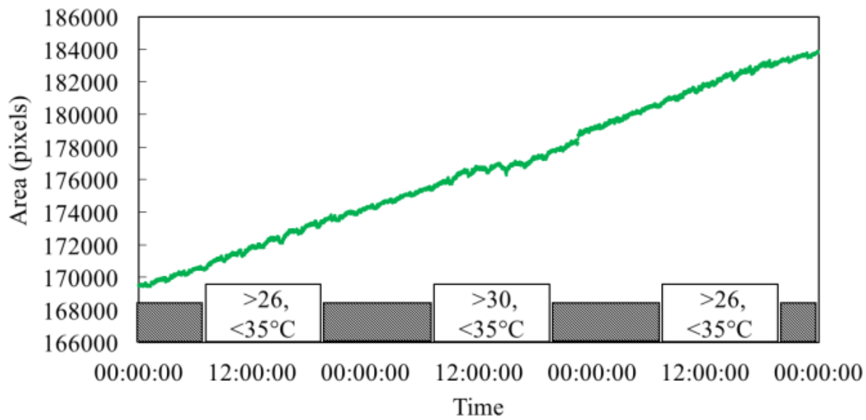

(a)

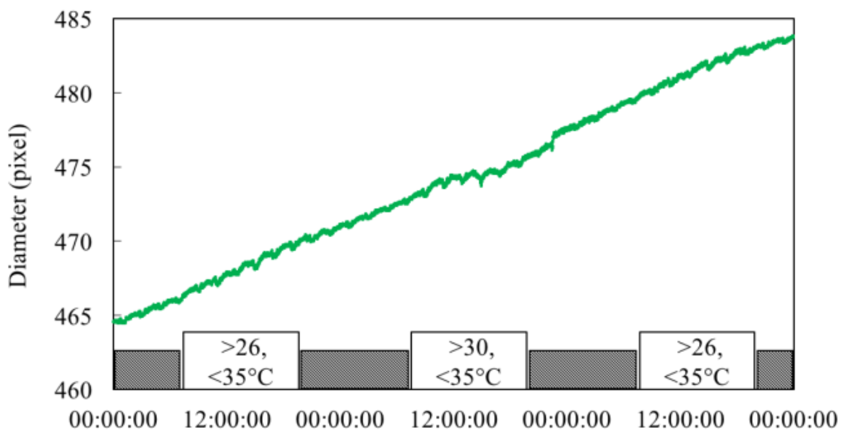

(b)

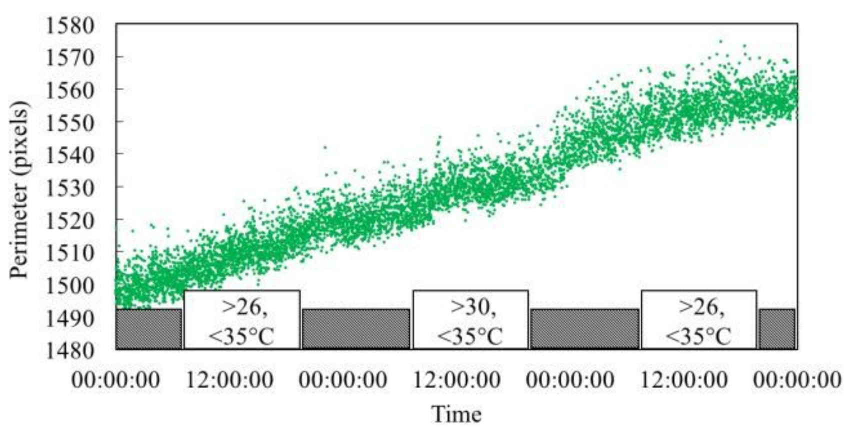

(c)

Figure 45. Diurnal area, diameter and perimeter patterns of the tomato fruit in pixels. The data presented is the result of an experiment conducted over three consecutive days under relatively moderate to warm daytime temperatures (26-35 °C), moderate daytime relative humidity (40-60%), high daytime VPD (2-5 kPa), and moderate solar radiation (1000 μmol·m^{-2}·s^{-1} > PAR > 1500 μmol·m^{-2}·s^{-1}).

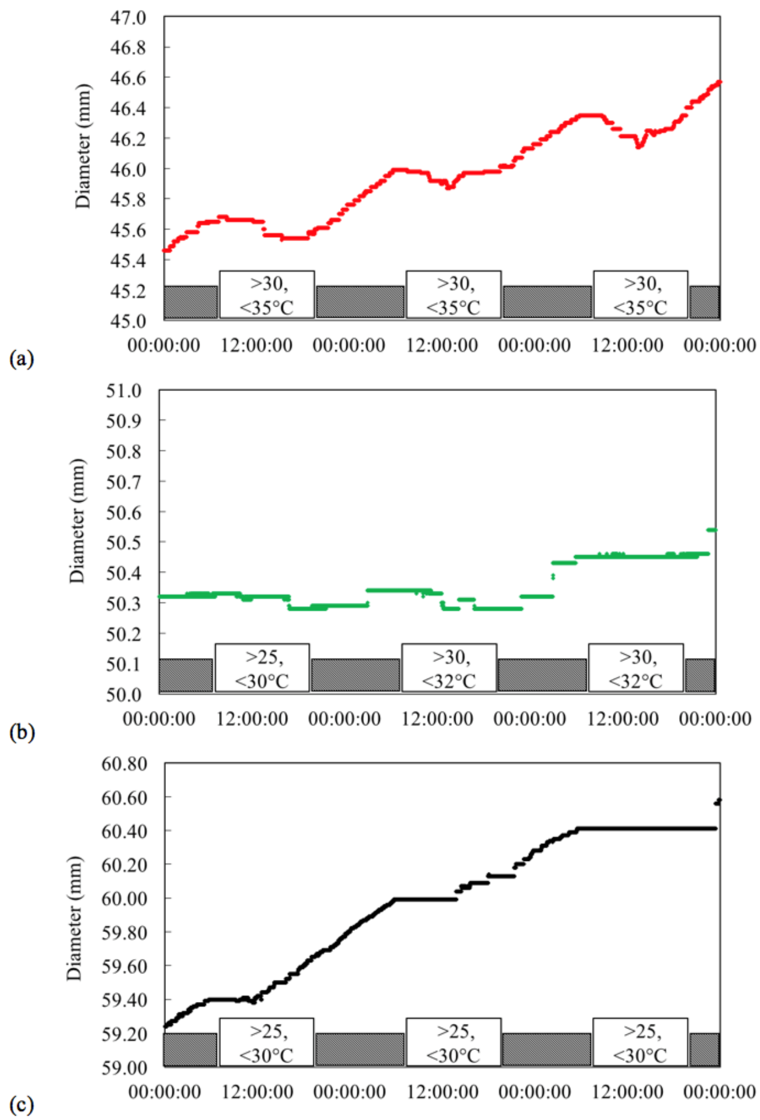

Figure 46. Diurnal patterns in tomato fruit diameter growth. The data presented in (a) is the result of an experiment conducted over three consecutive days under relatively high daytime temperatures (30-35 °C), low daytime relative humidity (30-50%), high daytime VPD (2-4.5 kPa), and moderate solar radiation (1000 µmol·m^{-2}·s^{-1} > PAR > 1500 µmol·m^{-2}·s^{-1}); in (b) under relatively moderate to warm daytime temperatures (25-32 °C), moderate daytime relative humidity (30-70%), high daytime VPD (1-3.5 kPa), and moderate solar radiation (1000 µmol·m^{-2}·s^{-1} > PAR > 1500 µmol·m^{-2}·s^{-1}); in (c) under relatively low daytime temperatures (25-30 °C), high daytime relative humidity (50-80%), low daytime VPD (0.5-2 kPa), and low solar radiation (200 µmol·m^{-2}·s^{-1} > PAR > 400 µmol·m^{-2}·s^{-1}). Note, the scale of the diameter axes varies according to the relative size of the fruit.

The increased precision in measurement of the imaging methodology revealed additional information besides the anticipated climate response data. What is apparent in Figure 45, but less apparent in Figures 43 and 44, is the response in fruit area (and diameter) to the irrigation schedule. The irrigation schedules used during the experiments, presented in Figures 44 and 45, were irregular compared to the schedule used during the experiment in Figure 45. Upon comparison of the on-and-off times of the irrigation system however, a relationship emerged. What initially appeared to be noise in the data was in fact responses to the activation of the NFT irrigation system. The irrigation schedule for the experiment in Figure 45 was regular: 30 min of irrigation every 2 h. Upon closer examination of Figure 45a, a very clear pattern can be discerned. It appears that the response to the irrigation schedule was more pronounced during the daytime than during the nighttime (Figure 47). This could be related to a higher plant transpiration rate during the daytime period. The same irrigation schedule as seen in Figure 45 was used for all LVDT experiments and this subtle pattern in fruit growth was not discernable with the LVDT.

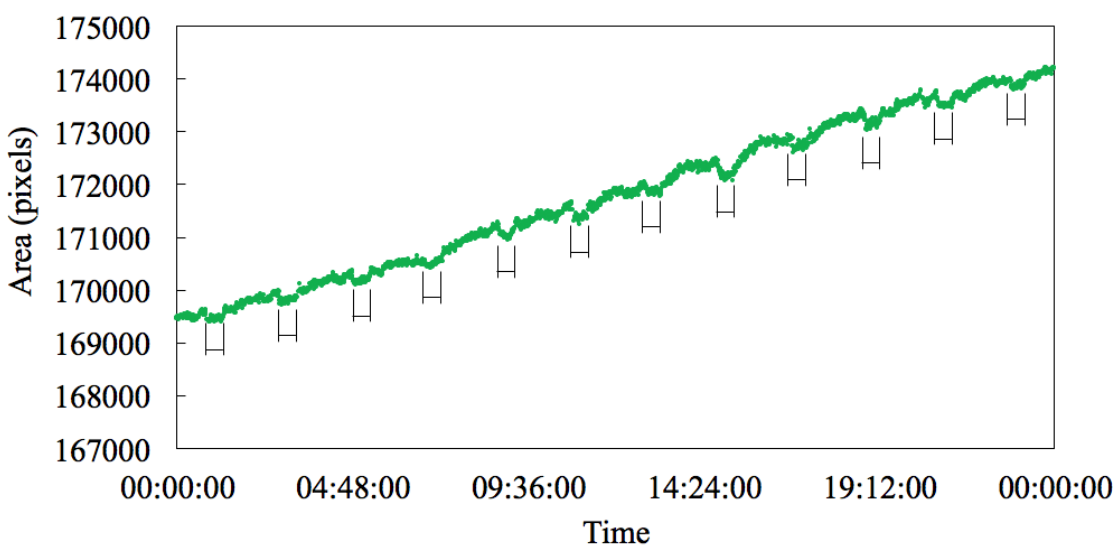

Figure 47. Measured fruit area over the course of 24 h. The irrigation schedule consisted of a 30-min irrigation period every 2 h. Inside the two-legged indicators are the 30-min irrigation periods.

Although this methodology and the experiments presented do not require true measurements to provide informative data, further steps in the image processing can be appended to obtain realistic measurements. Fruit size is an important physical property of all agricultural produce and the estimation of mean fruit size can be important in meeting quality standards and increasing market value of the produce (Wilhelm et al., 2005). In the event that the user requires true measurements, an immobile ruler can be included in the image. The *imdistline* function can be used to convert pixel count to other units either prior to, during or after the test. The tomato fruit can also be measured with a vernier caliper prior to or post-imaging to relate pixel count to physical measurement, although this method may not be accurate as it involves physical contact with the fruit. In previous work, the voltage readings from LVDTs were related to volume of the fruit by approximating the fruit shape as perfect spheres (Ehret & Ho, 1986). Some have used a water-displacement method to obtain the final volume of the fruit after measurement (Johnson et al., 1992). For the purpose of diurnal growth measurement, relative measurements are sufficient to provide information on the behavior of the fruit.

7.5 Conclusion

We have limited the use of the imaging methodology to only measure the diurnal growth patterns of tomato fruit. However, this methodology can be applied to a wide variety of fruit with slight modifications of the image thresholding limits and modification in the script. The image resolution was arbitrarily chosen to be 1024 × 576 pixels to speed-up the processing time, and the thresholding limits were visually and manually set. Further work should focus on comparing the results of different resolutions to investigate the necessity of high resolution imaging with respect to diurnal fruit measurement. Automation of the thresholding should be considered to reduce the need for human interaction with the measurement process and to standardize the fruit measurement data, regardless of the fruit size, fruit color, lighting or orientation scenarios.

A more streamlined image capturing device can be developed. From the prototype device presented here, a comprehensive device that includes the camera, light source and fruit stem support system should be developed. Investigation into the use of a bright light flash as opposed to a diffuse light source and ambient light shield could lead to a more practical device that does not require enclosing the fruit.

Lastly, in future studies, investigation into the very short-term behavior (i.e. periods of a few minutes) of the fruit could reveal more fruit growth and plant water status information. The irrigation response seen in this work can be further investigated to pinpoint the cause of the short-term variation in fruit diameter. This type of machine vision could then be used to control greenhouse climate and irrigation frequencies based on desired fruit quality.

Connecting Text

Chapter 8, *The study of diurnal growth patterns of tomato fruit under arid conditions and the conditions of the natural ventilation augmented cooling (NVAC) greenhouse* was authored by Lucas McCartney and Mark. G. Lefsrud. Chapter 8 will be submitted to the journal HortTechnology.

Based on published literature that suggests that fruit quality in greenhouse crops can be improved by optimizing the plant and fruit water statuses, the response in diurnal tomato fruit growth patterns was studied under high temperature conditions and under conditions provided by the NVAC greenhouse. Although the diurnal patterns in fruit growth cannot guarantee the final outcome of fruit crop in terms of quantity and quality, it can help understand how to improve the greenhouse climate, and its control, to reach yield goals. The machine vision methodology as presented in Chapter 7 was used for fruit measurement.

8. Chapter 8: The Study of Diurnal Growth Patterns of Tomato Fruit Under Hot Conditions and Conditions of the Natural Ventilation Augmented Cooling (NVAC) Greenhouse.

Lucas McCartney and Mark G. Lefsrud

Additional Word Index. Machine vision; Solanum lycopersicum L.; Water potential; Transpiration; Fruit growth; VPD; Fruit quality

8.1 Abstract

The optimization of fruit-water relations in response to environmental stress is critical, in particular under warm summer conditions with low humidity, such as that of an arid or Mediterranean climate. A machine vision methodology was used to measure and record diurnal changes in tomato (*Solanum lycopersicum* L.) fruit. Under harsh daytime greenhouse conditions consisting of high temperatures (peaking beyond 40 °C), low relative humidity (20 to 40%) and high vapor pressure deficit (VPD) (4 to 7 kPa), the diurnal growth patterns of tomato fruit were irregular. Fruit shrinkage occurred on all three days of the two experiments. Under the conditions provided by the natural ventilation augmented cooling (NVAC) greenhouse, the diurnal fruit growth patterns were regulated and fruit shrinkage did not occur. The NVAC greenhouse daytime conditions in the two experiments consisted of temperatures ranging from 25 to 30 °C, relative humidity ranging from 50 to 80% and VPD ranging from 0 to 2 kPa. In this study, observations found that relatively short-term variations in fruit size were highly related to the irrigation schedule and to drought stress conditions. The monitoring of fruit growth patterns, namely those involving fruit shrinkage, can be used for precision irrigation control which in turn could be used to reduce common crop quality issues such as fruit cracking and blossom end rot.

8.2 Introduction

The controlled environment provided by a greenhouse offers improved conditions for increased yield and quality of production. However, fruit quality in greenhouse production remains an important issue for greenhouse growers trying to meet the ever-increasing demand of consumers (Ho, 1998; Dorais et al., 2002; Flores et al., 2010). Fruit quality can combine various appearance characteristics such as size, shape and color, and taste properties, like sweetness, acidity and aroma (Bai & Lindhout, 2007). On average, a mature tomato fruit is composed of 92 to 95% water and only 5 to 8% dry matter (Davies and Hobson 1981). Phloem, xylem, and transpiration fluxes contribute water and nutrients to the fruit of a plant. Phloem influx is the main source of water, and it accounts for most of the increase in fruit volume. Therefore, quality characteristics of the tomato fruit such as dry matter content, taste, and incidence of cracking and blossom-end rot (BER) can be improved by optimizing the water relations and nutrient status of both the plant and fruit (Guichard et al., 2005; Ho & Adams 1995; Ho et al., 1993). BER, a physiological disorder related to calcium deficiency in the distal part of the fruit (Ho & Adams 1995), results from complex interactions (Saure, 2001) between stress factors but also from rapid fruit growth resulting from rapid influxes (Ho et al., 1993).

Variations in diurnal fruit growth rate are related to temporary water stresses associated with increased plant water demand as plant transpiration increases rapidly (Pearce et al. 1993a,b). For instance, fruit shrinkage is observed at midday under conditions that cause high plant transpiration such as high solar radiation (Johnson et al., 1992) and low relative humidity (Leonardi et al. 2000). Fruit shrinkage can occur early in the day when the plant is suddenly exposed to solar radiation and rising temperatures, which abruptly increase transpiration (Pearce et al., 1993a,b). The plant and fruit water status and associated growth patterns of tomato fruit have been linked to irrigation practices (Abbott et al., 1986) and plant fruit load (Demers et al., 2007; Guichard et al., 2005). Fruit cracking was reduced in tomatoes by increasing the irrigation frequency from one to four times daily (Abbott et al., 1986). Relieving plant water stress suddenly is the most certain means of drastically altering plant water status and causing cracking (Peet, 1992). Low fruit load per plant resulted in large variations in fruit water status and in an increase in tomato cracking (Demers et al., 2007), most likely due to the presence of less water sinks (Guichard et al., 2005).

Strong variations in fruit growth, including shrinkage, can have a major impact on the cracking of tomato fruit, as variations in tension forces on the fruit skin are associated with changes in fruit water status (Guichard et al. 2001). In pepper fruit (*Capsicum annuum* L.), a daily cycle of fruit shrinkage and expansion resulted in severe cracking (Aloni et al. 1999; Moreshet et al. 1999). Early morning and the end of the afternoon have been identified as the most likely moments of the day for initiation of cracking in most fruit (Guichard et al. 2001).

These moments are the times when the plant water status is drastically changing. Early in the morning before sunrise, the fruit is at its maximum relative size, as the plant is at a maximum stem water potential (Johnson et al., 1992) and transpiration is low (Chapter 6). Practically speaking, in a commercial operation in a warm climate, very little can be done to alter the fruit growth patterns during the nighttime, as dehumidification is a very unlikely practice and reducing irrigation to cause an efflux from the fruit while meeting the plant needs can be very difficult and counterproductive. Therefore, the focus is directed to the late-afternoon period during which cracking can also occur. After a daytime period of very little growth (e.g. plateau on a warm day) or negative growth (e.g. shrinkage on a hot sunny day), when late-afternoon air temperatures drop, humidity rises and solar radiation declines, the fruit can be subject to rapid water influx and rapid growth in response to the plant regaining a more normal water status.

Guichard et al. (2005) used high-pressure fogging to reduce greenhouse daytime vapor pressure deficit (VPD) to alleviate daytime fruit shrinkage. Similarly, in the present study, diurnal tomato fruit growth patterns were studied in response to the cooling and relative humidity control capabilities of the natural ventilation augmented cooling (NVAC) greenhouse. The resulting patterns were compared to the growth patterns of tomato fruit under stress conditions, consisting of high temperature, low relative humidity and high VPD. The fruit growth patterns of varying irrigation schedules and drought stress were investigated. The NVAC greenhouse is a low cost natural ventilation design that is improved by using an energy efficient misting system. An unconventional additional inside roof captures unevaporated water droplets before they reach the plants and strategically guides the evaporative cooled air into the plant space. From previous work on diurnal fruit growth patterns by Johnson et al. (1992), it was expected that the tomato fruit would show an irregular growth pattern in response to stress conditions, such as shrinkage during peak daytime heat. From the transpiration results presented in Chapter 6 and as seen in Guichard et al (2005), the NVAC greenhouse cooling system was expected to impact the tomato plant’s water status and regulate the diurnal growth patterns of the tomato fruit.

8.3 Methods and Materials

Experiments were conducted in June and July of 2017 in a research greenhouse at the McGill University Macdonald Campus in Ste-Anne-de-Bellevue, QC, Canada. The high-pressure fog system of the research greenhouse was used to simulate the temperature and relative humidity conditions of the NVAC greenhouse as reported in Chapters 4, 5 and 6. An experiment consisting of hot daytime conditions and an experiment consisting of colder, more humid daytime conditions, typical to the conditions provided by the NVAC greenhouse, were conducted. Each experiment was repeated once. The daytime conditions of the hot conditions experiment (Tests 1 and 2) consisted of high temperatures peaking beyond 40 °C but remained above 30 °C for the majority of the day, low relative humidity that ranged from 20 to 40% and a high VPD from 4 to 7 kPa. The daytime conditions of the colder NVAC greenhouse conditions experiment (Tests 3 and 4) consisted of temperatures ranging from 25 to 30 °C, relative humidity from 50 to 80% and VPD from 0 to 2 kPa. The temperature, relative humidity, VPD and photosynthetically active radiation (PAR) data from the four tests are presented in Figure 48.

Twenty-five 'Beefsteak' tomato plants were germinated in 1.5-inch by 1.5-inch rockwool cubes (A-Ok Starter Plugs™, The Rockwool Group, Hedehusene, Denmark) in a Conviron growth chamber (Model TC30, Controlled Environments Inc., Winnipeg, MB, Canada). Eight tomato plants were then grown to maturity in the greenhouse in 4-inch by 4-inch rockwool cubes (Grodan cubes, The ROCKWOOL Group) in a nutrient-film technique (NFT) hydroponic system. During growth (before experiments), the greenhouse climate settings were set to 26 °C and 60% relative humidity during daytime and 23 °C and 60% relative humidity during nighttime. The photoperiod was set to 16 h, 6:00 HR to 22:00 HR, with high-pressure sodium (HPS) supplemental lighting in the greenhouse and fluorescent lighting in the growth chamber. A twine and tomato clip trellis system held the mature plants in place. The plants were grown to six to eight feet in height. The plants were irrigated and fertilized with full-strength Hoagland's nutrient solution (Hoagland & Arnon, 1950). The irrigation schedule in Tests 1 and 4 provided 30 min of irrigation every 2 h. The irrigation schedule in Tests 2 provided 30 min of irrigation every 6 h. The irrigation schedule in Tests 3 provided randomized 30-min periods of irrigation 20 times during a 24-h period, separated by at least a 30-min period.

Similar experiments were conducted in a Conviron growth chamber in which the temperature, relative humidity and light were controlled. By nature, the growth chamber provided very constant settings in comparison to the greenhouse. Four plants that were germinated with the plants used in the greenhouse experiment were grown in the growth chamber on a trellis system and pruned to a maximum of three feet in height, as space was limited. An NFT system was installed in the growth chamber and the plants were also grown in four-inch by four-inch rockwool cubes. A total of two hot climate tests and two cooler NVAC greenhouse climate tests were conducted once the plants had each fruited two fruit. During hot conditions tests, daytime temperatures were maintained at 40.0 °C ± 1.0 °C and relative humidity at 30% ± 5% from 09:00 HR to 16:00 HR. Nighttime conditions were 26 °C and 80% relative humidity. The photoperiod was the same as in the greenhouse experiments, at 16 h from 06:00 HR to 22:00 HR. The light was controlled and measured at the plant level to be 150 $\mu mol \cdot m^{-2} \cdot s^{-1}$, far less than the natural light levels in the greenhouse experiment. During the NVAC greenhouse conditions tests, the nighttime conditions were maintained the same as in the hot conditions experiments, but daytime conditions were set to a temperature of 26 °C ± 1.0 °C and 70% ± 5% relative humidity. These conditions were colder than the conditions in the greenhouse.

The climate parameters inside the greenhouse and growth chamber were recorded using a data logger (HOBO U30 USB Data Logger U30-NRC, Onset Computer Corp., Bourne, MA) with temperature, relative humidity and solar radiation sensors calibrated as recommended by Both et al. (2015). The logged data was time stamped. Temperature and relative humidity sensors were placed 1.5 m above the root zone of the tomato plants in the greenhouse, and 0.75 m meters above the root zone in the growth chamber. PAR sensors were placed atop the plant canopy. The temperature sensors (S-TMB-M006, Onset Computer Corp.) provided < ± 0.2 °C total accuracy and resolution of < ± 0.03 °C, over the range of 0 to 50 °C. The humidity sensors (S-THB-M008, Onset Computer Corp.) provided an accuracy and resolution of ± 2.5% from 10% to 90% relative humidity and 0.1% relative humidity at 25 °C, and below 10% and above 90%, ±5%. The temperature and relative humidity sensors were shielded using perforated white Styrofoam cups or solar radiation shields (RS3 Solar Radiation Shield, Onset Computer Corp.). The photosynthetically active radiation (PAR) (S-LIA-M003, Onset Computer Corp.) sensors had an accuracy of ± 5 $\mu mol \cdot m^{-2} \cdot s^{-1}$, and a resolution of 2.5 $\mu mol \cdot m^{-2} \cdot s^{-1}$, with an additional temperature-induced error ±0.75 $\mu mol \cdot m^{-2} \cdot s^{-1}$ $°C^{-1}$ from 25 °C.

A machine vision and analysis methodology, as described in Chapter 7, was used to measure the diurnal fruit growth rate. The machine vision device encloses the fruit (not hermetically) and shades the fruit from all solar radiation, but shines a constant diffuse LED light (Philips 5.5 W soft white, 9290012036, Philips Lighting Canada Ltd., Markham, ON, Canada) for imaging purposes. The changes in fruit size are therefore in response to plant-fruit water status fluctuations, while the impact of warming of the fruit via solar radiation was minimized. Fruit area, diameter and perimeter were measured and recorded every 30 seconds. The experiments were repeated until data of three consecutive days with similar greenhouse climate conditions was obtained. Randomly chosen unripe tomato fruit of at least 4 cm in diameter were selected on healthy plants containing at least 2 other fruit, but no more than 4 other fruit. In the growth chamber, this was not possible as the plants only fruited one or two tomatoes. Tests on the fruit were stopped when the fruit began to ripen i.e. change from a green hue to a red hue.

Distilled water irrigation tests were conducted separately from the climate tests to investigate the relationship between irrigation water salinity and the subtle contracting and swelling patterns of the fruit that coincided with irrigation schedules, as reported in Chapter 7. A reservoir and pump system identical to the system providing Hoagland solution to the plants was installed. During daytime tests at moderate temperatures, the irrigation schedule remained the same but alternated between two consecutive irrigation periods with distilled water and one period with Hoagland solution. The data considered was from the second distilled water irrigation period in order to minimize trace amounts of nutrients remaining from preceding Hoagland solution irrigation periods.

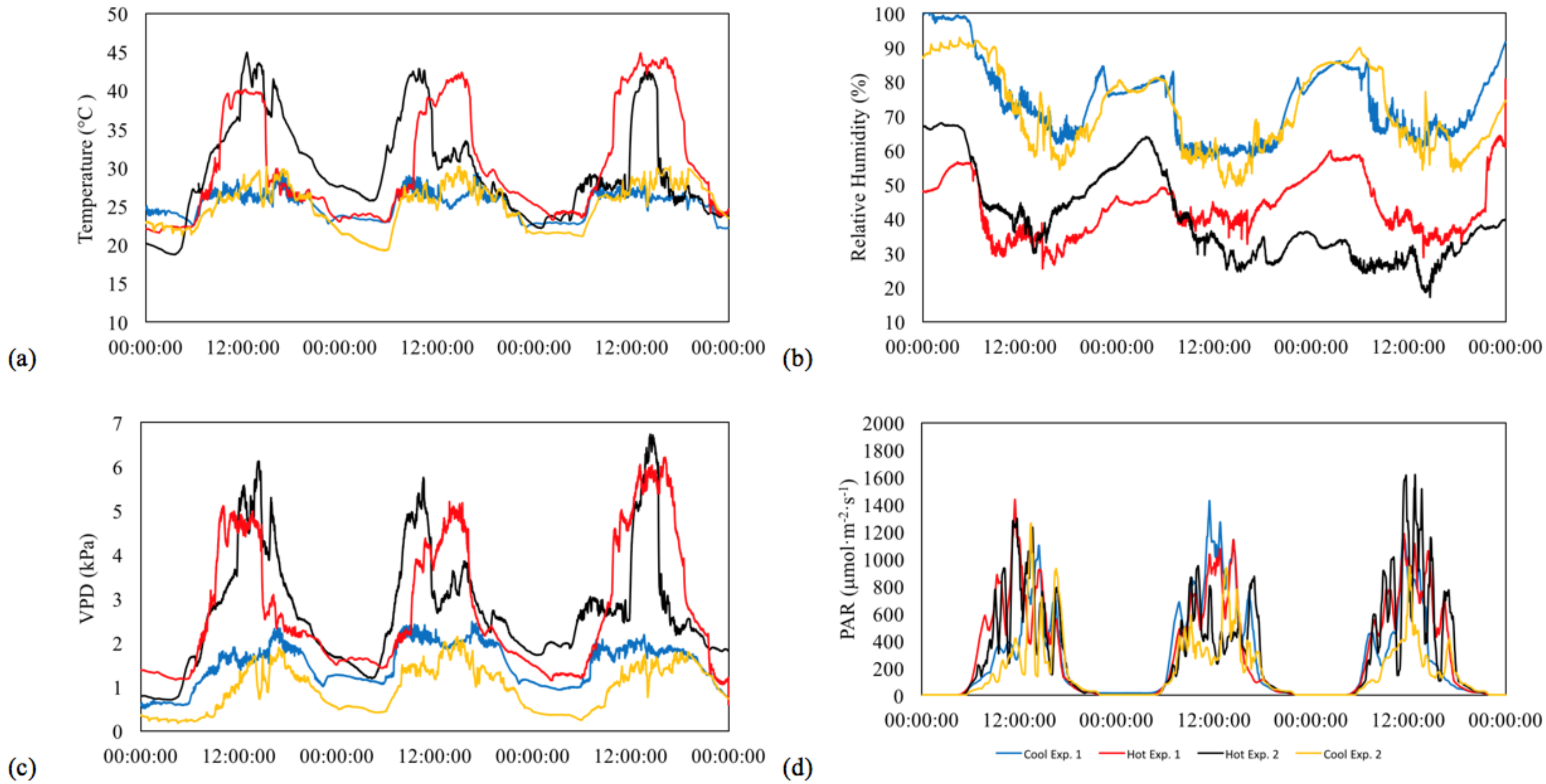

Figure 48. Graphical representations of the 3-day greenhouse climates under which the fruit growth experiments took place. In (a) temperature, (b) relative humidity, (c) vapor pressure deficit (VPD) and (d) photosynthetically active radiation (PAR). Each test consisted of a set of three consecutive days. In blue and yellow are the relatively cool conditions with higher humidity and in black and red are the hot conditions with lower humidity. Experiments were conducted at the Macdonald Campus of McGill University in Ste-Anne-de-Bellevue, QC, Canada.

8.4 Results

The diurnal tomato fruit growth pattern varied greatly in Tests 1 and 2, under hot and dry conditions, with a high VPD (Figures 49 and 50). Shrinkage occurred in the afternoon on each of the three days of each test. The nighttime growth patterns were more uniform, showing relatively consistent positive growth. In Test 1, day 1 and day 3 each showed shrinkage occurring shortly after 09:00 HR which coincided with the sharp increases in temperature, increase in VPD and decreases in relative humidity (Figure 48). Day 2 showed shrinkage later in the day, which also coincided with a later peak in temperature, increase in VPD and drop in relative humidity. With further analysis, what is apparent in Test 2 (Figure 50) but somewhat less apparent in Test 1 (Figure 49), is the impact of the irrigation schedule on the fruit growth. In Figure 49, a pattern of short wave cycles can be seen every 2 h. This coincides with the irrigation schedule of 30 min of irrigation every 2 h. This can be seen in greater detail in Figure 53 and this is discussed more later on. In Test 1, during the daytime when the fruit shrunk, the short waves of rapidly changing fruit growth were more pronounced. This same effect was especially apparent in Test 2 (Figure 50) where the irrigation frequency was less and the peak in VPD was higher than in all other tests. During day 1 of Test 2, the fruit initially shrunk by 2.90 mm in diameter in response to the greenhouse conditions, but then swelled by 0.92 mm in response to the irrigation period. After the 30-min irrigation period, the fruit further shrunk by 2.19 mm down to a daily minimum at 15:02 HR. By 17:00 HR, the fruit had regained positive growth after swelling by 1.47 mm. The following two days of the test showed similar patterns.

The stress caused by the harsh conditions of the three days of high temperatures and VPD and low relative humidity of Test 2 prevented the fruit from regaining its initial daily size. The size of the fruit 24 h after initiation of the experiment was lower than the initial fruit size, even after nighttime growth at the end of day 1. By the early morning of day 3 of Test 2, the fruit regained its initial size, but it is unsure if this is due to the continuous dry matter growth of the fruit or due to recovery of water and nutrients.

The greenhouse climate conditions of Tests 1 and 2 were similar, yet the growth patterns differed in the severity of daily shrinkage. The significantly more pronounced shrinkage seen in Test 2 (Figure 50) may be explained by the maturity of the tomato fruit. The larger fruit in Test 2 began to ripen in the hours following termination of the tests, indicating that it was well into the ripening stage of growth. Peet (1992) proposed that harvesting tomato fruit early while at the mature-green stage can help thwart cracking. The tensile strength of the skin is very high during the immature stages of fruit growth and decreases rapidly between mature-green to early-pink stages of ripening (Dorais et al., 2004). Jackman et al. (1990) showed that firmness in tomato fruit, as measured by the three different methods, progressively decreased with ripening from the mature-green stage into the following 10 days of ripening. This suggests that younger fruit may be less impacted by the varying water status of the plant, because they are inherently firmer, and can explain why the smaller, younger fruit in Test 1 did not show pronounced shrinkage as seen in Test 2.

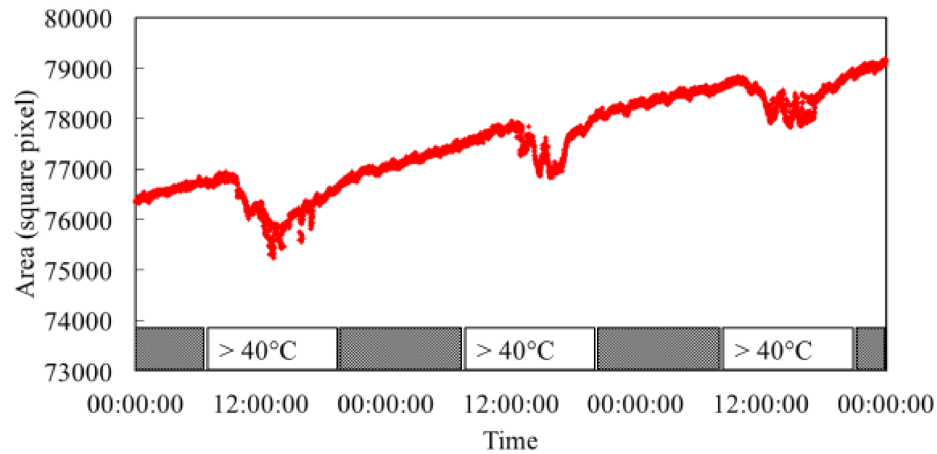

(a)

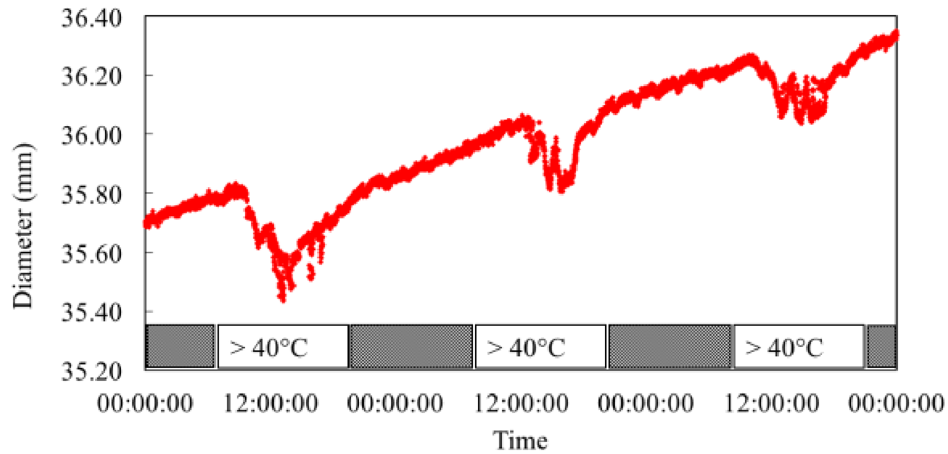

(b)

Figure 49. Diurnal growth area in (a) (pixels) and diameter in (b) (mm) patterns of the tomato fruit. The data presented is the result of Test 1 conducted over three consecutive days under relatively high daytime temperatures (peak > 40 °C), low daytime relative humidity (20-40%), high daytime VPD (4-7 kPa), and moderate solar radiation (1000 $\mu mol \cdot m^{-2} \cdot s^{-1}$ > PAR > 1500 $\mu mol \cdot m^{-2} \cdot s^{-1}$).

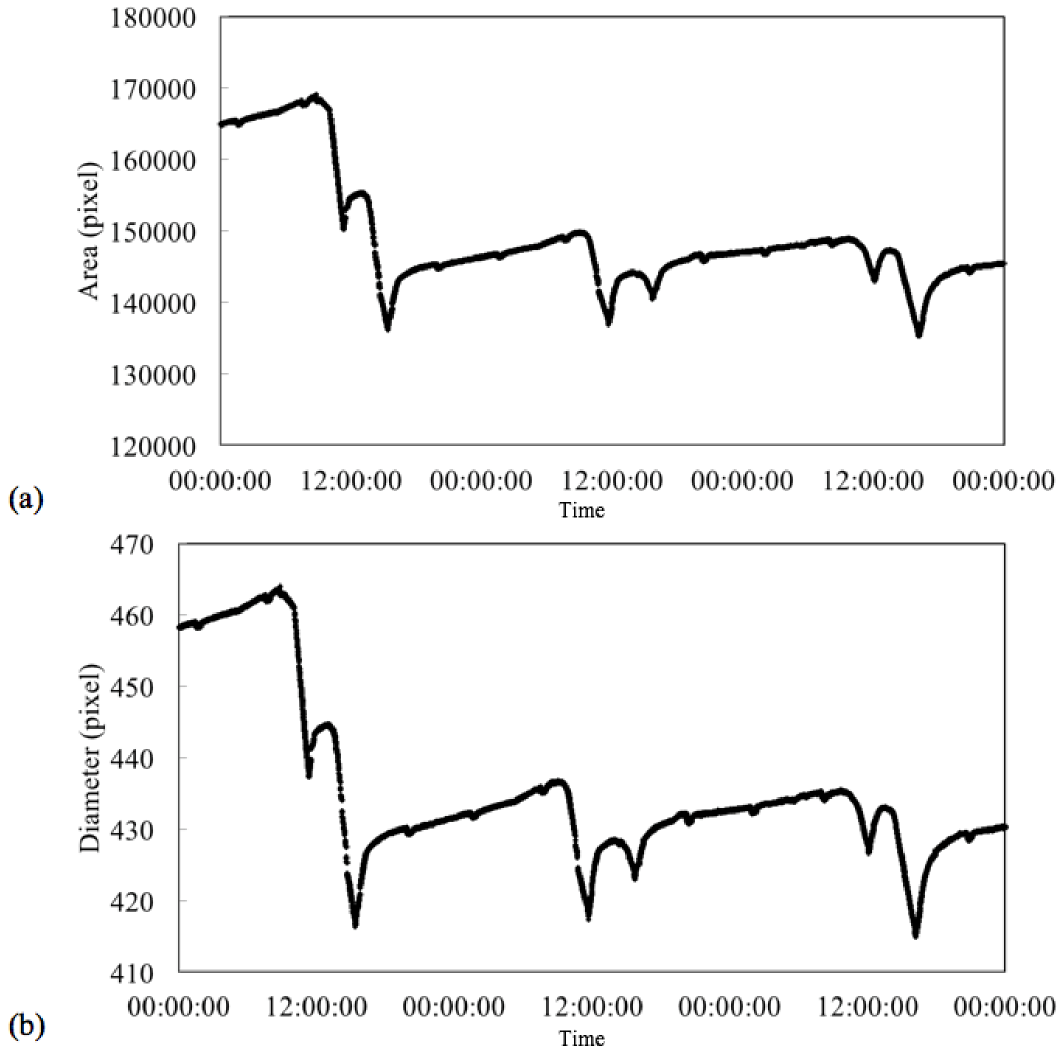

Figure 50. Diurnal growth area in (a) (pixels) and diameter in (b) (mm) patterns of the tomato fruit. The data presented is the result of Test 2, conducted over three consecutive days under relatively high daytime temperatures (peak > 40 °C), low daytime relative humidity (20-40%), high daytime VPD (4-7 kPa), and moderate solar radiation (1000 $\mu mol \cdot m^{-2} \cdot s^{-1}$ > PAR > 1500 $\mu mol \cdot m^{-2} \cdot s^{-1}$).

In Tests 3 and 4, under the NVAC greenhouse conditions, with lower temperatures and VPD and higher relative humidity the diurnal fruit growth patterns were stable from daytime to nighttime, in contrast to Tests 1 and 2 (Figures 51 and 52). No shrinkage occurred but day 1 and 3 of Test 3 showed plateaus in growth of varying lengths occurring shortly after 09:00 HR which coincided with the morning increases in temperature and VPD and decreases in relative humidity. The impact of the irrigation schedule on the fruit growth was apparent, even under NVAC greenhouse conditions. In Figure 51, an apparent random pattern of short waves can be seen. This coincides with the irrigation schedule that was randomized throughout the day. Over the course of the three days of Tests 3 and 4, the fruit diameter grew by 2.10 mm and 3.26 mm, respectively.

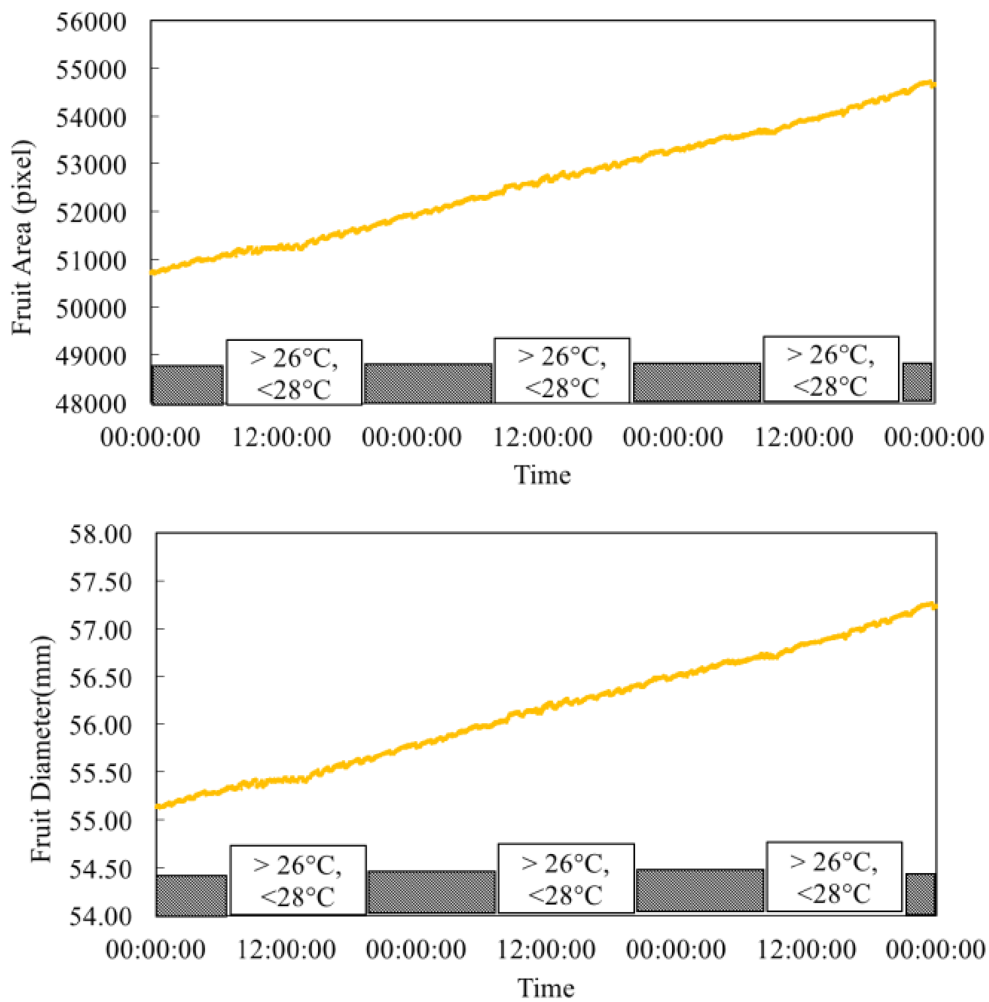

(a)

(b)

Figure 51. Diurnal growth area in (a) (pixels) and diameter in (b) (mm) patterns of the tomato fruit. The data presented is the result of Test 3, conducted over three consecutive days under NVAC greenhouse conditions consisting of relatively low daytime temperatures (26-28 °C), high daytime relative humidity (60-70%), low daytime VPD (1-2 kPa), and moderate solar radiation 1000 $\mu mol \cdot m^{-2} \cdot s^{-1}$ > PAR > 1500 $\mu mol \cdot m^{-2} \cdot s^{-1}$).

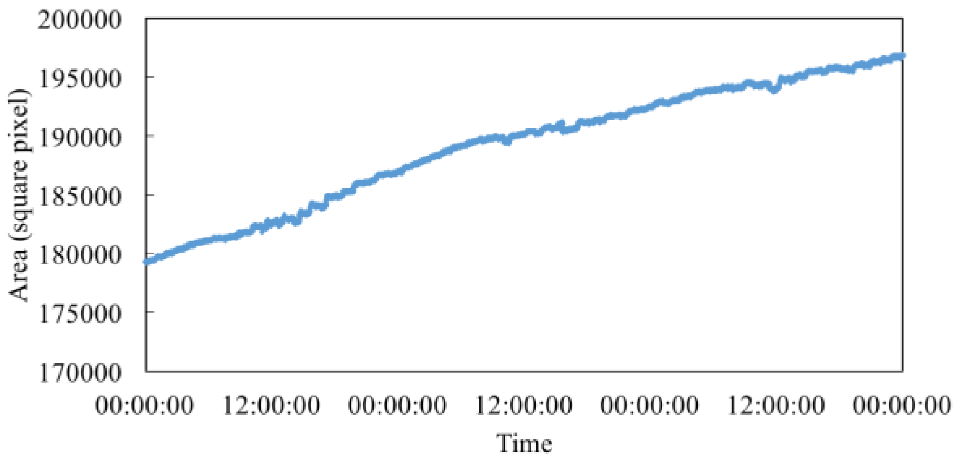

(a)

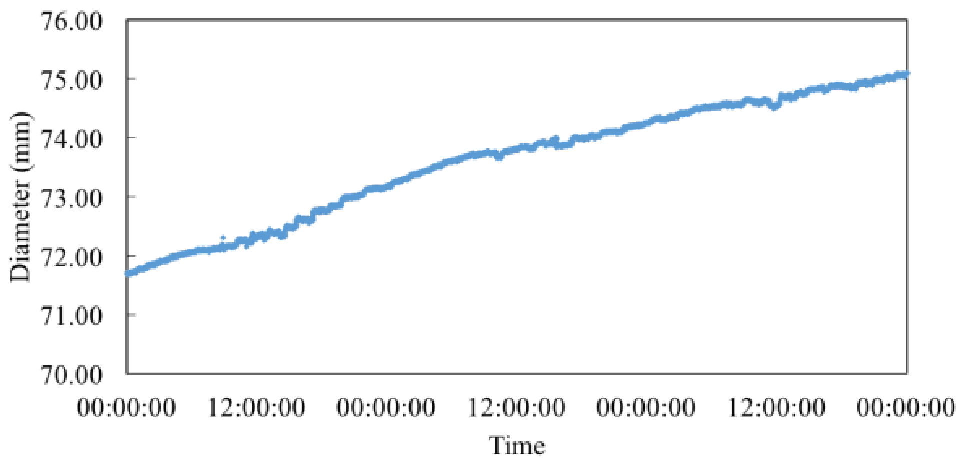

(b)

Figure 52. Diurnal area, diameter and perimeter patterns of the tomato fruit in pixels. The data presented is the result of Test 4, conducted over three consecutive days under NVAC greenhouse conditions consisting of relatively low daytime temperatures (28-30 °C), high daytime relative humidity (60-70%), low daytime VPD (1-2 kPa), and moderate solar radiation 1000 µmol·m^{-2}·s^{-1} > PAR > 1500 µmol·m^{-2}·s^{-1}).

Figure 53a shows a close-up of the area data over a 24-h period. Each wave in the growth pattern corresponds to a 30-min irrigation period. It appears that the fruit shrunk in response to the start of the irrigation system. When studied over a relatively longer irrigation period, the fruit appeared to eventually regain growth even if the irrigation was still occurring (Figure 53b).

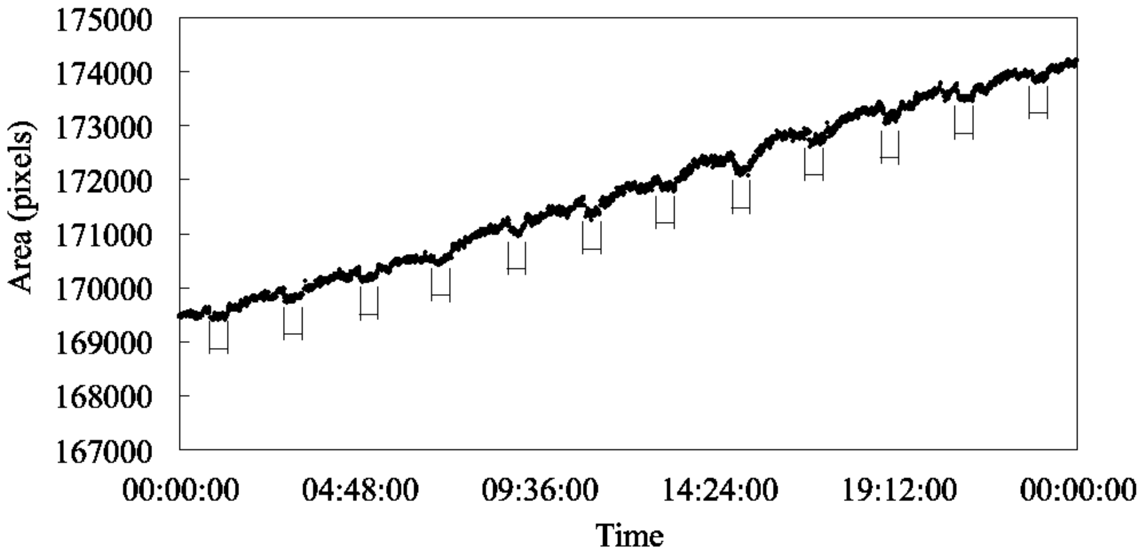

(a)

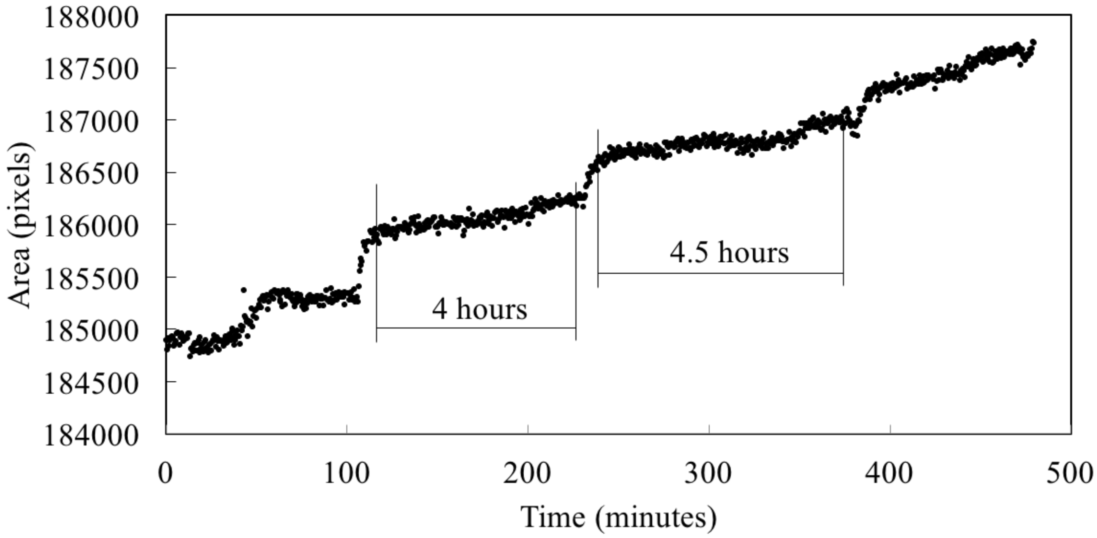

(b)

Figure 53. Measured fruit area (pixels) in response to irrigation schedules. In (a) over the course of 24 h with an irrigation schedule consisting of a 30-min irrigation period every 2 h. Inside the two-legged indicators are the 30-min irrigation periods; in (b) over the course of 9 h with an irrigation schedule consisting of a 4-h and 4.5-h irrigation period.

In a separate set of tests, irrigation salinity and drought stress were studied to investigate the unusual shrinkage of the fruit, in response to irrigation, seen during the three-day tests. Over the course of a 24-h period, under NVAC greenhouse conditions similar to the conditions presented in Figure 48, the change from Hoagland solution irrigation to distilled water irrigation did not affect the irrigation response patterns (waves) seen in fruit growth. Figure 54 shows 2-h snippets in the data of both irrigation tests, and a short-term reduction in fruit size can be seen four to 5 min after initiation of the irrigation. Conversely, 4 to 5 min after termination of the irrigation period, the fruit returns to regular growth.

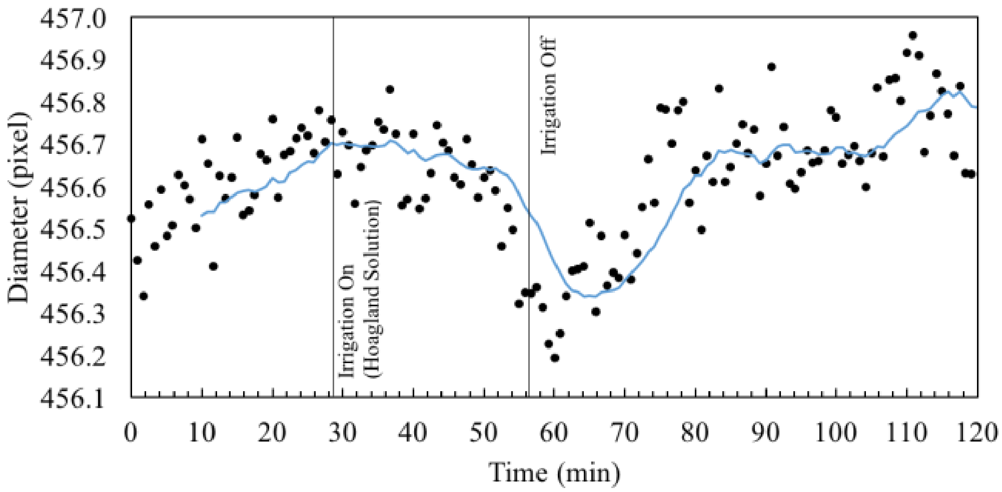

(a)

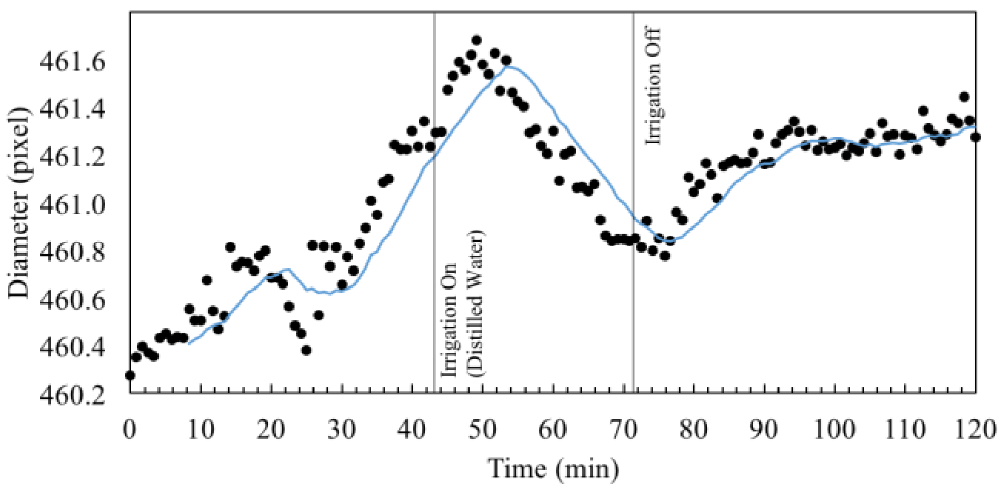

(b)

Figure 54. Measured fruit diameter (pixels) over the course of 120 min. The irrigation schedule in (a) consisted of a 30-min irrigation period with full strength Hoagland solution. The irrigation schedule in (b) consisted of a 30-min irrigation period with distilled water. Inside the two-legged indicators are the 30-min irrigation periods.

Drought stress was imposed on the tomato plants after the previously mentioned set of experiments were concluded. At 15:00 HR, under NVAC greenhouse conditions similar to the conditions presented in Figure 1, irrigation was ceased. A clear drop in fruit area and diameter ensued (Figure 55). The shrinkage lasted into the night, unaffected by the change in greenhouse conditions.

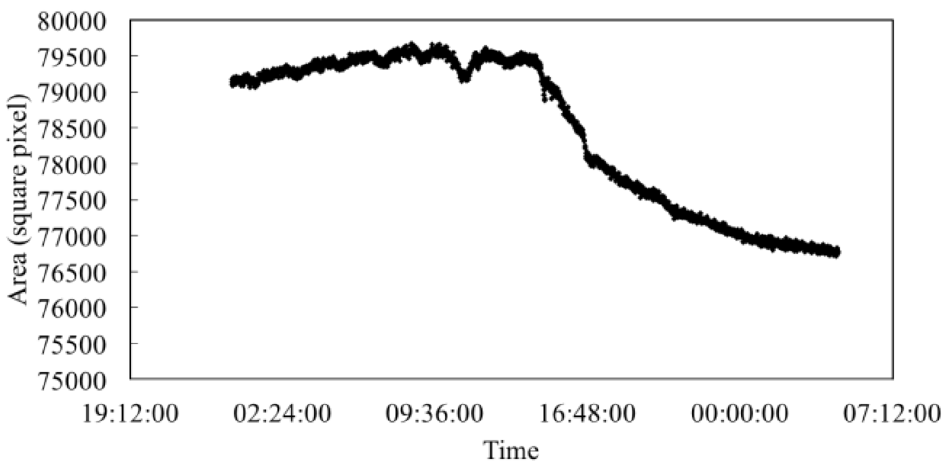

(a)

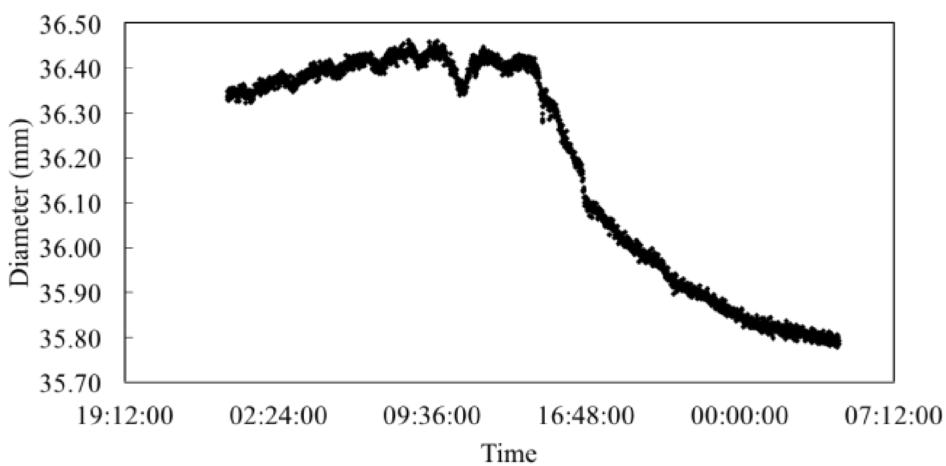

(b)

Figure 55. Growth area in (a) (pixels) and diameter in (b) (mm) patterns of the tomato fruit. The data presented is the result of a drought stress experiment. At 15:00 HR, the irrigation water was stopped.

Although the climate conditions of the growth chamber were closely similar to those of the greenhouse, no significant change in fruit area or diameter was measured in the growth chamber experiments with respect to changes in temperature, relative humidity, VPD or irrigation schedule. Regular and consistent growth over the course of the three-day periods was observed.

8.5 Discussion

From the observation of diurnal fruit growth in this study as in many others, the tomato fruit may seem to vary considerably in apparent growth rate. However, the fruit is in fact subject to a continuous true growth rate, with respect to dry matter accumulation (Johnson et al., 1992; Heuvelink, 1995). In the work by Johnson et al. (1992), tomato fruit water and dry matter content were determined at different times of the day from fresh and oven-dried weight of the fruit. Although the diameter of the tomato fruit was changing under high temperature and high solar radiation conditions, they reported that the percent dry matter did not significantly vary. On the other hand, Ehret and Ho (1986) found that true fruit growth rate is highest during the day, regardless of the water status of the fruit. Ho et al. (1987) found that during fruit development, the proportion of water imported via the xylem fell from 8-15% to 1-2% at maturity. The principal source of water for tomato fruit throughout growth was phloem sap.

As in the present study, fruit shrinkage was observed at midday under conditions that caused high plant transpiration by both Leonardi et al. (2000) and Johnson et al. (1992). Both used a linear voltage displacement transducer (LVDT) measurement technique. Johnson et al. (1992) found that higher solar radiation caused higher variation in diurnal fruit growth at the same air temperature. Day temperature was maintained at 22 ± 2 °C and night temperature was 18 ± 2°C. Relative humidity was maintained at 72 ± 5%. The fruit shrinkage was most likely caused by an increase in leaf temperature caused by the stronger solar radiation. They concluded that fruit growth is indeed closely linked to the movement of water to the fruit and that water potential gradients within a plant can directly influence fruit growth through their effects on phloem flow. Although solar radiation seems to have a great impact on diurnal fruit growth patterns, when comparing irradiance and temperature, the expansion rate of tomato fruit was most closely related to temperature (Pearce et al. 1993a). Guichard et al. (2005) indicated that tomato growth rate was highest at the end of the day (18:00 HR) and decreased to negative values (shrinkage) during the warmest and driest hours of the day, when VPD and temperature reached 2.7 kPa and 30°C, respectively. These observations are similar to those published by Lee et al., (1989), Grange and Andrews (1995), and van de Sanden and Uittien (1995), who all reported a decrease in fruit growth rate during the daytime and an increase at night. Guichard et al (2005) found that fruit diameter increased only at night unless misting was used during the day to regulate fruit shrinkage. The results from the experiments in the present study compare well with the findings of the various researchers mentioned herein.

Schilstra-vanVeelen and Bakker (1985) demonstrated an inverse relation between plant fruit load and fruit cracking. This suggests that the water status in the fruit on a low fruit load plant could vary considerably more than in the fruit on a plant with high fruit load. However, it was not clear if cracking increased because the supply of water via the phloem to each fruit was increased, or because the supply of water from the root was divided among fewer fruit. This relates to the present study: although the plants in the growth chamber produced no more than two tomato fruit each during the course of the experiments, no shrinkage or irregularities in diurnal growth pattern were noticed. All conditions were kept the same between greenhouse and growth chamber experiments except for the light reaching the plants. The fluorescent lighting of the Conviron growth chamber did not provide the same infrared radiation load. Under sunlight, the plant leaf temperature can be greatly affected by the solar radiation, beyond the effects of air temperature. It is crucial to also note that the plants grew small in comparison to the greenhouse experiments. The plant size and total leaf area was most likely not great enough to create significant variations in plant and fruit water status. Leonardi et al. (2000) reported that when more leaves were removed from tomato plants, lowering the leaf-to-fruit ratio, the effect of high VPD on fruit soluble solids and water content was less important. However, results by Demers et al. (2007) showed that cracking of greenhouse tomato was mostly influenced by total fruit load, and very little by the number of leaves between clusters. The plants in their study were nonetheless larger than the plants used for the current growth chamber experiments.

Leonardi et al., (2000) noted that if the goal is the optimization of tomato greenhouse production and quality, high VPD can reduce the mean fresh mass of fruits and their visual quality, but can also increase their soluble solid content. Their work showed that fruit growth and transpiration rates varied greatly during the daytime and that these variations were enhanced under high VPD conditions. The increase in VPD produced a significant reduction in fruit fresh mass and in fruit water content, and an increase in soluble solids, while fruit dry mass was not affected. Their results point out how improvements in the quality of tomato fruit and fresh mass yield can affect other aspects of the fruit such as soluble solid content.

Fruit cracking is a complex phenomenon because the incidence of cracking can be due to a variety of both independent and interacting environmental and physiological causes. Relatively large fruit with a large diameter (Gill & Nandpuri, 1970), thin skin and low fruit count per plant are all physiological factors that can lead to fruit cracking in tomato (Young, 1958). Raising fruit temperature dramatically increases the pressure exerted by the pulp on the skin and at the same time decreased skin stiffness and strength, increasing the incidence of cracking (Lang & During, 1990). Simard (2002) observed tomatoes under greenhouse conditions and found that cracking was positively and linearly correlated with daytime temperature averages and diurnal differences. Most environmental factors that lead to fruit cracking, including temperature, are tightly related to the plant's water status. Temperature, relative humidity and solar radiation indirectly affect the development of cracking and other issues through their influence on plant transpiration, and consequently plant and fruit water status (Dorais et al., 2004; Johnson et al., 1992). For instance, high relative humidity decreases leaf transpiration, which can result in increased fruit water supply and turgor pressure. Ho et al. (1993) found that the most likely causes of blossom end rot in susceptible cultivars was the interactions of solar radiation and temperature on fruit enlargement, as seen in this work, in addition to the plant-fruit competition for available calcium.

The easiest way to reduce the impacts of varying plant water status, such as fruit cracking, is to use commercial cultivars selected for cracking resistance (Peet, 1992). However, many cultivars susceptible to cracking are in demand or are grown for their resistances to other issues. Close-row spacing and shading have been shown to reduce cracking in tomato, but this is most likely because overall fruit size and soluble solids are reduced (Peet, 1992), which is counterproductive. Irrigation consistency is a key factor reducing cracking, but cannot entirely eradicate cracking. Therefore, greenhouse conditions that moderate the water status of the fruit, such as those created by the NVAC greenhouse, can be greatly beneficial in reducing fruit cracking and blossom end rot incidence.

Upon further examination of the data, it is clear that the tomato fruit responded to the irrigation schedule. The close-up of the area data over a 24-h period seen in Figure 53a shows how each wave in the growth pattern corresponds to a 30-min irrigation period. In an attempt to understand the irrigation response seen in the tomato fruit, the irrigation schedules of Tests 1, 2 and 3 were altered. The schedule of Test 1 was regular, at 30 min every 2 h. Test 2 was randomized, and Test 3 was 30 min every 5 h. The irrigation schedule had little impact of the amplitude of the waves, except for under severe stress conditions as seen in Test 2. Test 2 had longer periods of time between irrigation, which suggests that the plants may have been under drought stress, causing greater shrinkage. The length of the irrigation period did alter the pattern of the waves. Longer (4 and 4.5-h) irrigation periods caused an initial shrinkage, as in the 30-min periods, but in the long-term (over the 4 and 4.5-h period) caused a plateau and a subsequent regain of growth while the irrigation was sustained. The salinity of the irrigation water was modified by providing distilled water to the plants instead of full-strength Hoagland solution. The same short-term reduction in fruit size was observed in response to the activation of the irrigation, regardless of salinity.

Perhaps the sudden supply of water to the roots, with or without solutes, caused a strong enough change in plant water status to cause a short-term efflux from the fruit, but this is difficult to affirm. No similar findings have been reported. Especially under high transpiration conditions, the sudden supply of water via irrigation to the roots could cause a momentary spike in transpiration, causing the plant to draw water from elsewhere, including the water-rich fruit. Other potential causes of a fruit response to irrigation can relate to relatively brief osmotic potential difference across the various components of the plant, causing an efflux from the fruit. Dorais et al., (2001) investigated the electrical conductivity of the nutrient solution and its interactions with climatic factors and cultural practices on tomato yield and fruit quality and presented a variety of findings confirming that such interactions can be complex. Further work on the short-term responses of fruit to irrigation using machine vision measurement should be conducted.

The subtle patterns in the fruit growth measurements caused by the irrigation schedule were not observed in the growth chamber conditions. It is difficult to isolate the cause of this lack of response to the irrigation in the growth chamber experiment. However, two things are possibly involved: the use of a rockwool slab with a drip irrigation system and the smaller size of the plants. The larger reserve of water around the roots provided by the rockwool slab combined with less uptake from the smaller plants most likely moderated the variability in water relations of the plants and in turn of the fruit.

Future work should focus on the impact of varying plant and fruit water status with respect to fruit age. Adams et al. (2001) suggested that fluctuations in weekly fruit yields may result from fluctuations in temperature due to the increased sensitivity of maturing green fruits to temperature. For accurate yield and quality predictions further work is needed to quantify the precise time and degree to which fruits become more sensitive to temperature.

In somewhat contradicting work, the use of misting for increasing daytime humidity during the summer increased the incidence of fruit cracking (Bertin et al. 2000; Leonardi et al. 2000). This was reportedly due to a better plant water status, a lower plant transpiration, and an increase in the water and carbon fluxes entering the fruit (Guichard, 1999). Byari (1984) reported that high humidity increased tomato fruit cracking in the greenhouse, especially at high temperatures. Schilstra-van Veelen and Bakker (1985), on the other hand, found the least amount of cracking when greenhouse nighttime relative humidity was low and daytime relative humidity was high. Lastly, Demers et al. (2007) reported that no significant effect of varying day and night relative humidity regimens on fruit cracking was observed. Future work should study the diurnal fruit growth patterns and the final yield in fruit in terms of quality in fruit grown under the more humid daytime conditions of evaporatively cooled spaces to confirm if the findings of this study truly indicate that the NVAC system and other evaporative cooling measures lead to better quality tomato fruit.

8.6 Conclusion

We have provided direct evidence that under harsh daytime greenhouse conditions consisting of high temperatures, low relative humidity and high VPD the diurnal growth patterns of tomato fruit were irregular. Fruit shrinkage occurred on all three days of the two experiments. Under the conditions provided by the NVAC greenhouse, the diurnal fruit growth patterns were regulated and fruit shrinkage did not occur. Our work has suggested that momentary variations in fruit size were highly related to the irrigation schedule and to drought stress conditions. Based on previous literature relating common crop issues, such as cracking and blossom end rot, to highly variable fruit water status and growth, high-precision and real-time fruit growth monitoring can be useful for fruit quality improvements.

9. General Summary

9.1 General Conclusion

The objective of this research was to develop a simple and affordable method of cooling greenhouses that requires minimal energy input. A survey of current challenges in the protected agriculture industry shows that many areas of our planet can be candidate-regions for greenhouse cultivation, but that access to technology is often limiting. Moreover, the cost of the technology and the required energy input oftentimes offsets the potential revenue generated by the operations. In response to the need for a simple greenhouse climate control system in warm climates, a new method of greenhouse cooling was developed in this research project. The Natural Ventilation Augmented Cooling (NVAC) greenhouse relies on the evaporative cooling process of a misting system to provide greenhouse cooling and humidity control in an innovative way compared to traditional evaporative cooling systems, such as pad and fan systems and high-pressure fog systems. The NVAC greenhouse is naturally ventilated, with side vents and a roof vent, and improved by augmenting the thermal buoyancy and wind effects with a strategically placed misting system. The misting system is located above the gutters of the greenhouse and sprays a mist of water horizontally between the uppermost roof and an added inside roof. The added roof guides the cooled air to the plant space, prevents water droplets from reaching the crop foliage and recuperates unused misting water.

The NVAC greenhouse was tested under field conditions at two sites. A 28.1 m^2 NVAC greenhouse was built in Ste-Anne-de-Belleuve, QC, Canada for preliminary testing and validation of the NVAC system concept. A 438.4 m^2 NVAC greenhouse was built in Trents, Barbados for further development of material choice and final testing of the greenhouse design under field conditions. The final design of the NVAC greenhouse takes into consideration the constraints imposed by the climate, financial limitations and access to technology that regions of many arid and tropical climates are faced with. The NVAC greenhouse structural design was required to withstand the heavy rain and high winds typical of tropical storms but not hurricanes, as observed in Barbados. A tropical storm is defined as a tropical cyclone in which the maximum sustained surface wind speed ranges from 63 km/h to 118 km/h. For this reason, the NVAC greenhouse structures were built from existing natural ventilation greenhouses that showed proven resistance to harsh, warm climates, or built in-house entirely from locally sourced materials by using existing and proven structures as inspiration. Large gutters were incorporated into the final builds to provide rainwater harvesting for the irrigation or hydroponic systems, and for water supply to the NVAC misting system. The NVAC greenhouse design considers water and energy efficiency as it is a theme discussed across all types of protected agriculture. The components of the design that require electricity were carefully chosen to be both easily accessible in most regions of the world, affordable and energy efficient. Appendix B shows a recent build of an NVAC greenhouse in Holetown, Barbados, along with more images from the commercial build in Trents, Barbados. The 6.1 by 12.2 m greenhouse makes use of the design development accomplished in this research. This greenhouse serves as a demonstration of the potential for functional, affordable and sustainable protected agriculture projects in regions both accustomed and new to the greenhouse industry.

Field experiments were carried out on the NVAC greenhouse design throughout the course of the study. Variations in nozzle spacing, nozzle type, line pressure, misting line location, and structural design of the greenhouse were tested in similar climates under comparable daily conditions to optimize the design of the NVAC greenhouse for use in both relatively small-scale greenhouses and large-scale greenhouses. A water consumption of 0.54 $L \cdot h^{-1} \cdot m^{-2}$ at a pressure of 60 psi (414 kPa) was adequate for a 28.1 m^2 greenhouse, and 0.58 $L \cdot h^{-1} \cdot m^{-2}$ at 160 psi (1103 kPa) was sufficient for a 438.4 m^2 greenhouse. In comparison to average amounts of water used in greenhouse irrigation (1.9 to 2.5 $L \cdot m^{-2} \cdot day^{-1}$) and to the larger amount needed in arid climate greenhouse irrigation (greater than 6.8 $L \cdot m^{-2} \cdot day^{-1}$), the amount of water used in the NVAC misting system water demand represents 25% and 8%, respectively, of the irrigation water demand. In terms of performance, in its first design iteration, the NVAC greenhouse in Ste-Anne-de-Bellevue provided cooling varying from 3.1 to 4.6 °C and a relative humidity increase 2.9 to 12.1%, compared to the conditions found inside the greenhouse without the use of the NVAC system. When compared to outside conditions, the amount of cooling varied from 0.0 to 3.4 °C, and the increase in relative humidity varied from 0.0 to 25.4%. The solar radiation reaching the crop was reduced with the NVAC greenhouse design but a comparison of outside to inside PAR throughout the day showed that the transmission of PAR agreed with typical transmittance of 6-mil greenhouse cladding polyethylene film.

In the second design iteration, a different roof configuration was tested. It was assumed that a larger misting channel would increase the cooling potential of the design. The larger NVAC roof of the altered configuration had a more open arc compared to the previous configuration which reduced the PAR reaching the crop and thus reduced solar warming of the plant space. However, this second configuration did not provide cooling by means of the NVAC misting system. In comparison to conditions preceding the activation of the NVAC misting system, no temperature decrease was observed in the greenhouse when the NVAC system was activated, on the contrary there was an increase in temperature varying from 0.6 to 2.8 °C. Relative humidity did not change by any significant amount. When compared to outside conditions, the amount of cooling varied from 0.0 to 2.7 °C, and the increase in relative humidity varied from 0.0 to 15.1%. Given the poor results of this second configuration, we returned to the development of the NVAC greenhouse design based on the initial configuration.

The initial configuration of the NVAC greenhouse was scaled-up and built in Trents. After preliminary tests, the design was deemed unsuitable for the larger greenhouse size and environmental conditions of the region. A recurring draft created by the negative pressure of the prevailing wind gusts over the roof ridge pulled the mist from the rafters. Analysis of measurements showed that the system did not provide any significant cooling nor any change in relative humidity. It was deemed that the type of mist nozzle should be changed to reduce clogging and dripping, that the number of nozzles per area of greenhouse should be increased, and that the location of the misting line should be changed to reduce loss of the mist to the roof vent. Under this final configuration for larger greenhouse sizes, the responses in the greenhouse conditions to the NVAC misting system were evident. Cooling varied from 1.3 to 3.6 °C with a relative humidity increase varying from 5.6 to 17.7%, when comparing to outside conditions. When compared to the conditions inside the greenhouse without the NVAC misting system active, conditions of natural ventaltion without cooling, cooling varied from 5.2 to 6.0 °C and an increase in relative humidity varied from 2.1 to 15.8%.

A scaled-down model NVAC greenhouse was built in a controlled environment of the research greenhouse at the Macdonald Campus of McGill University. The model was tested in this controlled environment under a variety of conditions, simulating different climates ranging from mild and humid to hot and dry. Moreover, the controlled environment allowed us to limit external factors such as rain and wind, to isolate the performance of the NVAC greenhouse system. Cooling varied from 1.9 to 12.6 °C, and relative humidity was increased from 1.4 to 31.2% depending on the initial conditions in the greenhouse preceding the use of the NVAC system. Accordingly, the vapor pressure deficit (VPD) conditions were improved with the

NVAC greenhouse design. The VPD was lowered by 0.3 to 4.9 kPa, to within acceptable levels, when initial conditions were considered harsh (hot and low relative humidity). During very harsh trials with a very high initial temperature and a very low relative humidity (extremely high VPD), the system was unable to lower the VPD to within recommended levels, but nonetheless provided some relief by still significantly lowering the VPD. Use of the NVAC greenhouse in environments with very high VPD should seek a nozzle configuration with greater water flowrate by using alternate nozzles, or nozzle clusters. The water use efficiency of the NVAC greenhouse in this model study varied from 0.28 to 0.56 $L\cdot h^{-1}\cdot m^{-2}$ and is comparable to that of greenhouse fog evaporative cooling systems.

The average turbulence intensity in the plant space of the greenhouse increased to 0.32 with the use of the NVAC system, compared to 0.19 in the same structure under natural ventilation. This helped provide better ventilation and cooling across the plant space. Increased turbulence intensity in the roof vent provided the required air movement to allow the NVAC system's process to function effectively in the rafters of the greenhouse. The temperature gradient was more pronounced under NVAC system conditions, but the cooling performance of the system outweighed possible drawbacks of temperature heterogeneity.

The efficiency of the NVAC system was assessed using various methodologies and it is comparable to that of fog cooling systems, but is difficult to directly compare with that of a pad and fan cooling systems. It was determined that the NVAC greenhouse design offers performance improvements over that of fog evaporative cooling methods, for it can be used continuously rather than intermittently, limits wetting of foliage, can be used without active ventilation, and offers air movement. It is envisioned that the NVAC greenhouse design can be installed in gutter-connected multi-span greenhouses, provided each span has a roof vent. The added NVAC roof and misting system would be installed under each span.

Field and model tests on the NVAC greenhouse were conducted with no plants inside the greenhouses to simplify testing and provide uniformity across the tests. The plant responses to the NVAC greenhouse was assessed separately, first in the same model greenhouse in which the performance and air movement tests were conducted, and subsequently, under NVAC greenhouse conditions. In the plant response tests, the studied crops were subject to high stress conditions comparable to that found in a natural ventilation greenhouse in an arid semi-arid, or tropical climate. The same crops were subject to the conditions provided by the NVAC greenhouse, and comparisons were made. 'Bell Boy' pepper plants were selected as the study crop. Under daytime high temperature conditions (>35 °C but <40 °C) that also involved high vapor pressure deficit (VPD) (up to 3.9 kPa), net photosynthetic rate (P_n) and variable to maximum fluorescence ratio (F_v/F_m) in the pepper plants were significantly depressed (by 33%) compared to morning measurements. Transpiration rate was closely monitored and followed a diurnal cycle, being at a minimum rate overnight, and reaching a maximum rate shortly after 12:00 HR. It was determined that the transpiration rate followed a linear relationship with temperature, relative humidity and VPD, but was most tightly related to relative humidity. The maximum transpiration rate coincided with peak temperature and VPD. The conditions provided by the NVAC greenhouse offered an improved greenhouse climate in terms of plant growth. In contrast to when the plants were under conditions of high temperature, P_n in this case was increased by 28% from morning to afternoon. Moreover, F_v/F_m was not depressed and transpiration rate of the plants was moderated, by an average of 31%, with use of the NVAC greenhouse. By the results of the plant response study conducted, the NVAC greenhouse is able to provide an improved climate in terms of plant growth by reducing temperature stress, compared to the same greenhouse under natural ventilation and high temperature conditions. Based on known challenges in greenhouse cultivation in semi-arid, arid and tropical climates, such as saline growing media and irrigation water, the NVAC greenhouse can offer greenhouse climate control to improve crop yield and quality.

Considering the existing relationship between diurnal fruit growth rate, greenhouse climate conditions and plant water status, a device using machine vision for continuous and automatic fruit growth measurement can provide valuable information in terms of plant stress, and potential fruit yield and fruit quality. In past work, linear voltage displacement transducers (LVDTs) were used for measurement of fruit diameter in response to temperature, solar radiation and irrigation conditions. Although valuable data was obtained from these devices, certain mechanical limitations were shown to influence the measurements. A fruit growth monitoring device that makes use of automated imaging with an inexpensive camera was developed. The image capture rate was variable, allowing for real-time monitoring and longer-term monitoring of patterns. The analysis of the image provided tomato fruit area, perimeter and diameter measurements that were time-stamped and logged. This method of fruit growth monitoring is comparable to the known linear voltage displacement transducer (LVDT) method, but does not require contact with the fruit. Therefore, this imagery method offered faster response and better precision when compared to the LVDT method.

The diurnal fruit growth imagery device was used to assess the patterns in diurnal fruit growth in tomato under high temperature conditions and under NVAC system conditions. A comparison was made between the results from both sets of conditions, and it was apparent that the conditions provided by the NVAC greenhouse have a significant impact on the diurnal growth pattern of tomato fruit. It was shown by many in previous work that high temperature conditions, combined with high VPD and solar radiation, drastically increase plant transpiration rate, in some cases beyond the water uptake rate of the root system. This reaction alters the plant water status and can lead to an outflow of water from the fruit, thus causing the fruit to shrink. The exact rate of outflow and resulting fruit shrinkage can vary depending on plant size, fruit size and fruit count on the plant. Based on previous work on the plant reactions to the NVAC greenhouse system that showed control of the transpiration rate in pepper plants, it was suggested that the conditions provided by the NVAC system could also offer control over diurnal fruit growth patterns. With use of the NVAC system, the growth of the tomato fruit was kept relatively uniform on a diurnal basis. This is in contrast to the growth patterns seen under high temperature conditions, where significant shrinkage occurred during the daytime. It was suggested by many that the daily variation in fruit growth due to changing water fluxes could have a major impact on fruit cracking as variations in tension forces on the fruit skin are associated with changes in fruit turgor pressure. In earlier work, it was shown that early morning and late afternoon are the most likely moments of the day for initiation of cracking, for plant transpiration may be drastically low while water uptake remains high. In previous work on bell pepper, a daily cycle of fruit shrinkage and expansion resulted in severe cracking. Based on the fruit growth results obtained in this research, the use of the NVAC system in the cultivation of fruit bearing crops can potentially alleviate the incidence of fruit cracking by regulating the diurnal growth rate of the fruit. Additionally, secondary fruit response patterns were observed in response to irrigation schedules and drought conditions. Although conditions of high temperature, low humidity and high solar radiation can be causes of cracking, especially in plant species prone to cracking, high humidity conditions have also been related to cracking, amongst other more obvious problematic matters of high humidity such as disease. During use, proper attention to the greenhouse climate conditions provided by the NVAC greenhouse is important to not exceed the recommended humidity conditions for the given crop.

9.2 Further Suggested Studies

In this research project, the NVAC greenhouse design was developed and tested at two field locations and under a control environment. Two different sizes of greenhouse were tested and showed promising results in terms of climate control. The influence that the NVAC system has on the plants housed within the greenhouse were examined using a variety of methodologies. The NVAC system was able to improve the growing environment of the greenhouse in terms of reducing plant stress that can influence growth, yield and quality. Nonetheless, future studies could improve the use of the technology and our understanding of it.

- Climate measurements were done without plants in the greenhouse. The type of crop and the position of the crop can greatly impact the air movement in the greenhouse. Temperature and relative humidity are greatly affected by the presence of crop inside the greenhouse. Future studies should explore the climate and airflow characteristics of the NVAC greenhouse design with a crop.

- The NVAC greenhouse was designed for single-span greenhouses. It is likely that the NVAC greenhouse design can be installed in gutter-connected multi-span greenhouses, provided each span has a roof vent. An added inside NVAC roof and misting system would be installed under each span. The greenhouse climate provided by such a design would differ from a single-span greenhouse and significant design modifications may be required to tailor the NVAC greenhouse design to multi-span greenhouses. Future work should investigate the NVAC greenhouse design's applicability in multi-span greenhouses.
- Computational fluid dynamics (CFD) can be used to simulate and develop designs with complex systems, such as greenhouses. The NVAC greenhouse design can be potentially further developed and optimized with use of CFD simulation and analysis. The results of the greenhouse airflow and climate experiment in a controlled environment in this research can serve as a basis for future CFD work.
- A study of the long-term impact that the NVAC greenhouse design may have on the crop growth, yield and quality would generate valuable information for commercialization of

the design. A comprehensive set of experiments should quantify the yield and quality of certain important greenhouse crops, such as tomato and pepper, under the NVAC greenhouse design.

- Poultry and other agricultural operations make use of natural ventilation designs and evaporative cooling for climate control. Many renounce the use of high pressure fogging systems as the sanitary repercussions in animal husbandry are far more apparent than in plant cultivation. The NVAC system can potentially be used in the cooling of poultry houses by use inside the buildings, as in greenhouse operations, or outside the building by installing an NVAC misting channel over the air inlets.
- The machine vision fruit growth measurement device that was developed in this project can be refined to increase precision and ease of use. The script used to process and analyze the images can be improved to increase computing speed and flexibility in terms of different types of fruit.

9.3 Contributions to Knowledge

The work presented in this thesis demonstrates the performance and applicability of the natural ventilation augmented cooling (NVAC) greenhouse design in the protected agriculture industry. The experimental methods used and their results provide direct evidence that the NVAC greenhouse can provide an improved growing environment for greenhouse crop. A variety of experiments were conducted and the main contributions of this research include:

1. The development of a new greenhouse design and climate control system that provides cooling, humidity and air movement through evaporative cooling without the use of fans. Existing greenhouse operations can benefit from this technology by reducing energy consumption, and new operations can be made possible by offering climate control in a low cost, accessible and sustainable format.
2. The establishment of design characteristics including NVAC roof shape, mist nozzle count per greenhouse area and volume, nozzle location and system water consumption rates depending on the intended use of the NVAC greenhouse, such as greenhouse size, local climate and amount of cooling desired.
3. The establishment of certain greenhouse design characteristics and considerations that

make the use of greenhouse technologies possible in regions of the world where the required technologies are lacking or are not financially accessible.

4. The establishment of the cooling performance and efficiency of the NVAC greenhouse in different warm climates with varying temperatures, relative humidities and vapor pressure deficits.
5. The investigation of plant responses to climatic stresses including high temperatures, high vapor pressure deficit and low relative humidity. High temperature and low humidity conditions induced stress in plants by thermally induced damage and excessive transpiration.
6. The investigation of plant responses to the inside climate provided by NVAC greenhouse. The NVAC greenhouse was able to provide conditions that alleviated plant stresses seen under the climatic stresses mentioned in (5).
7. The development of a new machine vision method of fruit size measurement capable of measuring real-time and diurnal patterns of fruit growth. The precision of the new methodology surpasses previously used devices and is capable of detecting short-term changes in growth patterns in fruit that were previously undetectable.

10. References

Abbott, J. D., Peet, M. M., Willits, D. H., Sanders, D. C., & Gough, R. E. (1986). Effects of irrigation frequency and scheduling on fruit production and radial fruit cracking in greenhouse tomatoes in soil beds and in a soil-less medium in bags. Scientia Horticulturae, 28(3), 209-217.

Abdel-Ghany, A. M. & Kozai, T. (2006). Cooling efficiency of fogging systems for greenhouses. Biosystems Engineering, 94(1), 97-109.

Abdel-Ghany, A. M., Al-Helal, I. M., Alzahrani, S. M., Alsadon, A. A., Ali, I. M., & Elleithy, R. M. (2012). Covering materials incorporating radiation-preventing techniques to meet greenhouse cooling challenges in arid regions: a review. The Scientific World Journal.

Acock, B., Charles-Edwards, D. A., & Hand, D. W. (1976). An analysis of some effects of humidity on photosynthesis by a tomato canopy under winter light conditions and a range of carbon dioxide concentrations. Journal of Experimental Botany, 27(5), 933-941.

Adams, P., & Ho, L. C. (1995). Uptake and distribution of nutrients in relation to tomato fruit quality. In I International Symposium on Solanacea for Fresh Market, 412, 374-387.

Adams, S. R., Cockshull, K. E., & Cave, C. R. J. (2001). Effect of temperature on the growth and development of tomato fruits. Annals of Botany, 88(5), 869-877.

Ahmed, E. M., Abaas, O., Ahmed, M., & Ismail, M. R. (2011). Performance evaluation of three different types of local evaporative cooling pads in greenhouses in Sudan. Saudi Journal of Biological Sciences, 18(1), 45-51.

Al-Helal, I. M. (2007). Effects of ventilation rate on the environment of a fan-pad evaporatively cooled, shaded greenhouse in extreme arid climates. Applied Engineering in Agriculture, 23(2), 221-230.

Al-Helal, I. M., & Alhamdan, A. M. (2009). Effect of arid environment on radiative properties of greenhouse polyethylene cover. Solar Energy, 83(6), 790-798.

Al-Helal, I. M., & Abdel-Ghany, A. M. (2011). Measuring and evaluating solar radiative properties of plastic shading nets. Solar Energy Materials and Solar Cells, 95(2), 677-683.

Al-Helal, I. M., & Alhamdan, A. M. (2009). Effect of arid environment on radiative properties of greenhouse polyethylene cover. Solar Energy, 83(6), 790-798.

Al-Helal, I., Al-Abbadi, N., & Al-Ibrahim, A. (2004). A study of fan-pad performance for a photovoltaic powered greenhouse in Saudi Arabian summer. International Agricultural Engineering Journal, 1, 14.

Al-Ismaili, A. M., & Jayasuriya, H. (2016). Seawater greenhouse in Oman: A sustainable technique for freshwater conservation and production. Renewable and Sustainable Energy Reviews, 54, 653-664.

Al-Jamal, K. (1994). Greenhouse cooling in hot countries. Energy, 19(11), 1187-1192.

Al-Massoum, A., Haffar, I., & Mahmoud Ahmed, H. (1997). A similitude model for testing greenhouse evaporative cooling pads under the hot-arid conditions of the UAE. II Modelling Plant Growth, Environmental Control and Farm Management in Protected Cultivation 456, 329-338.

Al-Mulla, Y. A. (2006). Cooling greenhouses in the Arabian Peninsula. In International Symposium on Greenhouse Cooling, 719, 499-506.

Albaho, M., Thomas, B., Isathali, S., George, P., & Ghloum, D. (2013). Alternative growing media for Growbag tomato production in Kuwait. In International Symposium on New Technologies for Environment Control, Energy-Saving and Crop Production in Greenhouse, 1037, 1087-1091.

Albright, L. D. (1995). Controlling greenhouse ventilation inlets by pressure difference. HortTechnology, 5(3), 260-264.

Albright, L. D. (2001). Controlling greenhouse environments. International Symposium on Design and Environmental Control of Tropical and Subtropical Greenhouses, 578, 47-54.

Alhamdan, A. M., & Al-Helal, I. M. (2009). Mechanical deterioration of polyethylene greenhouses covering under arid conditions. Journal of Materials Processing Technology, 209(1), 63-69.

Ali, H. M., Moustafa, S., & El-Mansy, H. (1990). An efficient greenhouse design for hot climates. Energy Conversion and Management, 30(4), 433-437.

Alomran, A. M., Louki, I. I., Aly, A. A., & Nadeem, M. E. (2013). Impact of deficit irrigation on soil salinity and cucumber yield under greenhouse condition in an arid environment. Journal of Agricultural Science and Technology, 15(6), 1247-1259.

Aloni, B., Karni, L., Moreshet, S., Yao, C., & Stanghellini, C. (1999). Cuticular cracking in bell pepper fruit: II. Effects of fruit water relations and fruit expansion. The Journal of Horticultural Science and Biotechnology, 74(1), 1-5.

Aloni, B., Peet, M., Pharr, M., & Karni, L. (2001). The effect of high temperature and high atmospheric CO2 on carbohydrate changes in bell pepper (Capsicum annuum) pollen in relation to its germination. Physiologia Plantarum, 112(4), 505-512.

ASABE. (2003). ANSI/ASAE EP 406.4. 2003 Standard: heating, ventilation and cooling greenhouses. American Society of Agricultural and Biological Engineers, MI, USA

Anderson, B. (1995). Greenhouse Tomato Production Practices. University of Kentucky. Available from <http://www.uky.edu/Ag/CCD/anderson/gh_tom.htm>

Anderson, M. S., Ewert, M. K., Keener, J. F. & Wagner, S. A. (2015). Life Support Baseline Values and Assumptions Document. NASA/TP-2015-218570. Available from <http://ston. jsc. nasa. gov/collections/TRS/_techrep/TP-2015-218570. pdf.>

Andrews, J. R., Fryer, M. J., & Baker, N. R. (1995). Characterization of chilling effects on photosynthetic performance of maize crops during early season growth using chlorophyll fluorescence. Journal of Experimental Botany, 46(9), 1195-1203.

Aphalo, P. J., & Jarvis, P. G. (1991). Do stomata respond to relative humidity? Plant, Cell & Environment, 14(1), 127-132.

Arbel, A., Barak, M. & Shklyar, A. (2003). Combination of forced ventilation and fogging systems for cooling greenhouses, Biosystems Engineering, 84(1), 45–55.

Arbel, A., O. Yekutieli & M. Barak. (1999). Performance of a fog system for cooling greenhouses. Journal of Agricultural Engineering Research, 2(72): 129–136.

ASHRAE. (1985). Handbook of Fundamentals. American Society of Heating, Refrigerating and Air-Conditioning Engineers, Atlanta GA.

Bai, Y., & Lindhout, P. (2007). Domestication and breeding of tomatoes: what have we gained and what can we gain in the future?. Annals of Botany, 100(5), 1085-1094.

Bailey, B.J., Montero, J.I., Pérez-Parra, J., Robertson, A.P., Baeza, E., & Kamaruddin, R. (2003). Airflow resistance of greenhouse ventilators with and without insect screens. Biosystems Engineering, 86, 217–229.

Bailey, B.J., Montero, J.I., Pérez-Parra, J., Robertson, A.P., Baeza, E., & Kamaruddin, R. (2003). Airflow resistance of greenhouse ventilators with and without insect screens. Biosystems Engineering, 86, 217–229.

Baille, A. (2000). Trends in greenhouse technology for improved climate control in mild winter climates. 5th International Symposium on Protected Cultivation in Mild Winter Climates: Current Trends for Sustainable Technologies 559, 161-168.

Baille, A., Kittas, C., & Katsoulas, N. (2001). Influence of whitening on greenhouse microclimate and crop energy partitioning. Agricultural and forest meteorology, 107(4), 293-306.

Bakker, J.C., Bot, G.P.A., Challa, H. & Van de Braak, N.J. (1995). Greenhouse climate control. an integrated approach. Wageningen Academic Publishers, Wageningen.

Bamsey, M., Graham, T., Stasiak, M., Berinstain, A., Scott, A., Vuk, T. R., & Dixon, M. (2009). Canadian advanced life support capacities and future directions. Advances in Space Research, 44(2), 151-161.

Baptista, F. J., Bailey, B. J., Randall, J. M., & Meneses, J. F. (1999). Greenhouse ventilation rate: theory and measurement with tracer gas techniques. Journal of Agricultural Engineering Research, 72(4), 363-374.

Barbier, E. B. (2004). Explaining agricultural land expansion and deforestation in developing countries. American Journal of Agricultural Economics, 86(5), 1347-1353.

Barta, D. J., Tibbitts, T. W., Bula, R. J., & Morrow, R. C. (1992). Evaluation of light emitting diode characteristics for a space-based plant irradiation source. Advances in Space Research, 12(5), 141-149.

Bartok, J. & Grubinger, V. (2015). Horizontal air flow is best for greenhouse air circulation. The farm energy community of practice. Available from <http://articles.extension.org/pages/28043/horizontal-air-flow-is-best-for-greenhouse-air-circulation>

Basirat, M., & Davoodi, H. (2014). Study the possibility of soil less growing Media production from Local Resources For some greenhouse crops. The Food and Agriculture Organization of the United Nations.

Battisti, D. S., & Naylor, R. L. (2009). Historical warnings of future food insecurity with unprecedented seasonal heat. Science, 323(5911), 240-244.

Benoit, F., & Ceustermans, N. (1994). Horticultural aspects of ecological soilless growing methods. Hydroponics and Transplant Production, 396, 11-24.

Berlinger, M. J., Jarvis, W. R., Jewett, T. J., & Lebiush-Mordechi, S. (1999). Managing the greenhouse, crop and crop environment. In Integrated Pest and Disease Management in Greenhouse Crops (pp. 97-123). Springer Netherlands.

Berry, J., & Bjorkman, O. (1980). Photosynthetic response and adaptation to temperature in higher plants. Annual Review of Plant Physiology, 31(1), 491-543.

Bertin, N., Guichard, S., Leonardi, C., Longuenesse, J. J., Langlois, D., & Navez, B. (2000). Seasonal evolution of the quality of fresh glasshouse tomatoes under Mediterranean conditions, as affected by air vapour pressure deficit and plant fruit load. Annals of Botany, 85(6), 741-750.

Beshada, E., Zhang, Q., & Boris, R. (2006). Winter performance of a solar energy greenhouse in southern Manitoba. Canadian Biosystems Engineering, 48(5), 1-8.

Besthorn, F. H. 2013. Vertical farming: Social work and sustainable urban agriculture in an age of global food crises. Australian Social Work, 66(2), 187-203.

Böhme, M., Schevchenko, J., Pinker, I., & Herfort, S. 2005. Cucumber grown in sheepwool slabs treated with biostimulator compared to other organic and mineral substrates. In International Symposium on Growing Media, 779, 299-306.

Boone, R. M., Brown, R. J., Cole, N. A., & Thornton, S. R. 2007. Vegetable Production Facility Pilot for Arviat, Nunavut. University of Guelph, ON, Canada.

Bot, G. P. A. (1983). Greenhouse climate: from physical process to a dynamic model. Ph.D. dissertation, Agricultural University of Wageningen, Wageningen, The Netherlands.

Both, A. J., Benjamin, L., Franklin, J., Holroyd, G., Incoll, L. D., Lefsrud, M. G., & Pitkin, G. (2015). Guidelines for measuring and reporting environmental parameters for experiments in greenhouses. Plant Methods, 11(1), 43.

Boulard, T., & Draoui, B. (1995). Natural ventilation of a greenhouse with continuous roof vents: measurements and data analysis. Journal of Agricultural Engineering Research, 61(1), 27-35.

Boulard T; Papadakis G; Kittas C; Mermier M. (1997). Air flow and associated sensible heat exchanges in a naturally ventilated greenhouse. Agricultural and Forest Meteorology, 88, 111-119.

Boulard, T; Meneses, J. F., Mermier, M., Papadakis, G. (1996). The mechanisms involved in the natural ventilation of greenhouses. Agricultural and Forest Meteorology, 79, 61-77.

Boulard, T., Kittas, C., Papadakis, G., & Mermier, M. (1998). Pressure field and airflow at the opening of a naturally ventilated greenhouse. Journal of Agricultural Engineering Research, 71(1), 93-102.

Boulard, T., Kittas, C., Papadakis, G., & Mermier, M. (1998). Pressure field and airflow at the opening of a naturally ventilated greenhouse. Journal of Agricultural Engineering Research, 71(1), 93-102.

Boulard, T., Wang, S., & Haxaire, R. (2000). Mean and turbulent air flows and microclimatic patterns in an empty greenhouse tunnel. Agricultural and Forest Meteorology, 100(2), 169-181.

Boulard, T., S. Wang. (2000). Greenhouse crop transpiration simulation from external climate conditions. Agric. Forest Meteorol. 100:25-34.

Briassoulis, D., Waaijenberg, D., Gratraud, J., & Von Elsner, B. (1997). Mechanical properties of covering materials for greenhouses part 2: quality assessment. Journal of Agricultural Engineering Research, 67(3), 171-217.

Bruce, J. M. (1978). Natural convection through openings and its application to cattle building ventilation. Journal of Agricultural Engineering Research, 23(2), 151-167.

Bruce, J. M. (1982). Ventilation of a model livestock building by thermal buoyancy. Transactions of the American Society of Agricultural Engineers, 25(6), 1724-1726.

Buchholz, M., Jochum, P. & Zaragoza, G. (2005). Concept for water, heat and food supply from a closed greenhouse - The Watergy Project. Acta Horticulturae, 691, 509-516.

Buchholz, M., Buchholz, R., Jochum, P., Zaragoza, G. &Pérez-Parra, J. (2006). Temperature and humidity control in the Watergy greenhouse. In International Symposium on Greenhouse Cooling, 719, 401-408.

Bucklin, R. A., Leary, J. D., Rygalov, V., Mu, Y., & Fowler, P. A. (2001). Design parameters for Mars deployable greenhouses No. 2001-01-2428. Society of Automotive Engineers.

Bucklin. R. A. (2015). Florida Greenhouse Design BUL235/AE016. Available from <http://edis.ifas.ufl.edu/ae016>

Buffington, D. E., Bucklin, R. A., Henley, R. W., & McConnell, D. B. (2013). Greenhouse ventilation. The Institute of Food and Agricultural Sciences Extension Service, University of Florida, Publication AE-10.

Buffington, D.E., Bucklin, R.A., Henley, R.W., & McConnell, D.B. (2013). Greenhouse ventilation. The Institute of Food and Agricultural Sciences Extension Service, University of Florida, Publication AE-10.

Burns, S. P., Horst, T. W., Jacobsen, L., Blanken, P. D., & Monson, R. K. (2012). Using sonic anemometer temperature to measure sensible heat flux in strong winds. Atmospheric Measurement Techniques, 5(9), 2095-2111.

Byari, S. H. (1984). Physiological, Genetic, and Breeding Studies of Tolerance to High Temperature and High Relative Humidity in Tomatoes (Lycopersicon Esculentum Mill.). Ph.D. Dissertation. The University of Nebraska, Lincoln.

Camejo, D., Rodríguez, P., Morales, M. A., Dell'Amico, J. M., Torrecillas, A., & Alarcón, J. J. (2005). High temperature effects on photosynthetic activity of two tomato cultivars with different heat susceptibility. Journal of Plant Physiology, 162(3), 281-289.

Campra, P., Garcia, M., Canton, Y., & Palacios-Orueta, A. (2008). Surface temperature cooling trends and negative radiative forcing due to land use change toward greenhouse farming in southeastern Spain. Journal of Geophysical Research: Atmospheres, 113(D18).

Castilla, N. (2000). Current situation and future prospects of protected crops in the Mediterranean region. International Symposium on Mediterranean Horticulture: Issues and Prospects, 582, 135-147.

Castilla, N., & Hernández, J. (2005). The plastic greenhouse industry of Spain. Chronica Horticulturae, 45(3), 15-20.

Castilla, N., & Hernandez, J. (2006). Greenhouse technological packages for high-quality crop production. XXVII International Horticultural Congress-IHC2006: International Symposium on Advances in Environmental Control, Automation 761, 285-297.

Castilla, N. (1993). Greenhouses in the Mediterranean area: technological level and strategic management. International Symposium on New Cultivation Systems in Greenhouse, 361, 44-56.

Castilla, N., & Montero, J. I. (2008). Environmental control and crop production in Mediterranean greenhouses. International Workshop on Greenhouse Environmental Control and Crop Production in Semi-Arid Regions, 797, 25-36.

Castilla, N., Lopez-Galvez, J. (1994). Vegetable responses in improved low-plastic greenhouses. Journal of Horticultural Science, 69, 915-921.

Chaibi, M. T. (2000). An overview of solar desalination for domestic and agriculture water needs in remote arid areas. Desalination, 127(2), 119-133.

Chan, H. M., Fediuk, K., Hamilton, S., Rostas, L., Caughey, A., Kuhnlein, H., & Loring, E. (2006). Food security in Nunavut, Canada: barriers and recommendations. International Journal of Circumpolar Health, 65(5).

Chandra, P., Singh, J. K., & Majumdar, G. (1989). Some results of evaporative cooling of a plastic greenhouse. Journal of Agricultural Engineering, 26(3), 274-280.

Chau, J., Sowlati, T., Sokhansanj, S., Preto, F., Melin, S., & Bi, X. (2009). Economic sensitivity of wood biomass utilization for greenhouse heating application. Applied Energy, 86(5), 616-621.

Chinese, D., Meneghetti, A., & Nardin, G. 2005. Waste-to-energy based greenhouse heating: exploring viability conditions through optimisation models. Renewable Energy, 30(10), 1573-1586.

Choi, K. H. G. H., Lee, G., Han, Y. J., & Bunn, J. M. (1995). Tomato maturity evaluation using color image analysis. Transactions of the American Society of Agricultural Engineers, 38(1), 171-176.

Clawson, K. L., & Blad, B. L. (1982). Infrared thermometry for scheduling irrigation of corn. Agronomy journal, 74(2), 311-316.

Cohen, J. E., & Small, C. (1998). Hypsographic demography: The distribution of human population by altitude. Proceedings of the National Academy of Sciences, 95(24), 14009-14014.

Connellan, G. J. (2001). Selection of greenhouse design and technology options for high temperature regions. International Symposium on Design and Environmental Control of Tropical and Subtropical Greenhouses, 578,113-117.

Corral, F. J. C., Castaño, S. B., Fernández, M. D. F., García, M. R. G., & Hernández, J. C. L. (2016). Lysimetry methods for monitoring soil solution electrical conductivity and nutrient concentration in greenhouse tomato crops. Agricultural Water Management, 178, 171-179.

Corvalan, C., Hales, S., & McMichael, A. J. (2005). Ecosystems and human well-being: health synthesis. The World Health Organization.

Coulson, S., Hodkinson, I. D., Strathdee, A., Bale, J. S., Block, W., Worland, M. R., & Webb, N. R. (1993). Simulated climate change: the interaction between vegetation type and microhabitat temperatures at Ny Ålesund, Svalbard. Polar Biology, 13(1), 67-70.

Council of Canadian Academies. Expert Panel on the State of Knowledge of Food Security in Northern Canada. (2014). Aboriginal food security in Northern Canada: an assessment of the state of knowledge. Ottawa, ON, Canada.

Critten, D. L., & Bailey, B. J. (2002). A review of greenhouse engineering developments during the 1990s. Agricultural and forest Meteorology, 112(1), 1-22.

Dagtekin, M., Karaca, C., & Yıldız, Y. (2009). Performance characteristics of a pad evaporative cooling system in a broiler house in a Mediterranean climate. Biosystems engineering, 103(1), 100-104.

Davies, J. N., Hobson, G. E., & McGlasson, W. B. (1981). The constituents of tomato fruit—the influence of environment, nutrition, and genotype. Critical Reviews in Food Science & Nutrition, 15(3), 205-280.

Davies, P. A. (2005). A solar cooling system for greenhouse food production in hot climates. Solar Energy, 79(6), 661-668.

Davies, P. A., & Paton, C. (2005). The seawater greenhouse in the United Arab Emirates: thermal modelling and evaluation of design options. Desalination, 173(2), 103-111.

De Jong, T., (1990). Natural ventilation of large multi-span greenhouses. Ph.D. Dissertation, Wageningen Agricultural University, The Netherlands.

De Swaef, T., Verbist, K., Cornelis, W., & Steppe, K. (2012). Tomato sap flow, stem and fruit growth in relation to water availability in rockwool growing medium. Plant and Soil, 350(1-2), 237-252.

Dearborn, C. (1979). Horticultural limitations and potential of Alaska's Arctic, particularly the Kobuk River Region. Arctic. 32(3): 248-262.

Debevec, E. M., & MacLean Jr, S. F. (1993). Design of greenhouses for the manipulation of temperature in tundra plant communities. Arctic and Alpine Research, 56-62.

Deelstra, T., & Girardet, H. (2000). Urban agriculture and sustainable cities. In: Bakker, N., Dubbeling, M., Gündel, S., Sabel-Koshella, U., & de Zeeuw, H. Growing cities, growing food. Urban agriculture on the policy agenda. Feldafing, Germany: Zentralstelle für Ernährung und Landwirtschaft (ZEL), 43-66.

DeGannes, A., Heru, K.R., Mohammed, A., Paul, C., Rowe, J., Sealy, L., & Seepersad, G. (2014). Tropical greenhouse manual for the Caribbean. In: Increased production of vegetables and herbs through the use of protected agriculture in the Caribbean. St. Augustine, UWI Trinidad and Tobago. The Caribbean Agricultural Research and Development Institute (CARDI).

Demers, D. A., Dorais, M., & Papadopoulos, A. P. (2007). Yield and russeting of greenhouse tomato as influenced by leaf-to-fruit ratio and relative humidity. HortScience, 42(3), 503-507.

Despommier, D. (2009). The rise of vertical farms. Scientific American, 301(5), 80-87.

Despommier, D. (2011). The vertical farm: controlled environment agriculture carried out in tall buildings would create greater food safety and security for large urban populations. Journal für Verbraucherschutz und Lebensmittelsicherheit, 6(2), 233-236.

Despommier, D. (2013). Farming up the city: the rise of urban vertical farms. Trends in Biotechnology, 31(7), 388-389.

Dieckmann, J., Roth, K., & Brodrick, J. (2008). Liquid desiccant air conditioners. ASHRAE Journal, 50(10), 90-95.

Dixon, M. A., Grace, J., & Tyree, M. T. (1984). Concurrent measurements of stem density, leaf and stem water potential, stomatal conductance and cavitation on a spaling of Thuja occidentalis L. Plant, Cell & Environment, 7(8), 615-618.

Dorais, M., Demers, D. A., Papadopoulos, A. P., & Van Ieperen, W. (2004). Greenhouse tomato fruit cuticle cracking. Horticultural Reviews, 30, 163-184.

Dorais, M., Papadopoulos, A. P., & Gosselin, A. (2002). Greenhouse tomato fruit quality. Horticultural Reviews, 26, 239-349.

Dorais, M., Papadopoulos, A., & Gosselin, A. (2001). Influence of electric conductivity management on greenhouse tomato yield and fruit quality. Agronomie, 21(4), 367-383.

Drysdale, A., Ewert, M., & Hanford, A.J. (1999). Equivalent System Mass Studies of Missions and Concepts. Society of Automotive Engineers Technical Paper, ICES 1999-01-2081.

Dukes, M. D., & Scholberg, J. M. (2005). Soil moisture controlled subsurface drip irrigation on sandy soils. Applied Engineering in Agriculture, 21(1), 89-101.

Dvorak, B., & Volder, A. (2010). Green roof vegetation for North American ecoregions: a literature review. Landscape and Urban Planning, 96(4), 197-213.

El-Sharkawy, M. A., Cock, J. H., & Hernandez, A. (1985). Stomatal response to air humidity and its relation to stomatal density in a wide range of warm climate species. Photosynthesis Research, 7(2), 137-149.

Eder, C., Valente, V., Donaldson, N., & Demosthenous, A. (2014). A cmos smart temperature and humidity sensor with combined readout. Sensors, 14(9), 17192-17211.

Ehret, D.L., Ho, L.C. (1986). Effects of osmotic potential in nutrient solution on diurnal growth of tomato fruit. Journal of Experimental Botany, 37(9), 1294-1302.

Ehret, D., Lau, A., Bittman, S., Lin, W., & Shelford, T. (2001). Automated monitoring of greenhouse crops. Agronomie, 21(4), 403-414.

Eigenbrod, C., & Gruda, N. (2015). Urban vegetable for food security in cities. A review. Agronomy for Sustainable Development, 35(2), 483-498.

Environment Canada. 2016. Canadian Climate Normals 1981-2010 Station Data. 02 Feb. 2017. Accessible from < http://climate.weather.gc.ca/climate_normals/results_1981_2010_e.html?stnID=1750&autofwd=1>

Espi, E., Salmeron, A., Fontecha, A., García, Y., & Real, A. I. (2006). Plastic films for agricultural applications. Journal of Plastic Film and Sheeting, 22(2), 85-102.

Exner-Pirot, H. 2012. Guidelines for Establishing a Northern Greenhouse Project. International Center for Northern Governance and Development. Accessible from < https://www.usask.ca/icngd/publications/reports/Reports-Files/Northern%20Greenhouse%20Guidelines_FINAL.pdf >

Farrell, E., Hassan, M. I., Tufa, R. A., Tuomiranta, A., Avci, A. H., Politano, A., & Arafat, H. A. (2017). Reverse electrodialysis powered greenhouse concept for water-and energy-self-sufficient agriculture. Applied Energy, 187, 390-409.

Fereres, E., & Soriano, M. A. (2007). Deficit irrigation for reducing agricultural water use. Journal of Experimental Botany, 58(2), 147-159.

Fernandez, J. E., & Bailey, B. J. (1994). The influence of fans on environmental conditions in greenhouses. Journal of Agricultural Engineering Research, 58(2-3), 201-210.

Fernández, M. D., Bonachela, S., Orgaz, F., Thompson, R., López, J. C., Granados, M. R., & Fereres, E. (2010). Measurement and estimation of plastic greenhouse reference evapotranspiration in a Mediterranean climate. Irrigation Science, 28(6), 497-509.

Fernandes, C., Corá, J. E., & Araújo, J. A. C. D. (2003). Reference evapotranspiration estimation inside greenhouses. Scientia Agricola, 60(3), 591-594.

Ferreira, R. D. C., Bezerra, R. D. S., & Rosa, J. Q. (2014). Effects of light intensity modification by reflective aluminized screenhouse on sweet pepper growth and yield. Engenharia Agrícola, 34(4), 626-635.

Fischetti, M. (2008). Growing vertical. Scientific American, 18, 74-79.

Flores, F. B., Sanchez-Bel, P., Estan, M. T., Martinez-Rodriguez, M. M., Moyano, E., Morales, B. & Romojaro, F. (2010). The effectiveness of grafting to improve tomato fruit quality. Scientia Horticulturae, 125(3), 211-217.

Franco, A., Valera, D. L., & Peña, A. (2014). Energy Efficiency in greenhouse evaporative cooling techniques: cooling boxes versus Cellulose Pads. Energies, 7(3), 1427-1447.

Franco, A., Valera, D. L., Peña, A., & Pérez, A. M. (2011). Aerodynamic analysis and CFD simulation of several cellulose evaporative cooling pads used in Mediterranean greenhouses. Computers and Electronics in Agriculture, 76(2), 218-230.

Frausto, H.U. & J.G. Pieters. (2004). Modelling greenhouse temperature using system identification by means of neural networks. Neurocomputing 56: 423-428.

Fuchs, M., Dayan, E., & Presnov, E. (2006). Evaporative cooling of a ventilated greenhouse rose crop. Agricultural and Forest Meteorology, 138(1), 203-215.

Gale, J. 1981. Controlled environment agriculture for hot desert regions. Symposium-British Ecological Society.

Ganpat, W. G (2014). Impacts of climate change on food security in Small Island Developing States. IGI Global.

Garcia, M. L., Medrano, E., Sanchez-Guerrero, M. C., & Lorenzo, P. (2011). Climatic effects of two cooling systems in greenhouses in the Mediterranean area: External mobile shading and fog system. Biosystems Engineering, 108(2), 133-143.

Gaudet, P., Tawil, S., & Lefsrud, M. (2014). Canadian Integrated Northern Greenhouse (CING): Designing the Outer Structure and Pivoting Hydroponic Systems. American Society of Agricultural and Biological Engineers Annual International Meeting, Montreal, Canada.

Gastélum-Barrios, A., Bórquez-López, R. A., Rico-García, E., Toledano-Ayala, M., & Soto-Zarazúa, G. M. (2011). Tomato quality evaluation with image processing: A review. African Journal of Agricultural Research, 6(14), 3333-3339.

Ghidiu, G. M. & W. J. Roberts. (2002). Greenhouse Screening for Insect Control. Rutgers Coop. Ext., Publication FS640.

Ghosal, M. K., Tiwari, G. N., & Srivastava, N. S. L. (2004). Thermal modeling of a greenhouse with an integrated earth to air heat exchanger: an experimental validation. Energy and Buildings, 36(3), 219-227.

Giacomelli G, Castilla N, Vanhenten E, Mears D, Sase S (2008) Innovation in greenhouse engineering. Acta Hortic 801:75–88

Giacomelli, G. A., & Roberts, W. J. (1993). Greenhouse covering systems. HortTechnology, 3(1), 50-58.

Giacomelli, G., & Roberts, W. (1986). Try alternate methods of evaporative cooling. Energy Conservation and Solar Energy Utilization in Horticultural Engineering, 257, 29-30.

Giacomelli, G. A., Giniger, M. S., Krass, A. E., & Mears, D. R. (1985). Improved methods of greenhouse evaporative cooling. Symposium on Greenhouse Climate and its Control, 174, 49-56.

Giacomelli, G.A. (2003). Evaporative cooling system: mist and fog. Controlled Environment Agricultural Center, Agricultural & Biosystems Engineering Department, The University of Arizona.

Giaveno, C., & Ferrero, J. (2003). Introduction of tropical maize genotypes to increase silage production in the central area of Santa Fe, Argentina. Crop Breeding and Applied Biotechnology, 3, 89-94.

Gill, P. S., & Nandpuri, K. S. (1970). Lycopersicon esculentum Mill. Indian Journal of Agricultural Science, 40(1), 89-98.

Giroux, R., Berinstain, A., Braham, S., Graham, T., Bamsey, M., Boyd, K. & Cowing, K. (2006). Greenhouses in extreme environments: The Arthur Clarke Mars Greenhouse design and operation overview. Advances in Space Research, 38(6), 1248-1259.

Gómez, A. H., Hu, G., Wang, J., & Pereira, A. G. (2006). Evaluation of tomato maturity by electronic nose. Computers and Electronics in Agriculture, 54(1), 44-52.

Goto, E. (2012). Plant production in a closed plant factory with artificial lighting. VII International Symposium on Light in Horticultural Systems, 956, 37-49.

Grange, R. I., & Andrews, J. (1995). Respiration and growth of tomato fruit. Plant, Cell & Environment, 18(8), 925-930.

Grange, R. I., & Hand, D. W. (1987). A review of the effects of atmospheric humidity on the growth of horticultural crops. Journal of Horticultural Science, 62(2), 125-134.

Grossman, G. (2002). Solar-powered systems for cooling, dehumidification and air-conditioning. Solar energy, 72(1), 53-62.

Guichard, S., N. Bertin, C., Leonardi, C. & Gary. (2001). Tomato fruit quality in relation to water and carbon fluxes. Agronomie, 21, 385–392.

Guichard, S., Gary, C., Leonardi, C., & Bertin, N. (2005). Analysis of growth and water relations of tomato fruits in relation to air vapor pressure deficit and plant fruit load. Journal of Plant Growth Regulation, 24(3), 201.

Guinée, J., Heijungs, R., De Koning, A., Van, L., Geerken, T., Van Holderbeke, M., & Delgado, L. (2006). Environmental Impact of Products (EIPRO) Analysis of the life cycle environmental impacts related to the final consumption of the EU25. European Commission. Joint Research Centre (DG JRC). Institute for Prospective Technological Studies.

Guo, S., Tang, Y., Zhu, J., Wang, X., Yin, Y., Feng, H. & Qin, L. (2008). Development of a CELSS experimental facility. Advances in Space Research, 41(5), 725-729.

Hahn, F. (2002). Automation and Emerging Technologies: Multi-spectral prediction of unripe tomatoes. Biosystems Engineering, 81(2), 147-155.

Hanan, J. J. (1997). Greenhouses: advanced technology for protected horticulture. CRC press.

Hand, D. (1988). Effects of atmospheric humidity on greenhouse crops. Acta Horticulturae, 229: 143–158.

Hao, X., Little, C., & Khosla, S. (2012). LED inter-lighting in year-round greenhouse mini-cucumber production. VII International Symposium on Light in Horticultural Systems, 956, 335-340.

Haslavsky, V., Tanny J., & Teitel, M. (2006). Interaction between the mixing and displacement modes in a naturally ventilated enclosure. Building and Environment, 41(12), 1755–176.

Hatou, K., Nonami, H., Fukuyama, T., & Hashimoto, Y. (1994). Physiological diagnosis of tomato plants grown in hydroponic culture by using image analysis. Greenhouse Environment Control and Automation 399, 225-232.

Havaux, M., Greppin, H., & Strasser, R. J. (1991). Functioning of photosystems I and II in pea leaves exposed to heat stress in the presence or absence of light. Planta, 186(1), 88-98.

Havström, M., Callaghan T.V., Jonasson, S. (1993). Differential growthresponses of Cassiope tetragona, an arctic dwarf-shrub, to environmental perturbations among three contrasting high-and subarctic sites. Oikos, 66, 389-402.

Hayashi, M., & Kozai, T. (2005). Air and leaf temperatures and relative humidity in a naturally ventilated single-span greenhouse with a fogging system for cooling and its evaporative cooling efficiency. Environmental Control in Biology, 43(1), 3-11.

Hayashi, M., Goto, E., & Kozai, T. (2007). Experimental verification of control logic for operation of a fog cooling system for a naturally ventilated greenhouse. Environmental Control in Biology, 45(1), 47-58.

Hayden, A. L. (2006). Aeroponic and hydroponic systems for medicinal herb, rhizome, and root crops. HortScience, 41(3), 536-538.

Heber, A. J., Boon, C. R., & Peugh, M. W. (1996). Air patterns and turbulence in an experimental livestock building. Journal of Agricultural Engineering Research, 64(3), 209-226.

Hemming, S., Waaijenberg, D., Campen, J. B., & Bot, G. P. (2004). Development of a greenhouse system for tropical lowland in Indonesia. International Symposium on Greenhouses, Environmental Controls and In-house Mechanization for Crop Production in the Tropics, 710, 135-142.

Hemming, S., F. Kempkes, N. van der Braak, T. Dueck, and N. Marissen. (2006). Greenhouse cooling by NIR reflection. Acta Horticulturae, 719, 97-105.

Hepbasli, A. (2011). A comparative investigation of various greenhouse heating options using exergy analysis method. Applied Energy, 88(12), 4411-4423.

Hetzroni, A., Miles, G. E., Engel, B. A., Hammer, P. A., & Latin, R. X. (1994). Machine vision monitoring of plant health. Advances in Space Research, 14(11), 203-212.

Heuvelink, E. (1995). Growth, development and yield of a tomato crop: periodic destructive measurements in a greenhouse. Scientia horticulturae, 61(1), 77-99.

Heuvelink, E.B. (2008). Climate and yield in a closed greenhouse. Acta Horticulturae, 801:1083–1092.

Hickman, G. (2017). Cuesta Roble Greenhouse Vegetable Consulting. 13 June 2017. < http://cuestaroble.com/statistics.htm>

Ho, L. C., Grange, R. I., & Picken, A. J. (1987). An analysis of the accumulation of water and dry matter in tomato fruit. Plant, Cell & Environment, 10(2), 157-162.

Ho, L. C. (1998). The physiological basis for improving tomato fruit quality. VI International Symposium on Processing Tomato & Workshop on Irrigation & Fertigation of Processing Tomato, 487, 33-40.

Ho, L. C., Belda, R., Brown, M., Andrews, J., & Adams, P. (1993). Uptake and transport of calcium and the possible causes of blossom-end rot in tomato. Journal of Experimental Botany, 44(2), 509-518.

Hoagland, D. R., & Arnon, D. I. (1950). The water-culture method for growing plants without soil. Circular. California Agricultural Experiment Station, 347 (2nd edit).

Hoffman, G. J. (1979). Humidity. In Controlled Environment Guidelines for Plant Research, Academic Press London.

Hoffmann, S., & Waaijenberg, D. (2001). Tropical and subtropical greenhouses-A challenge for new plastic films. In International Symposium on Design and Environmental Control of Tropical and Subtropical Greenhouses, 578, 163-169.

Huber, L., & Gillespie, T. J. (1992). Modeling leaf wetness in relation to plant disease epidemiology. Annual Review of Phytopathology, 30(1), 553-577.

Humphries, M. & Landry-Cuerrier, M. (2013). State of knowledge in northern food production: An initial screening of published material. Internal Report. Department of Natural Resource Sciences Macdonald Campus, McGill University. Ste-Anne-de-Bellevue, QC, Canada.

Hussey, G. (1965). Growth and development in the young tomato III. The effect of night and day temperatures on vegetative growth. Journal of Experimental Botany, 16(3), 373-385.

Islam, S. (2008). Evaluating performance of ecologically sound organic substrates under different temperature regimes. International Journal of Agriculture and Biology, 10(3), 297-300.

Jackman, R. L., Marangoni, A. G., & Stanley, D. W. (1990). Measurement of tomato fruit firmness. HortScience, 25(7), 781-783.

Jackson, H.A. & Darby, D. E. (2010). Greenhouse Ventilation. Ontario Ministry of Agriculture, Food & Rural Affairs, ON, Canada. Publication 6704.

Jain, S., Dhar, P. L., & Kaushik, S. C. (1994). Evaluation of liquid dessicant based evaporative cooling cycles for typical hot and humid climates. Heat Recovery Systems and CHP, 14(6), 621-632.

Jain, D., & Tiwari, G. N. (2002). Modeling and optimal design of evaporative cooling system in controlled environment greenhouse. Energy Conversion and Management, 43(16), 2235-2250.

Janssen, L. H., Wams, H. E., & van Hasselt, P. R. (1992). Temperature dependence of chlorophyll fluorescence induction and photosynthesis in tomato as affected by temperature and light conditions during growth. Journal of Plant Physiology, 139(5), 549-554.

Jarvis, W. R. (1992). Managing diseases in greenhouse crops. American Phytopathological Society Press, 288.

Jensen, M. H. (2002). Deep flow hydroponics - Past, present and future. In Proceedings of the National Agricultural Plastics Congress, 30, 40-46.

Jensen, M. H. (2001). Controlled Environment agriculture in deserts, tropics and temperate regions-A World Review. International Symposium on Design and Environmental Control of Tropical and Subtropical Greenhouses 578, 19-25.

Jensen, M. H., & Malter, A. J. (1995). Protected agriculture: A global review. Washington, D.C: World Bank.

Jiménez-Hornero, F. J., De Ravé, E. G., Hidalgo, R., & Giráldez, J. V. (2005). Numerical study of the natural airflow in greenhouses using a two-dimensional lattice model. Biosystems Engineering, 91(2), 219-228.

Johnson, R. W., Dixon, M. A., & Lee, D. R. (1992). Water relations of the tomato during fruit growth. Plant, Cell & Environment, 15(8), 947-953.

Jokinen, K., Särkkä, L. E., & Näkkilä, J. (2012). Improving sweet pepper productivity by LED interlighting. VII International Symposium on Light in Horticultural Systems, 956, 59-66.

Jones, H. G. (2013). Plants and microclimate: a quantitative approach to environmental plant physiology. Cambridge University Press. Cambridge, United Kingdom.

Jolliet, O. & B.J. Bailey. (1992). The effect of climate on tomato transpiration in greenhouses: measurements and models comparison. Agricultural Forest Meteorology, 58:43-62.

Kacira, M., Sase, S., Okushima, L. & Ling, P.P. (2005). Plant response-based sensing for control strategies in sustainable greenhouse production. Journal of Agricultural Meteorology, 61(1), 15-22.

Kacira, M., Sadanori, S., & Okushima, L. (2004). Effects of side vents and span numbers on wind-induced natural ventilation of a gothic multi-span greenhouse. Japan Agricultural Research Quarterly, 38(4), 227-233.

Kacira, M., Ling, P. P., & Short, T. H. (2002). Machine vision extracted plant movement for early detection of plant water stress. Transactions of the American Society of Agricultural Engineers, 45(4), 1147.

Kacira, M., Short, T. H., & Stowell, R. R. (1998). A CFD evaluation of naturally ventilated, multi-span, sawtooth greenhouses. Transactions of the American Society of Agricultural Engineers, 41(3), 833.

Kamaruddin, R., Bailey, B. J., & Montero, J. I. (2001). A naturally ventilated greenhouse for temperate vegetable production in the tropics. International Symposium on Design and Environmental Control of Tropical and Subtropical Greenhouses, 578. 97-103.

Katsoulas, N., Elvanidi, A., Ferentinos, K. P., Kacira, M., Bartzanas, T., & Kittas, C. (2016). Crop reflectance monitoring as a tool for water stress detection in greenhouses: A review. Biosystems Engineering, 151, 374-398.

Katsoulas, N., Kittas, C., & Bartzanas, T. (2010). Microclimate distribution in a greenhouse cooled by a fog system. 28th International Horticultural Congress on Science and Horticulture for People, International Symposium, 927: 773-778.

Katsoulas, N., Savvas, D., Tsirogiannis, I., Merkouris, O., & Kittas, C. (2009). Response of an eggplant crop grown under Mediterranean summer conditions to greenhouse fog cooling. Scientia Horticulturae, 123(1), 90-98.

Katsoulas N; Baille A; Kittas C (2001). Effect of misting on transpiration and conductances of a greenhouse rose canopy. Agricultural and Forest Meteorology, 106, 233–247

Keller, L.M., Lazzara, M.A., Thom, J.E., Weidner, G.A. & Stearns, C.R. (2010). Antarctic Automatic Weather Station Data for the calendar year 2009. Space Science and Engineering Center University of Wisconsin.

Kennedy, A.D. (1995). Temperature effects of passive greenhouse apparatus in high-latitude climate change experiments. Functional Ecology, 9, 340–350.

Ould Khaoua, S., Bournet, P. E., Migeon, C., Boulard, T., & Chassériaux, G. (2006). Analysis of greenhouse ventilation efficiency based on computational fluid dynamics. Biosystems Engineering, 95(1), 83-98.

Kittas, C., Katsoulas, N., Bartzanas, T., Mermier, M., & Boulard, T. (2008). The impact of insect screens and ventilation openings on the greenhouse microclimate. Transactions of the ASABE, 51(6), 2151-2165.

Kittas, C., Bartzanas, T., & Jaffrin, A. (2003). Temperature gradients in a partially shaded large greenhouse equipped with evaporative cooling pads. Biosystems Engineering, 85(1), 87-94.

Kittas, C., Boulard, T., Bartzanas, T., Katsoulas, N., & Mermier, M. (2002). Influence of an insect screen on greenhouse ventilation. Transactions of the American Society of Agricultural Engineers, 45(4): 1083–1090

Kittas, C., N. Katsoulas, A. Baille. (2001). Influence of greenhouse ventilation regime on the microclimate and energy partitioning of a rose canopy during summer conditions. Journal of Agricultural Engineering Research. 79(3): 349-360.

Kittas, C., Bartzanas, T., & Jaffrin, A. (2000). Greenhouse evaporative cooling: measurement and data analysis. International Conference and British-Israeli Workshop on Greenhouse Techniques towards the 3rd Millennium, 534, 67-74.

Kittas, C., Baille, A., & Giaglaras, P. (1999). Influence of covering material and shading on the spectral distribution of light in greenhouses. Journal of Agricultural Engineering Research, 73(4), 341-351.

Kittas, C., Boulard, T., & Papadakis, G. (1997). Natural ventilation of a greenhouse with ridge and side openings: sensitivity to temperature and wind effects. Transactions of the American Society of Agricultural Engineers, 40(2), 415-425.

Koc, A. B. (2007). Determination of watermelon volume using ellipsoid approximation and image processing. Postharvest Biology and Technology, 45(3), 366-371.

Kopsell, D. A., Sams, C. E., & Morrow, R. C. (2015). Blue Wavelengths from LED Lighting Increase Nutritionally Important Metabolites in Specialty Crops. HortScience, 50(9), 1285-1288.

Kottek, M., Grieser, J., Beck, C., Rudolf, B., & Rubel, F. (2006). World map of the Köppen-Geiger climate classification updated. Meteorologische Zeitschrift, 15(3), 259-263.

Kozai, T. (2013). Resource use efficiency of closed plant production system with artificial light: Concept, estimation and application to plant factory. Proceedings of the Japan Academy, Series B, 89(10), 447-461.

Kozai, T., Kubota, C., Takagaki, M., & Maruo, T. (2014). Greenhouse environment control technologies for improving the sustainability of food production. In XXIX International Horticultural Congress on Horticulture: Sustaining Lives, Livelihoods and Landscapes (IHC2014): 1107: 1-14.

Kozai, T., Niu, G., & Takagaki, M. (2015). Plant Factory: An Indoor Vertical Farming System for Efficient Quality Food Production. Academic Press.

Kozai, T., & Sase, S. (1978). A simulation of natural ventilation for a multi-span greenhouse. In Symposium on Potential Productivity in Protected Cultivation, (87) 39-50.

Krause, G. H., & Weis, E. (1991). Chlorophyll fluorescence and photosynthesis: the basics. Annual review of plant biology, 42(1), 313-349.

Kuhnlein, H. V., & Receveur, O. (1996). Dietary change and traditional food systems of indigenous peoples. Annual Review of Nutrition, 16(1), 417-442.

Kulak, M., Graves, A., & Chatterton, J. (2013). Reducing greenhouse gas emissions with urban agriculture: a life cycle assessment perspective. Landscape and Urban Planning, 111, 68-78.

Kumar, K. S., Tiwari, K. N., & Jha, M. K. 2009. Design and technology for greenhouse cooling in tropical and subtropical regions: A review. Energy and Buildings, 41(12), 1269-1275.

Landsberg, J. J., White, B. & Thorpe, M. R. (1979). Computer analysis of the efficiency of evaporative cooling for glasshouses in high energy environments. Journal of Agricultural Engineering Research, 24, 29–39.

Langhans, R.W. & T.W. Tibbitts. (1997). Plant growth chamber handbook. Iowa Agriculture and Home Economics Experiment Station. Publ. 340.

Latimer, J.G. (2009). Dealing with the high cost of energy for greenhouse operations. Virginia Cooperative Extension, Virginia Polytechnic Institute and State University, VA. Publ. 430-101.

Lawrence, J. L., P. M. Titus & D. O. Clarke Harris. (2011). Protected agriculture and its potential role in achieving food and nutritional security in the Caribbean Region. University of the West Indies, St Augustine Campus. Caribbean Agricultural Research and Development Institute (CARDI).

Lawrence, J., L. Simpson and A. Piggott. (2014). Protected Agriculture: A Climate Change Adaptation. Impacts of Climate Change on Food Security in Small Island Developing States. 1 st ed. IGI Global, Hershey, PA.

Lee, D. R., Dixon, M. A., & Johnson, R. W. (1989). Simultaneous measurements of tomato fruit and stem water potentials using in situ stem hygrometers. Canadian Journal of Botany, 67(8), 2352-2355.

Lee, I. B., & Short, T. H. (2000). Two-dimensional numerical simulation of natural ventilation in a multi-span greenhouse. Transactions of the American Society of Agricultural Engineers, 43(3), 757.

Lee, I., Sase, S., Okushima, L., Ikeguchi, A., Choi, K., & Yun, J. (2003). A Wind Tunnel Study of Natural Ventilation for Multi-Span Greenhouse Scale Models Using Two-Dimensional Particle Image Velocimetry (PIV). Transactions of the American Society of Agricultural Engineers, 46(3), 763-772.

Lefsrud, M. G., Kopsell, D. A., & Sams, C. E. (2008). Irradiance from distinct wavelength light-emitting diodes affect secondary metabolites in kale. HortScience, 43(7), 2243-2244.

Leonardi, C., Guichard, S., & Bertin, N. (2000). High vapour pressure deficit influences growth, transpiration and quality of tomato fruits. Scientia Horticulturae, 84(3), 285-296.

LI-COR. (2017). LI-6400XT Portable Photosynthesis System. LI-COR Inc. Lincoln, NB. Accessible from < https://www.licor.com/env/products/photosynthesis/LI-6400XT/>

Li, Q., & Kubota, C. (2009). Effects of supplemental light quality on growth and phytochemicals of baby leaf lettuce. Environmental and Experimental Botany, 67(1), 59-64.

Li, S., & Willits, D. H. (2008). Comparing low-pressure and high-pressure fogging systems in naturally ventilated greenhouses. Biosystems Engineering, 101(1), 69-77.

Liao, C.M., K.H. Chiu. 2002. Wind tunnel modeling the system performance of alternative evaporative cooling pads in Taiwan region. Buildings and Environment, 37,177-187.

Lin, K., Chen, J., Si, H., & Wu, J. (2013). A review on computer vision technologies applied in greenhouse plant stress detection. Chinese Conference on Image and Graphics Technologies. Springer, Berlin, Heidelberg.

Lin, X., Hubbard, K G., & Walter-Shea, E A. (2001) Radiation loading model for evaluating air temperature errors with a non-aspirated radiation shield. Transactions of the American Society of Agricultural Engineers, 44, 1229–1306.

Ling, P. P., Giacomelli, G. A., & Russell, T. (1996). Monitoring of plant development in controlled environment with machine vision. Advances in Space Research, 18(4-5), 101-112.

Linsley-Noakes, G., Wilken, L., & de Villiers, S. (2004, September). High density, vertical hydroponics growing system for strawberries. V International Strawberry Symposium, 708, 365-370.

López, A., Valera, D. L., Molina-Aiz, F. D., & Peña, A. (2012). Sonic anemometry to evaluate airflow characteristics and temperature distribution in empty Mediterranean greenhouses equipped with pad–fan and fog systems. Biosystems Engineering, 113(4), 334-350.

López, A., Valera, D. L., & Molina-Aiz, F. (2011). Sonic anemometry to measure natural ventilation in greenhouses. Sensors, 11(10), 9820-9838.

López, A., Valera, D. L., Molina-Aiz, F. D., & Pena, A. (2010). Experimental evaluation by sonic anemometry of airflow in a Mediterranean greenhouse equipped with a pad-fan cooling system. Transactions of the American Society of Agricultural and Biological Engineers, 53(3), 945-957.

Lorenzo, P., Medrano, E., & Sánchez-Guerrero, M. C. (1993). Greenhouse crop transpiration: an implement to soilless irrigation management. International Symposium on Water Quality & Quantity-Greenhouse, 458, 113-122.

Luo, W., Stanghellini, C., Dai, J., Wang, X., de Zwart, H. F., & Bu, C. (2005). Simulation of greenhouse management in the subtropics, Part II: Scenario study for the summer season. Biosystems engineering, 90(4), 433-441.

Mahdavi, S., Kafi, M., Naderi, R., & Sadat, T. (2012). Vertical mobile planting system consistent with the pattern of solar radiation and effects of system on light exposure and growth of Gerbera cut flowers (Gerbera jamesonii cv. Antibes), in greenhouse culture. Journal of Agricultural Technology, 8, 1461-1468.

Mahmoudi, H., Spahis, N., Goosen, M. F., Ghaffour, N., Drouiche, N., & Ouagued, A. (2010). Application of geothermal energy for heating and fresh water production in a brackish water greenhouse desalination unit: A case study from Algeria. Renewable and Sustainable Energy Reviews, 14(1), 512-517.

Mannan, K.D. & Cheema, L.S. (1981). Year round studies on natural cooling and heating of greenhouses in Northern India. In: Proceedings of the National Solar Energy Convention Bhavnagar, India.

Maskan, A., Kaya, S., & Maskan, M. (2002). Hot air and sun drying of grape leather (pestil). Journal of Food Engineering, 54(1), 81-88.

Massa, G. D., Emmerich, J. C., Morrow, R. C., Bourget, C. M., & Mitchell, C. A. (2007). Plant-growth lighting for space life support: a review. Gravitational and Space Research, 19(2).

Massa, G. D., Kim, H. H., Wheeler, R. M., & Mitchell, C. A. 2008. Plant productivity in response to LED lighting. HortScience, 43(7), 1951-1956.

MATLAB® and Image Processing Toolbox Release 2017a, The MathWorks, Inc., Natick, MA.

Mattara C, S., Kalamegam, M. J., & Parveen, M. 2015. Upgradation of HVAC Systems in Exisiting Commercial Green House Using Evaporative Coolers in Middle East Climatic Conditions V06AT07A055. ASME 2015 International Mechanical Engineering Congress and Exposition. American Society of Mechanical Engineers.

Max, J. F., Horst, W. J., Mutwiwa, U. N., & Tantau, H. J. (2009). Effects of greenhouse cooling method on growth, fruit yield and quality of tomato (Solanum lycopersicum L.) in a tropical climate. Scientia Horticulturae, 122(2), 179-186.

Maxwell, K., & Johnson, G. N. (2000). Chlorophyll fluorescence - a practical guide. Journal of Experimental Botany, 51(345), 659-668.

McCartney, L., & Lefsrud, M.G. (2017). Field Trial of The Natural Ventilation Augmented Cooling (NVAC) Greenhouse. HortTechnology. Under Review.

McCartney, L. (2015). Cubic FarmingTM: Growing Fresh Produce in an Urban Setting. Resource Magazine, American Society of Agricultural and Biological Engineers 22(6), 20-21.

McCurdy, J.A. & Svoboda, J. (1989). Yield and productivity of radish (Raphanus sativus L. cultivar 'Cherry Belle') planted successfully over the growing season in the High Arctic. Musk-Ox, 37: 60–67.

Meca, D., López, J. C., Gázquez, J. C., Baeza, E., Parra, J. P., & Zaragoza, G. (2013). A comparison of three different cooling systems in parral type greenhouses in Almería. Spanish Journal of Agricultural Research, 5(3), 285-292.

Mendelsohn, R., & Dinar, A. (1999). Climate change, agriculture, and developing countries: does adaptation matter?. The World Bank Research Observer, 14(2), 277-293.

Meyer, G. E., Troyer, W. W., Fitzgerald, J. B., & Paparozzi, E. T. (1992). Leaf nitrogen analysis of poinsettia (Euphorbia Pulcherrima Will D.) using spectral properties in natural and controlled lighting. Applied Engineering in Agriculture, 8(5), 715-722.

Miguel, A. F., Van de Braak, N. J., & Bot, G. P. A. (1997). Analysis of the airflow characteristics of greenhouse screening materials. Journal of Agricultural Engineering Research, 67(2), 105-112.

Mitchell, C.A. (2012). Plant lighting in controlled environments for space and earth applications. VII International Symposium on Light in Horticultural Systems, 956, 23-36.

Mohammed, G. H., Binder, W. D., & Gillies, S. L. (1995). Chlorophyll fluorescence: a review of its practical forestry applications and instrumentation. Scandinavian Journal of Forest Research, 10(1-4), 383-410.

Mok, H. F., Williamson, V. G., Grove, J. R., Burry, K., Barker, S. F., & Hamilton, A. J. (2014). Strawberry fields forever? Urban agriculture in developed countries: a review. Agronomy for sustainable development, 34(1), 21-43.

Molina-Aiz, F. D., Valera, D. L., & Alvares, A. J. (2003). Using computational fluid dynamics tool to model the internal climate of an Almería-type greenhouse. International Workshop on Models for Plant Growth and Control of Product Quality in Horticultural Production, 654, 271-278.

Molina-Aiz, F. D., Valera, D. L., & Álvarez, A. J. (2004). Measurement and simulation of climate inside Almerıa-type greenhouses using computational fluid dynamics. Agricultural and Forest Meteorology, 125(1), 33-51.

Molina-Aiz, F. D., Valera, D. L., Peña, A. A., Gil, J. A., & López, A. (2009). A study of natural ventilation in an Almería-type greenhouse with insect screens by means of tri-sonic anemometry. Biosystems Engineering, 104(2), 224-242.

Mongkon, S., Thepa, S., Namprakai, P., & N. Pratinthong. 2014. Cooling performance assessment of horizontal earth tube system and effect on planting in tropical greenhouse. Energy Conversion Management. 78: 225-236.

Montero, J. I. (2006). Evaporative cooling in greenhouses: effect on microclimate, water use efficiency and plant response. International Symposium on Greenhouse Cooling, 719, 373-384.

Montero, J. I., Anton, A., Biel, C., & Franquet, A. (1989). Cooling of greenhouses with compressed air fogging nozzles. II Workshop on Greenhouse Construction and Design 281, 199-210.

Montero, J. I., Antón, A., Muñoz, P., & Lorenzo, P. (2001). Transpiration from geranium grown under high temperatures and low humidities in greenhouses. Agricultural and Forest Meteorology, 107(4), 323-332.

Morrow, R. C. (2008). LED lighting in horticulture. HortScience, 43(7), 1947-1950.

Morton, J. F. (2007). The impact of climate change on smallholder and subsistence agriculture. Proceedings of the national academy of sciences, 104(50), 19680-19685.

Muñoz, P., Montero, J. I., Antón, A., & Giuffrida, F. (1999). Effect of insect-proof screens and roof openings on greenhouse ventilation. Journal of Agricultural Engineering Research, 73(2), 171-178.

Murphy, G., & Ferguson, G. M. (2000). Screening of Greenhouses for Insect Exclusion Fact Sheet 290/626. Ministry of Agriculture, Food & Rural Affairs. Accessible from < http://www.omafra.gov.on.ca/english/crops/facts/00-021.htm>

Murray, F. W. (1967). On the computation of saturation vapor pressure. Journal of Applied Meteorology, 6, 203–204.

Mutwiwa, U. N., Elsner, B. V., Tantau, J. H., & Max, J. F. J. (2008). Cooling naturally ventilated greenhouses in the tropics by near-infra red reflection. Acta Horticulturae, 801, 259-266

Mutwiwa, U. N., Max, J. J. F., & Tantau, H. J. (2007). Effect of greenhouse cooling method on the growth and yield of tomato in the tropics. In: Conference on International Agricultural Research for Development. 13 Nov. 2015. Accessible from < http://www. tropentag. de/2007/abstracts/full/239. pdf. 2007.

Nagler, P. L., Glenn, E. P., & Thompson, T. L. (2003). Comparison of transpiration rates among saltcedar, cottonwood and willow trees by sap flow and canopy temperature methods. Agricultural and Forest Meteorology, 116(1), 73-89.

Nakamura, R., & Mahrt, L. (2005). Air temperature measurement errors in naturally ventilated radiation shields. Journal of Atmospheric and Oceanic Technology, 22(7), 1046-1058.

National Greenhouse Manufacturers Association. Ventilation and Cooling. 13 Jan. 2017. <https://www.ngma.com/standardpdf/VentandCool2010.pdf>.

National Oceanic and Atmospheric Administration. (2016). Climatic Data Online (CDO): 2014-2016 789540 99999 Grantley Adams Intl. Barbados. 02 Sept. 2016. Accessible from <https://www.ncdc.noaa.gov/cdo-web/datasets>.

National Renewable Energy Laboratory. (2004). Energy Snapshot Barbados. May 29, 2017. Accessible from <http://www.nrel.gov/docs/fy15osti/64118.pdf>

Neocleous, D., Kaittanis, C., Seraphides, N., & Polycarpou, P. (2010). Horizontal and vertical soilless growing systems under Cyprus conditions. Journal of Applied Horticulture, 12, 140-144.

Newbean Capital. (2016). The Rise of Asia's Indoor Agriculture Industry. Ag-Con Asia 2016.

Newbean Capital. (2017). Indoor Crop Production, Feeding the Future, 2nd Edition. Indoor Ag-Con 2017.

O'Flaherty, T., & Maher, M. J. (1987). Evaluation of Lining with PVC Panels as a Means of Reducing Heat Loss from a Glasshouse. Irish Journal of Agricultural Research, 77-86.

Ohta, K., Hosoki, T., Matsumoto, K., Ohya, M., Ito, N., & Inaba, K. (1997). Relationships between fruit cracking and changes of fruit diameter associated with solute flow to fruit in cherry tomatoes. Journal of the Japanese Society for Horticultural Science, 65(4), 753-759.

Olle, M., Ngouajio, M., & Siomos, A. (2012). Vegetable quality and productivity as influenced by growing medium: a review. Agriculture, 99(4), 399-408.

Olympios C. M. (1999) Overview of soilless culture: advantages, constraints and perspectives for its use in Mediterranean countries. Options Mediterraneennes, (31), 307–324

Orgaz, F., Fernández, M. D., Bonachela, S., Gallardo, M., & Fereres, E. (2005). Evapotranspiration of horticultural crops in an unheated plastic greenhouse. Agricultural Water Management, 72(2), 81-96.

Oberg, V., & Goswami, D. Y. (1998). A review of liquid desiccant cooling. Advances in solar energy, 12, 431-470.

Ouyang, Q., Dai, W., Li, H., & Zhu, Y. (2006). Study on dynamic characteristics of natural and mechanical wind in built environment using spectral analysis. Building and Environment, 41(4), 418-426.

Öztürk, H. H. (2003). Evaporative cooling efficiency of a fogging system for greenhouses. Turkish Journal of Agriculture and Forestry, 27(1), 49-57.

Papadakis, G., Frangoudakis, A., & Kyritsis, S. (1994). Experimental investigation and modelling of heat and mass transfer between a tomato crop and the greenhouse environment. Journal of Agricultural Engineering Research, 57(4), 217-227.

Papadakis, G., Mermier, M., Meneses, J. F., & Boulard, T. (1996). Measurement and analysis of air exchange rates in a greenhouse with continuous roof and side openings. Journal of Agricultural Engineering Research, 63(3), 219-227.

Papadopoulos, A.P. (1991). Growing greenhouse tomatoes in soil and in soilless media. Agriculture Canada. Publication 1865/E.

Parra, J. P., Baeza, E., Montero, J. I., & Bailey, B. J. (2004). Natural ventilation of parral greenhouses. Biosystems Engineering, 87(3), 355-366.

Pearce, B. D., Grange, R. I., & Hardwick, K. (1993a). The growth of young tomato fruit. I. Effects of temperature and irradiance on fruit grown in controlled environments. Journal of Horticultural Science, 68(1), 1-11.

Pearce, B. D., Grange, R. I., & Hardwick, K. (1993b). The growth of young tomato fruit. II. Environmental influences on glasshouse crops grown in rockwool or nutrient film. Journal of Horticultural Science, 68(1), 13-23.

Peel, M. C., Finlayson, B. L., & McMahon, T. A. (2007). Updated world map of the Köppen-Geiger climate classification. Hydrology and earth system sciences discussions, 4(2), 439-473.

Peet, M. M. (1992). Fruit cracking in tomato. HortTechnology, 2(2), 216-223.

Pettigrew, W. T., Hesketh, J. D., Peters, D. B., & Woolley, J. T. (1990). A vapor pressure deficit effect on crop canopy photosynthesis. Photosynthesis research, 24(1), 27-34.

Polder, G., & van der Heijden, G. W. A. M. (2010). Measuring Ripening of Tomatoes Using Imaging Spectrometry. In Hyperspectral Imaging for Food Quality Analysis and Control. Academic Press Elsevier.

Pollet, I. V. (2002). Radiation transmission through dry and condensate covered greenhouse cladding materials. Ph.D. Dissertation, Facultiet Landbouwkundige en Toegepaste, Biologische Werenschappen, Universitiet Gent.

Pollet, I. V., & Pieters, J. G. (2000). Condensation and radiation transmittance of greenhouse cladding materials, part 2: results for a complete condensation cycle. Journal of Agricultural Engineering Research, 75(1), 65-72.

Poulet, L., Massa, G. D., Morrow, R. C., Bourget, C. M., Wheeler, R. M., & Mitchell, C. A. (2014). Significant reduction in energy for plant-growth lighting in space using targeted LED lighting and spectral manipulation. Life Sciences in Space Research, 2, 43-53.

Prenger, J.J., & Ling, P.P. (2001). Greenhouse condensation control understanding and using vapor pressure deficit (VPD). Accessible from <http://citeseerx.ist.psu.edu/viewdoc/download?doi=10.1.1.183.8399&rep=rep1&type=pdf >

Prenger, J. J., Fynn, R. P., & Hansen, R. C. (2002). A comparison of four evapotranspiration models in a greenhouse environment. Transactions of the American Society of Agricultural Engineers, 45(6), 1779.

Public Health Agency of Canada. (2009). Inuvik Community Greenhouse – Building a strong sense of community through recreational gardening, food production, knowledge sharing, and volunteer support. Accessible from < http://www.phac-aspc.gc.ca/publicat/2009/be-eb/nwt-tno-eng.php>

Quinn, P. J., & Williams, W. P. (1985). Environmentally induced changes in chloroplast membranes and their effects on photosynthetic function. Photosynthetic Mechanisms and the Environment, 6, 1-47.

Rane K. (1989). Reducing humidity in the greenhouse. University of Massachusetts Cooperative Extension Floral Notes, 1(5): 7–8.

Rault, P. A. (1989). A tunnel greenhouse adapted to the tropical lowland climate. 2nd Workshop on Greenhouse Construction and Design, 281, 95-104.

Resh, H. M. (2012). Hydroponic food production: a definitive guidebook for the advanced home gardener and the commercial hydroponic grower. CRC Press. Boca Raton, FL.

Richardson, S. J., Brock, F. V., Semmer, S. R., & Jirak, C. (1999). Minimizing errors associated with multiplate radiation shields. Journal of Atmospheric and Oceanic Technology, 16(11), 1862-1872.

Roberts, W. J., Kazmierczak, J., & Chan, M. (1989). Energy conservation for commercial greenhouses. Cooperative Extension, Northeast Regional Agricultural Engineering Service, Cornell University, NY.

Romero-Aranda, R., & Longuenesse, J. J. (1995). Modelling the effect of air vapour pressure deficit on leaf photosynthesis of greenhouse tomatoes: the importance of leaf conductance to CO2. Journal of Horticultural Science, 70(3), 423-432.

Runkle S, Heins RD, Jaster P, Till, C. (2002). Environmental conditions under experimental near infrared reflecting greenhouse film. Acta Horticulturae, 578:181–185

Rylski, I., & Spigelman, M. (1986). Effect of shading on plant development, yield and fruit quality of sweet pepper grown under conditions of high temperature and radlation. Scientia Horticulturae, 29(1-2), 31-35.

Sabeh, N. C. (2007). Evaluating and minimizing water use by greenhouse evaporative cooling systems in a semi-arid climate. Ph.D. Dissertation. The University of Arizona.

Sabeh, N. C., Giacomelli, G. A., & Kubota, C. (2007). Water use by greenhouse evaporative cooling systems in a semi-arid climate. 2007 ASAE Annual Meeting. The American Society of Agricultural and Biological Engineers.

Sachs, J. D. (2001). Tropical underdevelopment no. w8119. National Bureau of Economic Research.

Samaniego-Cruz, E., Quezada-Martin, M.R., De La Rosa-Ibarra, M, Munguía-López, J., Benavides-Mendoza, A. & Ibarra-Jiménez, L. (2002). Tomato and bell pepper seedlings production under reflecting polyethylene covers to decrease temperature in greenhouse. Agrociencia, 36: 305-318.

Sánchez, A. C., David Uclés Aguilera, Tomás Agüera Camacho & Encarni de la Cruz Fernández. (2016). Análisis de la campaña hortofrutícola de Almería. Campaña 2015/2016. Cajamar Caja Rural. Spain.

Sanjuan, J. F. (2007), Deteccion de la superficie invernada en la provincia de Almeria a traves de imágenes Aster, edited by I. M. Cuadrado-Gomez, Fundacion para la Investigacion Agraria de la Provincia de Almeria, Almeria.

Santamouris, M., Mihalakakou, G., Argiriou, A., & Asimakopoulos, D. N. (1995). On the performance of buildings coupled with earth to air heat exchangers. Solar Energy, 54(6), 375-380.

Sase, S., Takakura, T., & Nara, M. (1984). Wind tunnel testing on airflow and temperature distribution of a naturally ventilated greenhouse. In III International Symposium on Energy in Protected Cultivation, 148, 329-336).

Sato, S., Kamiyama, M., Iwata, T., Makita, N., Furukawa, H., & Ikeda, H. (2006). Moderate Increase of Mean Daily Temperature Adversely Affects Fruit Set of Lycopersicon esculentum by Disrupting Specific Physiological Processes in Male Reproductive Development. Annals of Botany, 97, 731–738.

Savage, M. J. (2010). Field evaluation of polymer capacitive humidity sensors for Bowen ratio energy balance flux measurements. Sensors, 10(8), 7748-7771.

Sawan O. M., Eissa A. M., Abou-Hadid A. F. (1999). The effect of different growing media on cucumber seedling production, fruit yield and quality under greenhouse conditions. Acta Horticulturae, (491) 369–376

Schaik, W. V., Grooten, M., Wernaart, T., & Geld, C. V. D. (2010). High Accuracy Acoustic Relative Humidity Measurement in Duct Flow with Air. Sensors, 10(8), 7421-7433.

Schilstra-vanVeelen, I.M. & J.C. Bakker. (1985). Cracking of tomato fruits. Annual Report on Glasshouse Crops Research, Experiment Station Naaldwijk, The Netherlands.

Schulze, D., Philpot, C., Morfill, G., Klein, B., & Beck, T. (2016). Food Production in Space-Operating a Greenhouse in Low Earth Orbit. 14th International Conference on Space Operations, 2533.

Scott, J. W., Harbaugh, B. K., & Baldwin, E. A. (2000). Micro-Tina' and Micro-Gemma' Miniature Dwarf Tomatoes. HortScience, 35(4), 774-775.

Seginer, I., Elster, R. T., Goodrum, J. W., & Rieger, M. W. (1992). Plant wilt detection by computer-vision tracking of leaf tips. Transactions of the ASAE, 35(5), 1563-1567.

Sethi, V. P., & Sharma, S. K. (2007). Survey of cooling technologies for worldwide agricultural greenhouse applications. Solar Energy, 81(12), 1447-1459.

Shamshiri, R., & Ismail, W. I. W. 2013. A review of greenhouse climate control and automation systems in tropical regions. Journal of Agricultural Science and Applications, 2(3), 176-183.

Shaver, G. R., Chapin III, F. & Gartner, B.L. (1986). Factors Limiting Seasonal Growth and Peak Biomass Accumulation in Eriophorum Vaginatum in Alaskan Tussock Tundra. Journal of Ecology, 74(1): 257-278

Shear, C. B. (1975). Calcium-related disorders of fruits and vegetables. HortScience, 10, 361-365.

Shen, Y., & Yu, S. L. (2001). Cooling methods for greenhouses in tropical region. In International Symposium on Design and Environmental Control of Tropical and Subtropical Greenhouses, (578) 323-327.

Shimizu, H., & Heins, R. D. (1995). Computer-vision-based system for plant growth analysis. Transactions of the American Society of Agricultural Engineers, 38(3), 959-964.

Shipp, J. L., Zhang, Y., Hunt, D. W. A., & Ferguson, G. (2003). Influence of humidity and greenhouse microclimate on the efficacy of Beauveria bassiana (Balsamo) for control of greenhouse arthropod pests. Environmental Entomology, 32(5), 1154-1163.

Shukla, A., Tiwari, G. N., & Sodha, M. S. (2008). Experimental study of effect of an inner thermal curtain in evaporative cooling system of a cascade greenhouse. Solar Energy, 82(1), 61-72.

Simard, K., Gosselin, A., Papadopoulos, A. P., & Jobin-Lawler, F. (2000). The Influence of Solar Radiation and Boron-Calcium Fruit Application on Cuticle Cracking of a Winter Tomato Crop Grown under Supplemental Lighting. In IV International ISHS Symposium on Artificial Lighting, 580, 235-239.

Simonneau, T., Habib, R., Goutouly, J. P., & Huguet, J. G. (1993). Diurnal changes in stem diameter depend upon variations in water content: direct evidence in peach trees. Journal of Experimental Botany, 44(3), 615-621.

Singh, G., Singh, P. P., Lubana, P. P. S., & Singh, K. G. (2006). Formulation and validation of a mathematical model of the microclimate of a greenhouse. Renewable Energy, 31(10), 1541-1560.

Sivakumar, M. V. K., Das, H. P., & Brunini, O. (2005). Impacts of present and future climate variability and change on agriculture and forestry in the arid and semi-arid tropics. Climatic Change, 70(1-2), 31-72.

Small, C., & Cohen, J. (2004). Continental Physiography, Climate, and the Global Distribution of Human Population 1. Current Anthropology, 45(2), 269-277.

Snyder, R. L. & R. H. Shaw. (1984). Converting humidity expressions with computers and calculators. Cooperative Extension, Division of Agriculture and Natural Resources, University of California. Publication 21372.

Snyder, R.G. 1992. Greenhouse Tomato Handbook. Mississippi State University Cooperative Extension Service, Publication 1828.

Soni, P., Salokhe, V. M., & Tantau, H. J. (2005). Effect of screen mesh size on vertical temperature distribution in naturally ventilated tropical greenhouses. Biosystems Engineering, 92(4), 469-482.

Soto, F., Gallardo, M., Giménez, C., Peña-Fleitas, T., & Thompson, R. B. (2014). Simulation of tomato growth, water and N dynamics using the EU-Rotate_N model in Mediterranean greenhouses with drip irrigation and fertigation. Agricultural Water Management, 132, 46-59.

Specht, K., Siebert, R., Hartmann, I., Freisinger, U. B., Sawicka, M., Werner, A., & Dierich, A. (2014). Urban agriculture of the future: an overview of sustainability aspects of food production in and on buildings. Agriculture and Human Values, 31(1), 33-51.

Stanghellini, C. (1992). Environmental control of greenhouse crop transpiration. Journal of Agricultural Engineering Research, 51: 297-311.

Stapleton, S. & Hochmuth, R. C. (2001). Greenhouse production of several fresh-cut herbs in vertical hydroponic systems in north central Florida, Proc. Florida State Horticultural Society. Publication 114.

Stocking, M. A. (2003). Tropical soils and food security: the next 50 years. Science, 302(5649), 1356-1359.

Story, D., & Kacira, M. (2015). Design and implementation of a computer vision-guided greenhouse crop diagnostics system. Machine vision and applications, 26(4), 495-506.

Story, D., Kacira, M., Kubota, C., Akoglu, A., & An, L. (2010). Lettuce calcium deficiency detection with machine vision computed plant features in controlled environments. Computers and electronics in agriculture, 74(2), 238-243.

Strathdee, A. T., & Bale, J. S. (1993). A new cloche design for elevating temperature in polar terrestrial ecosystems. Polar Biology, 13(8), 577-580.

Sun, G., Li, Y., Zhang, Y., Wang, X., Chen, M., Li, X., & Yan, T. (2016). Nondestructive measurement method for greenhouse cucumber parameters based on machine vision. Engineering in Agriculture, Environment and Food, 9(1), 70-78.

Sutar, R. F., & Tiwari, G. N. (1995). Analytical and numerical study of a controlled-environment agricultural system for hot and dry climatic conditions. Energy and Buildings, 23(1), 9-18.

Swalls, A.A., & O'Leary, J.W. (1975). The effect of relative humidity on growth, water consumption and calcium uptake in tomato plants. Journal of the Arizona Academy of Science, 10, 87-9.

Swalls, A.A., & O'Leary, J.W. (1976). Growth, water consumption and salt uptake of tomato plants in high humidity-high carbon dioxide greenhouse environments. Journal of the Arizona Academy of Science, 11, 23-26.

Szmidt, R. A. K., & Graham, N. B. (1989). The effect of poly (ethylene oxide) hydrogel on crop growth under saline conditions. II International Symposium on Protected Cultivation of Vegetables in Mild Winter Climates, 287, 211-218.

Tanaka, F., Ide, Y., Kinjo, M., Genkawa, T., Hamanaka, D., & Uchino, T. (2010). Development of thick layer re-wetting model for brown rice packaged with LDPE and PBT films. Journal of Food Engineering, 101(2), 223-227.

Tanner, B. D., Swiatek, E., & Maughan, C. (1996). Field comparisons of naturally ventilated and aspirated radiation shields for weather station air temperature measurements. In Conference on Agricultural and Forest Meteorology, Symposium on Fire and Forest Meteorology, (22) 227-230).

Tanny, J., Haijun, L., & Cohen, S. (2006). Airflow characteristics, energy balance and eddy covariance measurements in a banana screenhouse. Agricultural and Forest Meteorology, 139(1), 105-118.

Tanny, J., Haslavsky, V., & Teitel, M. (2008). Airflow and heat flux through the vertical opening of buoyancy-induced naturally ventilated enclosures. Energy and Buildings, 40(4), 637-646.

Tantau, H. J., & Salokhe, V. M. (2006). Microclimate and air exchange rates in greenhouses covered with different nets in the humid tropics. Biosystems Engineering, 94(2), 239-253.

Teitel, M., O. Liran, J. Tanny & M. Barak. (2008). Wind driven ventilation of a mono-span greenhouse with a rose crop and continuous screened side vents and its effect on flow patterns and microclimate. Biosystems Engineering, 101(1): 111-122.

Teitel, M., Shklyar, A., Segal, I., & Barak, M. (1996). Effects of nonsteady hot-water greenhouse heating on heat transfer and microclimate. Journal of Agricultural Engineering Research, 65(4), 297-304.

Teitel, M., & Tanny, J. (1999). Natural ventilation of greenhouses: experiments and model. Agricultural and Forest Meteorology, 96(1), 59-70.

Teitel, M., Tanny, J., Ben-Yakir, D., & Barak, M. (2005). Airflow patterns through roof openings of a naturally ventilated greenhouse and their effect on insect penetration. Biosystems Engineering, 92(3): 341-353.

Thipe, E. L., Workneh, T., Odindo, A., & Laing, M. (2017). Greenhouse Technology for Agriculture Under Arid Conditions. In Sustainable Agriculture Reviews, 37-55. Springer International Publishing.

Tilman, D., Balzer, C., Hill, J., & Befort, B. L. (2011). Global food demand and the sustainable intensification of agriculture. Proceedings of the National Academy of Sciences, 108(50), 20260-20264.

Tiwari, G. N. (1985). Analysis of winter greenhouse. International Journal of Solar Energy, 3(1), 19-24.

Toida, H., Kozai, T., & Ohyama, K. (2006). Enhancing fog evaporation rate using an upward air stream to improve greenhouse cooling performance. Biosystems Engineering, 93(2), 205-211.

Toida, H., Ohyama, K., Kozai, T., & Hayashi, M. (2006). A method for measuring dry-bulb temperatures during the operation of a fog system for greenhouse cooling. Biosystems Engineering, 93(3), 347-351.

Touliatos, D., Dodd, I. C., & McAinsh, M. (2016). Vertical farming increases lettuce yield per unit area compared to conventional horizontal hydroponics. Food and Energy Security, 5(3), 184-191.

Tsai, W. Y., Chen, H. C., & Liao, T. L. (2005). An ultrasonic air temperature measurement system with self-correction function for humidity. Measurement science and technology, 16(2), 548.

Tüzel, Y., Öztekin, G. B., Tüzel, I. H., Tunali, U., & Tepecik, M. (2013). Automated irrigation management of organic greenhouse tomatoes. 2nd International Symposium on Organic Greenhouse Horticulture, 1041, 109-118.

Urban, L., & Langelez, I. (1992). Effect of high-pressure mist on leaf water potential, leaf diffusive conductance, CO2 fixation and production of cultivar 'Sonia'rose plants grown on rockwool. Scientia Horticulturae, 50(3), 229-244.

Ustymczuk, A., & Giner, S. A. (2011). Relative humidity errors when measuring dry and wet bulb temperatures. Biosystems Engineering, 110(2), 106-111.

Valerio, A. A., Mossman, M. A., & Whitehead, L. A. (2014). Light valve based on nonimaging optics with potential application in cold climate greenhouses 91910K. SPIE Optical Engineering Applications. International Society for Optics and Photonics.

Van de Sanden, P. A. C. M., & Uittien, J. J. (1994). Root environment water potential and tomato fruit growth. In International Symposium on Growing Media & Plant Nutrition in Horticulture, 401, 531-536.

Van Ooteghem, R. J. (2010). Optimal control design for a solar greenhouse. IFAC Proceedings Volumes, 43(26), 304-309.

Van Os, E. A. 1994. Engineering and environmental aspects of soilless growing systems. Hydroponics and Transplant Production, 396, 25-32.

Verlodt, H. (1999) Climate and vegetable management under greenhouse conditions. In: Greenhouse vegetable production and protection in Albania. Proceedings of The Food and Agriculture Organization, Workshop in Tirana, 9-11.

Verlodt, I., & Verschaeren, P. (1998). New interference film for climate control. XXV International Horticultural Congress, Part 4: Culture Techniques with Special Emphasis on Environmental Implications 514, 139-146.

Villarreal-Guerrero, F. (2011). Enhanced greenhouse cooling strategy with natural ventilation and variable fogging rates. Ph.D. Dissertation. The University of Arizona.

Von Elsner, B., & Xie, J. (2002). Effects of interference pigments in shading paint for greenhouses. Proceedings of the Thirty-First Agricultural Plastics Congress, 6-16.

Von Elsner, B., Briassoulis, D., Waaijenberg, D., Mistriotis, A., Von Zabeltitz, C., Gratraud, J. & Suay-Cortes, R. (2000a). Review of structural and functional characteristics of greenhouses in European Union countries: Part I, design requirements. Journal of Agricultural Engineering Research, 75(1), 1-16.

Von Elsner, B., Briassoulis, D., Waaijenberg, D., Mistriotis, A., Von Zabeltitz, C., Gratraud, J. & Suay-Cortes, R. (2000b). Review of structural and functional characteristics of greenhouses in European Union Countries, Part II: typical designs. Journal of agricultural engineering research, 75(2), 111-126.

von Zabeltitz, C. & Baudoin, W.O. (2005). Greenhouses and shelter structures for tropical regions. Food and Agriculture Organization of the United National.

von Zabeltitz, C. (2011). Integrated Greenhouse Systems for Mild Climates. Integrated Greenhouse Systems for Mild Climates Climate Conditions, Design, Construction, Maintenance, Climate Control. Springer-Verlag. Wedemark, Germany.

Waaijenberg, D., Hemming, S., & Campen, J. B. (2004). The solar greenhouse: a highly insulated greenhouse design with an inflated roof system with PVDF or ETFE membranes. International Conference on Sustainable Greenhouse Systems, 691, 561-568.

Wang, D., & Gartung, J. (2010). Infrared canopy temperature of early-ripening peach trees under postharvest deficit irrigation. Agricultural Water Management, 97(11), 1787-1794.

Wang, S., Feng, G., Chen, D., Cao, Z., Qi, Y., & Liu, Y. (1999). Study on macro-management of protected horticulture development in China. Transaction of the Chinese Society of Agricultural Engineering, 15(1), 153-158.

Wang, S., Yernaux, M., & Deltour, J. (1999). A networked two-dimensional sonic anemometer system for the measurement of air velocity in greenhouses. Journal of Agricultural Engineering Research, 73(2), 189-197.

Wang, S., & Deltour, J. (1997). Natural ventilation induced airflow patterns measured by an ultrasonic anemometer in Venlo-type greenhouse openings. Agricultural Engineering Journal, 6(3-4), 185-196.

Watanabe, H. (2009). Light-controlled plant cultivation system in Japan-development of a vegetable factory using LEDs as a light source for plants. 6th International Symposium on Light in Horticulture, 907, 37-44.

Wei, Y. Q., Bailey, B. J., & Stenning, B. C. (1995). A wetness sensor for detecting condensation on tomato plants in greenhouses. Journal of Agricultural Engineering Research, 61(3), 197-204.

Wees, D. (2016). The Greenhouse Handbook. McGill University.

Wheeler, E. F., & Both, A. J. (2002). Evaluating greenhouse mechanical ventilation system performance. E277Rutgers NJAES Cooperative Extension. New Jersey Agricultural Experiment Station. Rutgers, NJ.

Wheeler, R. M. (2015). Growing Food for Space and Earth: NASA's Contributions to Vertical Agriculture. Accessible from < https://ntrs.nasa.gov/archive/nasa/casi.ntrs.nasa.gov/20150015991.pdf>

Whiteman, C. D., Hubbe, J. M., & Shaw, W. J. (2000). Evaluation of an inexpensive temperature datalogger for meteorological applications. Journal of Atmospheric and Oceanic Technology, 17(1), 77-81.

Wilhelm, L. R., Suter, D. A., & Brusewitz, G. H. (2005). Physical properties of food materials. Food and Process Engineering Technology, American Society of Agricultural Engineers, St Joseph, MI.

Willits, D. H., & Li, S. (2005). A Comparison of Naturally Ventilated vs. Fan Ventilated Greenhouses in the Southeastern US. American Society of Agricultural and Biological Engineers Annual International Meeting.

Willits, D. H., & Peet, M. M. (2000). Intermittent application of water to an externally mounted, greenhouse shade cloth to modify cooling performance. Transactions of the American Society of Agricultural Engineers, 43(5), 1247.

Willits, D. H. (2003). Cooling fan-ventilated greenhouses: a modelling study. Biosystems engineering, 84(3), 315-329.

Wimberley, R., Fulkerson G., & Morris, L. (2007). Predicting a moving target. Rural Sociology, 28, 18–22.

Wittwer, S. H., & Castilla, N. (1995). Protected cultivation of horticultural crops worldwide. HortTechnology, 5(1), 6-23.

Wollaeger, H. & Runkle, E. (2015). Why should greenhouse growers pay attention to vapor-pressure deficit and not relative humidity? Michigan State University Extension. Accessible from < http://msue.anr.msu.edu/news/why_should_greenhouse_growers_pay_attention_to_vapor_pressure_deficit_and_n>

Wollaeger, H. & Runkle, E. (2015). Why should greenhouse growers pay attention to vapor-pressure deficit and not relative humidity? Michigan State University Extension. Accessible from < http://msue.anr.msu.edu/news/why_should_greenhouse_growers_pay_attention_to_vapor_pressure_deficit_and_n>

Wookey, P.A., Parsons, A.N., Welker, J.M., Potter, J.A., Callaghan, T.V., Lee, J.A., Press, M.C. (1993). Comparative responses of phenology and reproductive development to simulated environmental change in sub-arctic and high arctic plants. Oikos, 67, 490–502.

Young, H. W. (1958). Inheritance of fruit cracking. Tomato Genetics Cooperative, 8, 38.

Yu, J. Q., & Komada, H. (1999). Hinoki (Chamaecyparis obtusa) bark, a substrate with anti-pathogen properties that suppress some root diseases of tomato. Scientia Horticulturae, 81(1), 13-24.

Zabel, P., Bamsey, M., Schubert, D., & Tajmar, M. (2016). Review and analysis of over 40 years of space plant growth systems. Life Sciences in Space Research, 10, 1-16.

Zabel, P., Bamsey, M., Zeidler, C., Vrakking, V., Johannes, B. W., Rettberg, P., & Hoheneder, W. (2015). Introducing EDEN ISS-A European project on advancing plant cultivation technologies and operations. International Conference on Environmental Systems, 1-13.

Zandalinas, S. I., Mittler, R., Balfagón, D., Arbona, V., & Gómez-Cadenas, A. (2017). Plant adaptations to the combination of drought and high temperatures. Physiologia Plantarum.

Zhang, Y., Kacira, M., & An, L. (2016). A CFD study on improving air flow uniformity in indoor plant factory system. Biosystems Engineering, 147, 193-205.

Zhang, D., Zhang, Z., Li, J., Chang, Y., Du, Q., & Pan, T. (2015). Regulation of vapor pressure deficit by greenhouse micro-fog systems improved growth and productivity of tomato via enhancing photosynthesis during summer season. PLOS ONE, 10(7).

Zhang, J.H., Huang, W.D., Liu, Y.P., Pan, Q.H. (2005 Effects of Temperature Acclimation Pretreatment on the Ultrastructure of Mesophyll Cells in Young Grape Plants (Vitis vinifera L. cv. Jingxiu) Under Cross-Temperature Stresses. Journal of Integrative Plant Biology, 47(8), 959-970.

Zhang, Y. & Shipp, J.L. 2002. Manipulating. Plant Moisture. Conditions Using. Greenhouse High- pressure Fogging. HortTechnology 12(2): 261-267.

Zolnier, S., Gates, R. S., Buxton, J., & Mach, C. (2000). Psychrometric and ventilation constraints for vapor pressure deficit control. Computers and electronics in agriculture, 26(3), 343-359.

Zurigat, Y. H., & Abu-Arabi, M. K. (2004). Modelling and performance analysis of a regenerative solar desalination unit. Applied Thermal Engineering, 24(7), 1061-1072.

11. Appendix A

The natural ventilation augmented cooling (NVAC) greenhouse design was revealed to researchers and industry members at a variety of conferences, including ASABE Annual International Meetings and NCERA-101 Annual Meetings, offering critical review of progress made in research and development of the new greenhouse design. A notable response to the NVAC greenhouse in the industry was noticed subsequent to a press release on the horticultural news website HortiDaily.com. A website and video (Figure A-1) for the design, construction and performance NVAC greenhouse were created to provide information to the public and industry members interested in the technology. As of August 2017, this outreach has generated conversation with over 45 persons or groups showing interest in acquiring the NVAC greenhouse technology or knowing more about the protected agriculture industry in warm climates. The interested parties range in background from growers to greenhouse manufacturers. The need for energy efficient and affordable cooling technologies in greenhouse worldwide is clearly relevant. As of October 2017, the video published on YouTube has generated over 22 000 views and a noteworthy series of comments in the comment section.

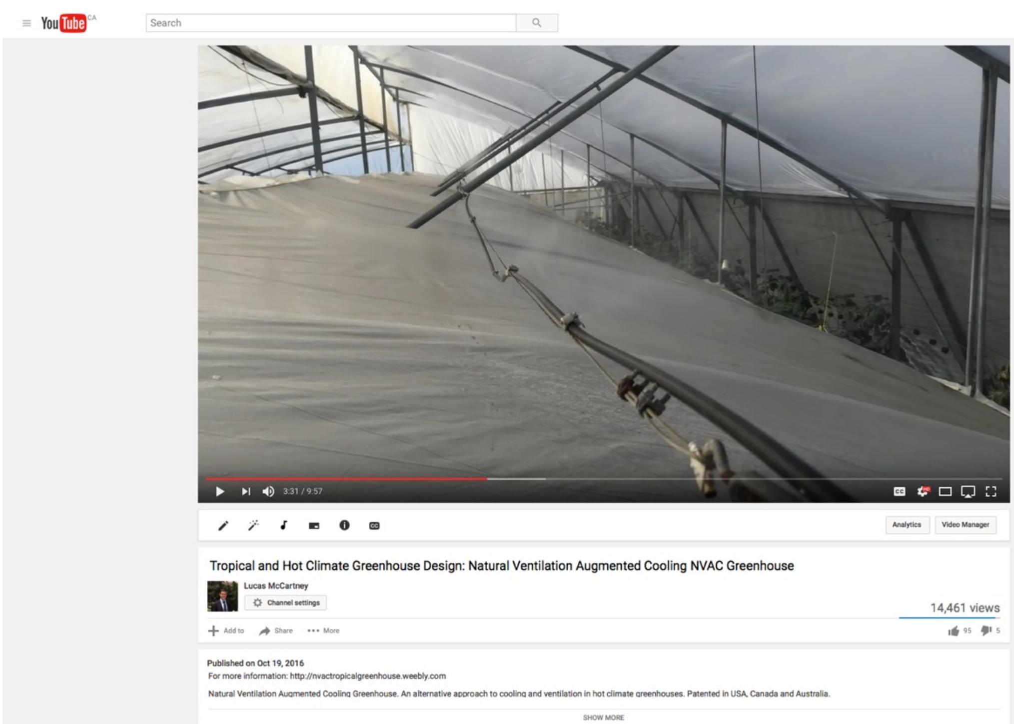

Figure A 1. Tropical and Hot Climate Greenhouse Design: Natural Ventilation Augmented Cooling NVAC Greenhouse. YouTube video available at <https://www.youtube.com/watch?v=GNezSZNfZpI>

12. Appendix B

Figure B-1. View of the NVAC roof being installed in the Natural Ventilation Augmented Cooling (NVAC) greenhouse in Trents, Barbados. Lucas McCartney (candidate) and Zainab Iqbal (undergraduate student in the McGill BITS Program) can be seen.

Figure B-3. View of the NVAC roof being installed in the Natural Ventilation Augmented Cooling (NVAC) greenhouse in Trents, Barbados. Ryan Knight and Dillon Fields (undergraduate students in the McGill BITS Program) can be seen working on the frame.

Figure B-3. View of the NVAC roof (above) in the Natural Ventilation Augmented Cooling (NVAC) greenhouse in Trents, Barbados. A pepper crop is seen in foreground with Lucas McCartney (candidate).

Figure B-4. View of a pepper crop in the Natural Ventilation Augmented Cooling (NVAC) greenhouse in Trents, Barbados. The NVAC roof is above the Aluminet on the left-hand side of the image. The NVAC roof gutter can be seen.

13. Appendix C

The Bellairs Research Institute is a McGill University facility located in Holetown, Barbados. It hosts many students and scientists from McGill and around the world for field courses, workshops and research projects. The institute prepares two or three meals a day during the week for the residents and students on the campus. The food bill is substantial and has averaged around $127 000 BBD per year for the campus. Over 50% of the food is sourced on the island but a very large percentage comes from outside Barbados. However, a large portion of this is fruits and vegetables that can be grown locally using a greenhouse. The construction of an NVAC greenhouse was funded by the McGill Office of Sustainability (MOOS) Sustainable Project Fund (SPF). The project introduced a sustainable and affordable solution to local food production. The candidate built the greenhouse and managed the project. The greenhouse is built with locally available materials and is off-grid with electricity provided by the Bellairs Research Institute's photovoltaic system. Water is provided sustainably from a rainwater harvesting system capable of providing water for both the natural ventilation augmented cooling (NVAC) system and drip-irrigation. The size of the structure is 4.5 by 9.0 m (Figure B-1, 2 and 3). It is suitable to supply the kitchen's cooking staff needs and provide the visitors to the campus with fresh produce. As a broad post-project objective, the greenhouse allows local students, greenhouse growers and future growers to educate themselves in the new and existing technologies and opportunities of sustainable protected agriculture in Barbados. Table B-1 offers a list of the materials used to build the NVAC greenhouse using only local material and their approximate cost.

Table B-1. Detailed cost of the 4.5 by 9.0 m NVAC greenhouse built at the Bellairs Research Institute in Holetown, Barbados.

Bellairs Research Institute NVAC Greenhouse Build						
Item	Description	Qu.	Unit Cost BBD	Unit Cost CAD	Sub Total BBD	Sub Total CAD
Greenhouse UV-Res. Poly Film	6mil 20'x100'	1	BBD 1,700.00	CAD 850.00	BBD 1,700.00	CAD 850.00
Concrete	3000 psi at 28 days	14	BBD 421.00	CAD 210.50	BBD 5,894.00	CAD 2,947.00

PCV Piping	3/4in, 1in (in feet lengths)	220	BBD 18.30	CAD 9.15	BBD 4,026.00	CAD 2,013.00
Nuts, Bolts and Washers	Various	1000	BBD 1.00	CAD 0.50	BBD 1,000.00	CAD 500.00
Single Groove Duralock2 System	3-piece system (4m length) (Base plate, insert strip and clips)	50	BBD 45.00	CAD 22.50	BBD 2,250.00	CAD 1,125.00
Snap Clamps	4’ by 1” (for 1” PVC pipe)	30	BBD 14.00	CAD 7.00	BBD 420.00	CAD 210.00
Fence Top Rail	1-3/8"x21' smaller gauge than^	42	BBD 41.00	CAD 20.50	BBD 1,722.00	CAD 861.00
Lockable Door	Fabricated	1	BBD 500.00	CAD 250.00	BBD 500.00	CAD 250.00
BRC (protective fencing)	A98 6' x 16'	12	BBD 86.50	CAD 43.25	BBD 1,038.00	CAD 519.00
Black Mesh	12' wide, 70% Shade from Agrochemicals	100	BBD 14.40	CAD 7.20	BBD 1,440.00	CAD 720.00
Gutter system	90ft of gutters, clamps, brackets etc. (13ft sections)	8	BBD 65.00	CAD 32.50	BBD 520.00	CAD 260.00
500-gal water tank	From Rotoplastics Barbados	3	BBD 400.00	CAD 200.00	BBD 1,200.00	CAD 600.00
Goulds Pump	1/2hp from ARC	2	BBD 795.00	CAD 397.50	BBD 1,590.00	CAD 795.00
Plumbing	Controller, Valves, Sensors.	2	BBD 500.00	CAD 250.00	BBD 1,000.00	CAD 500.00
High pressure pump	Orbit Irrigation Inc.	2	BBD 400.00	CAD 200.00	BBD 800.00	CAD 400.00
Control system	Various	1	BBD 6,000.00	CAD 3,000.00	BBD 6,000.00	CAD 3,000.00
Misting System	Orbit Irrigation Inc.	1	BBD 300.00	CAD 150.00	BBD 300.00	CAD 150.00

Plant Growing Systems for year 1, 2 and 3	Hydroponics and/or soil based systems	3	BBD 2,700.00	CAD 1,350.00	BBD 8,100.00	CAD 4,050.00
Year 2 and 3 operation and maintenance costs	~10% of total cost per year	2	BBD 5,000.00	CAD 2,500.00	BBD 10,000.00	CAD 5,000.00
Total					BBD 49,500.00	CAD 24,750.00

Figure B-1. The Natural Ventilation Augmented Cooling (NVAC) greenhouse at the Bellairs Research Institute in Holetown, Barbados.

Figure B-2. Phase 1 of the construction of the Natural Ventilation Augmented Cooling (NVAC) greenhouse at the Bellairs Research Institute in Holetown, Barbados.

Figure B-3. View of the crop irrigation system and water supply for the Natural Ventilation Augmented Cooling (NVAC) system in the NVAC greenhouse at the Bellairs Research Institute in Holetown, Barbados.

Figure B-3. View of the growth system with a light trellis system inside the Natural Ventilation Augmented Cooling (NVAC) system in the NVAC greenhouse at the Bellairs Research Institute in Holetown, Barbados.

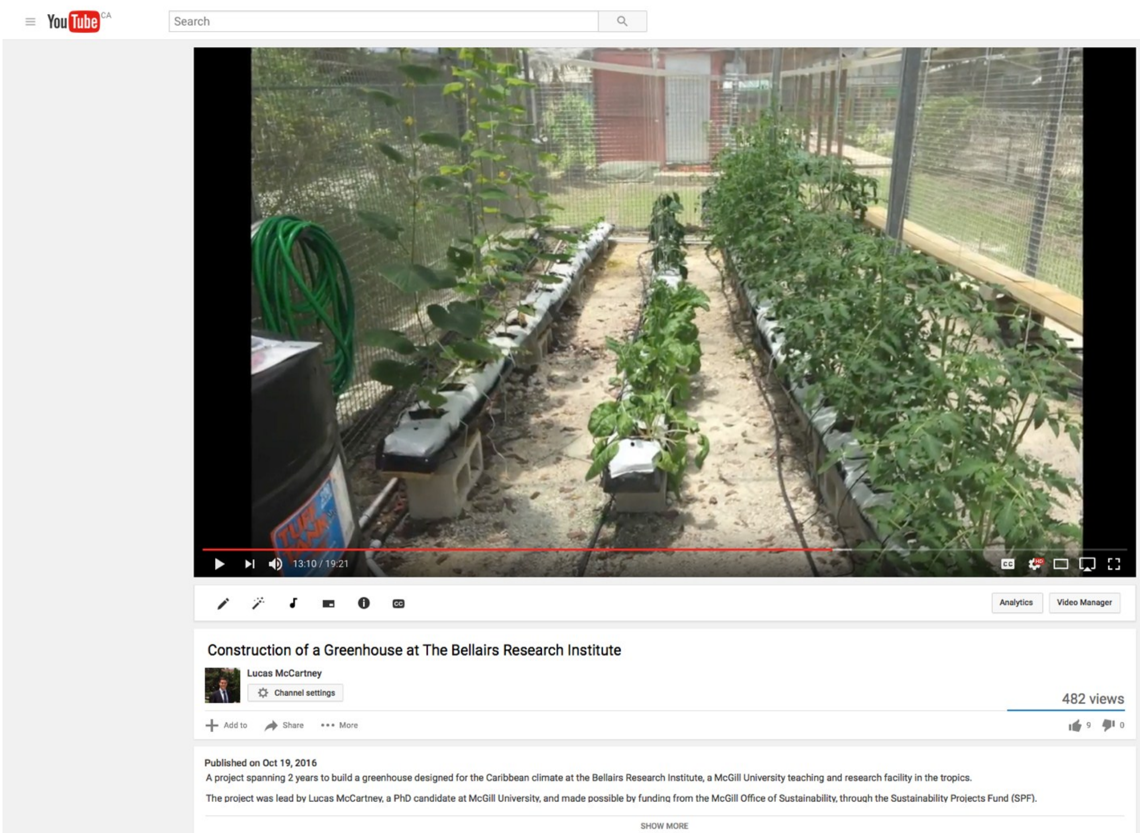

Figure B-3. A detailed account of the construction of the Bellairs Research Institute Natural Ventilation Augmented Cooling (NVAC) greenhouse is available in a video format. The video can be accessed at <https://www.youtube.com/watch?v=YRzF-yDBqHM>

14. Appendix D

The MATLAB script used for image capturing and processing in Chapter 7.

The script is separated into three sections: the main program with the image capturing components, recording of the data and saving of a data file. The main program calls upon two function scripts. The inspiration for some sections of these scripts was based on some publicly available script files on the MathWorks website. License is provided in Appendix E.

Main Script:

```
%Acquiring and Analyzing Image Sequences Tomato
%April 28 2017: set for red and green tomato with pure blue background

clear;
clc;
%ver % Display the user's toolboxes in their command window.

%Use imaqhwinfo to determine your deviceís identifier number and supported video
formats
%imaqhwinfo;
%imaqhwinfo('winvideo', 1);
%cam = webcam('Logitech')

counter=1;
%number of iterations of the image loop
n=1;
%2880 iterations for 24 hours, 8640 for 3 days exactly from start time.
numberofits = 10000;
areavaluesout = zeros(1,numberofits);
perivaluesout = zeros(1,numberofits);
%centroidvaluesout = zeros(2,numberofits);
diametervaluesout = zeros(1,numberofits);
timestampout = zeros(1, numberofits);

%Webcam image capture settings:
   W = webcam()

for n = 1:numberofits

   %W.Brightness = 128;
   %W.Contrast = 128;
   W.WhiteBalance = 2000;
   W.Resolution = '1024x576';
   %W.Gain = 102;
   %W.BacklightCompensation = 0;
   W.Focus = 50;
   %W.Saturation = 128;
   %W.Exposure = -4;
   W.Zoom = 155;
   %Need a ~5 second pause to allow camera to adjust to given settings
   pause(1);
```

```
    I = snapshot(W);
    imshow(I);                  % show the image
    imwrite(I, 'image.png');

    run('TomatoImageProcessing.m');
    run('FruitMeasurements.m');

    %%EXTRACT AREAS from function and save in matrix or array
    %The outputs of interest are: blobArea, blobPerimeter, blobCentroid, blobECD

    close;
    numbervaluesout(n) = n;
    areavaluesout(n) = max(blobArea);
    perivaluesout(n) = max(blobPerimeter);
    %centroidvaluesout(n) = blobCentroid;
    diametervaluesout(n) = max(blobECD);
    timestampout(n) = now;

    standardevA = std(numbervaluesout);
    standardevB = std(areavaluesout);
    standardevC = std(perivaluesout);
    standardevD = std(diametervaluesout);

    Image = numbervaluesout';
    AreaofTomato = areavaluesout';
    PerimeterofTomato= perivaluesout';
    %CentroidofTomato = centroidvaluesout';
    DiameterofTomato = diametervaluesout';
    TimeStamp = timestampout';

    delete image.png;
    delete HueMaskedImage.png
    delete coloredObjectsMask.png
    delete MaskedImageRed.png

    n = n+1

end

clc;
DataTable = table(Image, TimeStamp, AreaofTomato, PerimeterofTomato, DiameterofTomato)
stdTable = table(standardevA, standardevB, standardevC, standardevD)

typeoftest = 'tomato';
todaysdate = date;
filetype = '.xlsx';
filename = [typeoftest todaysdate filetype];
writetable(DataTable,filename,'Sheet',1,'Range','B1')
```

The color detection was accomplished using a modified form of a MathWorks File Exchange script. License is provided in Appendix E.

Color Detection by Hue Function Script:

```
% Function file for image processing of fruit
% HSV (Hue, Saturation, Value) color space.
% Requires the Image Processing Toolbox.

function FruitBrocessing()
clc;   % Clear command window
clear; % Delete all variables
close all;    % Close any leftover figures
imtool close all;    % Close all figure windows created by imtool
workspace;    % Show Workspace Panel
fprintf('Running TomatoImageProcessing.m\n'); % Message sent to command window.

% Change the current folder to the folder of this m-file.
if(~isdeployed)
       cd(fileparts(which(mfilename)));
end
       close all;
       fontSize = 16;
       figure;
       % Maximize the figure.
       set(gcf, 'units','normalized','outerposition',[0 0 1 1]);
       % Change the current folder to the folder of this m-file.
       % (The line of code below is from Brett Shoelson of The Mathworks.)

    if(~isdeployed)
              cd(fileparts(which(mfilename)));
    end

    %define the image
    fullImageFileName = 'image.png';

       % Read in image into an array.
       [rgbImage, storedColorMap] = imread(fullImageFileName);
       [rows, columns, numberOfColorBands] = size(rgbImage);
       % If it's monochrome (indexed), convert it to color.
       % Check to see if it's an 8-bit image needed later for scaling).
       if strcmpi(class(rgbImage), 'uint8')
              % Flag for 256 gray levels.
              eightBit = true;
       else
              eightBit = false;
       end
       if numberOfColorBands == 1
              if isempty(storedColorMap)
                     % Just a simple gray level image, not indexed with a stored color
map.
                     % Create a 3D true color image where we copy the monochrome image
into all 3 (R, G, & B) color planes.
                     rgbImage = cat(3, rgbImage, rgbImage, rgbImage);
              else
                     % It's an indexed image.
                     rgbImage = ind2rgb(rgbImage, storedColorMap);
                     % ind2rgb() will convert it to double and normalize it to the
range 0-1.
```

```
			% Convert back to uint8 in the range 0-255, if needed.
			if eightBit
				rgbImage = uint8(255 * rgbImage);
			end
		end
	end

	% Display the original image.
	subplot(3, 4, 1);
	hRGB = imshow(rgbImage);
	% Set up an infor panel so you can mouse around and inspect the value values.
	hrgbPI = impixelinfo(hRGB);
	set(hrgbPI, 'Units', 'Normalized', 'Position',[.15 .69 .15 .02]);
	drawnow; % Make it display immediately.
	if numberOfColorBands > 1
		title('Original Color Image', 'FontSize', fontSize);
	else
		caption = sprintf('Original Indexed Image\n(converted to true color with 
its stored colormap)');
		title(caption, 'FontSize', fontSize);
	end

	% Convert RGB image to HSV
	hsvImage = rgb2hsv(rgbImage);
	% Extract out the H, S, and V images individually
	hImage = hsvImage(:,:,1);
	sImage = hsvImage(:,:,2);
	vImage = hsvImage(:,:,3);

	% Display the hue image.
	subplot(3, 4, 2);
	h1 = imshow(hImage);
	title('Hue Image', 'FontSize', fontSize);
	% Set up an infor panel so you can mouse around and inspect the hue values.
	hHuePI = impixelinfo(h1);
	set(hHuePI, 'Units', 'Normalized', 'Position',[.34 .69 .15 .02]);

	% Display the saturation image.
	h2 = subplot(3, 4, 3);
	imshow(sImage);
	title('Saturation Image', 'FontSize', fontSize);
	% Set up an infor panel so you can mouse around and inspect the saturation 
values.
	hSatPI = impixelinfo(h2);
	set(hSatPI, 'Units', 'Normalized', 'Position',[.54 .69 .15 .02]);

	% Display the value image.
	h3 = subplot(3, 4, 4);
	imshow(vImage);
	title('Value Image', 'FontSize', fontSize);
	% Set up an infor panel so you can mouse around and inspect the value values.
	hValuePI = impixelinfo(h3);
	set(hValuePI, 'Units', 'Normalized', 'Position',[.75 .69 .15 .02]);

	% Compute and plot the histogram of the "hue" band.
	hHuePlot = subplot(3, 4, 6);
	[hueCounts, hueBinValues] = imhist(hImage);
	maxHueBinValue = find(hueCounts > 0, 1, 'last');
	maxCountHue = max(hueCounts);
	% Display with area() rather than bar, due to bug in bar().  The bug, and 
workaround of using area(), are discussed in
	% http://www.mathworks.com/matlabcentral/answers/103538-why-does-a-bar-subplot-
change-when-i-create-another-bar-subplot-on-the-same-figure-in-matlab-8-0-r
```

```
        % Supposedly it's been fixed in R2014b.
%       bar(hueBinValues, hueCounts, 'r');
        area(hueBinValues, hueCounts, 'FaceColor', 'r');
        grid on;
        xlabel('Hue Value');
        ylabel('Pixel Count');
        title('Histogram of Hue Image', 'FontSize', fontSize);

        % Compute and plot the histogram of the "saturation" band.
        hSaturationPlot = subplot(3, 4, 7);
        [saturationCounts, saturationBinValues] = imhist(sImage);
        maxSaturationBinValue = find(saturationCounts > 0, 1, 'last');
        maxCountSaturation = max(saturationCounts);
%       bar(saturationBinValues, saturationCounts, 'g', 'BarWidth', 0.95);
        area(saturationBinValues, saturationCounts, 'FaceColor', 'g');
        grid on;
        xlabel('Saturation Value');
        ylabel('Pixel Count');
        title('Histogram of Saturation Image', 'FontSize', fontSize);

        % Compute and plot the histogram of the "value" band.
        hValuePlot = subplot(3, 4, 8);
        [valueCounts, valueBinValues] = imhist(vImage);
        maxValueBinValue = find(valueCounts > 0, 1, 'last');
        maxCountValue = max(valueCounts);
%       bar(valueBinValues, valueCounts, 'b');
        area(valueBinValues, valueCounts, 'FaceColor', 'b');
        grid on;
        xlabel('Value Value');
        ylabel('Pixel Count');
        title('Histogram of Value Image', 'FontSize', fontSize);

        % Set all axes to be the same width and height.
        % This makes it easier to compare them.
        maxCount = max([maxCountHue,  maxCountSaturation, maxCountValue]);
        axis([hHuePlot hSaturationPlot hValuePlot], [0 1 0 maxCount]);

        % Plot all 3 histograms in one plot.
        subplot(3, 4, 5);
        plot(hueBinValues, hueCounts, 'r', 'LineWidth', 2);
        grid on;
        xlabel('Values');
        ylabel('Pixel Count');
        hold on;
        plot(saturationBinValues, saturationCounts, 'g', 'LineWidth', 2);
        plot(valueBinValues, valueCounts, 'b', 'LineWidth', 2);
        title('Histogram of All Bands', 'FontSize', fontSize);
        maxGrayLevel = max([maxHueBinValue, maxSaturationBinValue, maxValueBinValue]);
% Just for our information....
        % Make x-axis to just the max gray level on the bright end.
        xlim([0 1]);

        % Now select thresholds for the 3 color bands.

        % Assign the low and high thresholds for each color band.
    % April 28 2017: set for red and green of a tomato with pure blue background
              hueThresholdLow = 0;
                      hueThresholdHigh = 0.3;
                      saturationThresholdLow = 0;
                      saturationThresholdHigh = 0.7;
                      valueThresholdLow = 0;
                      valueThresholdHigh = 0.8;
```

```
	% Interactively and visually set/adjust thresholds using custom thresholding application.
	% Available on the File Exchange: http://www.mathworks.com/matlabcentral/fileexchange/29372-thresholding-an-image
%	[hueThresholdLow, hueThresholdHigh] = threshold(hueThresholdLow, hueThresholdHigh, hImage);
%	[saturationThresholdLow, saturationThresholdHigh] = threshold(saturationThresholdLow, saturationThresholdHigh, sImage);
%	[valueThresholdLow, valueThresholdHigh] = threshold(valueThresholdLow, valueThresholdHigh, vImage);


	% Now apply each color band's particular thresholds to the color band
	hueMask = (hImage >= hueThresholdLow) & (hImage <= hueThresholdHigh);
	saturationMask = (sImage >= saturationThresholdLow) & (sImage <= saturationThresholdHigh);
	valueMask = (vImage >= valueThresholdLow) & (vImage <= valueThresholdHigh);

	% Display the thresholded binary images.
	fontSize = 16;
	subplot(3, 4, 10);
	imshow(hueMask, []);
    imwrite(hueMask, 'HueMaskedImage.png');

	title('=   Hue Mask', 'FontSize', fontSize);
	subplot(3, 4, 11);
	imshow(saturationMask, []);
	title('&   Saturation Mask', 'FontSize', fontSize);
	subplot(3, 4, 12);
	imshow(valueMask, []);
	title('&   Value Mask', 'FontSize', fontSize);
	% Combine the masks to find where all 3 are "true."
	% Then we will have the mask of only the chosen parts of the image.
	coloredObjectsMask = uint8(hueMask & saturationMask & valueMask);
	subplot(3, 4, 9);
	imshow(coloredObjectsMask, []);
	caption = sprintf('Mask of Only Regions\nof The Specified Color');
	title(caption, 'FontSize', fontSize);

	% Tell user that we're going to filter out small objects.
	smallestAcceptableArea = 500; % Keep areas only if they're bigger than this.
    %close figure
    pause(5);
    close;
	% Open up a new figure, since the existing one is full.
	figure;
	% Maximize the figure.
	set(gcf, 'units','normalized','outerposition',[0 0 1 1]);

	% Get rid of small objects.  Note: bwareaopen returns a logical.
	coloredObjectsMask = uint8(bwareaopen(coloredObjectsMask, smallestAcceptableArea));
	subplot(3, 3, 1);
	imshow(coloredObjectsMask, []);
	fontSize = 13;
	caption = sprintf('bwareaopen() removed objects\nsmaller than %d pixels', smallestAcceptableArea);
	title(caption, 'FontSize', fontSize);

	% Smooth the border using a morphological closing operation, imclose().
	structuringElement = strel('disk', 4);
	coloredObjectsMask = imclose(coloredObjectsMask, structuringElement);
	subplot(3, 3, 2);
```

```
	imshow(coloredObjectsMask, []);
	fontSize = 16;
	title('Border smoothed', 'FontSize', fontSize);

	% Fill in any holes in the regions, since they are most likely red also.
	coloredObjectsMask = imfill(logical(coloredObjectsMask), 'holes');
	subplot(3, 3, 3);
	imshow(coloredObjectsMask, []);
	title('Regions Filled', 'FontSize', fontSize);
    imwrite(coloredObjectsMask, 'coloredObjectsMask.png');

	% You can only multiply integers if they are of the same type.
	% (coloredObjectsMask is a logical array.)
	% We need to convert the type of coloredObjectsMask to the same data type as
hImage.
	coloredObjectsMask = cast(coloredObjectsMask, 'like', rgbImage);
% 	coloredObjectsMask = cast(coloredObjectsMask, class(rgbImage));

	% Use the colored object mask to mask out the colored-only portions of the rgb
image.
	maskedImageR = coloredObjectsMask .* rgbImage(:,:,1);
	maskedImageG = coloredObjectsMask .* rgbImage(:,:,2);
	maskedImageB = coloredObjectsMask .* rgbImage(:,:,3);
	% Show the masked off red image.
	subplot(3, 3, 4);
	imshow(maskedImageR);
    imwrite(maskedImageR, 'MaskedImageRed.png');

	title('Masked Red Image', 'FontSize', fontSize);
	% Show the masked off saturation image.
	subplot(3, 3, 5);
	imshow(maskedImageG);
	title('Masked Green Image', 'FontSize', fontSize);
	% Show the masked off value image.
	subplot(3, 3, 6);
	imshow(maskedImageB);
	title('Masked Blue Image', 'FontSize', fontSize);
	% Concatenate the masked color bands to form the rgb image.
	maskedRGBImage = cat(3, maskedImageR, maskedImageG, maskedImageB);
	% Show the masked off, original image.
	subplot(3, 3, 8);
	imshow(maskedRGBImage);
	fontSize = 13;
	caption = sprintf('Masked Original Image\nShowing Regions of Only the Specified
Color');
	title(caption, 'FontSize', fontSize);
	% Show the original image next to it.
	subplot(3, 3, 7);
	imshow(rgbImage);
	title('The Original Image (Again)', 'FontSize', fontSize);

	% Measure the mean HSV and area of all the detected blobs.
	[meanHSV, areas, numberOfBlobs] = MeasureBlobs(coloredObjectsMask, hImage,
sImage, vImage);
	if numberOfBlobs > 0
		fprintf(1, '\n----------------------------------------------\n');
		fprintf(1, 'Blob #, Area in Pixels, Mean H, Mean S, Mean V\n');
		fprintf(1, '----------------------------------------------\n');
		for blobNumber = 1 : numberOfBlobs
			fprintf(1, '#%5d, %14d, %6.2f, %6.2f, %6.2f\n', blobNumber,
areas(blobNumber), ...
				meanHSV(blobNumber, 1), meanHSV(blobNumber, 2),
meanHSV(blobNumber, 3));
```

```
            end
        else
            % Alert user that no colored blobs were found.
            message = sprintf('No blobs of the specified color were found in the
image:\n%s', fullImageFileName);
            fprintf(1, '\n%s\n', message);
            uiwait(msgbox(message));
    end

    A = areas(1);
    save('areas1', 'A');
    pause(3);
    close;
return; % from SimpleColorDetection()


%Function to calculate and display the average hue, sat and value values of the
processed image to
%the user.
function [meanHSV, areas, numberOfBlobs] = MeasureBlobs(maskImage, hImage, sImage,
vImage)
try
        [labeledImage, numberOfBlobs] = bwlabel(maskImage, 8);     % Label each blob so
we can make measurements of it
        if numberOfBlobs == 0
            % Didn't detect any blobs of the specified color in this image.
            meanHSV = [0 0 0];
            areas = 0;
            return;
        end
        % Get all the blob properties.  Can only pass in originalImage in version
R2008a and later.
        blobMeasurementsHue = regionprops(labeledImage, hImage, 'area',
'MeanIntensity');
        blobMeasurementsSat = regionprops(labeledImage, sImage, 'area',
'MeanIntensity');
        blobMeasurementsValue = regionprops(labeledImage, vImage, 'area',
'MeanIntensity');

        meanHSV = zeros(numberOfBlobs, 3);  % One row for each blob.  One column for
each color.
        meanHSV(:,1) = [blobMeasurementsHue.MeanIntensity]';
        meanHSV(:,2) = [blobMeasurementsSat.MeanIntensity]';
        meanHSV(:,3) = [blobMeasurementsValue.MeanIntensity]';

        % Now assign the areas.
        areas = zeros(numberOfBlobs, 3);  % One row for each blob.  One column for each
color.
        areas(:,1) = [blobMeasurementsHue.Area]';
        areas(:,2) = [blobMeasurementsSat.Area]';
        areas(:,3) = [blobMeasurementsValue.Area]';
catch ME
        errorMessage = sprintf('Error in function %s() at line %d.\n\nError
Message:\n%s', ...
            ME.stack(1).name, ME.stack(1).line, ME.message);
        fprintf(1, '%s\n', errorMessage);
        uiwait(warndlg(errorMessage));
end
return; % from MeasureBlobs()

        % Function to show the low and high threshold bars on the histogram plots.
function PlaceThresholdBars(plotNumber, lowThresh, highThresh)
try
```

```
	% Show the thresholds as vertical red bars on the histograms.
	subplot(3, 4, plotNumber);
	hold on;
	yLimits = ylim;
	line([lowThresh, lowThresh], yLimits, 'Color', 'r', 'LineWidth', 3);
	line([highThresh, highThresh], yLimits, 'Color', 'r', 'LineWidth', 3);
	% Place a text label on the bar chart showing the threshold.
	fontSizeThresh = 14;
	annotationTextL = sprintf('%d', lowThresh);
	annotationTextH = sprintf('%d', highThresh);
	% For text(), the x and y need to be of the data class "double" so let's cast
both to double.
	text(double(lowThresh + 5), double(0.85 * yLimits(2)), annotationTextL,
'FontSize', fontSizeThresh, 'Color', [0 .5 0], 'FontWeight', 'Bold');
	text(double(highThresh + 5), double(0.85 * yLimits(2)), annotationTextH,
'FontSize', fontSizeThresh, 'Color', [0 .5 0], 'FontWeight', 'Bold');

	% Show the range as arrows.
	% Can't get it to work, with either gca or gcf.
%	annotation(gca, 'arrow', [lowThresh/maxXValue(2) highThresh/maxXValue(2)],[0.7
0.7]);

catch ME
	errorMessage = sprintf('Error in function %s() at line %d.\n\nError
Message:\n%s', ...
		ME.stack(1).name, ME.stack(1).line, ME.message);
	fprintf(1, '%s\n', errorMessage);
	uiwait(warndlg(errorMessage));
end
return; % from PlaceThresholdBars()
```

The tomato fruit measurements were accomplished using a modified form of a MathWorks File Exchange script. License is provided in Appendix E.

```
% Function file for image analysis for measurement of fruit

% Running time = 7.5 seconds the first run and 2.5 seconds on subsequent runs.

tic; % Start timer.
% Clear command window.
%clearvars; % Get rid of variables from prior run of this m-file.
fprintf('Running FruitMeasurements.m\n'); % Message sent to command window.
workspace; % Make sure the workspace panel with all the variables is showing.
imtool close all;  % Close all imtool figures.
format long g;
format compact;
captionFontSize = 14;

% Check that user has the Image Processing Toolbox installed.
hasIPT = license('test', 'image_toolbox');
if ~hasIPT
	% User does not have the toolbox installed.
	message = sprintf('Sorry, but you do not seem to have the Image Processing 
Toolbox.\nDo you want to try to continue anyway?');
	reply = questdlg(message, 'Toolbox missing', 'Yes', 'No', 'Yes');
	if strcmpi(reply, 'No')
		% User said No, so exit.
		return;
	end
end

baseFileName = 'MaskedImageRed.png';
folder = fileparts(which(baseFileName)); % Determine where demo folder is (works with 
all versions).
fullFileName = fullfile(folder, baseFileName);
if ~exist(fullFileName, 'file')
	% It doesn't exist in the current folder.
	% Look on the search path.
	if ~exist(baseFileName, 'file')
		% It doesn't exist on the search path either.
		% Alert user that we can't find the image.
		warningMessage = sprintf('Error: the input image file\n%s\nwas not 
found.\nClick OK to exit the demo.', fullFileName);
		uiwait(warndlg(warningMessage));
		fprintf(1, 'Finished running BlobsDemo.m.\n');
		return;
	end
	% Found it on the search path.  Construct the file name.
	fullFileName = baseFileName; % Note: don't prepend the folder.
end
% If we get here, we should have found the image file.
originalImage = imread(fullFileName);
% Check to make sure that it is grayscale, just in case the user substituted their own 
image.
[rows, columns, numberOfColorChannels] = size(originalImage);
if numberOfColorChannels > 1
	promptMessage = sprintf('Your image file has %d color channels.\nThis demo was 
designed for grayscale images.\nDo you want me to convert it to grayscale for you so 
you can continue?', numberOfColorChannels);
	button = questdlg(promptMessage, 'Continue', 'Convert and Continue', 'Cancel', 
'Convert and Continue');
```

```
	if strcmp(button, 'Cancel')
		fprintf(1, 'Finished running BlobsDemo.m.\n');
		return;
	end
	% Do the conversion using standard book formula
	originalImage = rgb2gray(originalImage);
end

% Display the grayscale image.
subplot(3, 3, 1);
imshow(originalImage);
% Maximize the figure window.
set(gcf, 'units','normalized','outerposition',[0 0 1 1]);
% Force it to display RIGHT NOW (otherwise it might not display until it's all done,
unless you've stopped at a breakpoint.)
drawnow;
caption = sprintf('Original "coins" image showing\n6 nickels (the larger coins) and 4
dimes (the smaller coins).');
title(caption, 'FontSize', captionFontSize);
axis image; % Make sure image is not artificially stretched because of screen's aspect
ratio.

% Just for fun, let's get its histogram and display it.
[pixelCount, grayLevels] = imhist(originalImage);
subplot(3, 3, 2);
bar(pixelCount);
title('Histogram of original image', 'FontSize', captionFontSize);
xlim([0 grayLevels(end)]); % Scale x axis manually.
grid on;

% Threshold the image to get a binary image (only 0's and 1's) of class "logical."
% Method #1: using im2bw()
%   normalizedThresholdValue = 0.4; % In range 0 to 1.
%   thresholdValue = normalizedThresholdValue * max(max(originalImage)); % Gray
Levels.
%   binaryImage = im2bw(originalImage, normalizedThresholdValue);       % One way to
threshold to binary
% Method #2: using a logical operation.
thresholdValue = 10;

binaryImage = originalImage > thresholdValue; % Bright objects will be chosen if you
use >.
% ========== IMPORTANT OPTION
============================================================
% Use < if you want to find dark objects instead of bright objects.
%binaryImage = originalImage < thresholdValue; % Dark objects will be chosen if you
use <.

% Do a "hole fill" to get rid of any background pixels or "holes" inside the blobs.
binaryImage = imfill(binaryImage, 'holes');

% Show the threshold as a vertical red bar on the histogram.
hold on;
maxYValue = ylim;
line([thresholdValue, thresholdValue], maxYValue, 'Color', 'r');
% Place a text label on the bar chart showing the threshold.
annotationText = sprintf('Thresholded at %d gray levels', thresholdValue);
% For text(), the x and y need to be of the data class "double" so let's cast both to
double.
text(double(thresholdValue + 5), double(0.5 * maxYValue(2)), annotationText,
'FontSize', 10, 'Color', [0 .5 0]);
text(double(thresholdValue - 70), double(0.94 * maxYValue(2)), 'Background',
'FontSize', 10, 'Color', [0 0 .5]);
```

```
text(double(thresholdValue + 50), double(0.94 * maxYValue(2)), 'Foreground',
'FontSize', 10, 'Color', [0 0 .5]);

% Display the binary image.
subplot(3, 3, 3);
imshow(binaryImage);
title('Binary Image, obtained by thresholding', 'FontSize', captionFontSize);

% Identify individual blobs by seeing which pixels are connected to each other.
% Each group of connected pixels will be given a label, a number, to identify it and
distinguish it from the other blobs.
% Do connected components labeling with either bwlabel() or bwconncomp().
labeledImage = bwlabel(binaryImage, 8);     % Label each blob so we can make
measurements of it
% labeledImage is an integer-valued image where all pixels in the blobs have values of
1, or 2, or 3, or ... etc.
subplot(3, 3, 4);
imshow(labeledImage, []);  % Show the gray scale image.
title('Labeled Image, from bwlabel()', 'FontSize', captionFontSize);

% Let's assign each blob a different color to visually show the user the distinct
blobs.
coloredLabels = label2rgb (labeledImage, 'hsv', 'k', 'shuffle'); % pseudo random color
labels
% coloredLabels is an RGB image.  We could have applied a colormap instead (but only
with R2014b and later)
subplot(3, 3, 5);
imshow(coloredLabels);
axis image; % Make sure image is not artificially stretched because of screen's aspect
ratio.
caption = sprintf('Pseudo colored labels, from label2rgb().\nBlobs are numbered from
top to bottom, then from left to right.');
title(caption, 'FontSize', captionFontSize);

% Get all the blob properties.  Can only pass in originalImage in version R2008a and
later.
blobMeasurements = regionprops(labeledImage, originalImage, 'all');
numberOfBlobs = size(blobMeasurements, 1);

% bwboundaries() returns a cell array, where each cell contains the row/column
coordinates for an object in the image.
% Plot the borders of all the coins on the original grayscale image using the
coordinates returned by bwboundaries.
subplot(3, 3, 6);
imshow(originalImage);
title('Outlines, from bwboundaries()', 'FontSize', captionFontSize);
axis image; % Make sure image is not artificially stretched because of screen's aspect
ratio.
hold on;
boundaries = bwboundaries(binaryImage);
numberOfBoundaries = size(boundaries, 1);
for k = 1 : numberOfBoundaries
       thisBoundary = boundaries{k};
       plot(thisBoundary(:,2), thisBoundary(:,1), 'g', 'LineWidth', 2);
end
hold off;

textFontSize = 14;  % Used to control size of "blob number" labels put atop the image.
labelShiftX = -7;   % Used to align the labels in the centers of the coins.
blobECD = zeros(1, numberOfBlobs);
% Print header line in the command window.
fprintf(1,'Blob #      Mean Intensity    Area     Perimeter        Centroid
Diameter\n');
```

```
% Loop over all blobs printing their measurements to the command window.
for k = 1 : numberOfBlobs           % Loop through all blobs.
	% Find the mean of each blob.  (R2008a has a better way where you can pass the
original image
	% directly into regionprops.  The way below works for all versions including
earlier versions.)
	thisBlobsPixels = blobMeasurements(k).PixelIdxList;  % Get list of pixels in
current blob.
	meanGL = mean(originalImage(thisBlobsPixels)); % Find mean intensity (in
original image!)
	meanGL2008a = blobMeasurements(k).MeanIntensity; % Mean again, but only for
version >= R2008a

	blobArea = blobMeasurements(k).Area;		% Get area.
	blobPerimeter = blobMeasurements(k).Perimeter;		% Get perimeter.
	blobCentroid = blobMeasurements(k).Centroid;		% Get centroid one at a
time
	blobECD(k) = sqrt(4 * blobArea / pi);					% Compute ECD
- Equivalent Circular Diameter.
	fprintf(1,'#%2d %17.1f    %11.1f   %8.1f    %8.1f %8.1f   % 8.1f\n', k, meanGL,
blobArea, blobPerimeter, blobCentroid, blobECD(k));
	% Put the "blob number" labels on the "boundaries" grayscale image.
	text(blobCentroid(1) + labelShiftX, blobCentroid(2), num2str(k), 'FontSize',
textFontSize, 'FontWeight', 'Bold');
end
```

15. Appendix E

© 1994-2017 The MathWorks, Inc.

License

16. Appendix F

The following is the license from Elsevier to reuse Figure 5 found in this thesis.

Expected completion date	Dec 2017
Estimated size (number of pages)	300
Requestor Location	Mr. Lucas McCartney 21,111 Lakeshore Dr. Ste-Anne-de-Bellevue, QC H9X3V9 Canada Attn: Mr. Lucas McCartney
Total	0.00 USD
Terms and Conditions	